AGE AND AFFINITY OF GRANITIC DETRITUS IN LOWER PALAEOZOIC CONGLOMERATES, S. W. SCOTLAND : IMPLICATIONS FOR CALEDONIAN EVOLUTION

Christopher David Longman

A thesis submitted for the degree of Doctor of Philosophy at the University of Glasgow

December 1980

CONTENTS

	Page
1. INTRODUCTION	
1.1 Prologue	1
1.2 Previous research and project development	3
1.3 Stratigraphy	5
1.4 Conglomerate composition and sampling	8
1.5 Depositional environment	12
1.6 Tectonic setting	17
1.7 Sample collection and preparation	19
2. GEOCHRONOLOGY	
2.1 Analytical methods	21
2.1.1 Rb-Sr geochronology	21
2.1.2 Isotope dilution	23
2.1.3 Mass spectrometry	25
2.1.4 Analytical precision	27
2.1.5 Data evaluation	30
2.1.6 U-Pb geochronology	32
2.2 Geochronological data	
2.2.1 Kirkland conglomerate	34
2.2.2 Benan conglomerate	34
2.2.3 Kilranny conglomerate	36
2.2.4 Tormitchell conglomerate	36
2.2.5 Craigskelly conglomerate	36
2.2.6 Corsewall conglomerate	37
2.3 Summary of geochronological framework	38
3.GEOCHEMISTRY & PETROGRAPHY	
3.1 Analytical techniques	59
3.1.1 XRF	59
3.1.2 'Wet' chemistry	60
3.1.3 Microprobe analyses	60
3.1.4 CIPW Norm	61
3.1.5 XTLFRAC	61
3.1.6 Analytical precision	62
3.2 Petrography	
3.2.1 Granites	88
3.2.2 Xenoliths	102

Page

3.3 Problems of granite classification 103
3.4 Major element chemistry 117
3.5 Trace element chemistry 136
3.6 Geothermometry 144
3.7 Summary 146

4. CALEDONIAN EVOLUTION OF SOUTHERN SCOTLAND
4.1 Previous plate-tectonic models 147
4.2 Evidence for a fore-arc regime 154
4.3 Island arc development 160
4.4 Midland Valley as a marginal basin 164
4.5 Plate-tectonic model for the development of southern Scotland 166
4.6 Implications of the model 169
4.6.1 Agreement/disagreement with previous models 169
4.6.2 Dalradian sedimentation 170
4.6.3 Timing of events 170
4.6.4 Relationship to other episodes of granite intrusion 174
4.7 Correlation east and west 177

5. ORDOVICIAN TIME SCALE
5.1 Present research applications 178
5.2 Published time scales 178
5.3 Implications of present data 180
5.3.1 Pluton emplacement to erosion timespan 180
5.3.2 Maximum age estimates for stratigraphic horizons 181
5.3.3 Comparisons with previous time scales 181

APPENDICES
I Thin section descriptions 184
II Ordovician conglomerates and the evolution of the Midland Valley 189
III Ordovician conglomerates : constraints on the time scale 191

REFERENCES 198

LIST OF TABLES

		Page
1A	Conglomerate constituents	11
2A	Replicate analyses	29
2B	U-Pb sample data	33
2C	Rb-Sr isochron data (Benan conglomerate)	53
2D	Rb-Sr isochron data (Corsewall, Craigskelly, Kilranny, Kirkland and Tormitchell conglomerates)	54
2E	Rb-Sr analytical data	55-58
3A	Detection limits	63
3B	Rb and Sr values	64
3C	Chemical rock analyses	67-80
3D	Norm and mode for analysed clasts	81-87
3E	Granite environmental characters	135
4A	Summary of plate-tectonic models for the north margin of the Iapetus Ocean	153
4B	Sequence of events	173
5A	Ordovician time scales	183

LIST OF FIGURES

		Page
1/1	Regional location map	2
1/2	Stratigraphic scheme	7
1/3	Geological map of Girvan showing sample localities	10
1/4	Facies relations	16
2/1	Nicolaysen diagram	23
2/2	Rb-Sr isochrons for samples 889 & 399	39
2/3	" 198 &1197	40
2/4	" 196 & 192	41
2/5	" 188 & 187	42
2/6	" 186 & 176	43
2/7	Pb " 101	44
2/8	Concordia diagram for sample 101	45
2/9	Rb-Sr isochrons for samples Benan WR & 996	46
2/10	" 993 & 988	47
2/11	" 985 & 982	48
2/12	" 591 & 587	49
2/13	" 580 & 579	50
2/14	" 284 & Kilranny WR	51
2/15	Frequency vs. age and $^{87}Sr/^{86}Sr^{o}$ vs. age	52
3/1	H_2O & CO_2 graphical determination	65
3/2	Microprobe analysis points for samples 101 &187	89
3/3	Microprobe analysis points for samples 176 & 182	90
3/4	Feldspar analyses plot for samples 182 & 187	91
3/5	Feldspar analyses plot for sample 176	92
3/6	Feldspar analyses plot for sample 101	93
3/7	Thin section sketch for sample 101	96
3/8	Thin section sketch for sample 187	97
3/9	Amphibole analyses plot for sample 187	98
3/10	Granophyric intergrowth shown by sample 197	99
3/11	Granophyric/graphic texture from sample 284	100
3/12	Thin section sketch for xenolith 179	102
	Note regarding figures 3/13 to 3/38	107
3/13	Streckeisen modal granite classifiacation	108
3/14	An-Ab-Or diagram (Heitanen & Streckeisen)	109
3/15	An-Ab-Or diagram (O'Connor, Barker & Glikson)	110

		Page
3/16	ANOR granite classification	111
3/17	Ca-Na-K diagram	112
3/18	K_2O/Na_2O vs. (Fe+Mg+Mn)	113
3/19	R_1-R_2 major cation granite classification	114
3/20	Normative data plotted on a Streckeisen diagram	115
3/21	Modal data plotted on a Streckeisen diagram	116
3/22	AFM ternary plot	123
3/23	Frequency of DI and normative plagioclase	124
3/24	K_2O+Na_2O and CaO vs. SiO_2	125
3/25	Log $(CaO/(Na_2O+K_2O))$ vs. SiO_2	126
3/26	AA vs. SiO_2	127
3/27	Corundum or Diopside (Normative) vs. SiO_2	128
3/28	Mgo vs. P_2O_5	129
3/29	Q-Ab-Or (Winkler & Breibart)	130
3/30	An-Ab-Or (Winkler & Breibart)	131
3/31	Molecular Al/(Ca + Na) vs Zr	132
3/32	Rb vs. Sr (annotated with age data)	133
3/33	Rb vs. Zr and Rb vs. Nb	134
3/34	K/Rb vs. DI	139
3/35	Ternary Ba-Rb-Sr diagram	140
3/36	Log Ba vs Rb	141
3/37	Log Sr vs. Rb	142
3/38	Log Ce vs. Rb	143
4/1	Plate-tectonic models for the northern margin of the Iapetus Ocean	150- 152
4/2	Anatomy of a volcanic	156
4/3	Development of a residual fore-arc basin	157
4/4	Evolution of the Midland Valley during part of the Ordovician	168
4/5	Northward subduction related granites	176

ACKNOWLEDGEMENTS

The author is grateful for facilities provided at the Scottish Universities Research and Reactor Centre by Professor H. Wilson and in the Department of Geology, Glasgow University by Professor B.E. Leake. Technical assistance was provided by Dr. M.Aftalion. Mr. J.Hutchinson, Mr. J.Jocelyn, Mr. D.Skinner, Mr. W.Neilson and Mrs. A. MacDougall for which the author is indebted.

The computations used in the study benefitted greatly from discussions with, and advice from, Drs. C.M. Farrow and M.R.Giles and Messrs. J.H.Hutchinson and B.E. Keeling.

Various aspects of the study were aided by discussion and communication with numerous geologists including Profs. P.Brown and K.Condie and Drs. M.Aftalion, G.Brown, C.Carter, H.Gabrielse, A.Halliday, J.Legget, D. Powell, A.Saunders, D.Strong and J.Whitacker. Also the staffand research students in the Glasgow Geology Dept. contributed to much useful, and much not so useful !, discussion.

My thanks also go to Henry Williams for a vain attempt to interest me in the delights of graptolithology and for leaving me a few square feet in which to work, in a room otherwise paying homage to the plethora of muck and paperwork surrounding palaeontologists !.

Financial support from the Natural Environment Research Council was greatly appreciated.

Drs. B.J.Bluck and O. van Breemen, who supervised this study, are thanked for the substantial help and patience afforded to me.

Finally I would like to thank my parents and brother for their support and interest.

The material presented herein is the result of independent research by the author undertaken between September 1977 and December 1980 at the Scottish Universities Research and Reactor Centre (East Kilbride) and the Department of Geology, Glasgow University. Any published or unpublished results of other workers have been given full acknowledgement in the text.

Christopher D. Longman

SUMMARY

Granitic clasts of hitherto unknown affinity are found in Ordovician and Silurian conglomerates of S.W. Scotland. The host conglomerates form part of a sequence envisaged to have accumulated on the southern margin of a continent under which Iapetus Ocean crust was being consumed in a northward dipping subduction zone. Palaeocurrent and clast size evidence suggests a provenance to the immediate north. The age and chemistry of the granitic clasts was thus important in elucidating the type, extent and evolution of magmatic activity north of the subduction zone, the crust into which the plutons were emplaced and regional chemical trends in rocks of comparable age.

The age data obtained show a spread in age from c. 580 Ma to 450 Ma, and the chemistry indicates that the granitoids originated in a compressional calc-alkaline environment. This evidence coupled with other clast types present suggests the existence of an island arc founded on continental crust in the region now occupied by the Midland Valley during the late Precambrian to Ordovician. Both to the north and south of this arc there is evidence, from the Ballantrae complex and the Highland Border series, of marginal basin oceanic crust having existed. This leads to the proposition of a new model for the evolution of the southern Caledonides involving volcanic/island arc and marginal basin development above a northward dipping subduction zone. The closure of marginal basins, prior to final Iapetus Ocean closure, results in arc-continent collisions manifest as tectonic effects in the Southern Highlands.

Magmatism in the volcanic arc may be correlated with progressively younger events to the north by this model through the effects of subduction enhanced melting at increasing depths.

The isotopic ages for the clasts also provide additional data points for the Lower Palaeozoic time scale due to the proximity of radiometric and stratigraphic ages, and show broad agreement with pre-existing Rb-Sr and K-Ar time scales.

1 INTRODUCTION

1.1 Prologue

Since the time of Lapworth the Ordovician and Silurian rocks of the Girvan district (S.W. Scotland) have played key roles in the understanding of the stratigraphical evolution of southern Scotland. More recently, beginning with the challenging papers of Dewey (1969 & 1971), workers have attempted to view the Girvan succession as a fundamental link in ascertaining the tectonic evolution of the Midland Valley and the rest of the southern Caledonides of Scotland.

Williams (1962) produced a detailed map of the Caradocian sequence at Girvan in which he noted the importance of conglomerate horizons. These conglomerate wedges contain a variety of clasts, many of which come from the underlying Ballantrae complex. Some detritus, however, is not of this provenance, the most notable exception being granitic material of hitherto unknown affinity. The interest in these granitic clasts is that they are derived from the north and that they have been suggested to represent the disintegration of a magmatic arc. This proposal has been made without any attempt to establish the age or chemistry of these granites and as such it is based on peripheral evidence.

It is with this in mind that the granitic detritus in the Lower Palaeozoic succession of S.W. Scotland was investigated. Samples have been collected from the Girvan area where Llanvirn to Caradoc and Llandovery conglomerates are exposed and from the Rhinns of Galloway where the Llanvirn/Landeilo is represented (Fig. 1/1).

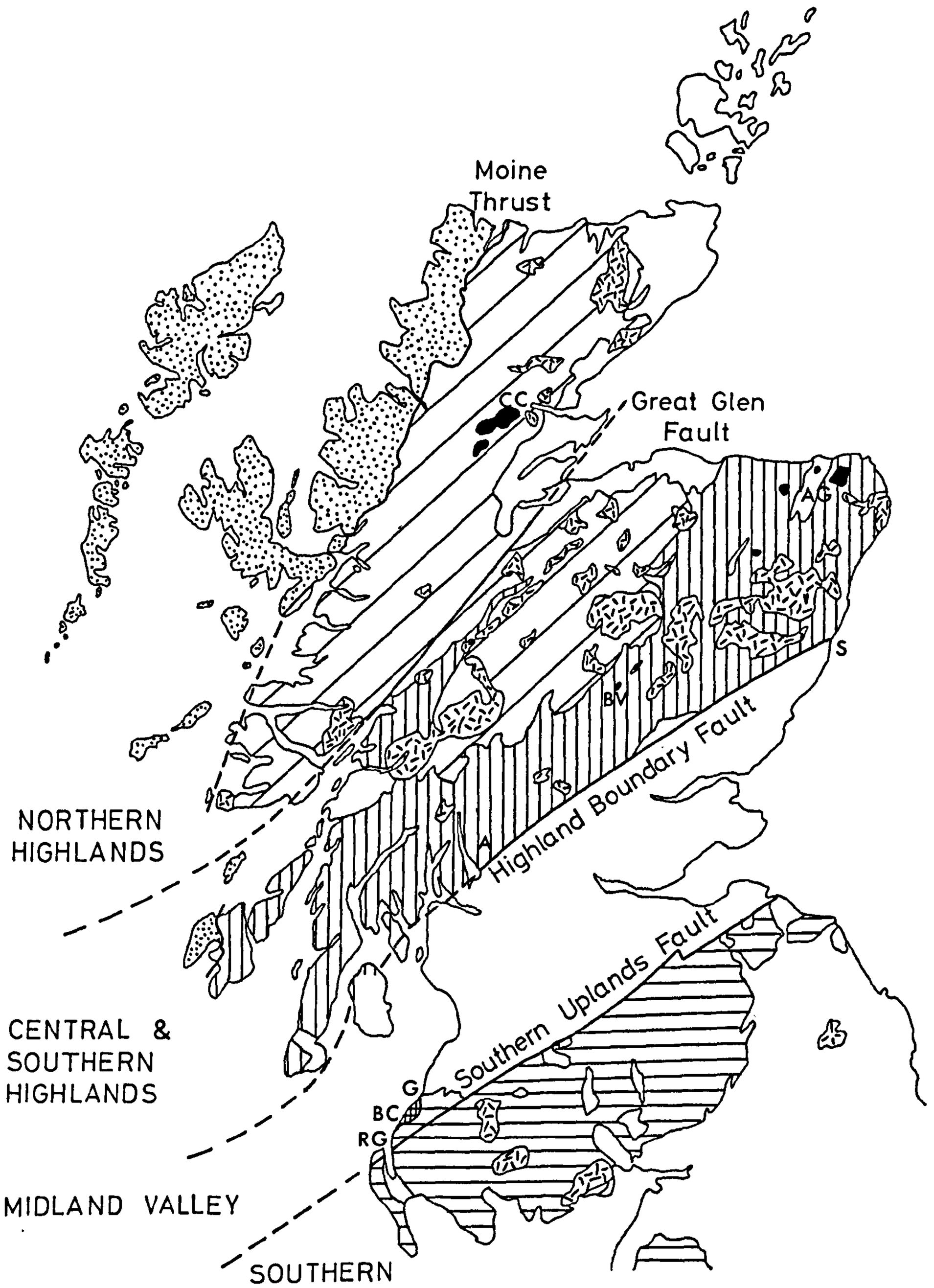

Fig. 1/1 Regional location map.

1.2 Previous research and project development

The previous research involving the succession presently under investigation has had a varying emphasis and a brief outline will be presented here. The very early work paled into insignificance with the classic publications of Lapworth (1882) and Peach & Horne (1899) which were mainly concerned with the stratigraphic succession and field relations. Henderson (1935) and Kuenen (1953 & 1956) investigated the sedimentology in an attempt to decipher the depositional environment. This was followed by the major work of Williams (1962) on the stratigraphy, palaeogeography and palaeontology of the area. This paper was a key publication regarding the Girvan area as it established the stratigraphic relations and, as it turned out, more importantly indicated that the fauna (mainly brachioppda) had an American affinity rather than a similarity to the rest of the U.K.. This feature was somewhat of a mystery at the time. The next contribution was that of Hubert (1969) and was concerned with the sedimentology and palaeoenvironment. With regard to the Rhinns of Galloway many of these works refer to that sequence as well but the major work for the stratigraphy and structure of that area is Kelling (1961).

The development of the sea floor spreading concept in the late 1960's provided a new frame of reference for the Girvan sediments to be viewed in. Wilson (1966) envisaged a proto-Atlantic ocean separating Laurasia from the European continent. This suddenly made the faunal provinces of Williams (1962) more understandable and the first plate-tectonic model to explain the British Caledonides appeared (Dewey 1969). Through much of the 1970's the main emphasis was on the development of various models for the Caledonides (e.g. Fitton & Hughes 1970; Dewey 1971; Jeans 1973; Gunn 1973; Church & Gayer 1973; Lambert & McKerrow 1976; Phillips et al. 1976; Wright 1976 & 1977; McKerrow et al. 1977) with additional refinement of the statigraphic ages (e.g. Bergstom 1971; Ingham 1979). A bit of variation was provided by Harland & Gayer (1972)

who produced the mythological name for the proto-Atlantic, the father of Atlas (from whom the name Atlantic is derived) namely Iapetus. This name gained acceptance and most papers now use the term 'Iapetus Ocean' in preference to 'proto-Atlantic'.

The plate-tectonic models for the Caledonides also threw new light on the Girvan sediments. The sequence overlies the Ballantrae complex, itself re-defined as an ophiolite (Dewey 1969), and has many characters typical of fore-arc basins situated on the landward side of subduction zones. This clarified several points but also created more unknowns, one of which was the role of the Midland Valley during plate closure. All the sedimentological work indicated that the provenance for the conglomerates was to the north and the size of the clasts (up to 80 cm in longest dimension) mitigates against a long transport distance. Consequently the source of the conglomerates is the area now occupied by the Midland Valley and the clast type must therefore indicate the nature of the Midland Valley during the Iapetus closure. Much of the detritus indicates the exposure of the Ballantrae Complex but other clasts include a granitic suite which could not be matched to any known Scottish plutons. Thus this project arose to determine the age and chemistry of the granite detritus in order to explicate the evolution of the Midland Valley.

1.3 Stratigraphy

The stratigraphy of the Girvan area has long been of interest. The main 19th century works were those of Lapworth (1882) and Peach & Horne (1899) which both provided much the same stratigraphic succession. After that little major stratigraphic work was done until Williams (1962) published the classic memoir on the Barr and Lower Ardmillan Series (Caradoc) of the Girvan district. This covers all the Girvan conglomerate horizons sampled except the Silurian Craigskelly unit, and it is taken as the base work defining their stratigraphic relationship. The mainstay of this system was the diverse brachiopod fauna present in many horizons which enabled both local and regional, mostly with North American sections, correlation. This was then combined with graptolite data (Ingham & Wright 1970; Dewey et al. 1970; Toghill 1970) and conodont information (Lamont & Lindstrom 1957) to provide the stratigraphic position of the Girvan succession as published in Williams et al. (1972).

Bergstrom (1971) used further conodont evidence in comparison with their Swedish counterparts, to amend the position of the Llanvirn/Llandeilo boundary. Ingham (1979) then used the graptolite fauna, and in conjunction with Tripp (1980) the trilobite fauna to modify the position of the Llandeilo series.

The Rhinns of Galloway is generally outside the scope of the above works but was the subject of detailed investigation by Kelling (1961) who assigned the Corsewall conglomerate to the lower Glenkiln. At that time this was equated to the Llandeilo/Caradoc but is now put at the Nemagraptus gracilis zone of Llandeilo age (S.H.Williams pers. comm. 1980). It should also be mentioned that the similarity between the Corsewall conglomerate, the Glenn App conglomerate (an horizon exposed geographically between the Rhinns of Galloway and Girvan) and the Benan conglomerate suggest that they may be lateral equivalents (Walton 1963).

The other horizon sampled,the Craigskelly conglomerate, lies unconformably on Ordovician sediments and has been placed as basal Silurian (Llandovery) by all

authors e.g. Lapworth (1882) and Cocks & Toghill (1973).

Thus the stratigraphic scheme used in this study is based on the correlations of Williams et al. (1972) and the subsequent modifications shown in Tripp (1980) and is portrayed in Fig. 1/2 and also in Table 5A.

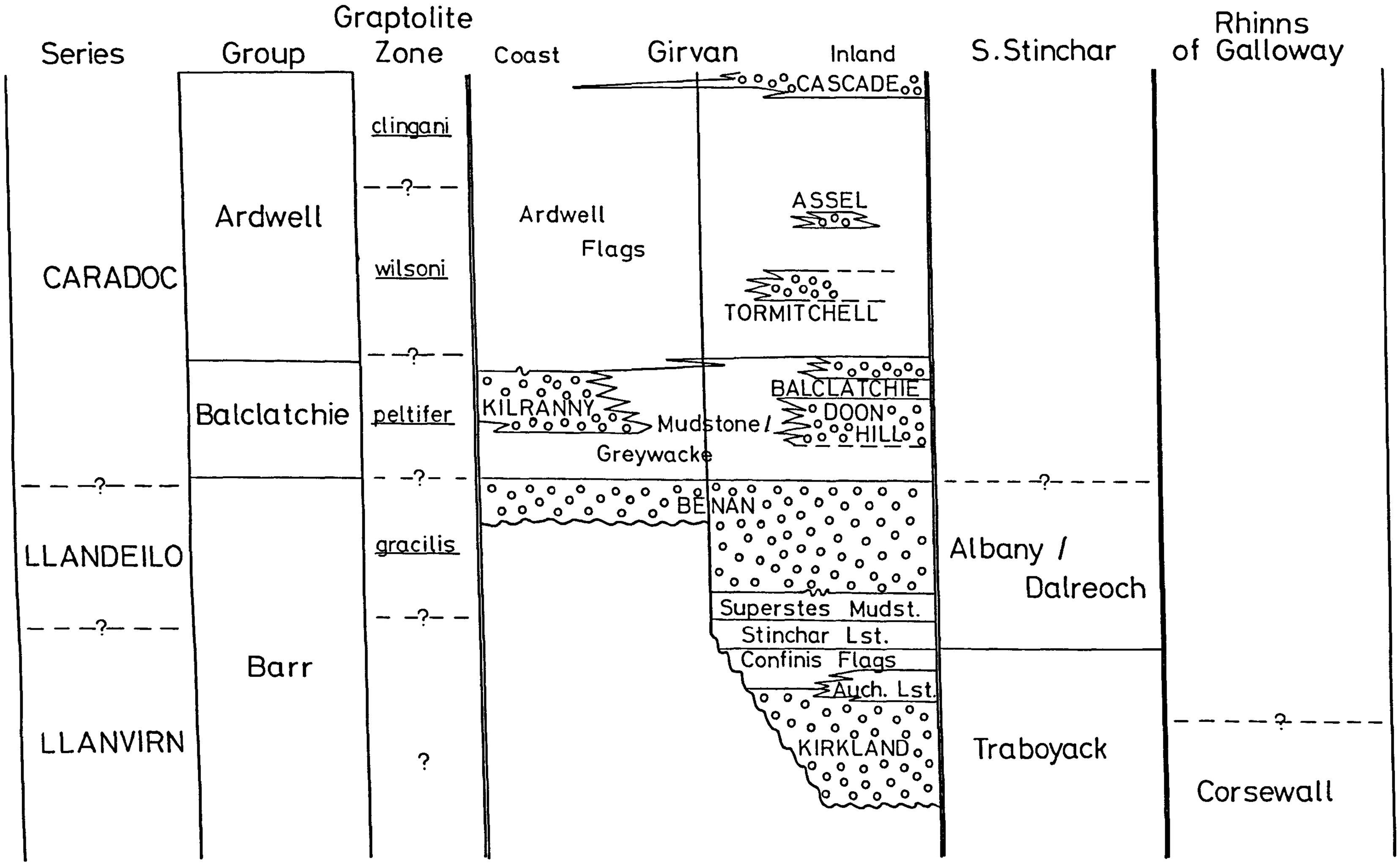

Fig. 1/2 Stratigraphic scheme after Williams et al. (1972) and Tripp (1980)

1.4 Conglomerate composition and sampling

The Lower Palaeozoic conglomerate horizons are polymict though have much in common. The northwesterly transgression over the Ballantrae complex indicates that it was exposed during Upper Llanvirn to Caradoc times. As a consequence of this there is an almost ubiquitous presence of detritus derived from the Ballantrae Complex in all conglomeratic units. This takes the form of serpentinite, spilite, dolerite, gabbro etc. from the volcanic and 'sheeted dyke' groups, and cherts and shale from the intercalated sediments. In addition to these other typical clasts include acid intrusives and extrusives, intra-formational sediments, vein quartz and quartzite. Each horizons' complement of major clasts is summarized in Table 1A.

It is the granitic clasts that are of interest here, although they have only been mentioned briefly by ealier workers. Williams (1962) noted "red granite of unknown provenance" and Hubert (1969) referred to "fragments of microperthite-bearing granite (which) cannot be matched locally, but may be derived from oldest Caledonian intrusives".

All the major rudaceous units in the succession from the Traboyack series to the Craigskelly conglomerate were examined by the author between 1977 and 1980. Granitic detritus was not found at all horizons. The Traboyack series has few rudaceous units and they are lacking in large granite clasts. In the greywackes, however, there are abundant fragments of potassium feldspar up to ~1 cm in diameter which are most likely to have a plutonic origin. The Balclatchie conglomerate yielded no acid plutonic clasts and although the Cascade and Assel horizons had small fragments of granitic material no specimens large enough for isotopic or chemical analysis were located. Small clasts were also present in the lensoid grits/conglomerates of the Lower Whitehouse group but again none were suitable for analysis.

The remaining conglomerates did however reveal

large (>10 cm in longest dimension) granitic clasts. The locations from which samples were collected are indicated in Fig. 1/3 and those localities yielding samples for analysis are as follows :-

Craigskelly conglomerate : Craigskelly rock and the Haven, foreshore south of Girvan.

Tormitchell conglomerate : N.E. of Pinmery Farm (near Tormitchell)

Kilranny conglomerate : Kennedy's Pass south of Girvan.

Benan conglomerate : Byne Hill.

Corsewall conglomerate : Corsewall lighthouse, Rhinns of Galloway.

Kirkland conglomerate : Benan burn, Stinchar valley.

(See section 1.7 for details of sample collection and preparation.)

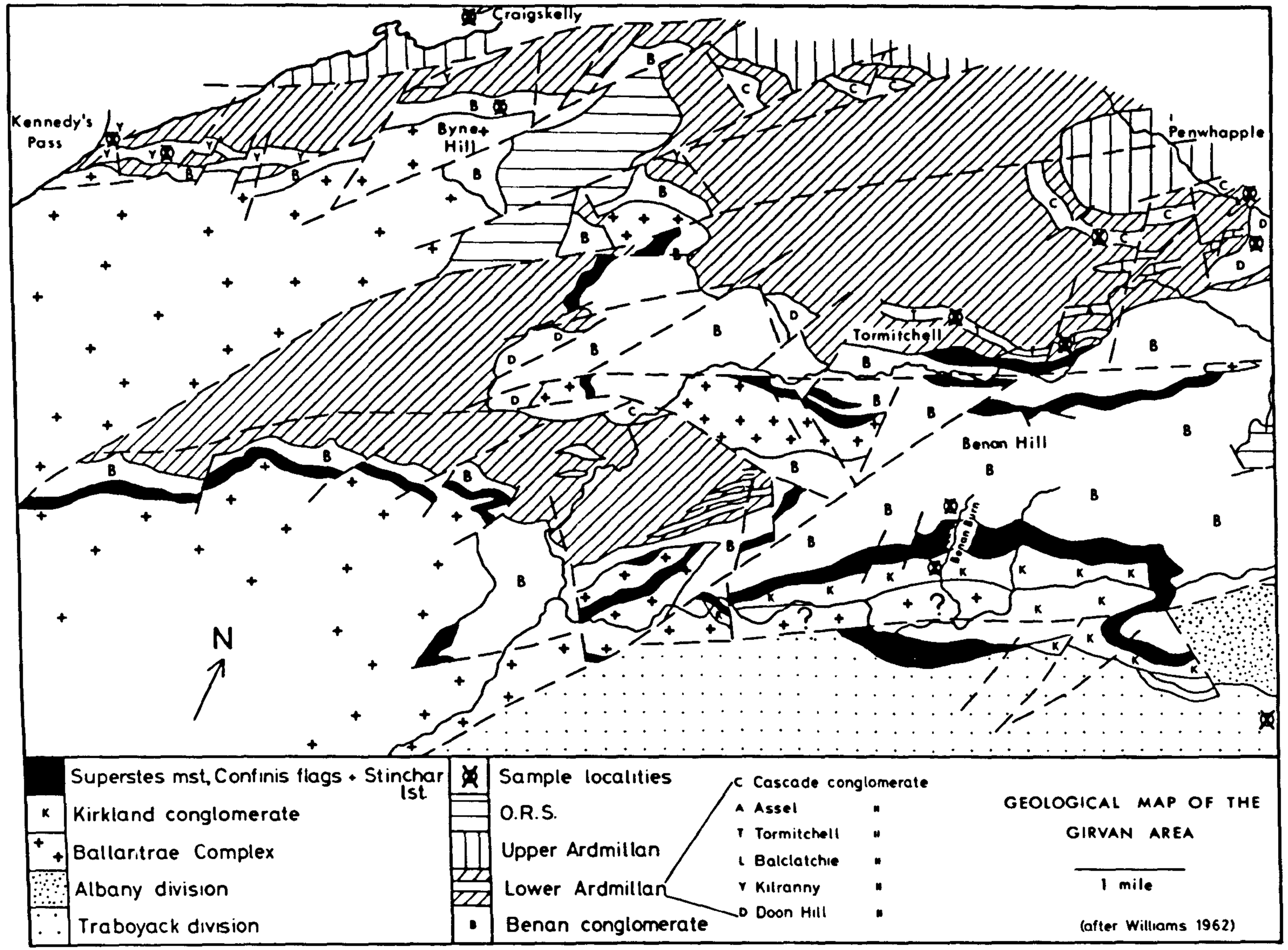

Fig. 1/3 Sample location map

	Vein quartz	Spilite	Serpentinite	Quartzite	Porphyry	Metamorphics	Intraformational sediments	Granite	Gabbro	Dolerite	Chert	Andesite
Craigskelly	X	X			X	X	X	X		X	X	
Cascade		X					X	x	X	X		
Assel	X	X						x	X	X		
Tormitchell		X						X		X		
Kilranny	X	X			X	X	X	X	X	X		
Doon Hill	X	X			X	X		X	X	X		
Balclatchie	X	X			X	X		X	X	X		
Benan	X	X			X	X	X	X	X	X		
Kirkland	X	X			X	X		X	X	X		
Corsewall	X	X			X	X	X	X	X	X		
Traboyack	X	X			X	X		x*	X	X		
Series												

* No granitic clasts but abundant potassium feldspar fragments.

Table 1A Major constituents of individual conglomerates

1.5 Depositional environment

Detailed work on the environment of deposition was sparse prior to that of Williams (1962). Henderson (1935) noted that much of the Barr and Lower Ardmillan sequence was shallow water platform sedimentation but that to account for the brecciation of the Auchensoul and Stinchar limestones a process such as minor sea-quakes may be required. Kuenen (1953 & 1956) made a brief foray into the area and decided that the Ardwell group had a deep water affinity and a northwesterly source. These two studies indicate that the main problem regarding the Girvan succession is that there is a juxtaposition of deep and shallow water sediments, and a general dominance of greywackes, often taken to indicate deep water, in conjunction with a broad transgression of the sequence onto the eroded Ballantrae Complex.

Williams (1962) found that the Tappins Group to the south of the Stinchar valley contained much graded greywacke with thin black shales of presumed anoxic nature. Thus this represents a basin with periodic influx of detritus but with tranquil periods enabling a return to euxinic conditions. The base of the Barr series to the north of the Stinchar appears to represent a change to a fault bounded basin with conglomerates accumulating against the fault scarps, but below wave base to account for the lack of sorting, and mudstones and limestones on the platform during periods of fault quiescence. This, however, makes the accumulation of sediment above the faults a problem. A possibility may be one of limestone development on the shelf with gravels being channeled past this shelf to be deposited in the basin. With the onset of the Benan conglomerate the environment changed with the platform no longer stable and the faults becoming more active causing submarine slides of material accumulated at the head of the fault scarps. After the Benan conglomerate the sequence becomes interbedded greywackes and conglomerates reflecting some equilibration of the basin but still with periodic fault activity producing mass flow.

The Tappins Group sediments exhibit flute casts

and current bedding indicating an easterly source but in the Barr and Lower Ardmillan series the sedimentary structures and lateral thickness variations indicate a notherly source, but with components varying from northeast to northwest (Williams 1962).

Hubert (1969) further investigated the sediments at Girvan and the Rhinns of Galloway but came to slightly different conclusions. He regarded the Kirkland and Benan conglomerates as current laid deposits, relying somewhat on evidence provided by a cross-bedded sandstone found near the top of the Benan conglomerate. The presence of imbrication, thin laminated sandstone and some cross-bedding caused Hubert to dispute the slide conglomerate origin postulated for the Kilranny conglomerate by Kuenen (1953). Instead he favoured deposition in 'relatively shallow water, perhaps nearshore, by strong bottom currents of widely fluctuating velocity'. Hubert's palaeocurrent data agree with a northerly source, including the pebble imbrication, for the coarser units of the Barr, Balclatchie and Ardwell groups.

Ingham (1978) produced a synthesis of the depositional environments agreeing with the broad picture of Williams (1962) and including some of the modifications proposed by Hubert (1969). Ingham also used the intra-formational folds within the Ardwell group (see 1.6) to additionally establish a palaeoslope from the northwest in agreement with previous results. The Silurian Craigskelly conglomerate was also referred to by Ingham and is thought to represent down slope channeling from the north.

The Corsewall conglomerate was interpret ed by Pettijohn (1943) and Walton (1956) as being similar to piedmont deposits on a broad floodplain with occasional marine incursions. This appears an unlikely interpretation due to the absence of features such as lamination and mud horizons. Kelling (1961) and Walton (1963) favoured a nearshore non-turbidite facies. Hubert (1969) again considered the rudaceous Corsewall units to represent deposition from strong bottom currents in relatively shallow water.

Kelling and Holroyd (1978) looked at the Craigskelly and Corsewall conglomerates in the light of submarine canyon and fan deposits. They produced a broad division of basin margin canyon-fan rudites into channeled and non-channeled varieties with subdivisions into organised and disorganised forms. Within this framework they classified the Corsewall conglomerate as a disorganised channeled deposit and this typical of proximal canyon-fan facies, and the Craigskelly (and Kilranny) conglomerates as non-channeled and organised, exhibiting imbrication and envisaged to represent distal facies.

Although no detailed sedimentological work was done as part of this study several observations are pertinent to the environment of deposition. The clasts, especially granitic, found in the Benan conglomerate are generally well rounded but frequently this unit is matrix supported. This implies a two stage development as straight slide deposit would produce poorly sorted, unrounded matrix supported clasts. Well rounded clasts imply a period of abrasion and/or transport. (Although in the instance of the granitic clasts it is worth bearing in mind that typical granite weathering may produce somewhat rounded boulders). The size of some of the granitic clasts (>80 cm in longest dimension) mitigates against long transport distances and reduces the possible environments in which to abrade the clasts. In the light of the previously postulated palaeoenvironment and the above factors it appears that the clasts underwent a fairly short transport to a coastal platform where a temporary residence time above the wave base enabled rounding of the clasts before fault movement caused mass flow into the basin producing slide conglomerates. The presence of occasional interbedded arkosic sandstones also suggests that between debris flows bottom currents may be active and they may also be responsible for some of the smaller lensoid rudites. All these features are indeed typical of many fault dominated basin and platform areas.

The Kilranny conglomerate exhibits well developed imbrication of larger clasts at some levels with other areas containing rounded boulders scattered through a greywacke

type matrix. As Hubert (1969) noted the imbrication obviously mitigates against a purely slide origin and the imbricated units are taken to represent deposition from tractional currents. The matrix supported units may, however, still indicate the effects of mass flow. The Corsewall conglomerate is seen to comprise rudaceous units again in a greywacke dominated succession and the presence of cross bedding in the latter suggests deposition from currents.

Thus the broad pattern of sedimentation is taken to be one of a platform and fault bounded basin. The platform was periodically stable producing shallow water muds and limestone, but repeated faulting produced slide conglomerates e.g. Kirkland and Benan horizons. Strong bottom currents appear important in the basin and dominate several other rudaceous units. This produces a pattern of major conglomerates and smaller lensoid rudites transgressing northwards over the Ballantrae Complex. This is summarized in Fig. 1/4, modified after Williams (1962) and Ingham (1979).

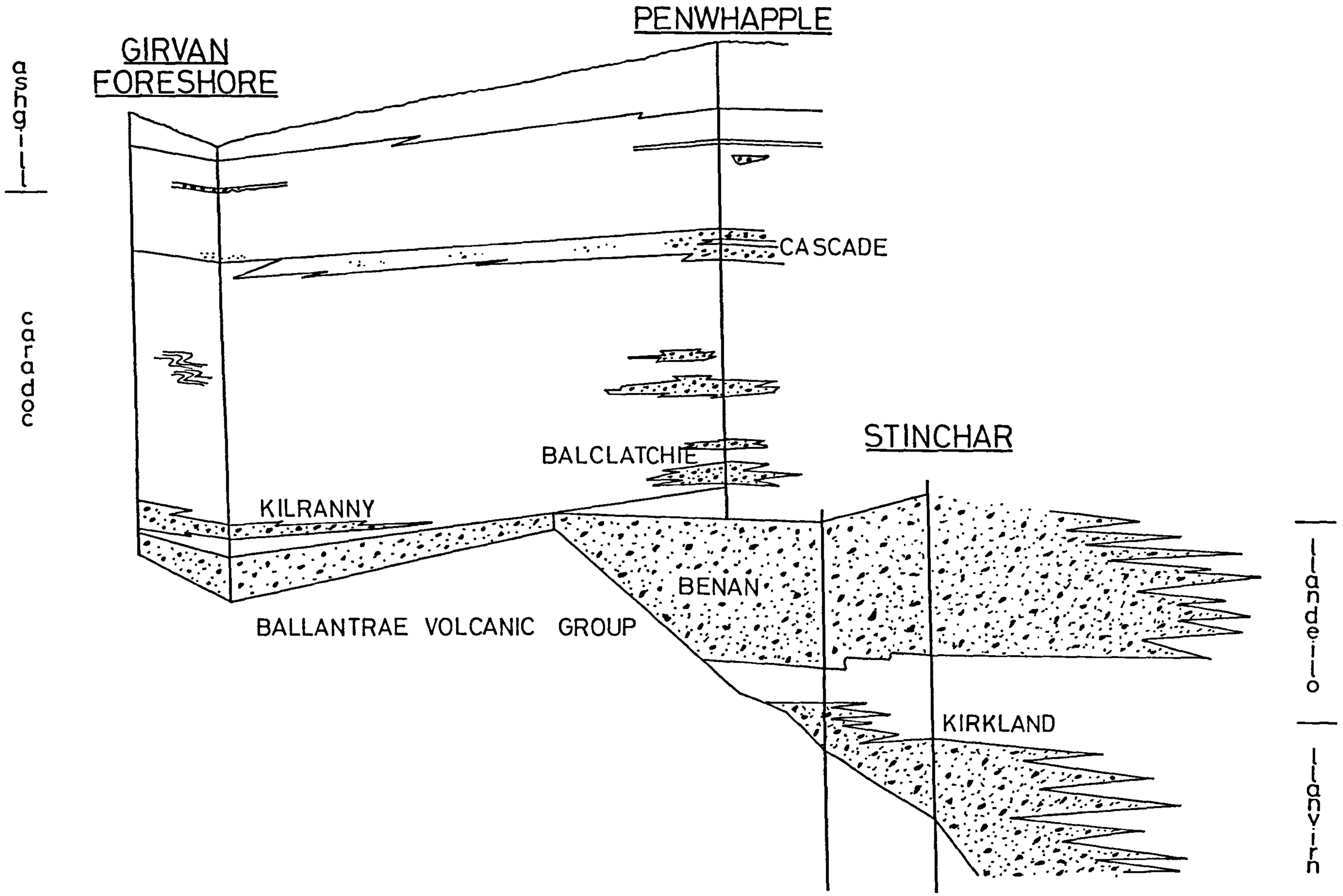

Fig. 1/4 Facies relations in the Girvan region (after Ingham 1979)

1.6 Tectonic setting

The Lower Palaeozoic of the Midland Valley forms part of the British Caledonides. The term Caledonian was first used by Suess (1906) to define a period of Lower Palaeozoic deformation and later extended to the term Caledonides covering rocks associated with this orogeny. Today this is taken to represent, in broad terms, the events from around 700 Ma to 400 Ma ago. Attempts have been made to subdivide the Caledonian orogenic sequence. Lambert & McKerrow (1976) differentiated between a Grampian Orogeny (confined to the northern margin of the Iapetus Ocean) comprising pre middle Ordovician events, and a Caledonian Orogeny covering episodes from late Ordovician to Lower Devonian. In this study the term Caledonides is used in the broad sense and both the Grampian and Caledonian orogeny will be referred to.

The Caledonides have been divided into the metamorphic and non-metamorphic portions. The rocks investigated in this work belong to the Midland Valley structural unit and have been variously classified, but the succession has been subjected to essentially no metamorphic effects and is best placed in the non-metmorphic zone e.g. Fettes (1980). Structural effects are, however, widespread and complicated but mainly evident as brittle deformation with some folding.

The major structural interpretation is that of Williams (1959). He deduced nine phases of deformation with thrusting and overfolding, wrench faulting and cross-folds of Caledonian age, oblique-slip faulting of Hercynian aspect and Tertiary tension joints. Little structural investigation has been done since but there is an element of doubt concerning some of the cross-folds. The well exposed folds on the Ardwell shore are stratigraphically constrained and show additional features such as sandstone mobility at fold axes. These tend to suggest a slump sheet syn-sedimentary cause (e.g. B.Bluck pers. comm. 1978) rather than a post consolidation tectonic effect.Opinion, however, is not unified.

Whichever way the folds are interpret ed the structural effects are unimportant in the context of this study. The outcrop patterns may be complicated but the effects on the conglomerates and their constituents are manifest only as minor calcite veining.

1.7 Sample collection and preparation

Analytical data are obviously only of value if they are representative of the rock being analysed. To this end several factors are considered important in the sample selection:-

1. Samples should be visually representative of the host.
2. Xenoliths, dykes, veins etc. should be avoided.
3. Weathered specimens should be excluded.

Where one is dealing with an exposed rock outcrop these guide lines are easily adhered to. In this study, however, the samples are clasts from conglomerates. This implies that weathering has taken place and also means that the specimens are of a finite size. The weathering is thought to have taken place during a short erosion/sedimentation period as the presently exposed conglomerates are not unduly weathered, and as such has not caused too much alteration (3.2.1). In addition to this many of the conglomerates exhibit veins (mainly calcite) cutting the matrix and clasts.

In selecting the clasts to be analysed only those greater than 10 cm in longest dimension were considered, and xenoliths and veins were avoided as far as possible, as were any unduly weathered specimens.

Once collected samples were washed and broken into chips of approximately 1 cm^3 and any excessively weathered, veined or xenolithic chips discarded. Further crushing in a tungsten steel jaw crusher was followed by grinding in a chalcedony Tema mill for about 90 seconds. The sample was then split into quarters and one fraction ground in a chalcedony ball mill to <250 mesh for X-ray fluorescence and isotopic analysis. Another fraction was washed, sieved to 210-175 µm (or occasionally 500-210 µm), washed in acetone and weight fractions obtained by using heavy liquid (Tetrabromoethane) separation. Another acetone wash was followed by magnetic separation and/or hand picking where necessary. The fractions so obtained were then stored in new glass bottles until analysed.

The one zircon separation involved crushing 25 Kg of a specimen to a fine grain size (so that single minerals

result) and collecting the heavy minerals by washing the sample over a 'Wiltly' jigging table. Washing in acetone was followed by heavy liquid (tetrabromoethane and methylene iodide) separation, another acetone wash, sieving and magnetic separation resulting in several size fractions of varying magnetic susceptiblity.

2 GEOCHRONOLOGY

Geochronological data presented herein comprise Rb-Sr whole rock/mineral isochrons and individual Rb-Sr mica ages for granitic detritus from six Lower Palaeozoic conglomerate horizons in S.W.Scotland, coupled with U-Pb zircon analyses for one sample. The isotope analysis was carried out at the Scottish Universities Research and Reactor Centre (S.U.R.R.C.) in East Kilbride. All Rb-Sr determinations were performed by the author and the chemistry and mass spectrometry for the U-Pb analyses was generously undertaken by Dr. M.Aftalion.

2.1 Analytical methods

2.1.1 Fundamentals of Rb-Sr geochronology

The Rb-Sr method of dating geological events is based on the β decay of ^{87}Rb to ^{87}Sr. The parent isotope, ^{87}Rb is one of two Rb isotopes, the others being non-radioactive ^{85}Rb. The daughter product, ^{87}Sr, is one of four stable natural Sr isotopes (88, 87, 86 + 84) but the only one produced by decay of another element. The radioactive decay of ^{87}Rb to ^{87}Sr takes place at a rate which is unaffected by geological processes and consequently measuring the current isotopic composition of rocks and minerals and applying the rate of decay produces the age of the specimen.

This is obviously an idealised case and in practise more problems are apparent. The decay constant used by geochronologists varied by 5% until the I.U.G.S. Subcommission on Geochronology chose an appropriate value to try and unify age calculations. This figure was reported by Steiger and Jäger (1977), namely a half-life of $48.8 \times 10^{9}\ y^{-1}$ corresponding to a decay constant of $\lambda^{87}Rb = 1.42 \times 10^{-11}\ y^{-1}$. Within this framework all Sr isotopic ratios are normalised to $^{86}Sr/^{88}Sr = 0.1194$. These figures are used in all calculations presented in this study.

In an ideal system a crystallizing mineral would only incorporate the parent isotope. This is obviously never the case as the decay is a continuous process so pre-existing daughter isotopes will also be incorporated in the mineral. This initial contribution of ^{87}Sr is measured relative to non-radiogenic ^{86}Sr, expressed as $^{87}Sr/^{86}Sr^{o}$, and must be accounted for before the age can be determined. This is evident from the basic age equation which is :-

$$t = \frac{1}{\lambda} \log_e \left(1 + \frac{^{87}Sr}{^{87}Rb} \text{ (radiogenic)} \right)$$

which can be re-expressed as

$$t = \frac{1}{\lambda} \log_e \left(1 + \frac{^{87}Sr/^{86}Sr^{p} - ^{87}Sr/^{86}Sr^{o}}{^{87}Rb/^{86}Sr} \right)$$

where t = age, λ = decay constant, $^{87}Sr/^{86}Sr^{p}$ = present ratio and $^{87}Sr/^{86}Sr^{o}$ = initial ratio. In rocks and minerals with a high Rb content the measured $^{87}Sr/^{86}Sr^{p}$ may be large when compared to the uncertainty in estimating the $^{87}Sr/^{86}Sr^{o}$ value. In this case an age determination may be made from a single analysis.

Another approach to this problem is the isochron method of Nicolaysen (1961). He reasoned that a suite of cogenetic minerals in a rock will all evolve from the same $^{87}Sr/^{86}Sr^{o}$ value, and will lie along a line, with the distance along the line proportional to their Rb content (Fig. 2/1).In this instance the basic decay equation can be further rearranged to give:-

$$^{87}Sr/^{86}Sr^{p} = (e^{\lambda t} - 1)\ ^{87}Rb/^{86}Sr + ^{87}Sr/^{86}Sr^{o}$$

which is in the form $y = mx + c$, the equation for a straight line. Thus the best fit line through the measured points will yield the age (proportional to slope) and $^{87}Sr/^{86}Sr^{o}$ (the point where the line intersects $^{87}Rb/^{86}Sr = 0$).

In this study the isochron procedure is used extensively as although the potassium feldspars are rich in

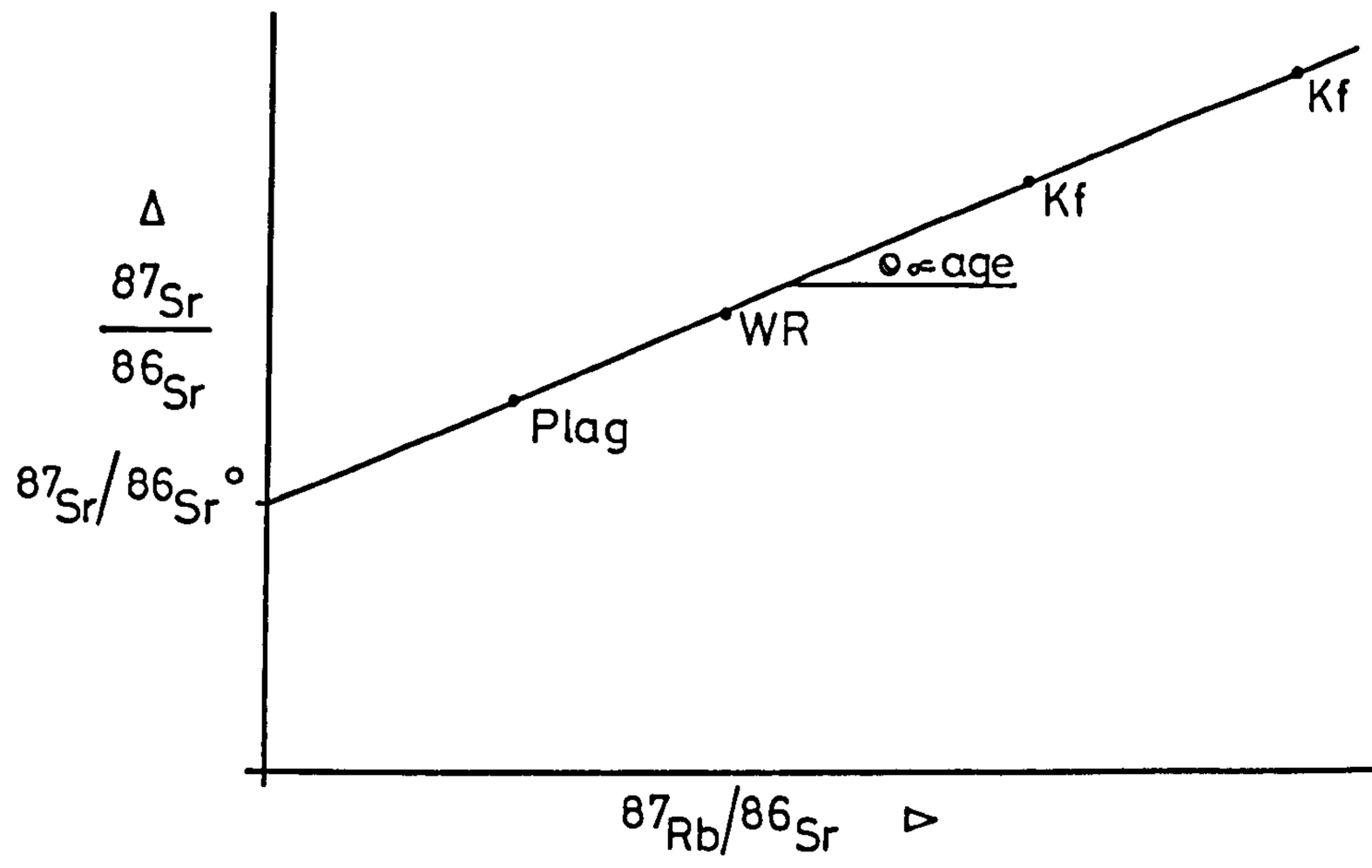

Fig. 2/1 Nicolaysen diagram

Rb the whole rock Rb/Sr ratios are low and there is no independent method of estimating the $^{87}Sr/^{86}Sr^{o}$ value.

2.1.2 Isotope dilution

Samples are processed in batches of up to ten selected from the preliminary X-ray fluorescence Rb and Sr analyses. The samples, either whole rock powders or mineral separates, are weighed (to 0.01 mg) directly into Teflon beakers. Problems with static charges on the beakers are frequently encountered, particularly with micaceous specimens, but reduced by using an anti-static gûn. Sample weights are typically around 0.2 g but vary depending on the Rb and Sr concentrations.

Beakers are then spiked by direct addition of enriched ^{87}Rb and ^{84}Sr solutions. The spikes (solutions of known isotopic composition) used are the United States National Bureau of Standards Sr spike (NBS 988) containing 99.783 % ^{84}Sr and United Kingdom Atomic Energy Authority Rb spike containing 99.2 % ^{87}Rb. The spikes are calibrated for concentration by reference to NBS RbCl and $SrCO_3$

stochiometric salts. The spiking is adjusted to produce analytical ratios of around $^{87}Rb/^{85}Sr = 1.2$ and $^{84}Sr/^{86}Sr = 1$.

Dissolution is achieved by adding 20 ml of reagent grade HF, covering with a Teflon lid, and heating overnight. Evaporation to dryness follows through removal of the lid and heating on a thermostatically controlled hot plate. At this stage care is taken to avoid any spitting or boiling of the sample and as an additional precaution guards of aluminium foil were placed around the beakers. The residue is re-dissolved in Analar HNO_3 [1] and again evaporated. A few drops of 6N HCl are added, again reduced to dryness and then finally the residue is taken up in a few millilitres of 2.5N HCl.

Separation of Rb and Sr is achieved by eluting the sample through a cation exchange col umn containing Biorad AG 50W-X8 (200-400 mesh) resin. The position of the elution peaks for Rb and Sr is determined using flame photometry and periodically checked by passing dissolved RbCl and $SrCO_3$ through the columns and visually inspecting the resultant solutions. The Rb and Sr 'cuts' are collected in Teflon beakers, evaporated , wrapped in thin plastic film and may then be stored for a short time until the mass spectrometry is undertaken.

During the isotope dilution great care is taken to avoid any contamination and all laboratory ware is scrupulously cleaned between samples. Teflon beakers are scrubbed in tap water, rinsed in acetone to remove the identification marks and rinsed in H_2O^*. Heating in 50% Analar HNO_3 is followed by heating in 50% Analar HCl, both for twelve hours. The beakers are then heated and rinsed in H_2O^*, dried in an oven and wrapped in plastic film for storage. The beakers used to collect the eluted Rb cut are those used for the dissolution but which have been cleaned through the addition of 6N HCl (30-40 ml), heating and rinsing in H_2O^*.

1. Note : all acids used in the isotope dilution (except HF which is "from the bottle" Merck Suprapure grade) are twice distilled from Analar grade and where necessary diluted by addition of twice pyrex distilled H_2O (referred to as H_2O^*).

Ion exchange columns are cleaned by passing 40 ml of 6N HCl through, blowing out the resin (either into the bowl of the column or into a small beaker) and rinsing in 20 ml H_2O^*, adding 80 ml of 6N HCl and finally re-equilibrating the column with the addition of 100 ml of 2.5N HCl. The dissolved sample is placed in the ion exchange column by means of a macropipette with plastic tips. In the early part of this work these tips were reused after heating in dilute 6N HCl, rinsing in H_2O^* and drying, but in the later stages disposable tips were utilised.

2.1.3 Mass spectrometry

Rubidium and Strontium are loaded onto thin tantalum filaments for analysis. Sr is taken up in a small quantity of 10% H_3PO_4 and loaded as a phosphate by placing a drop in the middle of a single filament bead and evaporating to dryness by means of an electric current. Rb is dissolved in H_2O^* and loaded as a chloride on one side of a triple filament bead [2].

During the course of this study the machine used for the Rb-Sr isotopic measurements changed from an AEI MS12 to a Micromass MM30 mass spectrometer. It will thus be necessary to outline the design of both machines and the analytical procedures used thereon. In the isotopic data presented in section 2.2 samples with the first three digits being 101, 176, 186, 187, 194, 197 or 198 were analysed on the former machine the rest on the latter.

The AEI MS12 mass spectrometer has a 12" radius, 90^o sector and uses a Faraday Cup in conjunction with a

2. Note : The beads consist of tantalum strip spot welded between nickel posts and mounted in a refractory glass base. These beads are cleaned by removing the tantalum filament(s) boiling briefly in weak HCl, rinsing in H_2O^* and drying. Prior to reuse the beads are filamented and outgassed to avoid excessive volatilization of the filament(s) in the mass spectrometer.

Cary 401 vibrating reed electrometer (incorporating a 10^{-11} ohm resistor) linked to an on-line mini-computer (Data General). For both Rb and Sr analyses an initial zero is taken by averaging 10 values. The Sr peaks are measured in ascending order (84, 86, 87 and 88; but including 85 as a Rb monitor) by an automatic peak switching routine using two second count times. The peak sequence is measured 10 times and the mean 86/84, 88/86 and 87/86 ratios calculated and printed out with complimentary standard deviation, standard error and percentage error. Normally at least 10 'sets' of data are taken and the mean calculated, discarding those with excessive errors. The two Rb peaks, 85 and 87, are measured in similar fashion and typically three to five sets are averaged.

The Micromass MM30 mass spectrometer is a semi-automated machine with a 30 cm tube, VGCA2 collector amplifier and digital integrator (again incorporating a 10^{-11} ohm resistor) connected to an on-line Nova 3 mini-computer. Sr analysis involves measuring six peaks, as the zero is taken (at mass 84.7) within the data set rather than outside in order to compensate for any slight machine drift during the analytical cycle. The collecting order is normally 86, 87, 88, 84, 85, 84.7 chosen to protect the 85 peak on which Rb correction is made from the large 88 peak. Again the peak sequence is scanned ten times and the mean 87/86 ratio and error printed for each set. The number of sets taken varies with the precision required but is normally ten to fifteen. Three peaks are measured in the Rb analysis (87, 85, 89.5) as the zero is again determined during the run and as before typically three to five seta are averaged.

Several other factors need to be accounted for on both machines. The automatic peak switching routine is subject to the decay characteristics of the recording device. This decay can be measured and a correction factor applied using a digital representation of the decay curve. During Sr analysis there is a tendency for the light isotopes to volatilize more readily than the heavy ones. This fractionation effect can be nullified by recalculating

each set of data to be compatible with the first recorded 88/86 ratio. Fractionation may also occur during Rb analysis but with only two natural Rb isotopes a correction is not possible and so to minimise the effect the lowest possible running temperature is used.(This is also the reason for loading Rb onto one side of a triple filament assembly. Current may then be passed through the centre filament hence avoiding direct heating of the sample and any associated tendency to boil). Although Rb normally volatilizes before the Sr running temperature is reached some may still be present. This is why the 85 peak is measured during Sr runs to enable a correction for any minor Rb contamination. Peak centring is important to maintain consistent analyses and frequently needs checking during the run. On the AEI MS12 the centring was checked and adjusted manually but on the MM 30 a sub-programme in the computing routine maintains the centring on a pre-selected peak.

2.1.4 Analytical precision

Chemical procedures involved in the analyses are periodically checked by running a blank, containing only a small measured amount of the Rb and Sr spike solutions, through the complete process. Blanks of <10 ng are deemed acceptable and typically results in the laboratory are around 5 ng for both Rb and Sr. Consequently no blank corrections were made on any of the presented analyses.

Individual machine Sr analyses were measured to an accuracy of $\pm$ 0.0002 or better on the AEI MS12 and $\pm$ 0.0001 or better on the MM30 for the 87/86 ratio. These figures don't represent the capabilities of the machines but mark a level beyond which, in the nature of the study, it appeared unrealistic to proceed.

Internal laboratory precision is checked through periodic measurements of samples GGU 86035 and NBS 987. GGU 86035 is an whole rock sample from the top of a well defined eight point isochron from the Hviddal composite dyke, Gardar, S. Greenland (van Breemen & Upton 1972). NBS

987 is a prepared potassium feldspar sample. The isotopic results of repeated analyses on these samples and two whole rock samples duplicated within this study, are shown in Table 2A. The agreement between analyses is extremely good, and the variation of 23 analyses of GGU 86035 made over a period of eight years is $\pm$ 1% at the 2σ level.

These replicate analyses, in conjunction with those carried out by other workers in the laboratory, are used to estimate the reproducibility of isotopic determinations, and hence the errors assigned to the points used in isochron regression. The errors are in the parameters $^{87}Rb/^{86}Sr$ and $^{87}Sr/^{86}Sr$ and care is needed in calculating them, particularly as sample inhomogeneity, best seen in samples with a high Rb/Sr ratio, may lead to positive correlation of parameters.

Variations in replicate analyses are expressed as percentage errors e.g. Brooks et al. (1972), calculated as 100 (xmax - xmin)/ xmin. This is most frequently calculated from two values and the denominator is taken as xmin to give the slightly larger error figure rather than using the mean of the two. What one is trying to quantify is the variability of the measured values. A better method of determining this may be to use the precision, defined as "the closeness of agreement between measurements" (Topping 1965), also called the coefficient of variation and expressed as $100\sigma/\bar{x}$ (where σ = standard deviation and $\bar{x}$ = mean). In the case of two values this is not really applicable, simply halving the percentage error value, but if many replicate values were obtained the coefficient of variation would give a more realistic error expectation.

The errors on individual analyses and the replicate values enable the errors to be assigned to the isotopic data used in the isochron determination. The analyses from the AEI MS12 instrument are assigned errors, at the 1σ level, of 0.7% and 0.03% for $^{87}Rb/^{86}Sr$ and $^{87}Sr/^{86}Sr$ respectively. The data obtained from the MM30 are of higher quality and it is possible to use the individual errors from each Sr analysis. However, for the calculations in this study blanket errors are again used

Sample	Analyst	Date	Rb(ppm)	Sr(ppm)	$^{87}Rb/^{86}Sr$	$^{87}Sr/^{86}Sr$
988	CDL	27/07/79	83.0	208.1	1.15630	0.72525
988	CDL	05/10/79	82.4	207.4	1.15092	0.72538
284	CDL	04/08/79	82.9	115.5	2.07948	0.72100
284	CDL	06/09/79	82.6	114.8	2.07237	0.72099
86035	CDL	16/06/79	227.2	19.59	35.4311	1.28046
86035	CDL	"	186.8	16.13	35.3881	1.27977
86035	OvB	11/07/79	225.0	19.61	35.0730	1.28453
86035	CDL	23/07/79	225.5	19.67	35.0239	1.27989
86035	CDL	23/11/79	224.1	19.45	35.2047	1.28189
86035	AGM	26/11/79	226.1	19.68	35.1140	1.28456
86035	CDL	03/04/80	226.1	19.67	35.2310	1.27937
86035	OvB	15/04/80	227.1	19.60	35.4000	1.28171
86035	OvB	23/04/80	226.9	19.56	35.4410	1.28241

In addition to the above 35 analyses were performed by various analysts on the Sr standard NBS 987 (Potassium feldspar). The values obtained for $^{87}Sr/^{86}Sr$ varied between 0.71043 $\pm$6 and 0.71011 $\pm$ 4 with a mean of 0.71027 $\pm$ 1.

Table 2A Replicate analyses. The analysts are the author (CDL), Otto van Breemen (OvB) and Andrew McCormick (AGM).

and calculated as 0.5% for $^{87}Rb/^{86}Sr$ and 0.014% for $^{87}Sr/^{86}Sr$.

2.1.5 Data evaluation

The measured isotopic ratios are combined with the sample and spike weights and spike concentrations to reveal the Rb and Sr content and $^{87}Rb/^{86}Sr$ and $^{87}Sr/^{86}Sr$ values for the specimen. If these data are then used for direct age determination the error on the age is a function of the analytical precision of the measured isotopic ratios and the uncertainty in estimating $^{87}Sr/^{86}Sr^{o}$. In most cases in this study, however, the isochron method of Nicolaysen (1961) is used (see 2.1.1) with the errors on each point being those defined in the previous section.

The calculation of the best fit isochron line through the data points has been examined by many authors e.g. York (1966 & 1969), MacIntyre et al. (1966), Brooks et al. (1968), reviewed by Brooks et al. (1972) and further discussed by Titterington & Halliday (1979). All these methods utilize a least squares linear regression procedure giving the best fit slope and intercept value and produce essentially the same results for a particular data set. The main variations are in the way they handle the errors on each individual point. Most use percentage errors for both parameters ($^{87}Rb/^{86}Sr$ and $^{87}Sr/^{86}Sr$) but MacIntyre et al. (1966) treated the error on $^{87}Sr/^{86}Sr$ as fixed onvvalues between 0.72 and 2.80. York (1969) is the only calculation which takes into account any positive correlation between $^{87}Rb/^{86}Sr$ and $^{87}Sr/^{86}Sr$ by using the correlation coefficient between errors.

The laboratory precision provides a limit to the accuracy within which the isochron age can be determined. The scatter about the regression lineeshould be accounted for by the laboratory error and if this is not the case one may assume that a true isochron does not exist. In an attempt to quantify this, a parameter, the mean square of the weighted deviates (MSWD) was computed by MacIntyre et al. (1966) and an equivalent value the minimised weighted

sum of the squares of the residuals SUMS/N-2 [3] where N = the number of points, calculated by Brooks et al. (1972). If the points fit the line within the laboratory error limits SUMS should approximate to N-2, though this is only true for large numbers of data points. Therefore in isochrons with large sample populations a value of MSWD < 1 indicates a 'perfect fit' within experimental error and values of MSWD ≥ 1 show scatter outside laboratory error and hence imply some'geological scatter'.

The next problem is to set a nominal value for the MSWD to differentiate between geologically vaid isochrons and geologically invalid or dubious 'errorchrons'. Brooks et al. (1972) accounted for the average number of datapoints and replicate analyses and decided on MSWD ≤ 2.5 to deem an acceptable isochron. The figure 2.5 has come into general use as the cut off limit but care must be taken in comparing values from paper to paper. The Brooks et al. figure used MSWD = $(SUMS/(N-2))^{1/2}$ and some authors still use this equation e.g. Rundle (1979), thus in this case their figures must be squared before comparison with the MSWD values presented in this study.

Another minor problem is the dependence of the MSWD parameter on the laboratory error estimates. A consequence of this is that increasing error figures reduces the MSWD by allowing more analytical scatter about the line.

The isochron results presented here are achieved by utilisization of the York (1969) model with errors expressed at the 2σ level and the MSWD parameter calculated as SUMS/(N-2) (Tables 2C and 2D). The decay constant used in all calculations is $\lambda^{87}Rb = 1.42 \times 10^{-11} y^{-1}$ and previously published results have been recalculated using the above figure where necessary.

3. Note: Originally defined as $(SUMS/(N-2))^{1/2}$ but is in fact (SUMS/(N-2)).

2.1.6 U-Pb geochronology

As previously mentioned the U-Pb zircon analyses were performed on samples separated by the author by Dr. M. Aftalion at the Scottish Universities Research and Reactor Centre. Chemical techniques follow those of Krogh (1973) and the isotopic analyses were obtained using the Micromass MM30 mass spectrometer. The decay constants were taken as $\lambda^{235}U = 9.84850 \times 10^{-10} y^{-1}$ and $\lambda^{238}U = 1.55125 \times 10^{-10} y^{-1}$ (Steiger & jäger 1977). Corrections for common lead were made using the following parameters ; $^{206}Pb/^{204}Pb = 17.3$, $^{207}Pb/^{204}Pb = 15.5$ and $^{208}Pb/^{204}Pb = 37.1$.

The U-Pb data for the various zircon size and magnetic fractions (Table 2B) are interpret ed through a concordia diagram (Wetherill 1956) and compared with the apparent Pb-Pb ages obtained from each fraction.

Sample	Size (μm)	Pb (ppm)	U (ppm)	$^{207}Pb/^{206}Pb$ ($\times 10^{-2}$)	$^{207}Pb/^{235}U$ ($\times 10^{-2}$)	$^{206}Pb/^{238}U$ ($\times 10^{-2}$)	$^{207}Pb/^{206}Pb$ Ages (Ma)
688	-85+65 NM	104.6	1379.4	5.65930	56.3075	7.21563	476
689	-85+65 M1°	202.3	2694.1	5.64694	55.3200	7.10460	471
690	-65+53 M1°	195.3	2591.3	5.66405	55.5318	7.11026	478
707	-85+65 M3°	249.1	3423.7	5.66486	53.1698	6.80685	478
708	-65+53 M3°	228.7	3139.4	5.65071	53.1488	6.82121	472

Table 2B U-Pb sample data (after common lead correction) for zircon fractions separated from Benan conglomerate sample 101 and individual $^{207}Pb/^{206}Pb$ ages

2.2 Geochronological data

The following sections indicate the geochronological data obtained for the six conglomerate horizons investigated. In all cases a brief petrographic description of the analysed samples is presented in Appendix 1, and the isotope data used in the calculations are given in Table 2E.

2.2.1 Kirkland conglomerate

One deformed granitic sample typical of the Kirkland conglomerate, has been analysed. Specimen 889 has low Rb/Sr ratios but the five samples lie on a well defined isochron (MSWD = 0.83) yielding an age of 486 $\pm$ 29 Ma and $^{87}Sr/^{86}Sr^{o}$ of 0.7034 $\pm$ 4 (Fig. 2/2).

2.2.2 Benan conglomerate

The Benan conglomerate has the most prolific selection of granitic clasts and accordingly nine samples have been analysed. The clasts range in composition from tonalites through granite to granite rich in alkalies (see 3.3). These isotopic determinations were made on two different machines and consequently the parameters used in the isochron calculation vary (see 2.1.4). The results are shown in Figs. 2/3 to 2/9 and demonstrate a spread in ages from 559 $\pm$ 20 to 466 $\pm$ 13 Ma and in $^{87}Sr/^{86}Sr^{o}$ from 0.7051 $\pm$ 2 to 0.7126 $\pm$ 6. All the isochrons have low or very low MSWD values except sample 198 which although having a reasonable spread of Rb/Sr ratios shows a marked scatter about the best fit line.

Sample 101 has been investigated most thoroughly with 10 Rb/Sr determinations. This being a perthite bearing sample two different size fractions were separated and investigated. The coarse fraction 500-210 microns (µm) gives an age of 463 $\pm$ 4 Ma and the fine, 210-175 µm, 470 $\pm$ 2 Ma. Although these two figures don't quite overlap they are in close agreement and as the coarse fraction has

a limited spread of Rb/Sr ratios and gives the younger age, no significant variation in age proportional to sample size is thought to occur. In consequence a combined nine point isochron was calculated providing an age of 467 $\pm$ 3 Ma (Fig. 2/7). Muscovite has also been separated from 101 and an analysis gives an individual age of 483 $\pm$ 2 Ma. This figure is significantly older than the mineral isochron and, in view of petrographic considerations, not thought to be real. The cause of this figure is thought to be spiking inaccuracies as a function of the huge $^{87}Rb/^{86}Sr$ ratio of 1084.75.

In addition to the Rb-Sr determinations on sample 101 there are the five U-Pb analyses on various zircon size fractions. These results (Fig. 2/8 and Table 2B) show a concordia with an upper intercept of 475 $^{+17}_{-9}$Ma and a lower intercept of -1 $^{+121}_{-123}$ Ma, and amean Pb-Pb age of 475 $\pm$ 3 Ma. These figures obviously agree well and indicate crystallization at 475 Ma, no lead loss since then and no evidence of an inherited zircon component. The figures are marginally older than the Rb-Sr value which being based on whole rock and feldspar points should be representative of emplacement. This suggests that there might possibly have been minor pulling down of the Rb-Sr ages due to subsolidus feldspar exsolution or weathering. However, the group of ages around 470 Ma (101, 186, 187 and 197) are thought to represent a real magmatic event and any possible minor reduction in Rb-Sr ages is insignificant in the context of this study.

In consideration of the closeness of the ages for samples 101, 186, 187 and 197 they were plotted along with 194 (a petrographically similar clast) and produced an age of 459 $\pm$ 10 Ma (Fig. 2/9). Not much reliance can be placed on this value but it is close to the isochron ages for individual clasts and may be seen to be younger through the effects of weathering on a whole rock scale in comparison to the unaltered potassium feldspars used in the mineral isochrons.

2.2.3 Kilranny conglomerate

The Kilranny conglomerate shows fairly limited variation in the type of granitic clasts it contains, particularly at the acid end of the spectrum. This is borne out by the fact that isotopic analyses from three separate clasts (284, 286 and 299) plot on a statistical straight line of age 447 $\pm$ 5 Ma (Fig. 2/14). Due to this only one clast, 284, was subjected to individual mineral analysis, with the resultant four point isochron yielding an age of 470 $\pm$ 6 Ma. This figure is regarded as the 'true' age and the composite whole rock isochron value as anomalously low for the same reasons as cited for the Benan composite example.

2.2.4 Tormitchell conglomerate

The Tormitchell conglomerate is a sequence comprising grits, siltstones and conglomerates. The rudaceous units contain few boulders but one large sample (399) has been analysed and provided an age of 462 $\pm$ 8 Ma and $^{87}Sr/^{86}Sr^{o}$ of 0.7062 $\pm$ 8 (Fig. 2/2).

2.2.5 Craigskelly conglomerate

The basal Silurian in the Girvan area is represented by the Craigskelly conglomerate. This again contains a variety of granitic detritus and four samples have been dated, 591, 587, 580 and 579 (Figs. 2/12 & 2/13). Sample 591 is a deformed one with very low Rb/Sr ratios and yields a meaningless figure of 391 $\pm$ 180 Ma. Clast 580 shows some evidence of possible recrystallization but produces an age of 593 $\pm$ 28 Ma and $^{87}Sr/^{86}Sr^{o}$ of 0.7154 $\pm$ 7. The two other specimens, 587 and 579, give ages of 462 $\pm$ 8 and 458 $\pm$ 4 Ma and $^{87}Sr/^{86}Sr^{o}$ of 0.7105 $\pm$4 and 0.7102 $\pm$ 3 respectively.

2.2.6 Corsewall conglomerate

The Corsewall conglomerate of similar age to the Benan conglomerate is in contrast to the rest being exposed in the Rhinns of Galloway. The granitic clasts are generally more basic in character and many exhibit the effects of deformation. The low Rb/Sr ratios, low potassium feldspar content and mixed quality of the analyses mean that the MSWD figures are generally high. Three essentially undeformed clasts, 993, 985 and 982 give ages of around 570 and 460 Ma and $^{87}Sr/^{86}Sr^{o}$ values between 0.706 and 0.709 (Figs. 2/10 & 2/11). Sample 996, which is foliated, produces an age of 525 $\pm$ 22 Ma and $^{87}Sr/^{86}Sr^{o}$ of 0.7059 $\pm$ 6 (Fig. 2/9). Clast 988 is another foliated sample which has proved problematical. The feldspar minerals yield an unnacceptable isochron of 798 $\pm$ 84 Ma and $^{87}Sr/^{86}Sr^{o}$ of 0.7152 $\pm$ 11 (Fig. 2/10). It does, however, contain biotite and muscovite and individual ages, assuming an $^{87}Sr/^{86}Sr^{o}$ figure of 0.715, are respectively 448 $\pm$ 5 and 473 $\pm$ 23 Ma. Any emphasis that may be placed on these figures is unfortunately reduced by the uncertainty of the $^{87}Sr/^{86}Sr^{o}$ value and the chloritization of the biotite.

2.3 Summary of geochronological data

The spread of ages obtained from the clasts is summarized in Tables 2C & 2D and shown graphically in Fig. 2/15. Certain features are evident :-

1. There is an overall spread in ages from 590 to 450 Ma with no gap of more than 30 Ma.
2. An apparent concentration of ages around 470 Ma. This may be partly explained by the early sampling of more acid clasts which facilitated more accurate isotopic determinations. The acid clasts do, however, predominate and consistently give ages around 470 Ma and as such the concentration peak is probably real.
3. A tendency for the stratigraphically higher conglomerates to contain numerically younger granites.
4. A greater proportion of the Corsewall samples cluster around 550 Ma.
5. Ages from deformed clasts are generally poorly defined but appear to give older ages.

The plot $^{87}Sr/^{86}Sr^{o}$ versus age (Fig. 2/15) also indicates certain points :-

1. Benan samples (excluding 186 & 187 which have poorly defined and anomalously low values) show a spread in $^{87}Sr/^{86}Sr^{o}$ from 0.705 to 0.710.
2. Corsewall samples (excluding 988) show consistent values of 0.707-0.708 regardless of age or deformation.
3. Craigskelly clasts show higher $^{87}Sr/^{86}Sr^{o}$ values in the range 0.710-0.715.
4. Sample 889 has a very low value of 0.703.
5. A tentative relationship of increasing $^{87}Sr/^{86}Sr^{o}$ with increasing age.

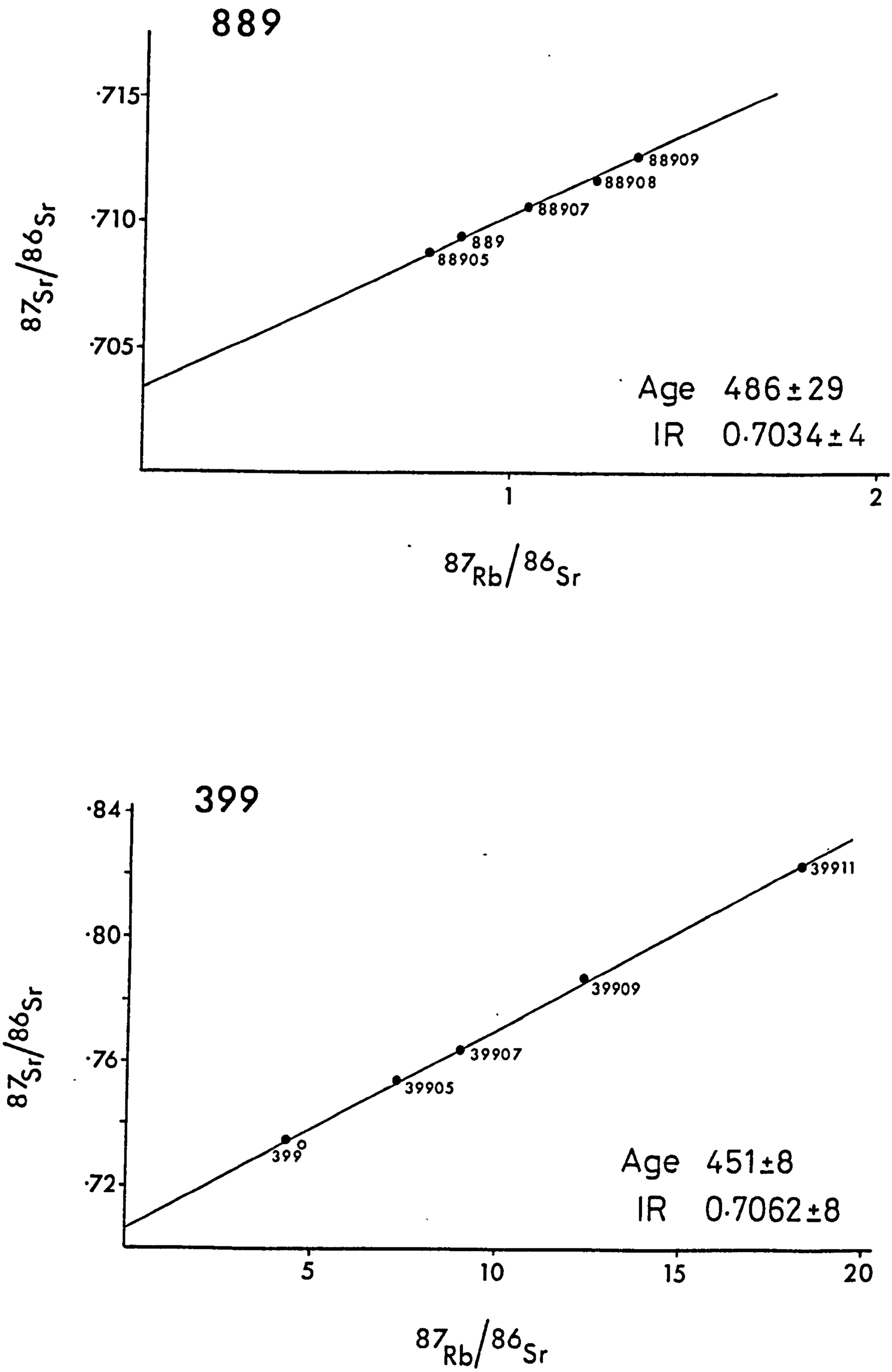

Fig. 2/2 Isochrons for the Kirkland (889) and Tormitchell (399) clasts. Analytical data is given in Table 2E.

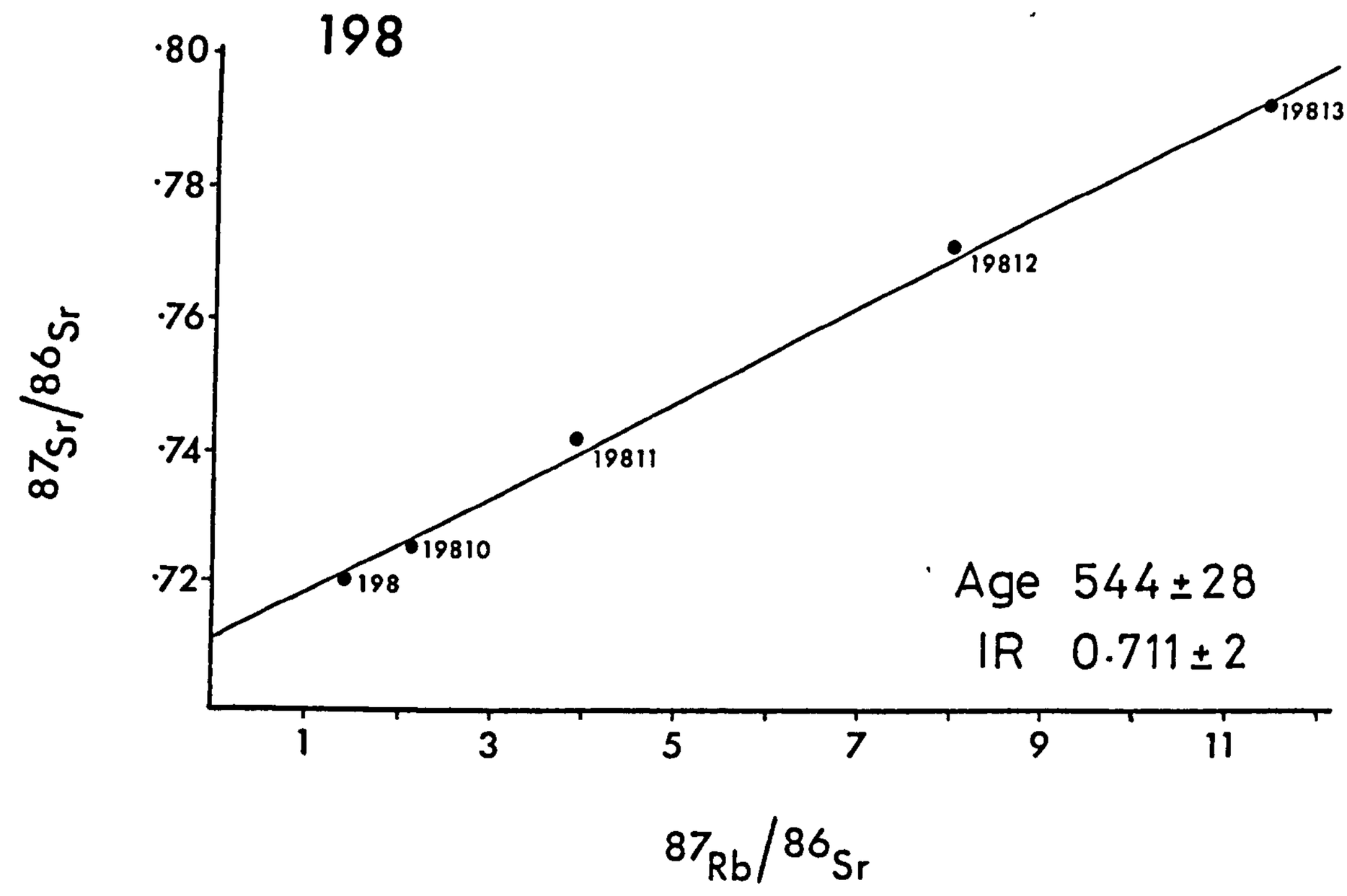

Fig. 2/3 Isochrons for two Benanaconglomerate clasts (198 &197). Analytical data are given in Table 2E.

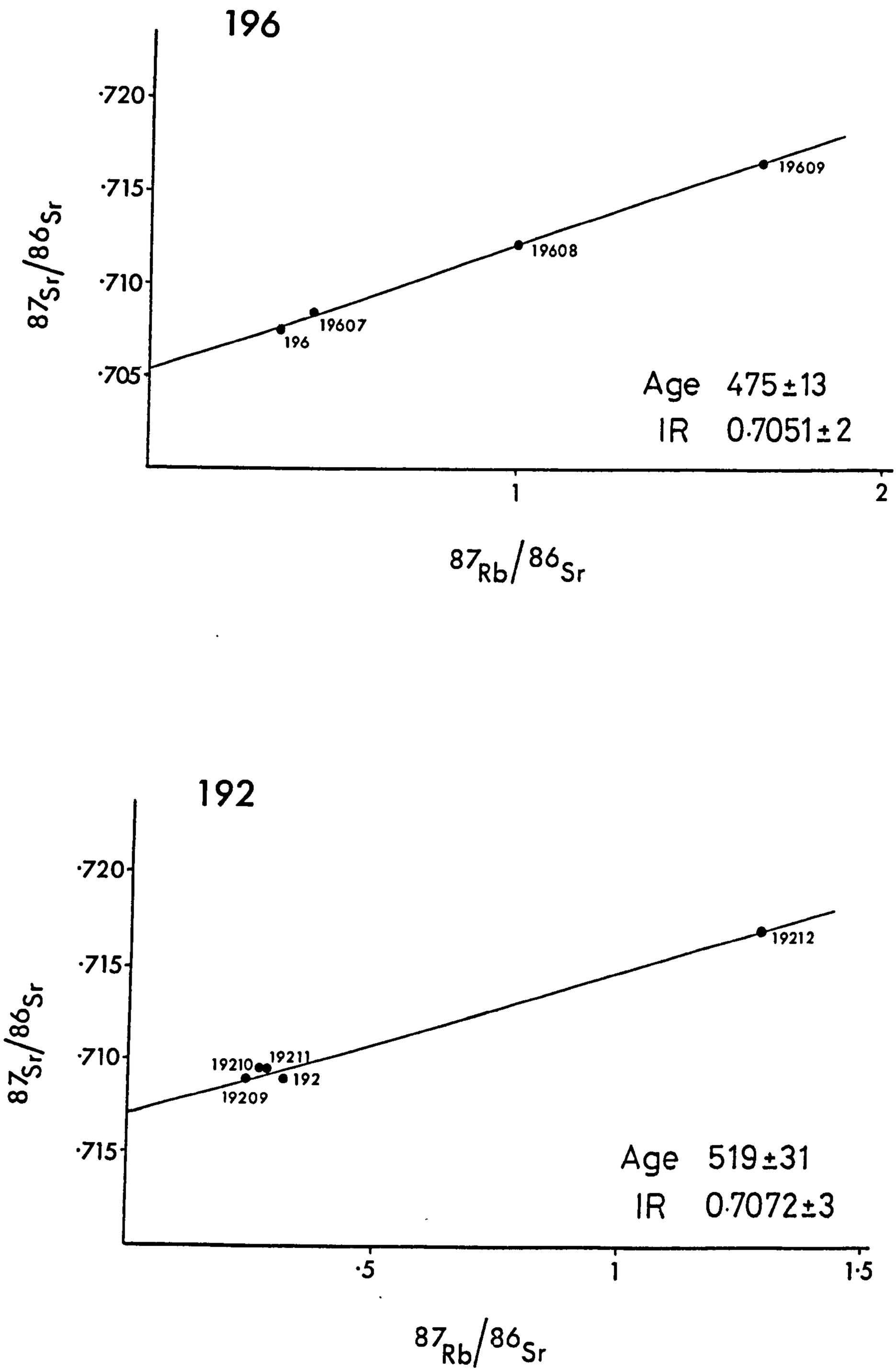

Fig. 2/4 Isochrons for two Benan conglomerate clasts (196 & 192). Analytical data are given in Table 2E.

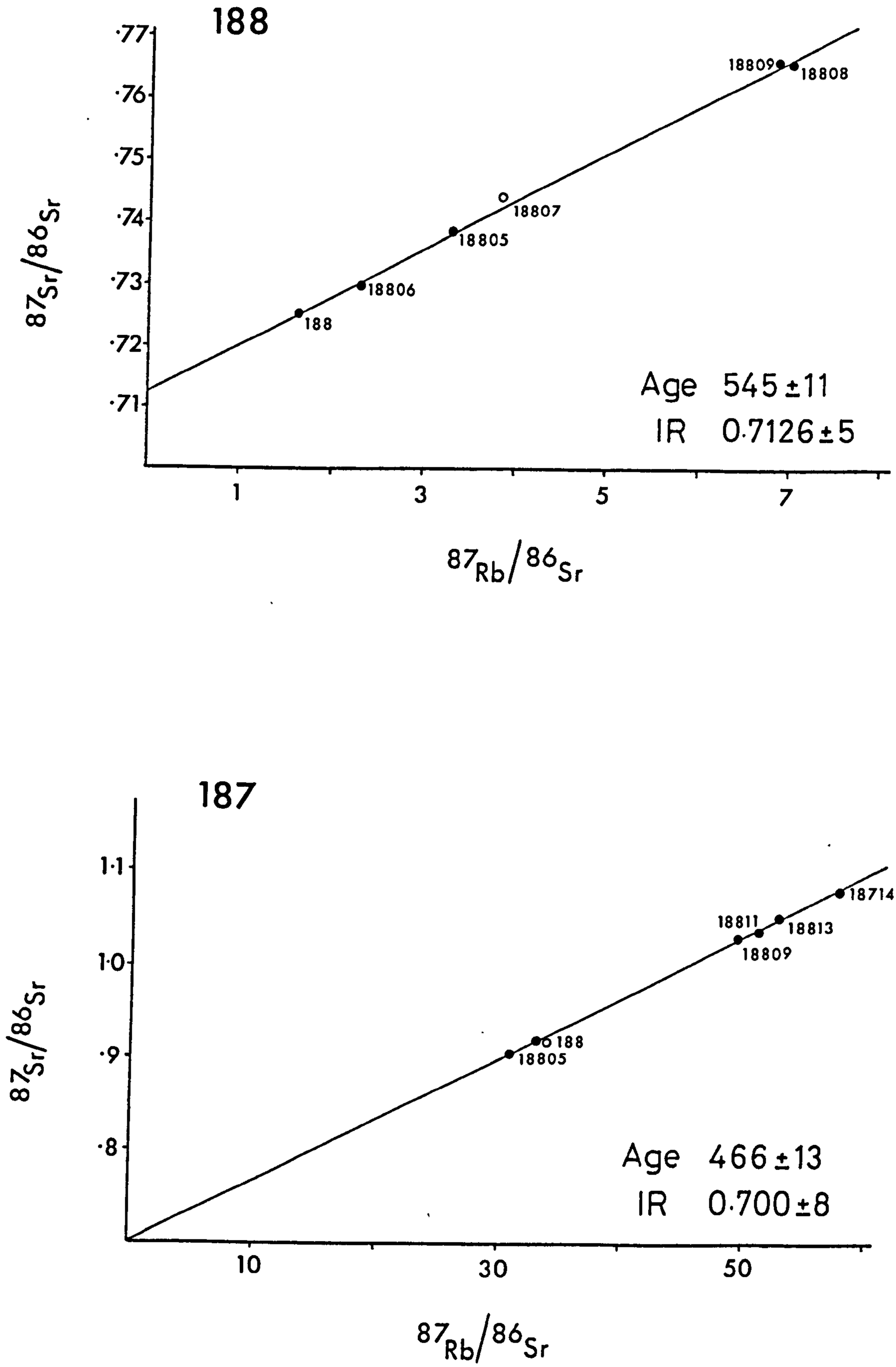

Fig. 2/5 Isochrons for two Benan conglomerate clasts (188 & 187). Analytical data are given in Table 2E.

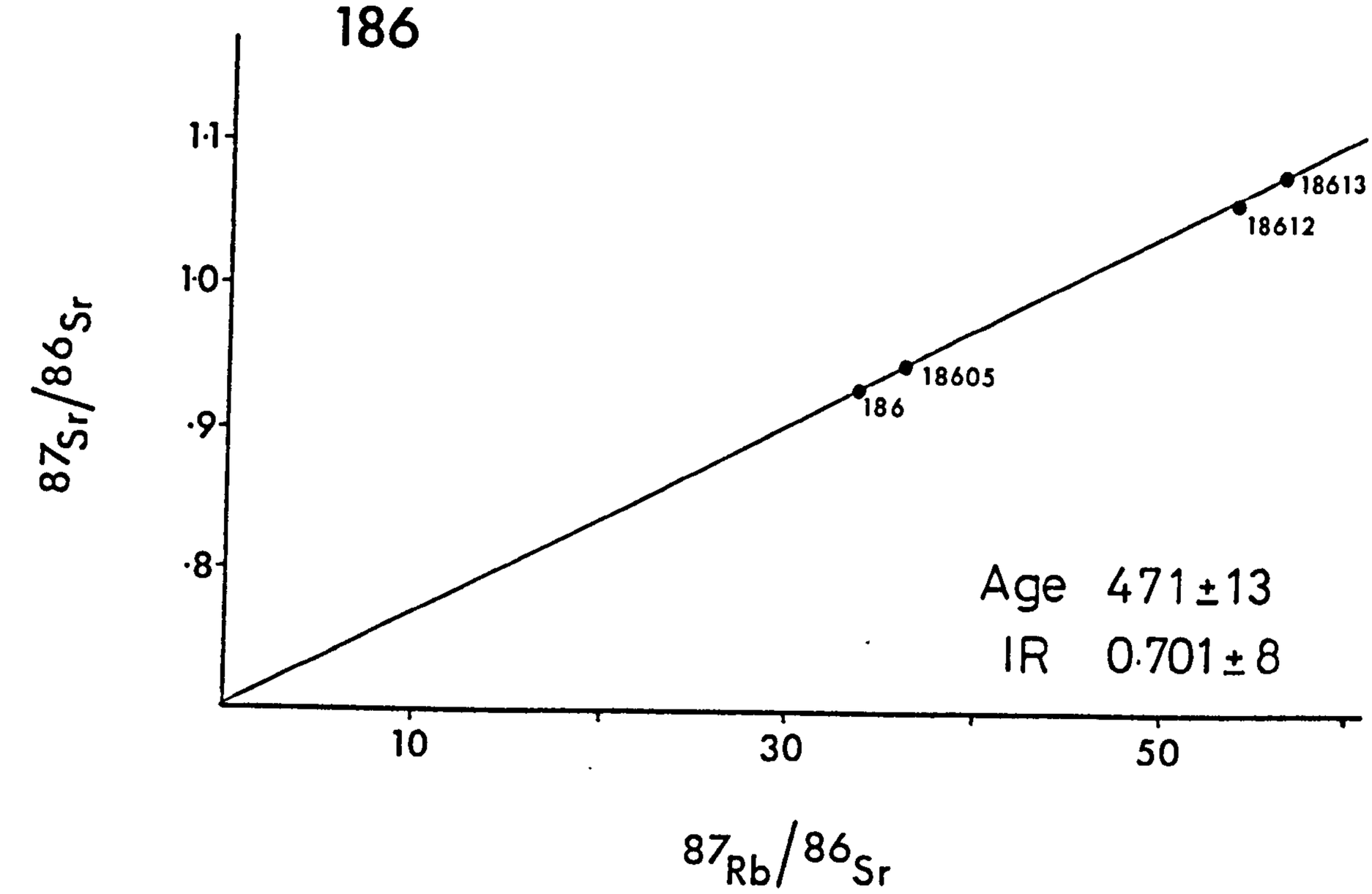

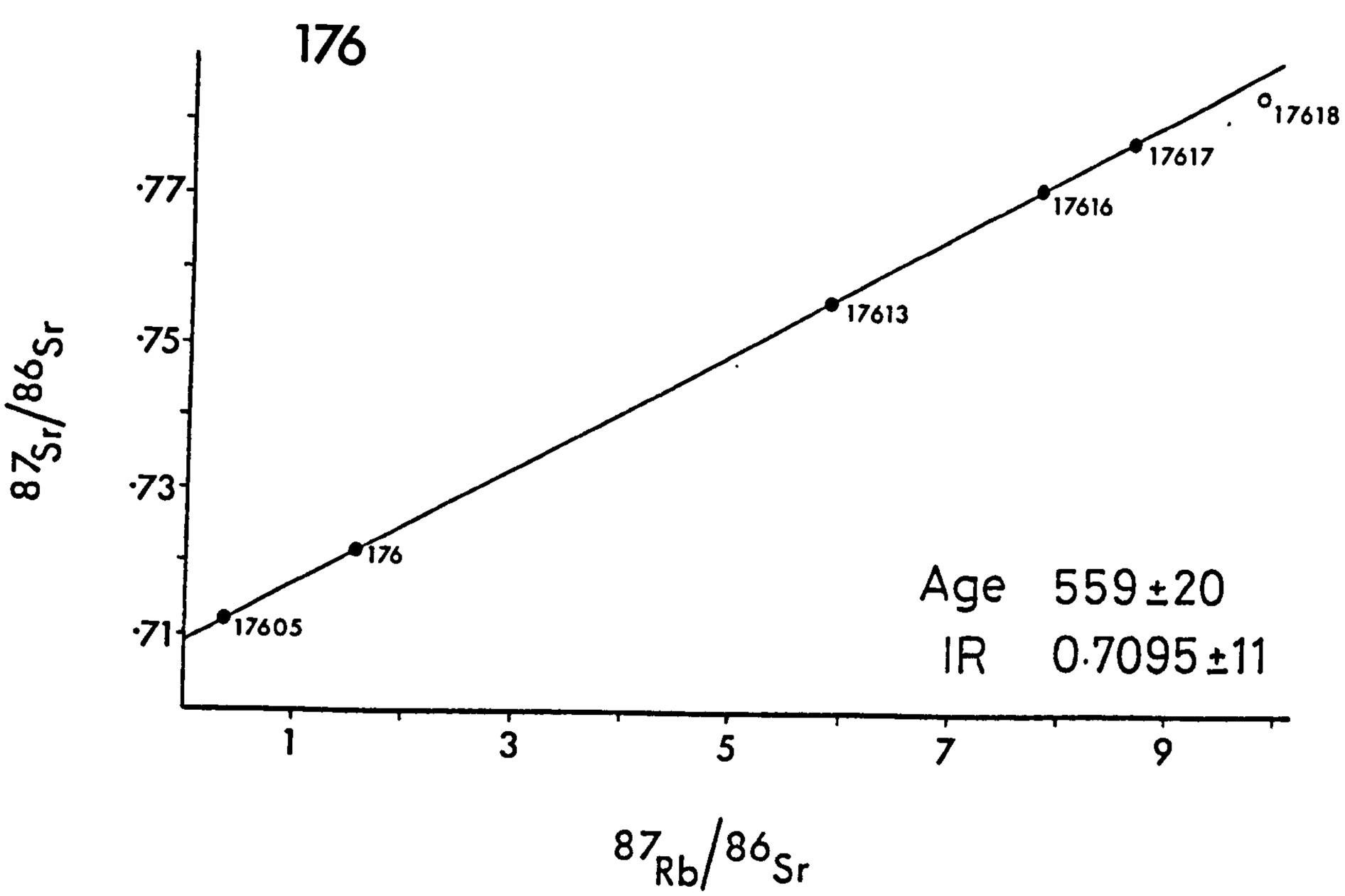

Fig. 2/6 Isochrons for two Benan conglomerate clasts (186 & 176). Analytical data are given in Table 2E.

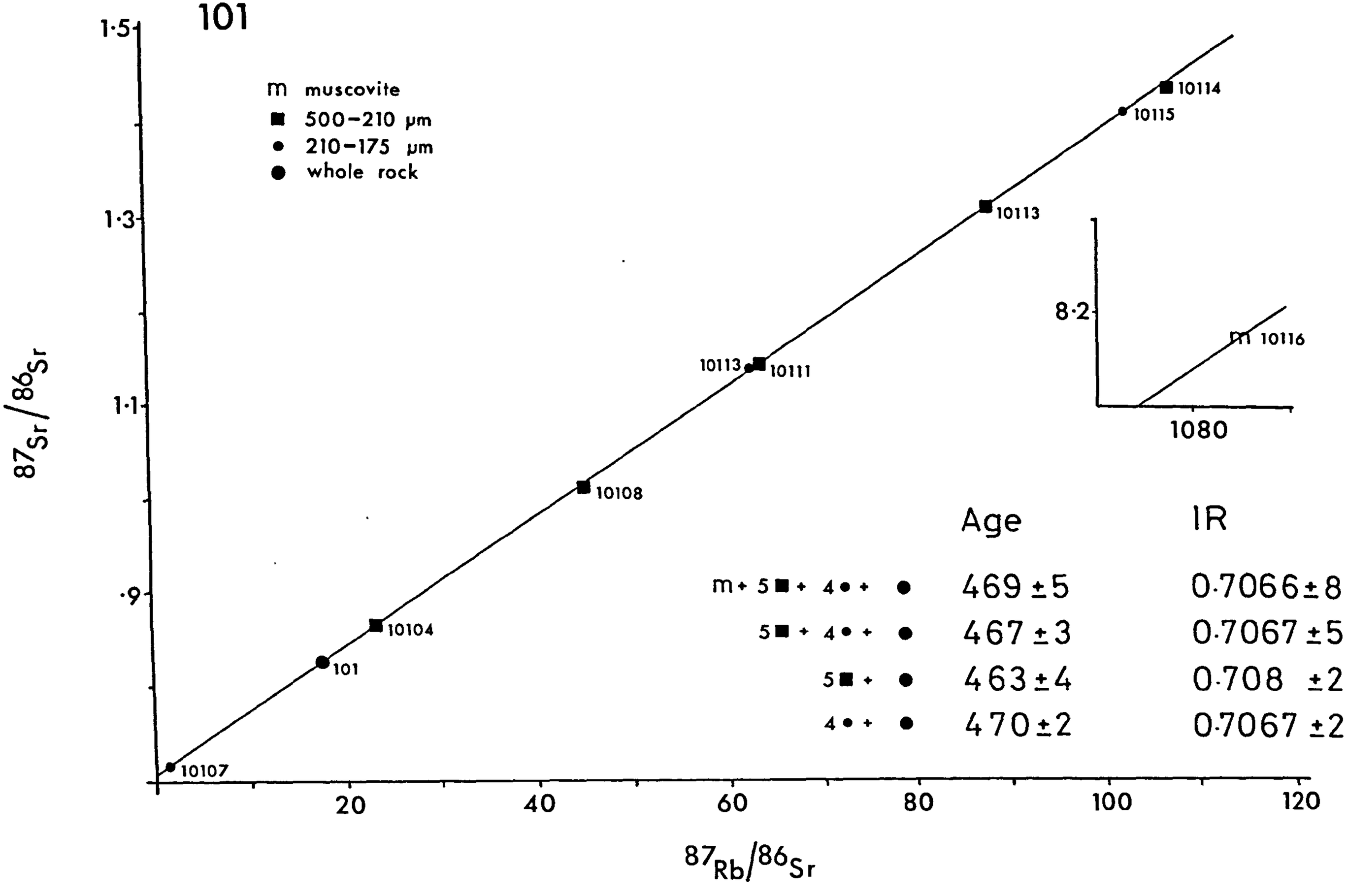

Fig. 2/7 Isochrons for sample 101 from the Benan conglomerate. Data in Table 2E.

101

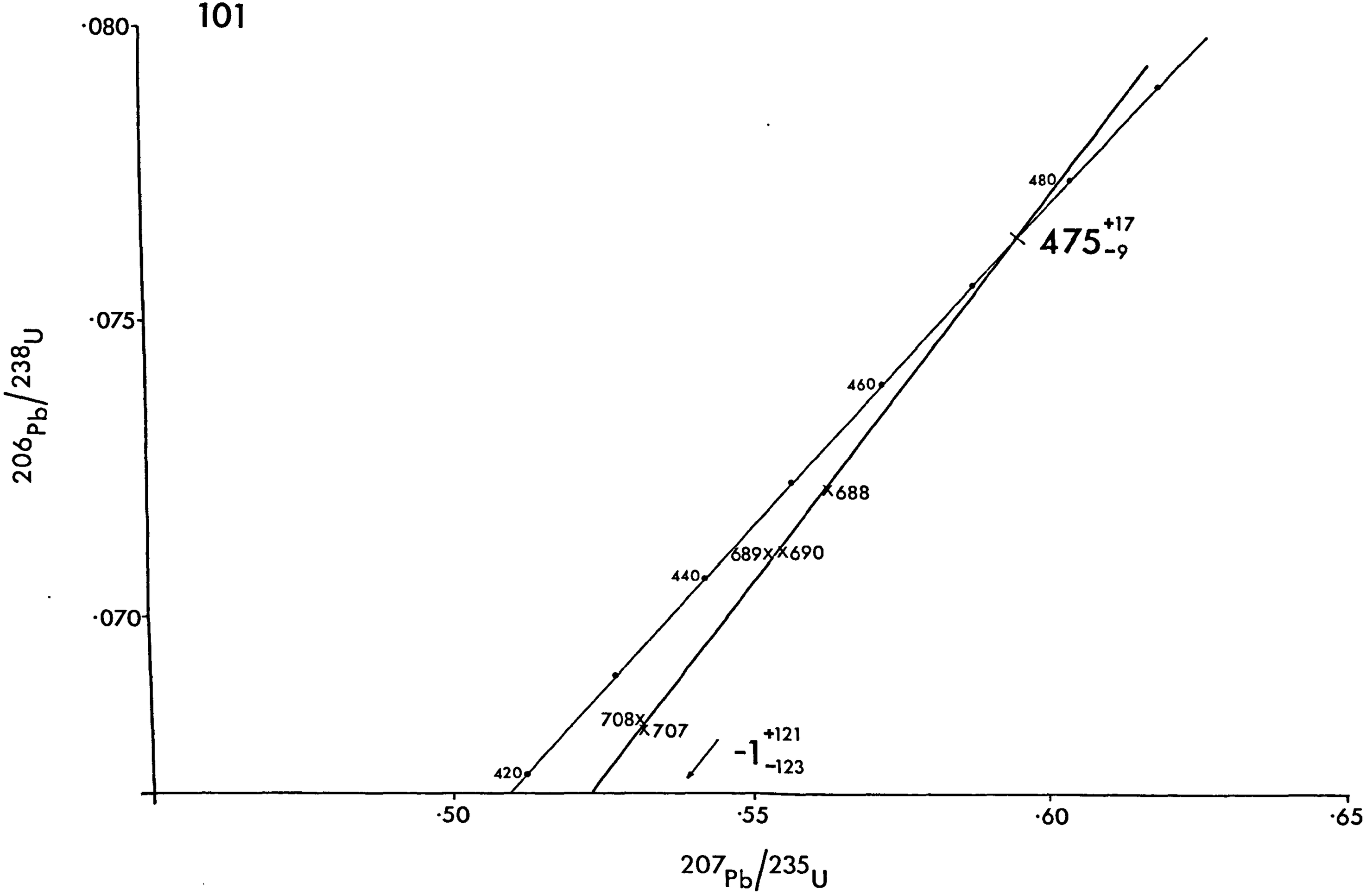

Fig. 2/8 Concordia diagram for sample 101 from the Benan conglomerate. Data in Table 2B.

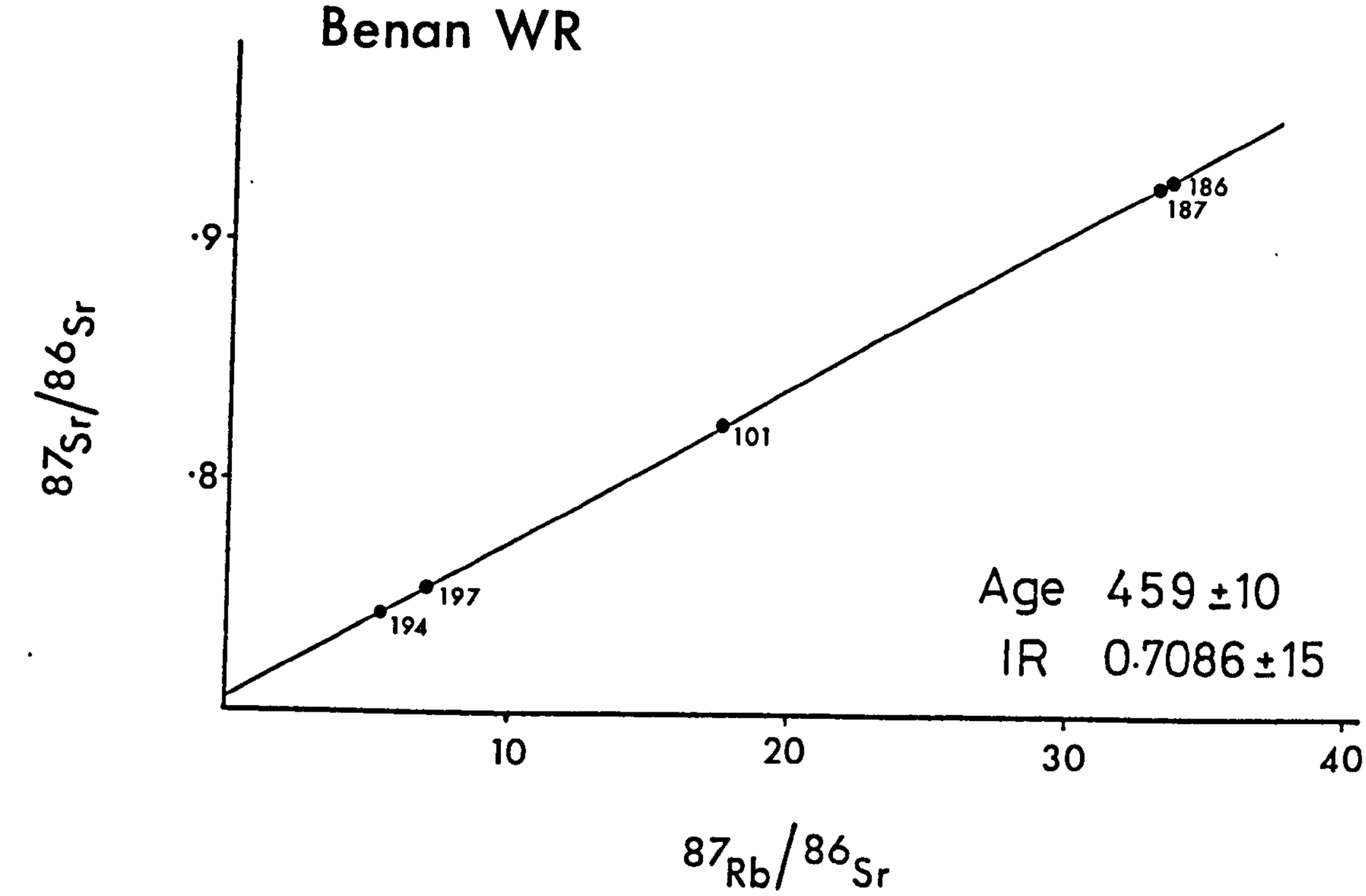

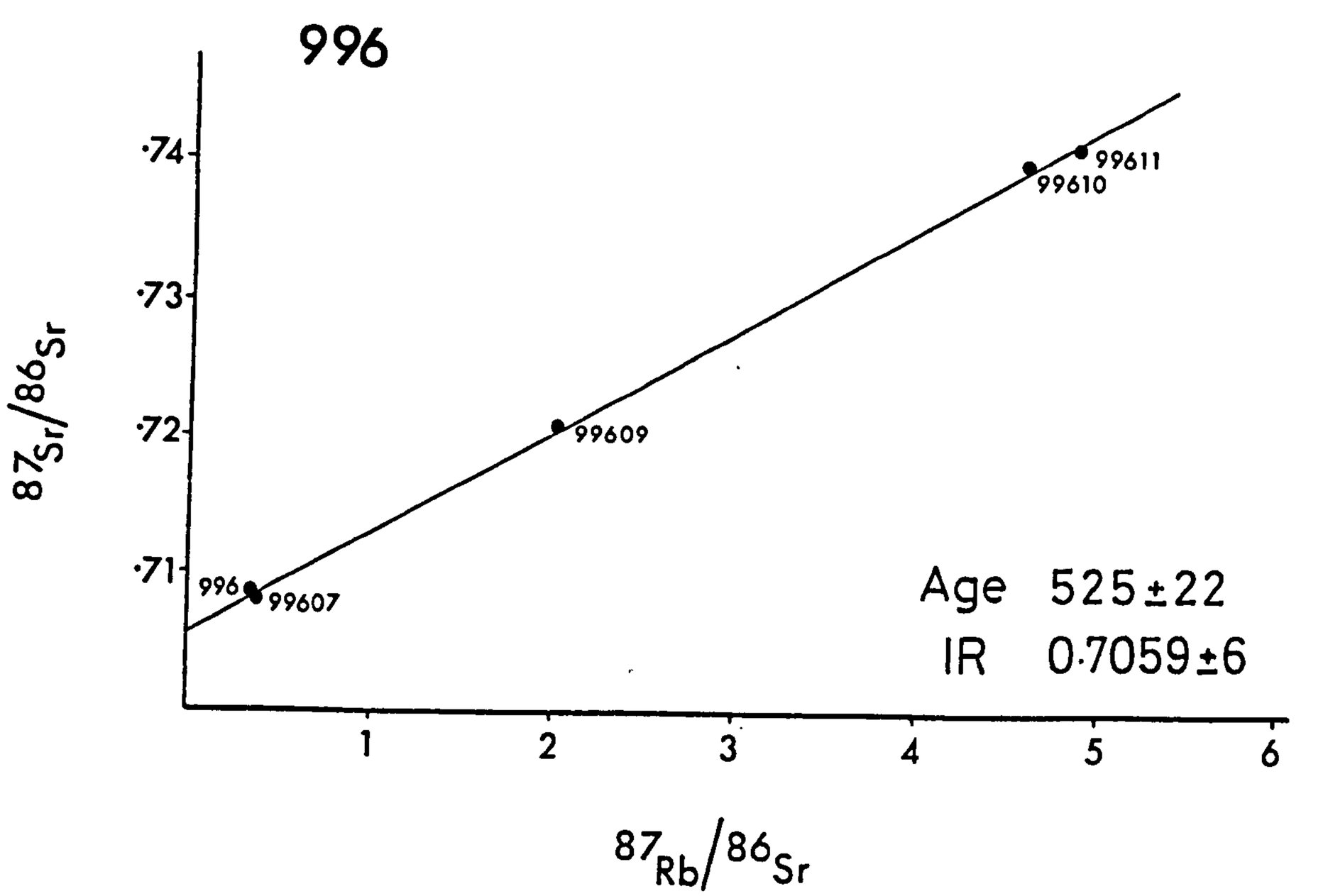

Fig. 2/9 Benan conglomerate whole rock isochron and Corsewall clast 996 isochron. Analytical data are given in Table 2E.

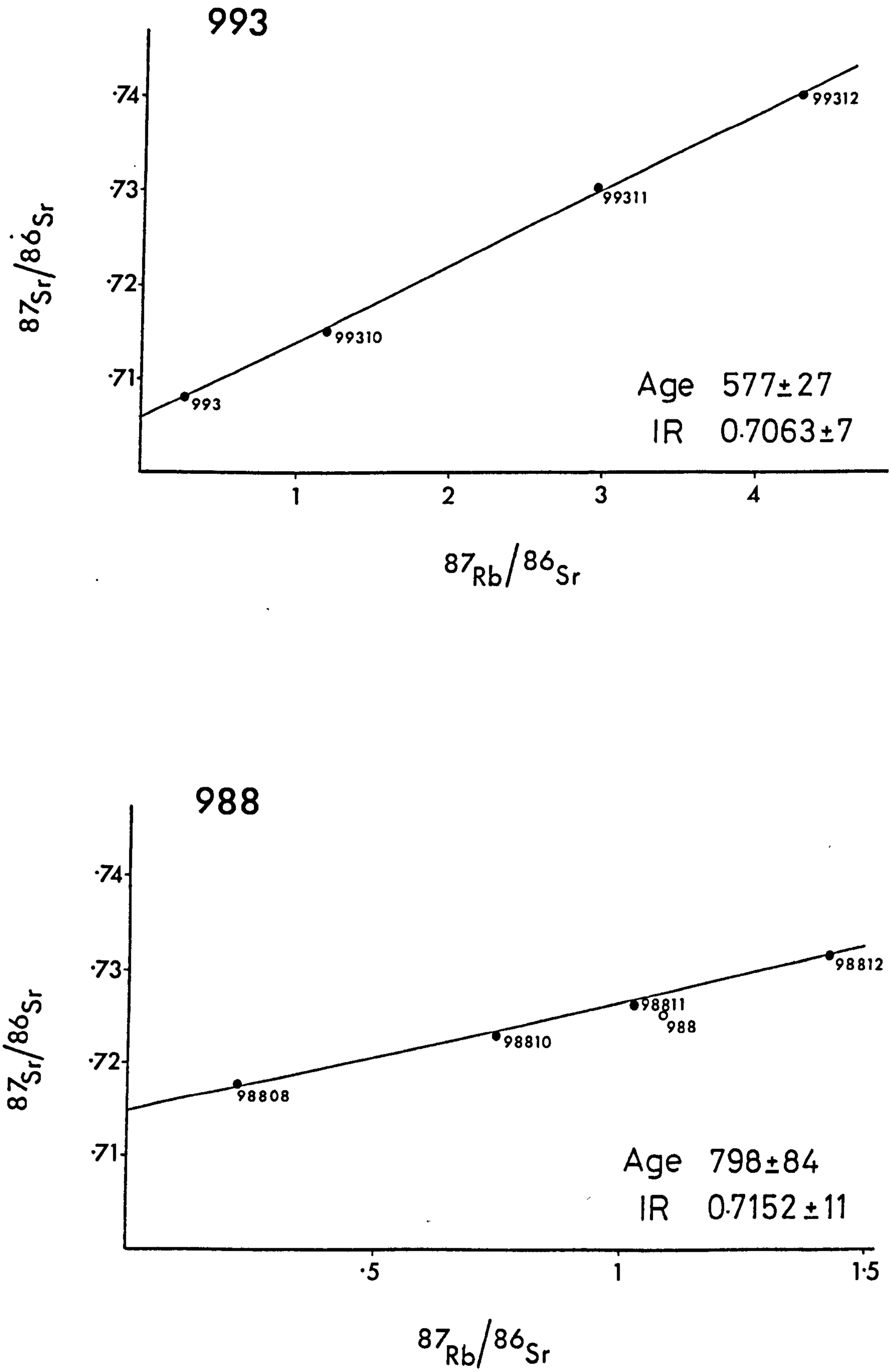

Fig. 2/10 Isochrons for two Corsewall conglomerate clasts (993 & 988). Analytical data are given in Table 2E.

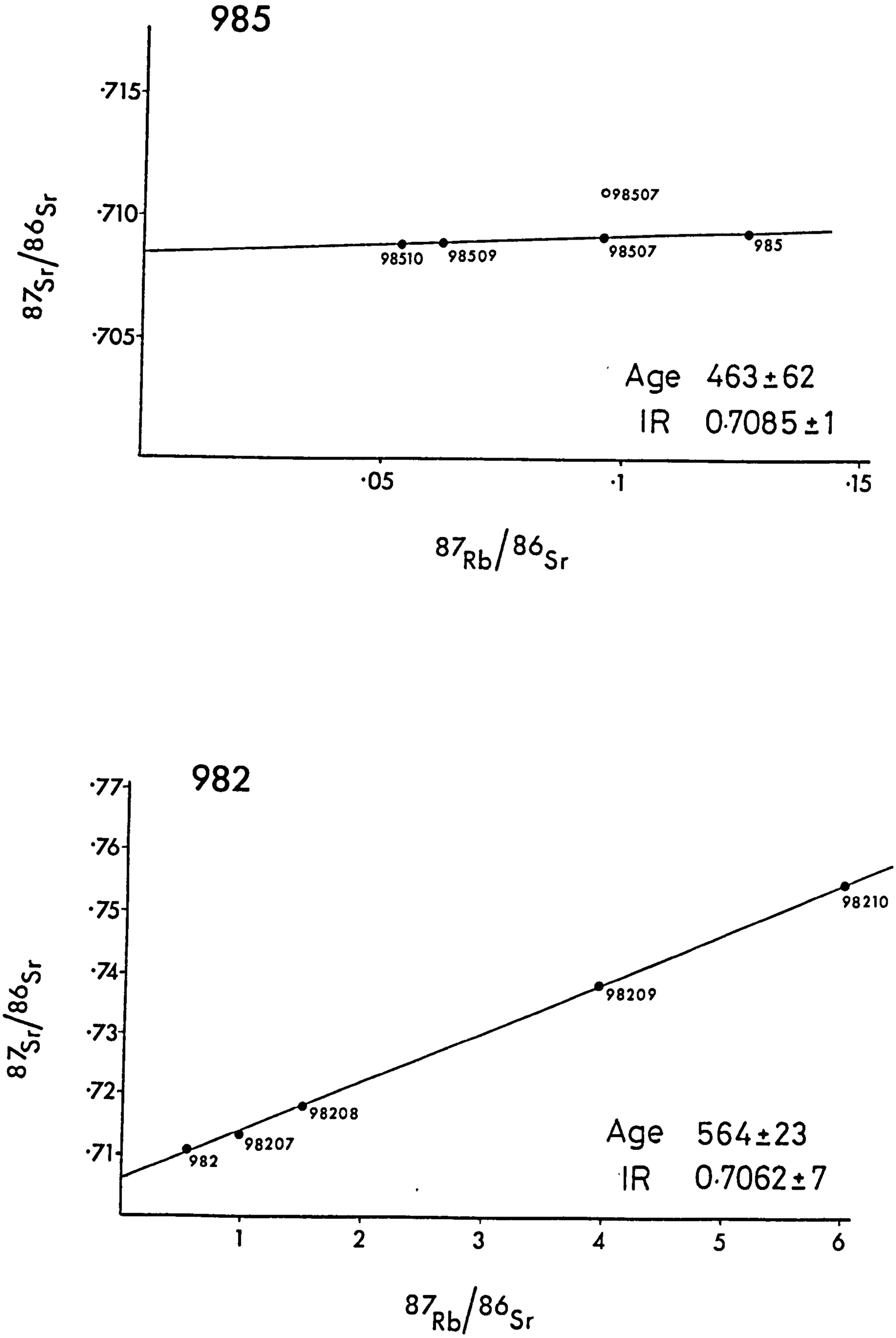

Fig. 2/11 Isochrons for two Corsewall conglomerate clasts (985 & 982). Analytical data are given in Table 2E.

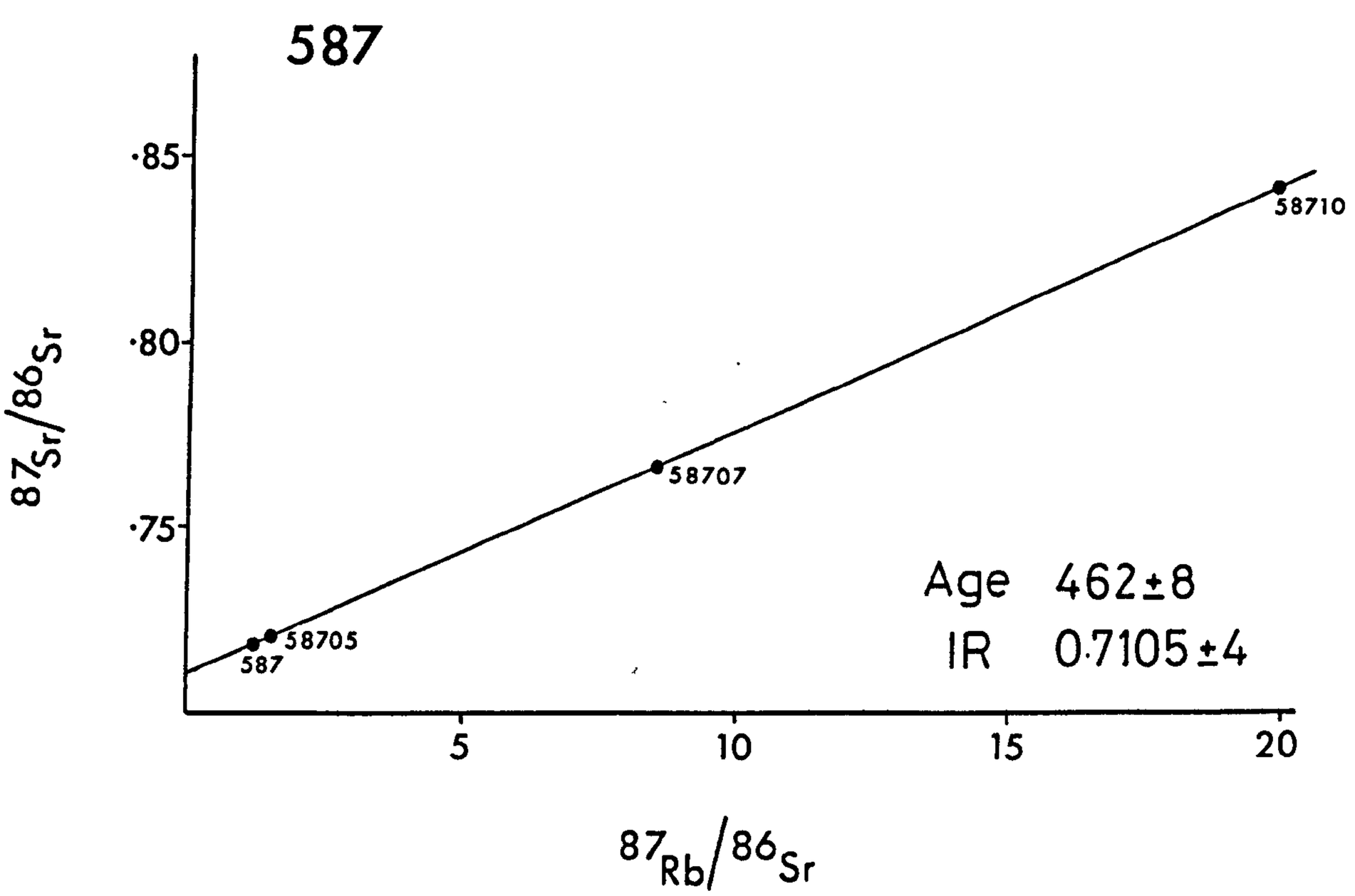

Fig. 2/12 Isochrons for two Craigskelly conglomerate clasts (591 & 587). Analytical data are given in Table 2E.

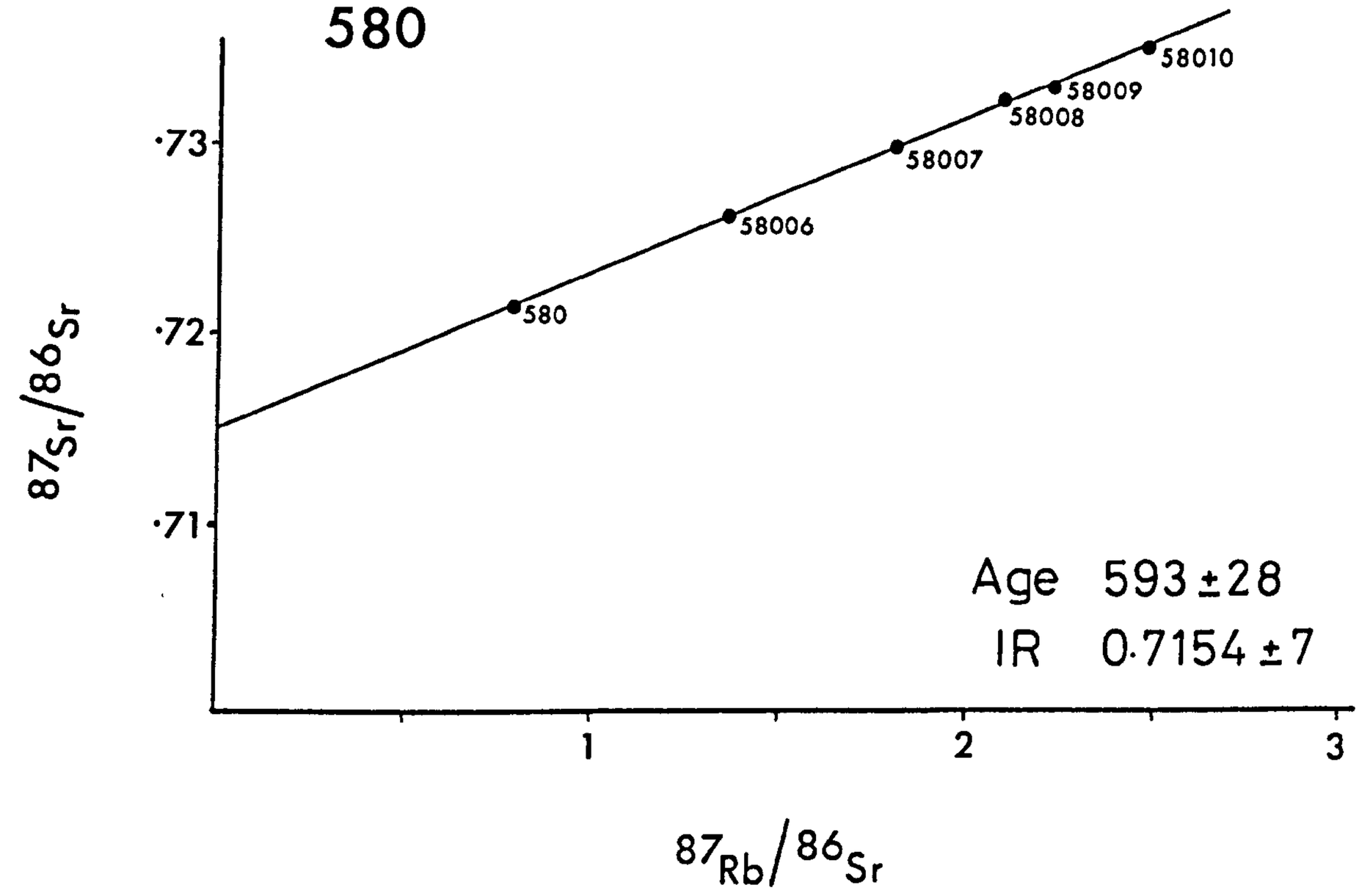

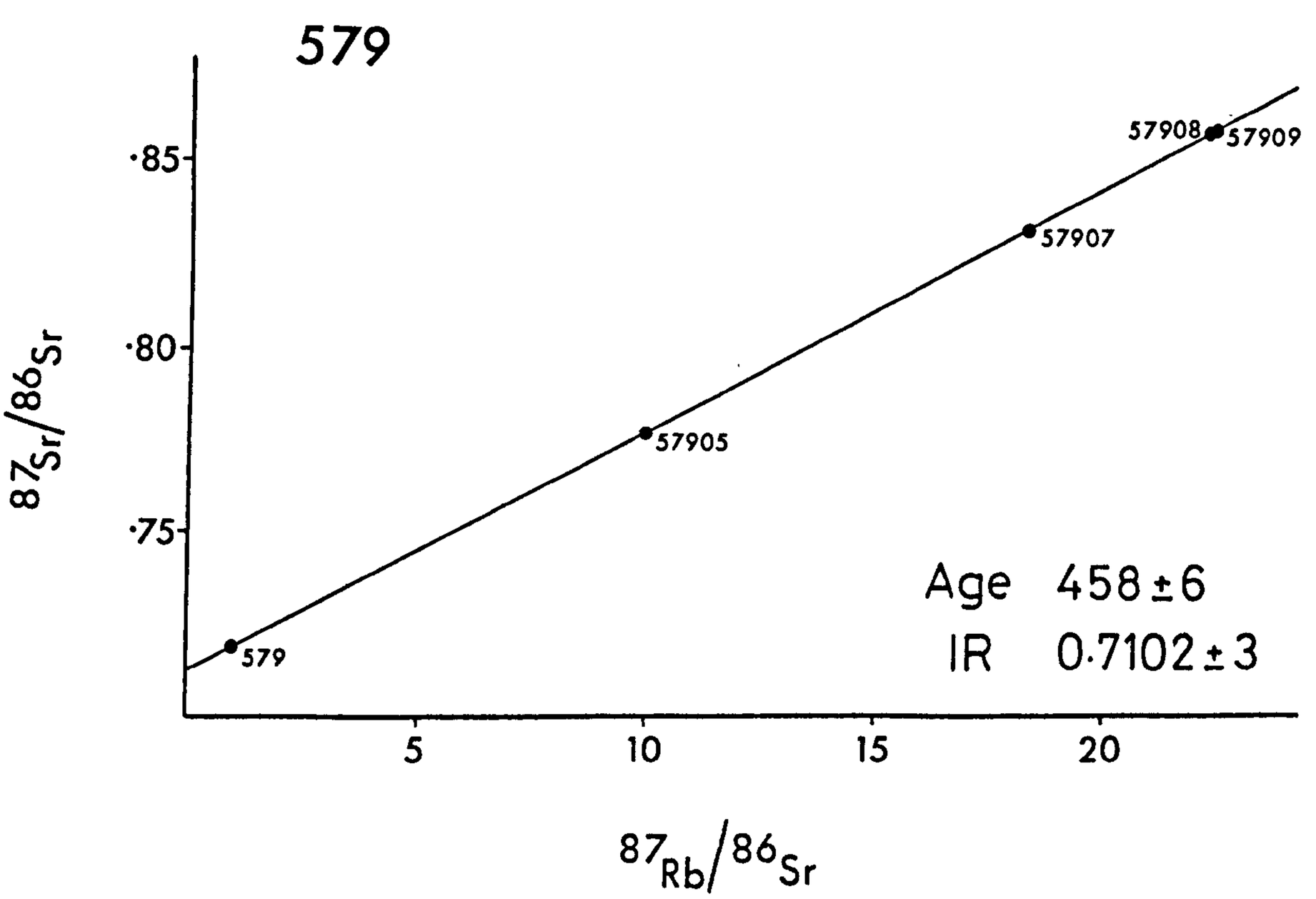

Fig. 2/13 Isochrons for two Craigskelly conglomerate clasts (580 & 579). Analytical data are given in Table 2E.

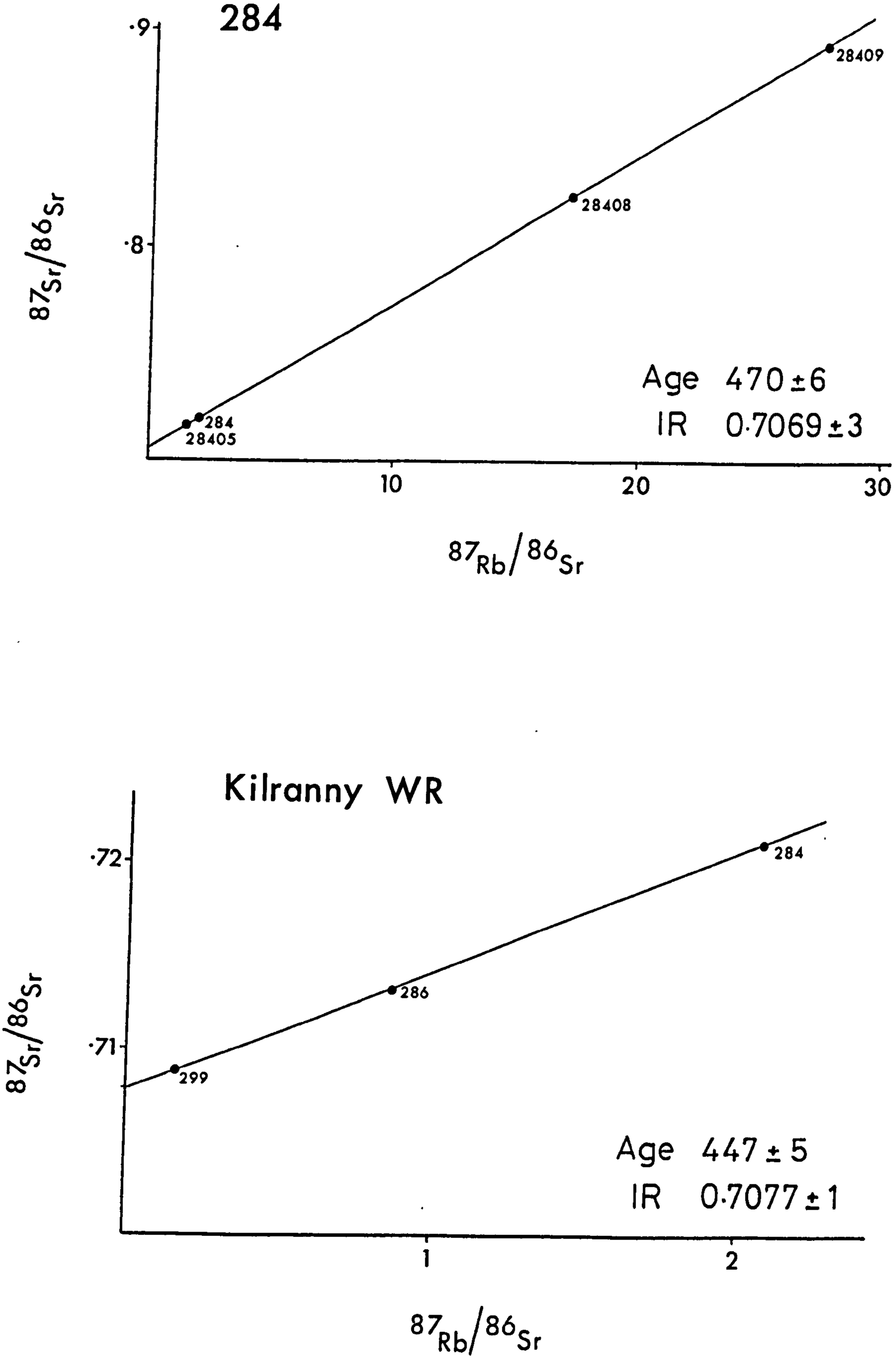

Fig. 2/14 Isochrons for clast 284 and combined whole rock points from the Kilranny conglomerate. Analytical data are given in Table 2E.

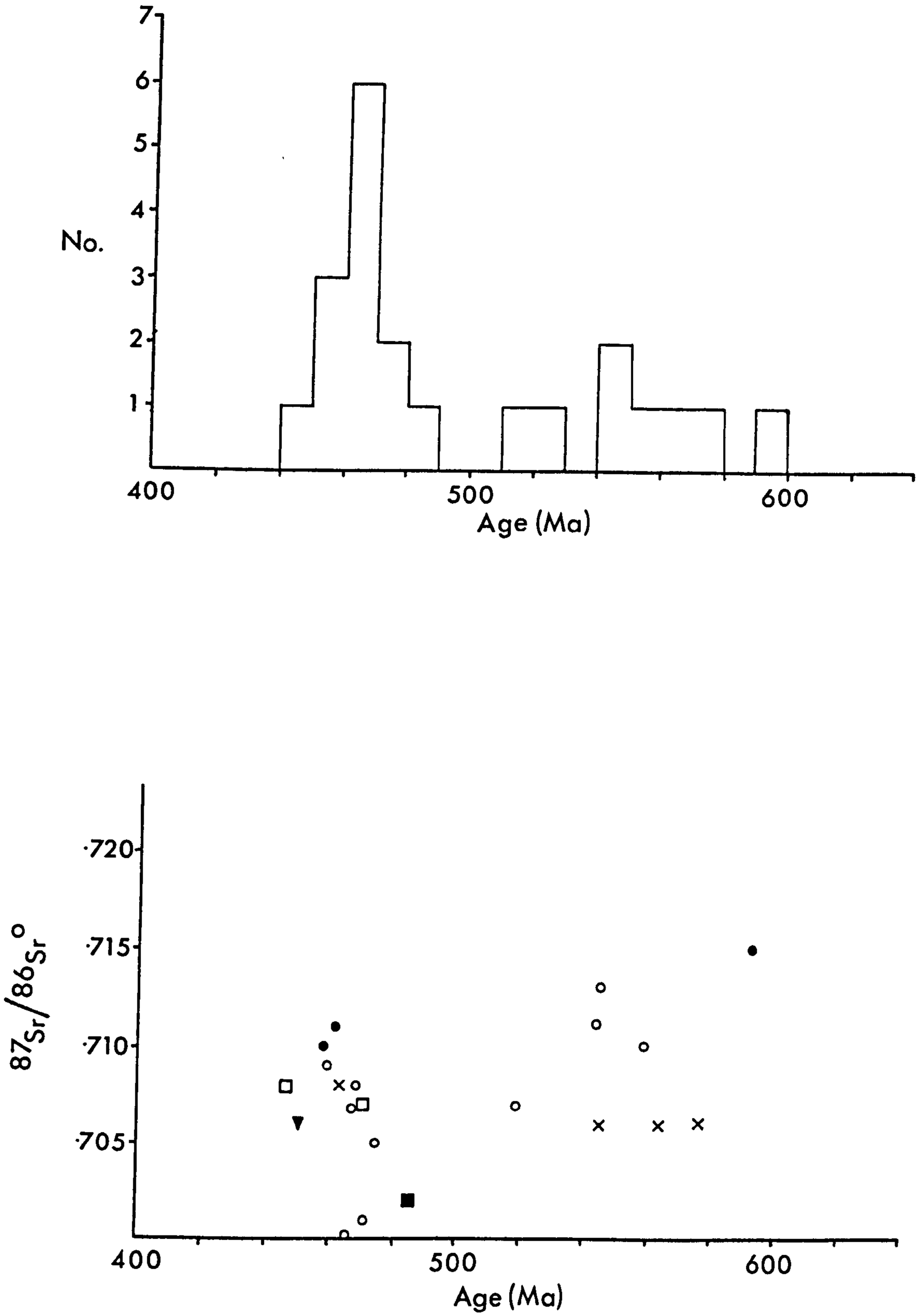

Fig. 2/15 Plots of frequency versus age and $^{87}Sr/^{86}Sr^{o}$ versus age for all the clasts analysed geochronologically. The data are summarized numerically in Tables 2C & 2D.

Sample	No. of points	Regression errors (%) $^{87}Rb/^{86}Sr$	$^{87}Sr/^{86}Sr$	Intercept	Age (Ma)	MSWD
198	5	0.5	0.014	0.711 ± 2	544 ± 48	88.13
197	5	0.7	0.030	0.7081 ± 7	468 ± 5	0.57
196	4	0.5	0.014	0.7051 ± 2	475 ± 13	0.75
192	5	0.5	0.014	0.7072 ± 3	519 ± 31	3.28
188	5	0.5	0.014	0.7126 ± 5	545 ± 11	3.36
187	6	0.7	0.030	0.700 ± 8	466 ± 13	1.46
186	4	0.5	0.014	0.701 ± 8	471 ± 13	1.42
176	5	0.7	0.030	0.7095 ± 11	559 ± 20	8.25
101	9	0.7	0.030	0.7067 ± 5	467 ± 3	1.12
101	10 (9 + musc.)	0.7	0.030	0.7066 ± 8	469 ± 5	3.66
101	4 (210-175 µm)	0.7	0.030	0.7067 ± 2	470 ± 2	0.26
101	6 (500-210 µm)	0.7	0.030	0.708 ± 2	463 ± 4	0.69
Whole rocks	5	0.7	0.030	0.7086 ± 15	459 ± 10	3.42

Table 2C Rb-Sr isochron data for Benan conglomerate samples

Sample	No. of points	Intercept	Age (Ma)	MSWD
Corsewall conglomerate				
996	5	0.7059 ± 6	525 ± 22	17.54
993	4	0.7063 ± 7	577 ± 27	15.42
988	4	0.7152 ± 11	798 ± 84	21.93
985	4	0.7085 ± 1	463 ± 62	0.07
982	5	0.7062 ± 7	564 ± 23	15.29
Craigskelly conglomerate				
591	4	0.7085 ± 8	391 ± 181	19.10
587	4	0.7105 ± 4	462 ± 8	4.06
580	6	0.7154 ± 7	593 ± 28	4.98
579	5	0.7102 ± 3	458 ± 4	2.11
Kilranny conglomerate				
284	4	0.7069 ± 3	470 ± 6	2.64
Whole rocks	3	0.7077 ± 1	447 ± 5	0.16
Kirkland conglomerate				
889	5	0.7034 ± 4	486 ± 29	0.83
Tormitchell conglomerate				
399	5	0.7062 ± 8	451 ± 8	2.45

Table 2D Rb-Sr isochron data for samples from the Corsewall, Craigskelly, Kilranny, Kirkland and Tormitchell conglomerates. In all cases the regression errors are $^{87}Rb/^{86}Sr$ 0.5% and $^{87}Sr/^{86}Sr$ 0.014%

Sample	Rb (ppm)	Sr (ppm)	$^{87}Rb/^{86}Sr$	$^{87}Sr/^{86}Sr$
996	45.8	369.2	0.359084	0.708859
99607	81.0	625.0	0.375191	0.708251
99609	196.8	284.2	2.00651	0.721229
99610	255.0	161.3	4.58838	0.740630
99611	256.6	153.6	4.84834	0.741384
993	44.7	467.8	0.276434	0.708518
99310	119.2	284.3	1.21401	0.716152
99311	176.8	173.0	2.96220	0.731322
99312	191.1	129.5	4.28330	0.740816
988	83.0	208.1	1.15630	0.725250
988	82.4	207.4	1.15092	0.725380
98800	357.7	16.7	64.8030	1.14408
98801	372.1	11.6	98.6554	1.35026
98802	187.9	36.0	15.2579	0.822922
98808	10.5	134.3	0.225312	0.718010
98811	120.3	339.3	1.02789	0.726714
98812	169.9	346.4	1.42261	0.731795
985	11.5	261.9	0.127210	0.709389
98507	11.4	339.0	0.096908	0.711706
98507	11.5	346.7	0.095867	0.709156
98509	7.5	349.6	0.061837	0.708977
98510	6.6	356.0	0.053243	0.708878
982	67.5	363.1	0.538820	0.710959
98207	120.0	367.6	0.944737	0.713328
98208	166.6	324.7	1.48580	0.717983
98209	234.4	172.0	3.95398	0.738475
98210	254.6	123.4	5.99403	0.754173
889	56.3	189.5	0.859181	0.709434
88905	62.5	231.7	0.778256	0.708774
88907	86.2	240.9	1.03526	0.710453
88908	104.8	248.1	1.22246	0.711814
88909	114.4	247.3	1.33970	0.712746

Table 2E Rb-Sr Analytical data

Sample	Rb (ppm)	Sr (ppm)	$^{87}Rb/^{86}Sr$	$^{87}Sr/^{86}Sr$
591	22.3	267.5	0.241442	0.710371
59107	11.0	271.3	0.116967	0.709072
59108	16.1	256.4	0.181215	0.709209
59109	48.4	249.2	0.562726	0.711552
587	105.0	231.1	1.31658	0.719007
58705	168.8	318.4	1.53606	0.720858
58707	317.5	107.4	8.60581	0.767492
58710	374.5	55.3	19.8476	0.840721
580	76.7	277.8	0.799573	0.722060
58006	131.0	278.2	1.36491	0.727055
58007	177.3	284.0	1.81090	0.731087
58008	196.5	271.5	2.09906	0.733388
58009	203.1	264.9	2.22348	0.734195
58010	214.6	250.8	2.48224	0.735996
579	77.0	248.2	0.898785	0.716095
57905	234.4	68.6	9.94946	0.774520
57907	281.8	45.1	18.2756	0.829294
57908	307.7	40.5	22.3009	0.855595
57909	322.6	42.3	22.4001	0.857662
399	32.1	19.8	4.71684	0.733358
399	32.1	22.2	4.20598	0.733056
39905	40.8	16.5	7.20444	0.752978
39907	54.0	17.5	8.99568	0.763500
39909	75.8	18.0	12.2792	0.785127
39911	111.8	18.0	18.2032	0.822819
299	9.3	170.0	0.157596	0.708762
286	29.0	97.5	0.861470	0.713194
284	82.9	115.5	2.07948	0.721004
284	82.6	114.8	2.07237	0.720990
28405	78.9	144.1	1.58662	0.717329
28408	255.9	43.0	17.4264	0.823603
28410	317.8	33.8	27.6791	0.891727

Table 2E (cont.) Rb-Sr analytical data

Sample	Rb (ppm)	Sr (ppm)	$^{87}Rb/^{86}Sr$	$^{87}Sr/^{86}Sr$
198	85.0	174.0	1.41505	0.721676
19810	178.4	241.7	2.13857	0.726770
19811	231.9	171.4	3.92905	0.743752
19812	280.2	101.2	8.06752	0.773527
19813	324.2	83.1	11.3786	0.795467
197	117.2	48.1	7.08988	0.755694
19704	133.2	65.4	5.91436	0.747306
19706	256.6	45.8	16.4009	0.817892
19708	280.2	45.4	18.0603	0.827994
19709	306.0	43.5	20.6541	0.857651
196	40.7	322.1	0.365491	0.707556
19607	45.9	285.8	0.464337	0.708389
19608	85.4	291.4	0.847600	0.710849
19609	135.2	232.4	1.68434	0.716557
192	22.8	207.6	0.318246	0.709337
19209	18.2	213.9	0.245578	0.709028
19210	21.9	223.7	0.283832	0.709464
19211	23.0	234.9	0.283873	0.709467
19212	81.7	182.9	1.29384	0.716810
188	100.0	179.1	1.61901	0.725181
18805	211.7	187.3	3.28012	0.738399
18806	180.8	225.0	2.33015	0.730498
18807	232.6	171.8	3.93148	0.744335
18808	268.3	112.5	6.93997	0.765976
18809	268.5	114.1	6.85098	0.766066
187	127.1	11.1	33.9507	0.923199
18705	142.4	13.7	30.6406	0.904313
18709	227.1	13.7	49.2947	1.02998
18711	226.9	13.4	50.5927	1.03354
18713	235.9	13.4	52.6500	1.05118
18714	258.0	13.4	57.8238	1.08135

Table 2E (cont.) Rb-Sr Analytical data

Sample	Rb (ppm)	Sr (ppm)	$^{87}Rb/^{86}Sr$	$^{87}Sr/^{86}Sr$
186	120.0	10.5	33.8337	0.927767
18605	173.3	14.0	36.7596	0.948655
18612	244.5	13.6	53.9222	1.06083
18613	258.9	13.7	56.7424	1.08367
176	94.9	177.8	1.54599	0.722118
17607	57.8	374.8	0.446481	0.712741
17613	264.0	130.0	5.90438	0.758005
17616	287.7	106.9	7.83619	0.771326
17617	296.1	100.1	8.62048	0.776867
17618	312.3	92.5	9.84506	0.784170
101	163.8	27.1	17.6832	0.825362
10107	35.2	86.0	1.18325	0.714598
10113	450.6	21.5	63.1951	1.13128
10115	591.6	17.7	103.374	1.39660
10116	1049.1	4.8	1084.75	8.17221
10104*	284.3	35.0	23.8428	0.864756
10108*	389.5	25.6	45.3412	1.00714
10111*	445.5	20.9	64.1603	1.13346
10113*	521.6	18.1	88.2863	1.29343
10114*	607.6	16.9	111.411	1.43777

Table 2E (cont.) Rb-Sr Analytical data. Analyses marked with a * are of size 500-210 μm, all others are 210-175 μm.

3 CHEMISTRY & PETROGRAPHY

A selection of 57 granitic clasts, including all those analysed geochronologically, have been subjected to chemical determinations. The importance of these analyses, along with petrographic studies, is to obtain further details regarding their origin and intrusive nature. This information, when combined with the age and provenance studies, will enable a more detailed interpretation of the Caledonian palaeoenvironment.

3.1 Analytical techniques

3.1.1 X-ray fluorescence (XRF)

X-ray fluorescence analysis has been undertaken for 28 elements, 10 major element oxides (SiO_2, TiO_2, Al_2O_3, FeO^{Total}, MnO, MgO, CaO, Na_2O, K_2O and P_2O_5) and 16 trace elements (Ba, Ce, Co, Cr, Cu, Ga, La, Nb, Ni, Pb, Rb, Sr, Th, Y, Zn & Zr). Major elements are measured on fused beads made from sieved rock powder (<68 µm) and flux (lithium tetraborate) in a weight ratio of 1:5.3. Trace elements are measured on pressed pellets comprising whole rock powder (<68 µm) and thermal binder (phenol formaldehyde) of weight ratio 6:1.

All the trace elements were analysed on a Philips PW 1220 semi-automated X-ray spectrometer as were the major elements during the early part of the study (those samples with the first digit being 1). The rest of the major element determinations were performed on a Philips PW 1450 sequential automatic X-ray spectrometer. The analyses used three different detector tubes (W, Cr and Mo) and five different reflecting crystals (Ge, LiF 220, LiF 200 P.E. (Penta erythritol) and T.A.P. (Thalium acid phthalate)). The combinations of tubes and crystals and the details of current, voltage, scintillation or flow detection and analysing angles follow those, with occasional minor modifications, described by Leake et al. (1969).

3.1.2 'Wet' chemistry

Traditional wet chemical analysis is necessary to determine the FeO, H_2O and CO_2 values which are not suitable for X-ray fluorescence methods.

FeO determination is by titration with standard dichromate solution after dissolution of the whole rock powder in sulphuric and hydrofluoric acid. This then enables the Fe_2O_3 content to be evaluated by reference to the total iron (FeO + Fe_2O_3 expressed as FeO) figure from the XRF data.

In the early work the H_2O and CO_2 values were determined using the Penfield method of combustion, absorbtion and gravimetry (as is the case for samples with first digit 1). In later analyses a total volatiles figure was produced by graphical methods as the H_2O and CO_2 percentages for granitic rocks have little practical use but help to verify the analysis total (see 3.1.6)

In addition to the above some Na_2O determinations were done by flame photometry to act as a check for the XRF values.

3.1.3 Microprobe analysis

Individual mineral analyses were possible using a Cambridge Instruments Microscan 5 machine. This utilizes X-ray radiation generated by an electron beam striking a finely polished thin section. Each element produces a characteristic X-ray energy spectrum which is measured by a solid state detector for a count time of 100 seconds. The total spectrum is processed by an on-line Data General Corporation Nova 2 mini-computer using a programme designed by Statham (1976) and modified by C.Farrow, which produces the analysis in weight percent oxides.

3.1.4 CIPW Norm

The major element oxides may be expressed in terms of an hypothetical series of arbitrarily selected minerals; the norm. Several methods of doing this are available. The original version was produced by Cross, Iddings, Pirsson and Washington (1903) and referred to as the CIPW norm. This system has survived with few modifications and the version used in this study is that of Kelsey (1965). The main feature of this norm is that no water is assumed to be present. In addition all Al_2O_3 is assigned to feldspar or feldspathoid until CaO, K_2O and Na_2O are exhausted, all CO_2 is combined with CaO to make calcite and the Mg:Fe ratio of ferromagnesian minerals is kept constant.(In many of the analyses in this study CO_2 was not determined and when applied to the norm this means that no calcite is made and there is marginally more CaO available for plagioclase incorporation. This factor has a very minimal effect in most cases, except sample 889 which exhibits extensive calcite veining).

There are other norms which use molecular rather than weight percents and incorporate hydrous minerals in the assemblage e.g. those of Niggli (1954) and Barth (1955), but they are not used in this study.

3.1.5 XTLFRAC

XTLFRAC is a computer programme devised by Stormer & Nicholls (1978). It assesses the feasibility of deriving one magma from another through the fractionation of selected mineral phases. This is achieved by using major oxide analyses of the magmas (rock samples) and fractionating minerals expressed in terms of major oxide components (microprobe analyses). The amount of each oxide removed by the minerals is compared with overall difference between the two magmas by minimizing the sum of residuals from a series of simultaneous equations through a least squares method. The amount of each phase removed (or added if so desired) is then expressed as a percentage of the

total removed and as a percentage of the initial magma.

The programme can also be modified to fit selected minerals to a magma composition and hence produce weight percent modes for individual rocks. This has been done by using microprobe analyses of minerals, or end member compositions, and fitting mineral phases observed in thin section to the whole rock chemical analysis (see 3.3). This approach works well but with the main problem being the presence of two or more mafic phases. In this case the programme tends to account for the minor oxides e.g. P_2O_5, MnO, TiO_2 in a way which frequently results in reasonable amount of one mafic phase and a small negative amount of the other. In many cases it was found best to only use the dominant mafic phase in the calculation. In absolute terms this would be a major problem but in the role used here its effects are minor (see 3.3).

3.1.6 Analytical precision

All XRF measurements are made in at least duplicate and averaged, using a peak - background measure to define the intensity for each element when compared with a ratio pellet. The absolute concentrations are calculated by comparison with international (NBS) and internal (Glasgow) calibration standards using a computing routine devised by C.Farrow. These standards are run with every batch of samples to act as a check on machine operation.

The detection limit and precision varies from element to element and are shown in Table 3A. Only in one instance have correction factors been applied to the data as a function of consistent variation from the recommended standard values. This is for Zr which is a poorly defined element, but overall the figures are thought to be broadly representative. The Rb and Sr values have the best precision but they too have been subjected to minor amendment. This is not through deviation from the standard values but due to the additional control provided by the isotopic measurements (Table 2E). The isotopic determinations are made on non-dehydrated rock powders and this may lead to variations of the order of $\pm$ 1%. They are, however, taken

Element or oxide	Method	RMS (%)	Detection limit (ppm)	Precision
SiO_2	XRF	2.00		Fair
Al_2O_3	"	1.80		"
TiO_2	"	0.06		Good
Fe_2O_3	"	0.30		"
FeO	Wet	--		V.Good
MgO	XRF	0.20		Good
CaO	"	0.16		"
Na_2O	"	0.16		"
K_2O	"	0.13		"
MnO	"	0.04		"
P_2O_5	"	0.04		"
H_2O)	Wet /			
CO_2)	graph	--		Poor
Ba	XRF		7	Fair
Ce	"		2	"
Co	"		10	Poor
Cr	"		2	"
Cu	"		3	Fair
Ga	"		3	Good
La	"		6	Fair
Nb	"		2	Good
Ni	"		4	Fair
Pb	"		14	"
Rb	XRF/MS		3	V.Good
Sr	"		3	"
Th	XRF		9	Fair
Y	"		3	"
Zn	"		3	"
Zr	"		6	Poor

Table 3A Parameters for whole rock chemical analyses

Sample	Rb			Sr		
	XRF	XRF*	MS	XRF	XRF*	MS
199	26	24	22.8	229	211	212.9
198	89	84	85.0	190	175	174.0
197	122	115	117.2	52	48	48.1
196	45	42	40.7	347	320	322.1
194	132	124	117.4	69	64	61.2
191	80	75	77.1	154	142	142.4
188	109	102	100.0	197	181	179.1
187	134	126	127.1	12	11	11.1
186	128	120	120.0	10	10	10.5
176	95	89	94.9	185	170	177.8
101	167	157	163.8	30	28	27.1
299	13	12	9.3	177	172	170.0
286	34	31	29.0	98	95	97.5
284	88	81	82.9	116	113	115.5
399	39	36	32.1	22	21	22.1
591	26	24	22.3	270	263	267.5
587	115	106	105.0	235	229	231.1
580	80	73	76.7	279	271	277.8
579	84	77	77.0	261	254	248.2
889	61	56	56.3	195	190	189.5
988	87	80	83.0	213	208	208.1
996	50	46	45.8	379	369	369.2
993	48	44	44.7	482	470	467.8
985	13	12	11.5	272	265	261.9
982	70	64	67.6	369	360	363.1

Table 3B Comparison of Rb and Sr values determined by X-ray fluorescence (XRF) and mass-spectrometry (MS). Column XRF* = XRF value x averaged difference between XRF and MS values.

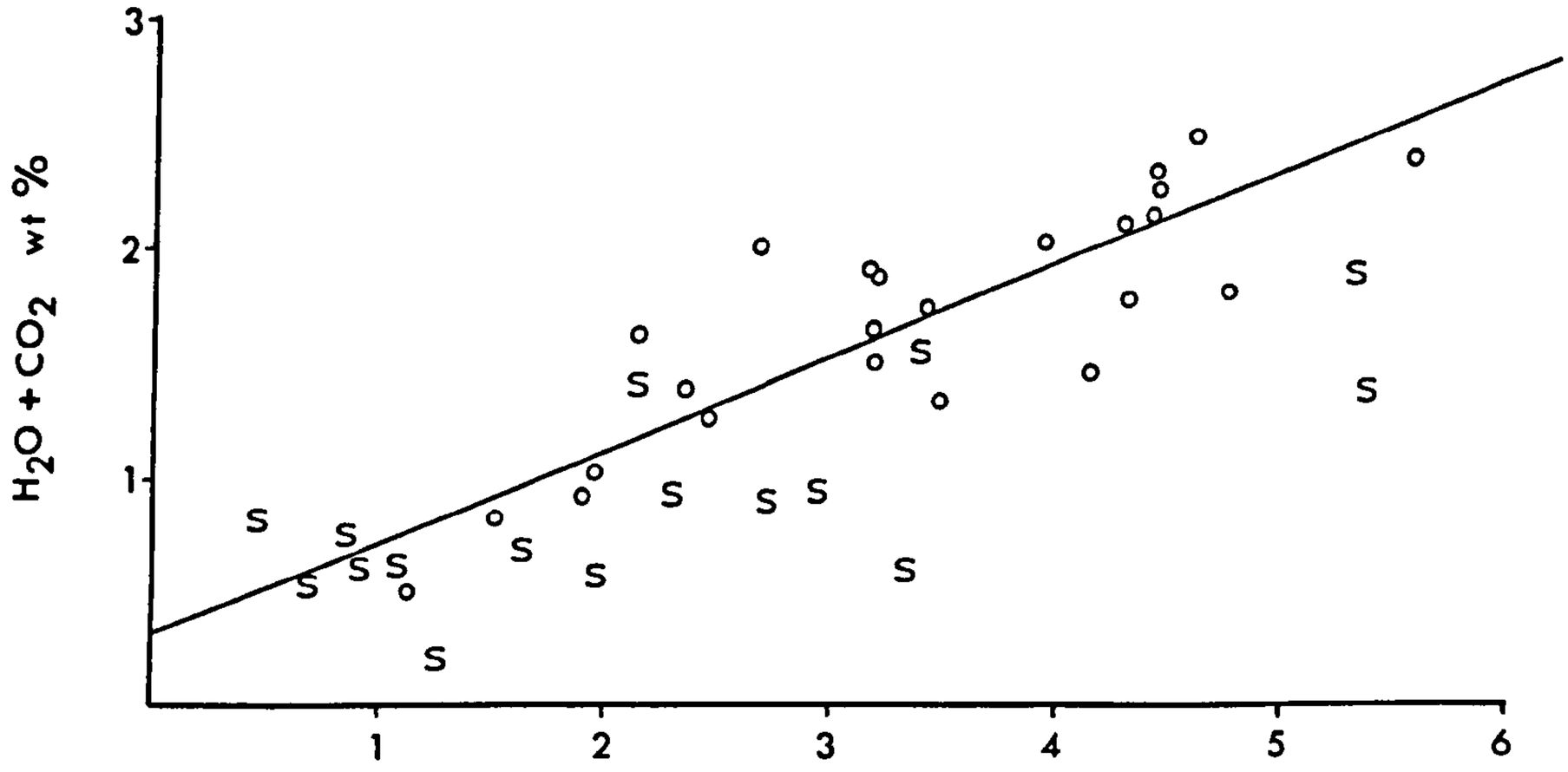

Fig. 3/1 Graph used in $H_2O + CO_2$ determinations.

to be more accurate than the XRF values. Table 3B shows the comparison between XRF and isotopic Rb and Sr determinations for 25 whole rock samples. The raw XRF data are consistently higher than the isotopic values and correction factors have been applied which reduce the XRF values. These correction factors, of around 5%, vary between two groups (101-199 and 284-996) were in different batches of XRF analyses.

The wet chemical determinations of FeO show good agreements between replicates and check well with the standards. The H_2O and CO_2 values are less reproduceable with often 3,4 or more values necessary to ensure agreement.

The graphical approach for determining total volatiles ($\sim H_2O + CO_2$) and used for all analyses with the first digit being 2,3,5,8 or 9, involved plotting $H_2O + CO_2$ weight percent versus percentage loss on ignition + FeO for wet analysed samples. This revealed a straight line with a correlation coefficient (r) of 0.83 (Fig. 3/1). The total volatile content of the later samples was read from this graph with an accuracy of around $\pm$ 10%.

The oxides are summed and ideally should total 100%. Naturally this is rarely the case with the bulk of the analyses falling in the range 97-103%. These totals

have been recalculated to 100 $\pm$ 1%, but keeping any 'wet' determinations and MnO and P_2O_5 the same. Analyses marked with an asterisk fell outside these limits but have been recalculated and included for comparative purposes. The data are presented in Table 3C.

Table 3C Chemical analyses of individual clasts.

The first digit of the analysis number refers to the horizon from which the specimen was collected in the following manner :-

First digit	Horizon
1	Benan conglomerate
2	Kilranny conglomerate
3	Tormitchell conglomerate
5	Craigskelly conglomerate
8	Kirkland conglomerate
9	Corsewall conglomerate

PAGE
MISSING
IN
ORIGINAL

No.	199	198	197	196	195 *
Name	Tonalite	Granite	Granite	Tonalite	Granod.
SiO_2	69.96	72.67	75.96	63.74	62.87
TiO_2	0.41	0.29	0.07	0.39	0.26
Al_2O_3	14.63	12.14	12.02	15.98	16.39
Fe_2O_3	1.40	1.23	0.33	3.02	2.91
FeO	2.55	1.64	0.81	2.43	2.58
MnO	0.09	0.06	0.02	0.08	0.10
MgO	1.95	1.51	0.38	3.17	3.15
CaO	3.02	1.51	0.67	3.70	1.94
Na_2O	3.51	2.78	4.22	3.31	5.00
K_2O	1.04	3.21	3.71	1.84	2.33
P_2O_5	0.09	0.06	0.03	0.12	0.11
H_2O	1.95	1.73	0.67	2.05	2.22
CO_2	0.13	0.17	0.11	0.09	0.12
Total	100.73	99.01	99.00	99.92	99.98
Ba	211	699	592	496	571
Ce	11	39	29	20	24
Co	10	7	2	12	16
Cr	13	24	15	26	41
Cu	0	0	8	0	0
Ga	15	12	13	14	17
La	5	24	15	6	13
Nb	5	10	8	7	6
Ni	1	6	2	1	7
Pb	6	21	16	6	9
Rb	25	85	117	43	53
Sr	211	175	48	320	154
Th	4	9	11	4	9
Y	12	20	31	9	11
Zn	47	34	10	38	41
Zr	88	162	101	61	68

Table 3C Chemical analyses of individual clasts. Those analyses marked thus (*) are recalculated from outside the range 97-103%.

NO.	194	193	192	191	190
Name	Granite	Granod.	Tonalite	Granod.	Granite
SiO_2	77.63	69.15	72.34	67.55	73.26
TiO_2	0.07	0.40	0.30	0.38	0.28
Al_2O_3	12.43	13.22	13.28	13.56	13.07
Fe_2O_3	0.38	1.66	1.55	2.15	0.66
FeO	0.81	2.43	1.74	2.54	1.85
MnO	0.02	0.08	0.06	0.09	0.06
MgO	0.31	3.20	1.46	2.84	1.11
CaO	0.47	2.16	2.08	1.90	1.46
Na_2O	3.99	2.71	3.68	2.53	2.86
K_2O	3.64	2.69	1.15	2.93	3.62
P_2O_5	0.04	0.10	0.08	0.08	0.07
H_2O	0.66	2.27	1.65	2.33	1.44
CO_2	0.15	0.60	0.14	0.17	0.06
Total	100.60	99.77	99.51	99.07	99.82
Ba	548	616	252	640	802
Ce	40	32	8	16	59
Co	4	10	5	13	3
Cr	45	37	13	35	22
Cu	0	30	31	26	16
Ga	10	10	12	12	10
La	19	14	3	9	28
Nb	8	9	6	8	8
Ni	0	10	2	6	5
Pb	16	14	6	10	20
Rb	124	76	25	75	94
Sr	64	180	207	142	190
Th	12	7	3	7	10
Y	36	7	8	11	21
Zn	9	51	44	50	29
Zr	97	129	119	119	121

Table 3C

No.	189 *	188	187	186	185 *
Name	Granod.	Granite	Granite	Granite	Granite
SiO_2	70.28	73.43	75.84	74.72	74.77
TiO_2	0.30	0.28	0.10	0.11	0.26
Al_2O_3	14.49	13.73	12.28	12.51	12.68
Fe_2O_3	2.14	0.76	0.99	0.46	1.18
FeO	1.31	1.93	0.94	1.21	1.58
MnO	0.06	0.05	0.04	0.01	0.05
MgO	1.84	1.14	0.29	0.76	1.45
CaO	1.79	1.26	0.17	0.48	1.15
Na_2O	3.08	2.63	4.75	4.35	2.59
K_2O	2.76	3.51	4.13	3.69	3.45
P_2O_5	0.06	0.08	0.04	0.03	0.07
H_2O	1.82	1.62	0.68	0.88	1.47
CO_2	0.21	0.17	0.20	0.56	0.14
Total	100.14	100.60	100.45	99.76	100.84
Ba	511	829	79	91	712
Ce	38	52	90	71	52
Co	11	7	0	0	7
Cr	34	29	33	21	34
Cu	41	4	12	18	40
Ga	11	11	28	24	13
La	20	32	38	31	26
Nb	10	11	54	59	14
Ni	8	4	2	1	5
Pb	16	19	8	84	25
Rb	72	102	126	120	95
Sr	235	181	11	10	166
Th	8	14	18	21	13
Y	9	19	75	103	15
Zn	41	31	114	114	36
Zr	126	151	512	585	134

Table 3C

No.	184	183	182	181	180
Name	Granod.	Granod.	Tonalite	Granite	Granod.
SiO_2	70.19	71.87	68.07	74.53	60.20
TiO_2	0.39	0.26	0.54	0.20	0.48
Al_2O_3	13.33	14.24	14.64	13.25	16.88
Fe_2O_3	1.63	1.14	2.61	0.83	3.10
FeO	2.56	1.95	2.28	1.34	3.47
MnO	0.07	0.07	0.08	0.05	0.11
MgO	2.67	1.06	2.46	1.15	3.82
CaO	1.74	2.06	3.26	0.98	4.23
Na_2O	2.96	3.89	3.19	2.91	3.04
K_2O	2.68	2.41	1.07	4.02	2.88
P_2O_5	0.07	0.06	0.11	0.06	0.12
H_2O	2.14	1.28	1.94	1.20	2.19
CO_2	0.12	0.06	0.20	0.08	0.25
Total	100.55	100.35	100.45	100.60	100.78
Ba	510	447	181	970	555
Ce	14	28	12	31	34
Co	10	7	12	22	23
Cr	75	40	19	22	54
Cu	37	8	12	17	39
Ga	12	12	15	13	21
La	8	7	4	15	12
Nb	11	8	6	7	6
Ni	6	1	3	6	10
Pb	7	13	5	16	2
Rb	70	63	33	93	72
Sr	155	270	181	170	291
Th	15	7	0	9	7
Y	13	14	4	9	13
Zn	50	38	54	25	51
Zr	173	116	124	80	54

Table 3C

No.	179	178	177	176	101
Name	Tonalite	Granite	Granite	Granite	Granite
SiO_2	70.96	74.60	76.94	73.85	77.08
TiO_2	0.33	0.26	0.07	0.20	0.05
Al_2O_3	13.32	12.32	11.92	12.56	12.34
Fe_2O_3	1.71	1.03	0.15	0.95	0.24
FeO	2.36	1.68	0.84	1.20	0.65
MnO	0.09	0.06	0.02	0.04	0.04
MgO	2.12	1.43	0.33	1.03	0.32
CaO	2.69	1.15	0.40	1.01	0.28
Na_2O	3.49	2.98	4.39	3.13	3.60
K_2O	1.49	3.29	3.60	3.96	4.33
P_2O_5	0.07	0.07	0.03	0.05	0.03
H_2O	1.64	1.32	0.79	1.42	0.37
CO_2	0.18	0.16	0.23	0.24	0.17
Total	100.35	100.36	99.71	99.64	99.50
Ba	266	629	542	817	581
Ce	13	50	31	15	31
Co	10	6	3	10	3
Cr	23	22	7	31	19
Cu	21	40	17	20	8
Ga	13	14	12	10	13
La	6	23	15	10	18
Nb	1	7	3	0	9
Ni	1	5	1	2	3
Pb	7	20	13	17	22
Rb	41	87	116	89	157
Sr	169	152	54	170	28
Th	8	11	10	11	13
Y	12	14	25	10	18
Zn	48	34	15	20	16
Zr	78	117	76	35	41

Table 3C

No.	100	999	996	995	994
Name	Granod.	Granod.	Granod.	Granod.	Granod.
SiO_2	74.08	66.66	74.24	73.86	69.63
TiO_2	0.21	0.66	0.11	0.36	0.41
Al_2O_3	13.04	14.70	13.64	13.08	13.90
Fe_2O_3	0.24	1.73	1.26	1.02	1.82
FeO	2.13	3.37	0.48	1.69	2.45
MnO	0.06	0.08	0.07	0.07	0.10
MgO	0.89	2.79	0.58	1.20	2.44
CaO	1.49	3.60	1.45	1.59	1.84
Na_2O	3.93	2.96	4.71	3.25	3.22
K_2O	2.44	1.42	2.27	3.16	2.67
P_2O_5	0.05	0.11	0.05	0.08	0.08
H_2O	1.40	2.85	1.15	1.50	2.35
CO_2	0.34				
Total	100.31	100.93	100.01	100.86	100.89
Ba	458	445	696	1098	699
Ce	21	12	36	51	26
Co	4	20	0	5	9
Cr	10	51	9	19	35
Cu	13	59	16	13	9
Ga	14	17	13	16	13
La	11	6	16	25	8
Nb	5	8	10	9	7
Ni	2	13	2	4	8
Pb	21	8	21	13	11
Rb	75	40	46	59	69
Sr	161	369	369	288	497
Th	5	5	10	14	8
Y	18	15	24	17	7
Zn	35	56	32	38	51
Zr	93	208	59	154	131

Table 3C

No.	993	989	988	985	982
Name	Granod.	Tonalite	Granod.	Tonalite	Granod.
SiO_2	68.56	68.11	72.62	74.93	68.51
TiO_2	0.39	0.42	0.64	0.27	0.41
Al_2O_3	14.34	14.50	12.59	11.35	13.89
Fe_2O_3	1.67	2.15	1.23	1.20	1.62
FeO	2.49	2.68	3.06	1.78	2.73
MnO	0.11	0.11	0.09	0.08	0.10
MgO	2.05	2.19	1.68	1.27	2.27
CaO	2.66	4.43	1.89	2.18	2.22
Na_2O	2.97	2.96	2.39	4.91	2.97
K_2O	2.09	0.72	2.77	0.53	2.76
P_2O_5	0.07	0.08	0.03	0.05	0.08
H_2O) CO_2)	2.33	1.77	1.98	1.45	1.87
Total	99.75	100.12	100.97	100.00	99.43
Ba	761	188	756	110	833
Ce	26	36	53	10	16
Co	6	11	12	7	13
Cr	50	89	53	26	50
Cu	15	8	9	22	15
Ga	12	14	20	16	21
La	11	15	32	5	11
Nb	7	9	11	6	7
Ni	8	8	22	6	7
Pb	12	5	14	5	14
Rb	44	16	80	12	64
Sr	470	538	208	265	360
Th	9	9	18	3	8
Y	10	14	9	4	11
Zn	57	35	51	51	54
Zr	113	162	213	115	137

Table 3C

No.	591	589	587	583	581
Name	Tonalite	Granite	Granod.	Tonalite	Granod.
SiO_2	70.99	76.46	76.24	76.32	74.57
TiO_2	0.36	0.07	0.15	0.15	0.24
Al_2O_3	14.06	11.78	11.92	12.42	13.07
Fe_2O_3	1.26	0.39	0.53	0.85	0.87
FeO	2.27	0.69	0.91	0.82	1.10
MnO	0.12	0.03	0.05	0.04	0.07
MgO	1.29	0.28	0.37	0.60	0.79
CaO	2.42	0.50	0.63	1.53	1.42
Na_2O	5.18	2.58	4.08	5.47	4.51
K_2O	0.91	6.47	3.36	0.95	2.73
P_2O_5	0.09	0.02	0.04	0.04	0.07
H_2O) CO_2)	1.77	0.93	0.95	0.90	0.76
Total	100.72	100.20	99.23	100.09	100.20
Ba	492	755	971	404	936
Ce	11	20	47	26	33
Co	0	3	6	0	6
Cr	22	8	8	17	17
Cu	16	22	13	8	14
Ga	16	12	11	17	13
La	5	7	23	9	15
Nb	5	17	9	3	6
Ni	0	0	0	1	0
Pb	4	8	9	3	6
Rb	24	125	106	14	64
Sr	263	34	229	193	305
Th	4	10	11	4	9
Y	42	42	25	17	15
Zn	66	14	24	32	26
Zr	103	36	65	78	70

Table 3C

No.	580	579	299	297	296
Name	Granite	Granod.	Tonalite	Tonalite	Granod.
SiO_2	76.18	76.36	77.75	66.40	77.45
TiO_2	0.20	0.15	0.21	0.69	0.20
Al_2O_3	12.82	11.73	12.05	14.22	11.95
Fe_2O_3	0.74	0.55	0.94	2.15	0.78
FeO	0.67	0.82	0.79	2.98	0.83
MnO	0.03	0.04	0.03	0.07	0.04
MgO	0.43	0.54	0.47	1.26	0.48
CaO	1.30	1.11	2.09	2.78	1.04
Na_2O	3.58	3.90	5.30	6.55	4.33
K_2O	3.96	3.36	0.52	0.81	2.66
P_2O_5	0.04	0.04	0.04	0.21	0.04
H_2O) CO_2)	1.04	0.75	1.02	1.98	0.69
Total	100.99	99.35	100.61	100.22	100.49
Ba	5021	1135	115	155	475
Ce	113	31	19	43	25
Co	3	0	4	2	2
Cr	4	17	12	9	10
Cu	12	20	14	7	16
Ga	10	10	9	15	10
La	60	12	9	12	12
Nb	4	5	8	8	6
Ni	0	3	6	0	0
Pb	16	6	8	7	5
Rb	73	77	12	16	67
Sr	271	254	172	205	97
Th	25	11	11	9	6
Y	7	14	21	42	21
Zn	19	19	9	21	17
Zr	?	64	142	152	107

Table 3C

No.	289	286	284	283	281
Name	Tonalite	Granod.	Granod.	Tonalite	Granite
SiO_2	77.34	76.07	76.88	73.80	78.69
TiO_2	0.20	0.21	0.20	0.35	0.11
Al_2O_3	12.39	11.89	12.33	13.15	11.10
Fe_2O_3	0.94	0.90	1.34	1.69	0.82
FeO	0.74	1.03	0.76	1.58	0.32
MnO	0.03	0.05	0.04	0.06	0.02
MgO	0.57	0.63	0.50	1.15	0.24
CaO	1.15	1.22	0.88	0.97	0.33
Na_2O	6.30	5.14	4.25	6.08	4.36
K_2O	0.41	1.81	2.73	0.50	3.66
P_2O_5	0.04	0.04	0.04	0.08	0.03
H_2O) CO_2)	0.72	0.91	0.79	0.96	0.66
Total	100.83	99.90	100.74	100.37	100.34
Ba	79	702	437	72	451
Ce	33	21	26	25	33
Co	2	5	0	6	1
Cr	17	11	11	11	16
Cu	14	10	13	17	24
Ga	14	12	12	15	11
La	16	13	14	9	17
Nb	6	6	6	7	6
Ni	1	2	0	0	1
Pb	2	7	6	4	10
Rb	6	31	81	8	114
Sr	123	95	113	117	52
Th	7	9	11	12	14
Y	24	18	25	28	31
Zn	14	18	17	31	16
Zr	153	107	111	187	105

Table 3C

No.	889	399
Name	Q. Monz.	Granod.
SiO_2	57.44	77.03
TiO_2	0.09	0.14
Al_2O_3	15.76	11.70
Fe_2O_3	2.43	1.08
FeO	0.76	0.67
MnO	0.09	0.04
MgO	1.72	0.30
CaO	7.80	0.28
Na_2O	6.66	6.09
K_2O	3.29	2.16
P_2O_5	0.06	0.02
H_2O) CO_2)	3.38	0.59
Total	99.48	100.10
Ba	176	57
Ce	26	86
Co	11	2
Cr	8	14
Cu	6	13
Ga	21	20
La	8	37
Nb	61	25
Ni	30	1
Pb	0	0
Rb	56	36
Sr	190	21
Th	2	16
Y	2	43
Zn	61	69
Zr	853	484

Table 3C

No.	599	595	593	585	582
Name	Porphyry	Porphyry	Porphyry	Porphyry	Porphyry
SiO_2	71.20	70.02	67.51	70.67	70.13
TiO_2	0.16	0.17	0.17	0.26	0.27
Al_2O_3	14.79	16.00	14.50	14.69	14.63
Fe_2O_3	0.44	0.63	0.56	1.06	1.04
FeO	0.52	0.58	0.88	0.73	0.74
MnO	0.03	0.04	0.08	0.05	0.04
MgO	0.73	0.72	1.94	1.25	1.01
CaO	2.20	1.89	3.64	2.39	2.15
Na_2O	6.04	6.37	6.24	6.40	6.55
K_2O	2.29	1.89	1.96	1.86	2.20
P_2O_5	0.05	0.06	0.07	0.13	0.15
H_2O) CO_2)	1.54	1.63	2.43	0.83	1.04
Total	99.99	100.00	99.98	100.32	99.95
Ba	1625	1535	1818	993	1332
Ce	18	13	11	42	45
Co	4	0	0	2	6
Cr	9	9	7	48	10
Cu	18	22	20	15	17
Ga	14	16	12	13	22
La	4	6	2	21	25
Nb	6	2	6	4	5
Ni	2	4	4	15	3
Pb	10	12	12	6	5
Rb	15	25	19	18	29
Sr	1203	1089	1096	1198	1146
Th	2	2	2	9	7
Y	1	0	6	10	9
Zn	10	46	12	23	22
Zr	89	107	74	116	102

Table 3C

Norm	199	198	197	196	195	194	193	192	191
Ap	0.21	0.14	0.07	0.28	0.26	0.09	0.23	0.19	0.19
Il	0.78	0.55	0.13	0.74	0.49	0.13	0.76	0.57	0.72
Or	6.15	18.97	21.93	10.87	13.77	21.51	15.90	6.80	17.32
Ab	29.69	23.52	35.70	28.00	42.30	33.75	22.93	31.13	21.40
An	13.57	6.03	2.43	17.00	8.15	1.12	6.27	8.91	7.83
C	2.76	1.88	0.17	2.31	2.66	1.52	3.55	2.72	3.36
Mt	2.03	1.78	0.48	4.38	4.22	0.55	2.41	2.25	3.12
DiWo	-	-	-	-	-	-	-	-	-
DiEn	-	-	-	-	-	-	-	-	-
DiFs	-	-	-	-	-	-	-	-	-
HyEn	4.86	3.76	0.95	7.89	7.85	0.77	5.73	3.64	7.07
HyFs	2.85	1.52	1.10	1.32	1.90	1.06	2.43	1.42	2.26
Q	35.50	38.67	35.10	24.77	15.79	39.06	35.85	39.86	32.98
Cc	0.30	0.39	0.25	0.21	0.27	0.34	1.37	0.32	0.39

Mode (Weight Percent)

Ab	30.38	23.73	34.62	26.99	41.67	34.21	23.18	32.50	22.52
An	15.56	7.57	2.54	17.80	9.34	2.72	10.87	11.24	10.17
Kf	2.46	17.23	21.66	5.06	8.23	21.62	12.59	4.46	13.76
Q	35.47	37.85	35.50	26.73	17.36	37.63	34.56	37.84	32.06
Bi	16.13	13.62	5.69	23.41	23.40	3.82	18.80	13.95	21.49
Hb	-	-	-	-	-	-	-	-	-
Mu	-	-	-	-	-	-	-	-	-
Cc	-	-	-	-	-	-	-	-	-
Ep	-	-	-	-	-	-	-	-	-
Sums	0.10	0.93	0.56	1.03	0.87	0.12	1.13	0.35	1.46

Table 3D CIPW norm and weight percent mode for analysed clasts (Sums represents the goodness of fit in the mode calculation, values < 2.5 are acceptable)

Norm	190	189	188	187	186	185	184	183	182
Ap	0.16	0.14	0.19	0.09	0.07	0.16	0.16	0.14	0.26
Il	0.53	0.57	0.53	0.19	0.21	0.49	0.74	0.49	1.03
Or	21.39	16.31	20.74	24.41	21.81	20.39	15.84	14.24	6.32
Ab	24.19	26.06	22.26	40.16	36.80	21.91	25.04	32.91	26.99
An	6.41	7.16	4.65	-	0.04	4.36	7.42	9.45	14.19
C	2.10	3.81	3.90	-	1.35	3.09	2.84	1.77	3.03
Mt	0.94	3.10	1.10	1.43	0.67	1.71	2.36	1.65	3.78
DiWo	-	-	-	0.03	-	-	-	-	-
DiEn	-	-	-	0.02	-	-	-	-	-
DiFs	-	-	-	0.02	-	-	-	-	-
HyEn	2.76	4.58	2.84	0.71	1.89	3.61	6.65	2.64	6.13
HyFs	2.45	0.14	2.45	0.73	1.66	1.50	2.71	2.21	1.13
Q	37.23	35.90	39.87	31.62	33.39	41.77	34.30	33.35	35.10
Cc	0.14	0.38	0.39	0.18	0.77	0.32	0.27	0.14	0.46
Mode	(Weight Percent)								
Ab	25.05	28.52	25.23	37.83	36.28	23.62	25.55	32.93	27.21
An	7.85	10.59	8.35	-	2.02	6.98	9.09	10.35	16.46
Kf	20.31	14.65	20.31	24.71	21.47	19.17	12.15	11.80	1.51
Q	36.14	31.99	35.88	31.11	32.61	39.50	34.91	33.30	34.76
Bi	10.66	14.25	10.23	1.97	6.78	10.73	18.29	11.61	20.06
Hb	-	-	-	4.38	0.84	-	-	-	-
Mu	-	-	-	-	-	-	-	-	-
Cc	-	-	-	-	-	-	-	-	-
Ep	-	-	-	-	-	-	-	-	-
Sums	0.13	0.46	0.58	0.01	0.27	0.30	0.67	0.09	0.22

Table 3D

Norm	181	180	179	178	177	176	101	100	999
Ap	0.14	0.28	0.16	0.16	0.07	0.12	0.07	0.12	0.26
Il	0.38	0.91	0.63	0.49	0.13	0.38	0.10	0.40	1.25
Or	23.76	17.02	8.81	19.44	21.28	23.40	25.60	14.42	8.39
Ab	24.62	25.72	29.52	25.21	37.14	26.48	30.45	33.25	25.04
An	3.96	18.62	11.75	4.24	0.33	3.17	0.12	4.92	17.14
C	2.66	1.94	1.66	2.30	0.68	1.96	1.69	2.13	2.01
Mt	1.20	4.50	2.48	1.49	0.22	1.38	0.35	0.35	2.51
DiWo	-	-	-	-	-	-	-	-	-
DiEn	-	-	-	-	-	-	-	-	-
DiFs	-	-	-	-	-	-	-	-	-
HyEn	2.86	9.51	5.28	3.56	0.82	2.57	0.80	2.22	6.95
HyFs	1.45	3.02	2.38	1.81	1.30	1.09	0.91	3.37	3.67
Q	38.13	16.38	35.64	39.89	36.40	37.09	38.62	36.90	30.77
Cc	0.18	0.57	0.41	0.36	0.52	0.55	0.39	0.77	-

Mode (Weight Percent)

Ab	26.27	22.45	28.27	25.78	36.43	26.89	30.79	33.41	24.86
An	6.07	19.03	12.63	6.17	1.48	5.26	1.61	7.54	12.43
Kf	23.34	9.09	4.27	17.77	21.21	22.72	24.99	12.80	9.02
Q	35.91	21.73	37.83	39.08	36.22	35.45	37.05	36.45	33.15
Bi	8.41	27.70	17.00	11.21	4.66	9.67	3.51	9.79	16.00
Hb	-	-	-	-	-	-	-	-	-
Mu	-	-	-	-	-	-	2.05	-	-
Cc	-	-	-	-	-	-	-	-	-
Ep	-	-	-	-	-	-	-	-	4.54
Sums	0.26	1.46	0.29	0.09	0.24	0.30	0.04	0.10	1.65

Table 3D

Norm	996	995	994	993	989	988	985	982	599
Ap	0.12	0.19	0.19	0.16	0.19	0.07	0.12	0.19	0.12
Il	0.21	0.68	0.78	0.74	0.80	1.22	0.51	0.78	0.30
Or	13.42	18.68	15.78	12.35	4.26	16.37	3.13	16.31	13.53
Ab	39.84	27.49	27.24	25.13	25.04	20.22	41.54	25.13	51.10
An	6.87	7.36	8.61	12.74	21.46	9.18	7.36	10.49	6.48
C	0.92	1.61	2.56	2.52	0.99	2.30	-	2.17	-
Mt	1.23	1.48	2.64	2.42	3.12	1.78	1.74	2.35	0.64
DiWo	-	-	-	-	-	-	1.30	-	1.72
DiEn	-	-	-	-	-	-	0.78	-	1.30
DiFs	-	-	-	-	-	-	0.45	-	0.24
HyEn	1.44	2.99	6.03	5.11	5.45	4.18	2.40	5.65	0.51
HyFs	-	1.67	2.32	2.55	2.45	3.55	1.38	3.00	0.10
Q	34.32	37.13	32.30	33.57	34.49	40.03	37.74	31.39	22.38
Cc	-	-	-	-	-	-	-	-	-

Mode (Weight Percent)

Ab	39.90	27.51	27.82	26.00	24.53	19.65	37.21	25.14	47.96
An	7.24	8.01	9.56	13.82	17.55	9.18	7.96	11.08	8.72
Kf	12.53	16.74	12.01	9.06	-	10.84	-	12.55	11.96
Q	33.44	37.19	33.01	33.17	36.63	41.62	42.01	32.34	25.12
Bi	6.90	10.56	17.60	17.95	17.56	16.25	12.82	18.89	6.24
Hb	-	-	-	-	-	-	-	-	-
Mu	-	-	-	-	-	2.45	-	-	-
Cc	-	-	-	-	-	-	-	-	-
Ep	-	-	-	-	3.73	-	-	-	-
Sums	0.11	0.02	0.29	0.46	0.26	0.07	1.53	0.49	1.75

Table 3D

Norm	595	593	591	589	587	585	583	582	581
Ap	0.14	0.16	0.21	0.05	0.09	0.30	0.09	0.35	0.16
Il	0.32	0.32	0.68	0.13	0.29	0.49	0.29	0.51	0.46
Or	11.17	11.58	5.39	38.24	19.86	10.99	5.61	13.00	16.13
Ab	53.89	52.79	43.82	21.83	34.52	54.14	46.27	55.41	38.15
An	8.99	5.77	11.42	1.45	2.86	5.86	6.53	4.02	6.59
C	0.18	-	0.37	-	0.52	-	-	-	0.28
Mt	0.91	0.81	1.83	0.57	0.77	1.54	1.23	1.51	1.26
DiWo	-	4.94	-	0.37	-	2.14	0.33	2.37	-
DiEn	-	3.76	-	0.17	-	1.84	0.23	2.01	-
DiFs	-	0.68	-	0.20	-	0.02	0.08	0.04	-
HyEn	1.79	1.08	3.21	0.53	0.92	1.27	1.27	0.50	1.97
HyFs	0.26	0.19	2.53	0.63	0.99	0.01	0.46	0.01	0.91
Q	20.66	15.37	29.37	35.07	37.41	20.80	36.72	19.12	33.45
Cc	-	-	-	-	-	-	-	-	-

Mode (WeightPercent)

Ab	53.78	44.93	41.76	20.15	34.19	49.36	44.50	50.41	36.76
An	9.21	12.60	10.77	1.42	2.86	8.67	6.48	7.28	6.18
Kf	13.49	7.07	2.49	40.35	19.53	7.45	3.51	9.67	14.31
Q	18.10	23.65	31.02	34.16	37.02	25.56	38.47	23.53	34.88
Bi	-	11.76	10.70	-	6.41	8.96	6.96	9.11	7.87
Hb	5.42	-	3.26	3.93	-	-	-	-	-
Mu	-	-	-	-	-	-	-	-	-
Cc	-	-	-	-	-	-	-	-	-
Ep	-	-	-	-	-	-	-	-	-
Sums	1.30	9.71	0.16	0.12	0.38	1.99	0.31	2.52	0.13

Table 3D

Norm	580	579	299	297	296	295	289	286	284
Ap	0.09	0.09	0.10	0.48	0.10	0.12	0.10	0.10	0.10
Il	0.38	0.29	0.40	1.31	0.38	0.84	0.38	0.40	0.38
Or	23.40	19.86	3.07	4.79	15.72	9.63	2.42	10.70	16.13
Ab	30.29	32.99	44.84	55.41	36.63	21.74	53.30	43.48	35.95
An	6.19	4.58	7.55	7.01	4.90	24.53	4.32	4.03	4.10
C	0.38	-	-	-	0.15	-	-	-	0.88
Mt	1.07	0.80	1.36	3.12	1.13	3.13	1.36	1.31	1.87
DiWo	-	0.28	1.07	5.88	-	5.78	0.47	0.74	-
DiEn	-	0.17	0.76	3.14	-	3.48	0.36	0.46	-
DiFs	-	0.10	0.21	2.56	-	1.99	0.06	0.23	-
HyEn	1.07	1.18	0.41	-	1.20	12.03	1.06	1.11	1.25
HyFs	0.29	0.71	0.12	-	0.55	6.87	0.19	0.56	-
Q	36.75	37.52	39.67	13.67	39.00	7.24	36.05	35.82	39.10
Cc	-	-	-	-	-	-	-	-	-

Mode (Weight Percent)

Ab	29.43	31.44	42.12	36.38	35.76	51.69	41.03	35.47
An	5.93	4.43	8.60	21.52	4.67	4.74	4.43	4.17
Kf	23.58	18.95	0.32	-	17.07	2.75	8.29	14.65
Q	36.38	38.74	42.18	23.06	37.39	35.38	38.14	38.90
Bi	3.15	6.45	6.78	-	-	-	8.11	6.81
Hb	1.54	-	-	19.04	5.11	5.44	-	-
Mu	-	-	-	-	-	-	-	-
Cc	-	-	-	-	-	-	-	-
Ep	-	-	-	-	-	-	-	-
Sums	0.04	0.52	0.54	7.53	0.27	0.31	0.62	0.19

Table 3D

Norm	283	281	889	399
Ap	0.18	0.10	0.13	0.04
Il	0.67	0.21	0.17	0.27
Or	2.96	21.63	19.44	12.77
Ab	51.43	36.71	44.42	48.14
An	4.29	-	3.39	-
C	1.04	-	-	-
Mt	2.45	0.71	2.19	0.08
DiWo	-	0.60	4.60	0.53
DiEn	-	0.52	4.28	0.23
DiFs	-	-	-	0.29
HyEn	2.86	0.08	-	0.52
HyFs	0.93	-	-	0.66
Q	32.53	38.69	-	32.96
Cc	-	-	-	-
			Wo 9.62	
			Ne 6.46	
Mode (Weight Percent)				
Ab	50.29	34.84	52.74	48.31
An	4.18	0.31	2.37	-
Kf	-	20.80	15.10	13.11
Q	33.43	39.89	6.59	32.54
Bi	12.09	4.15	10.86	-
Hb	-	-	-	6.04
Mu	-	-	-	-
Cc	-	-	12.34	-
Ep	-	-	-	-
Sums	0.11	0.27	0.86	0.19

Table 3D

3.2 Petrography

The petrographic aspects of the Ayrshire granitic suite will be discussed in broad terms, with more extensive descriptions of the individual clasts dated given in Appendix I.

3.2.1 Granitoids

All the samples contain quartz, plagioclase and opaque minerals in varying proportions ± potassium feldspar, biotite and hornblende as the major constituents. The minor minerals include muscovite, zircon, sphene, apatite and epidote. The modal composition of the chemically analysed clasts has been determined using the XTLFRAC programme (3.1.5) and the resulting weight percent modes, along with the CIPW norm values, are presented in Table 3D.

The presence of plagioclase as discrete grains in all samples classifies them as subsolvus in the terminology of Tuttle & Bowen (1958). The plagioclase is, however, often present as exsolution lamellae in perthites which tend to develop in the more acid clasts. The potassium feldspar, as well as being the host in the perthite exsolution, may also form discrete crystals.

The overall plagioclase composition, as determined from the CIPW norm, varies from An 00 in clast 187 to An 46 in 989. These figures, however, represent the average composition and in detail many rocks contain well developed optically zoned plagioclase. Microprobe analyses of three clasts containing zoned plagioclases (Figs. 3/2 &3/3) are presented graphically in Figs. 3/4 to 3/6. Sample 182, a tonalite[1], shows equal dominance of Ca and Na with minor K in the zones (Fig. 3/4) but with no specific compositional trend although the extreme margins show a drop in Ca reflecting late alkali enrichment. Granite 176 shows plagioclase with a lower Ca content and with a trend from a calcic core (An43 Ab56 Or01) to a sodic rim (An01 Ab98 Or01) (Fig. 3/5). The most acidic clast with

1. Note : Where a definitive name is used, refer to 3.3.

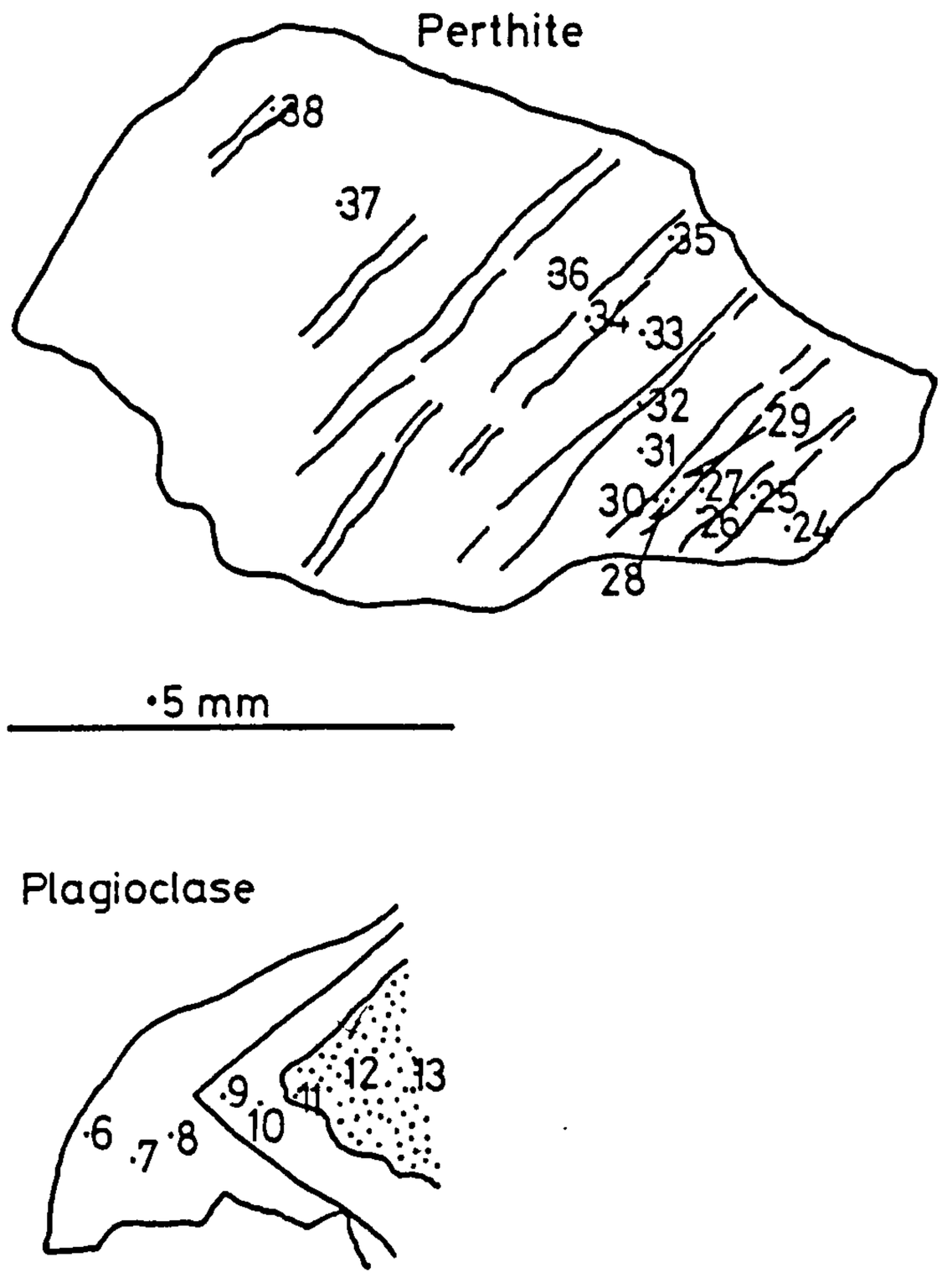

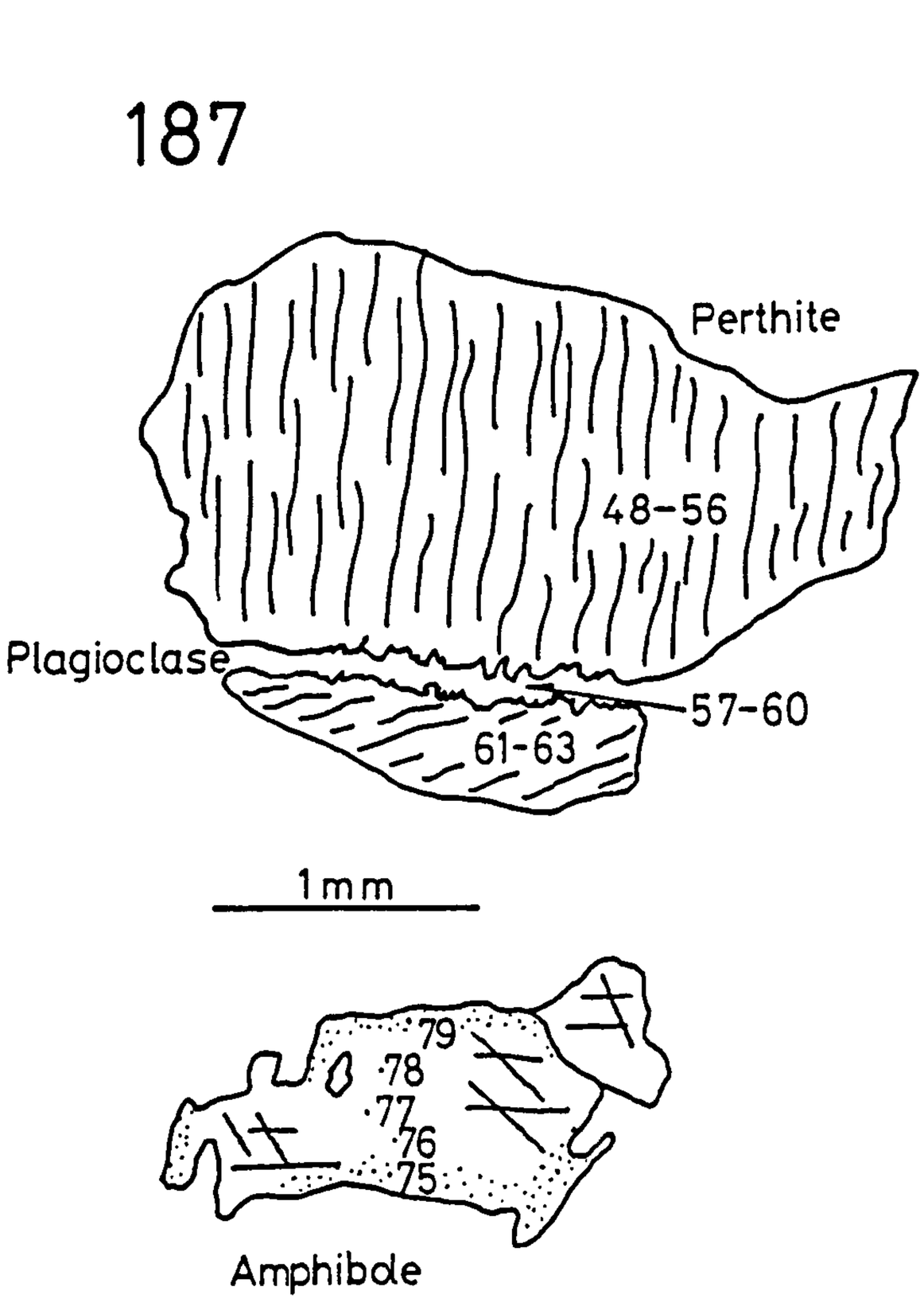

Fig. 3/2 Location of microprobe analyses

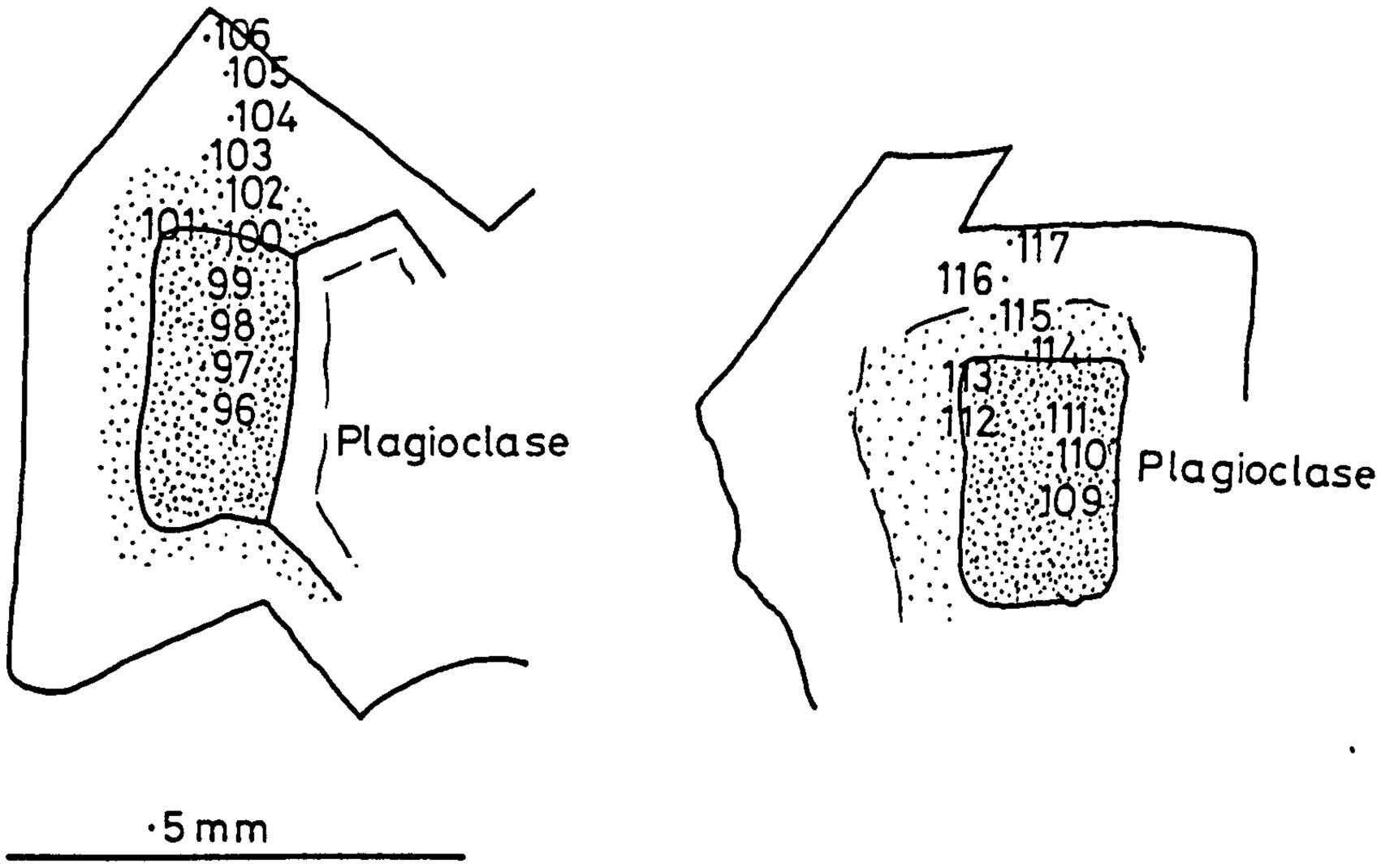

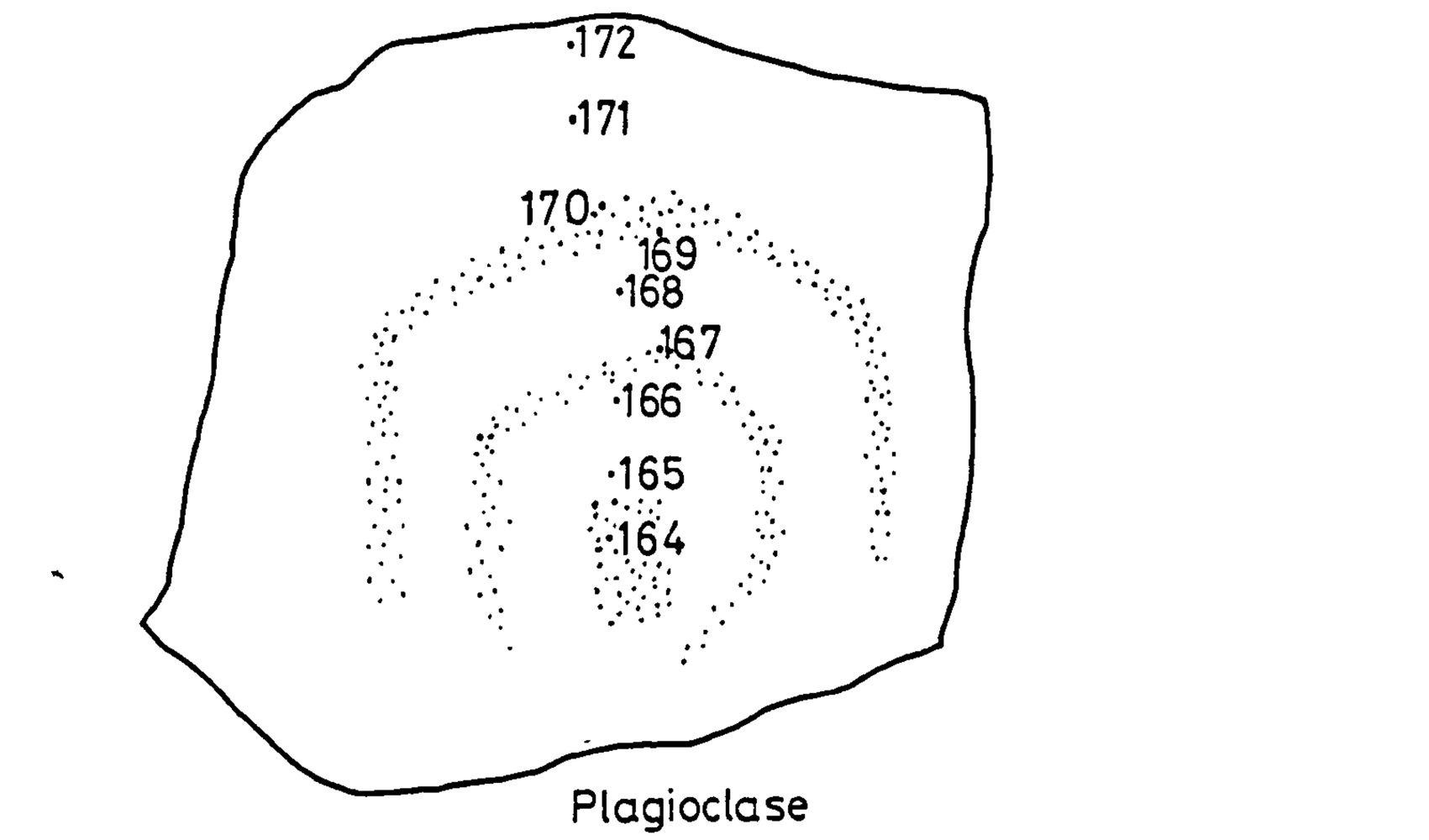

Fig. 3/3 Location of microprobe analyses

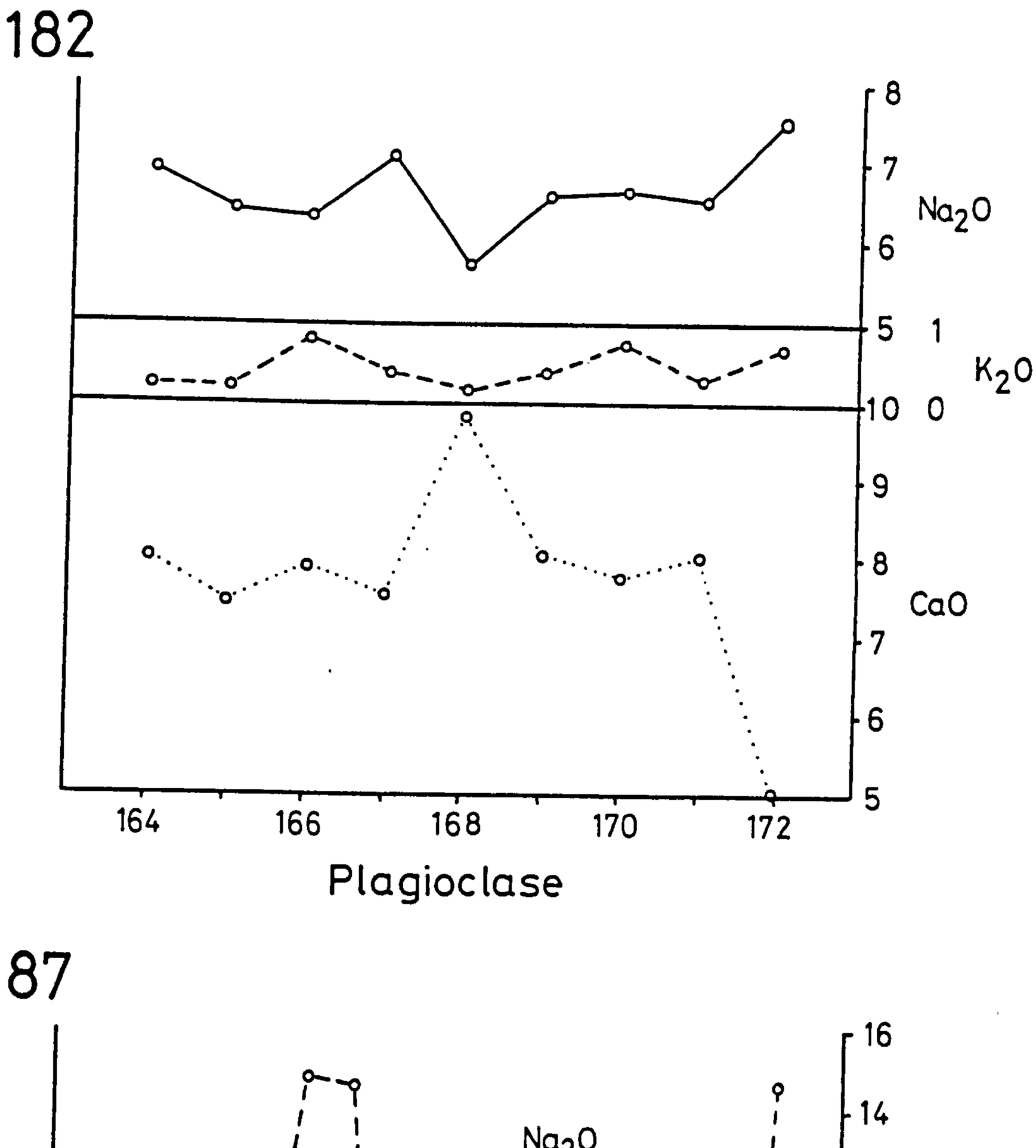

Fig. 3/4 Microprobe feldspar analyses plots for clasts 182 and 187

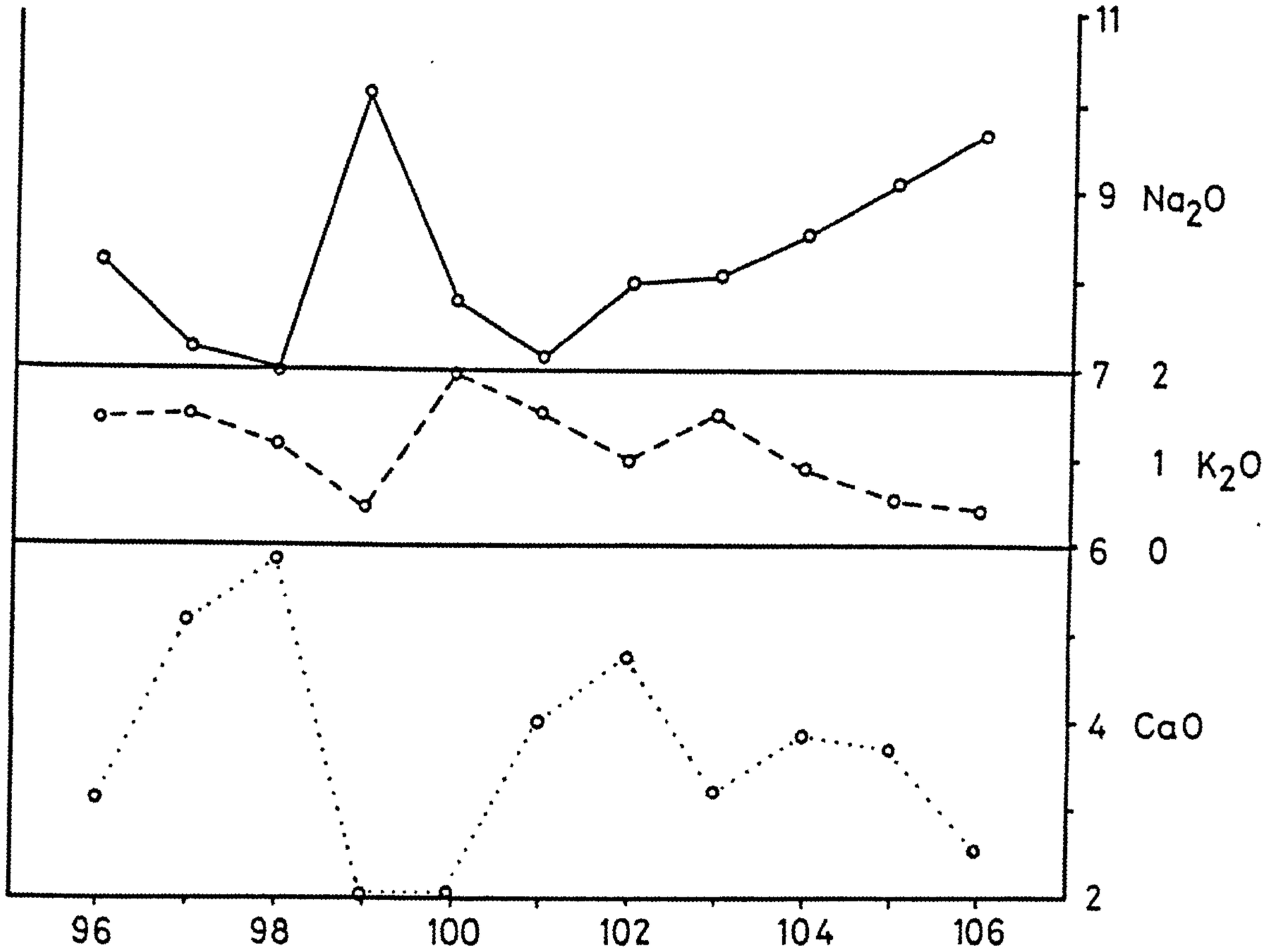

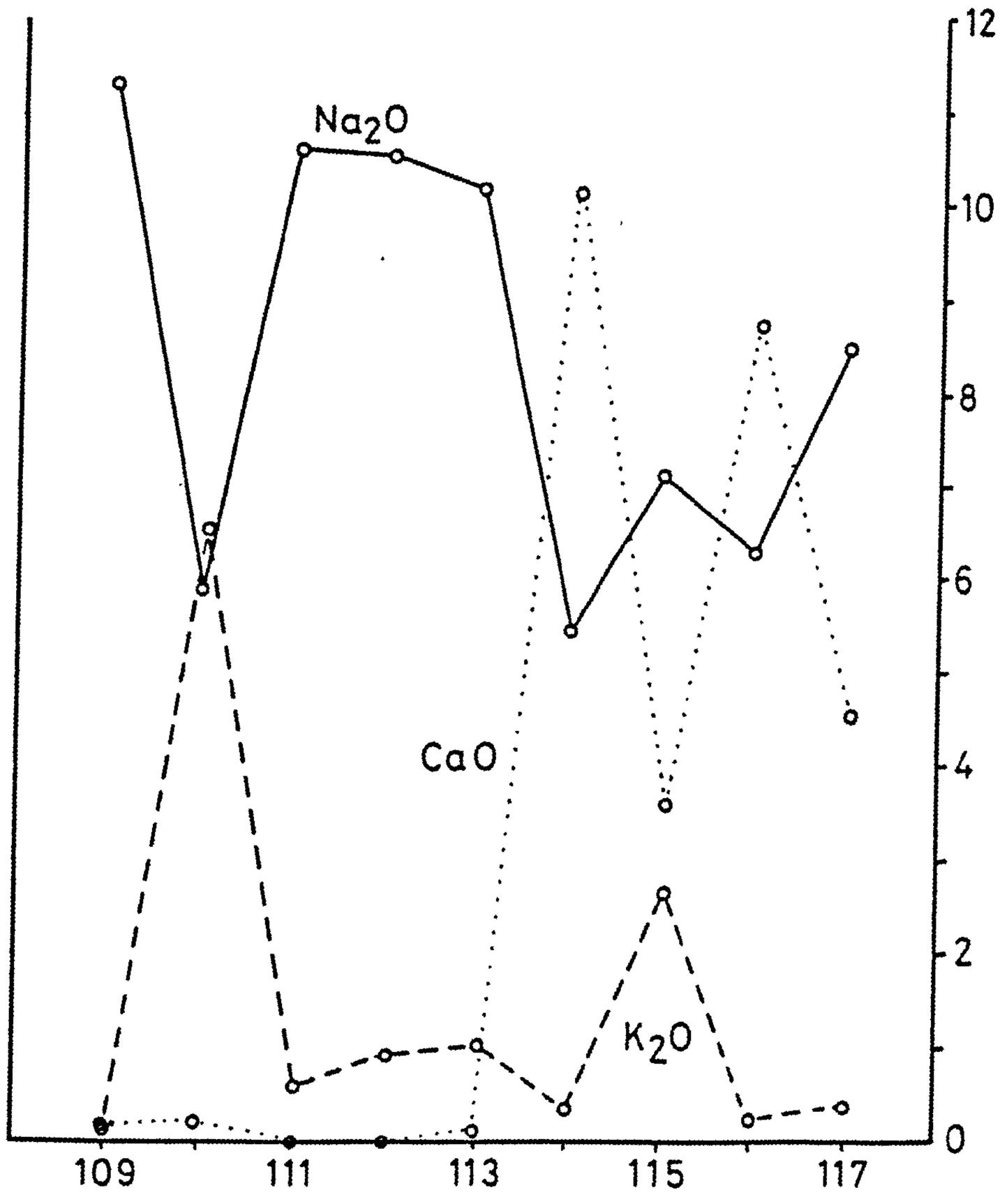

Fig. 3/5 Microprobe feldspar analyses plots for clast 17

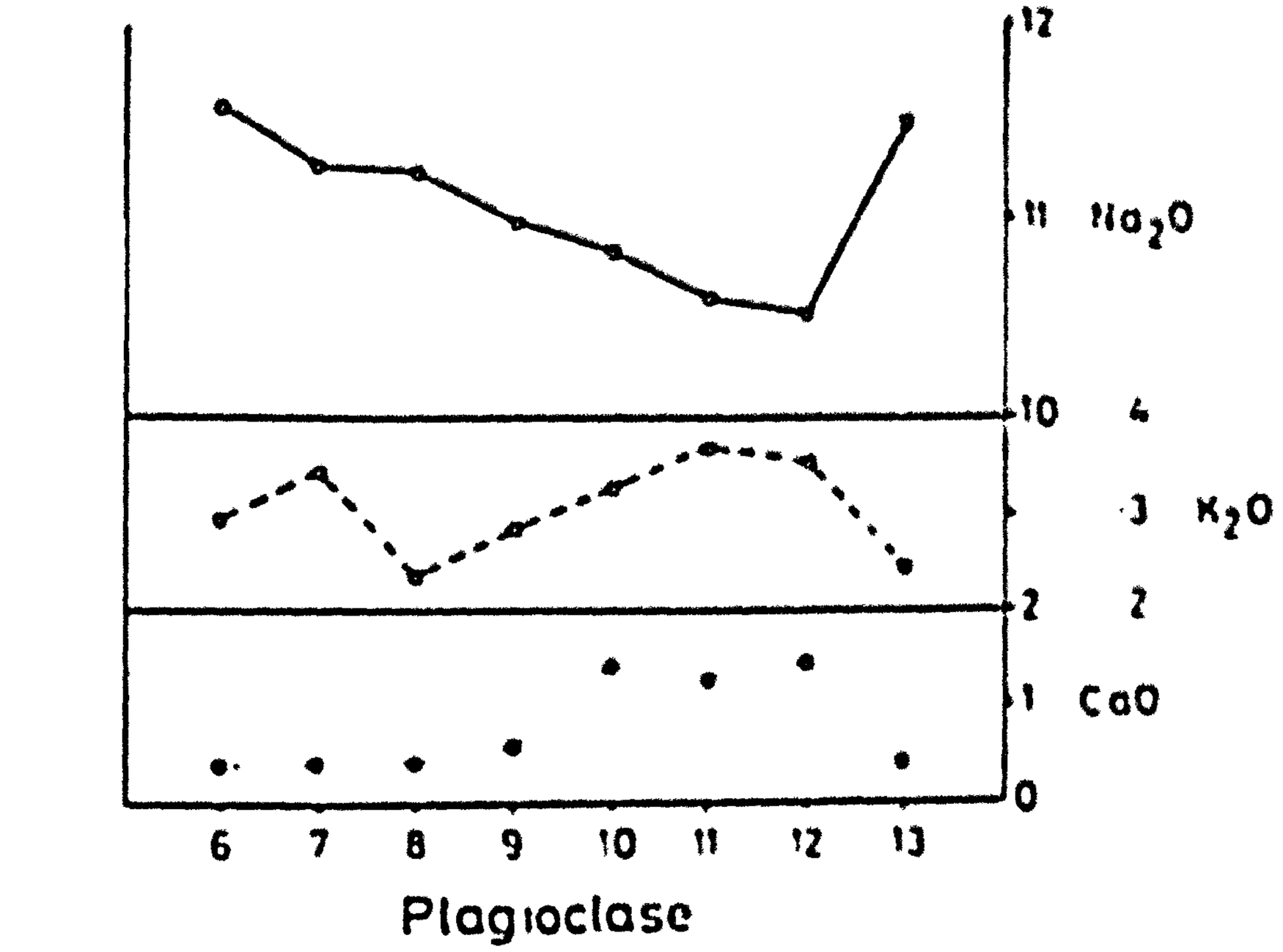

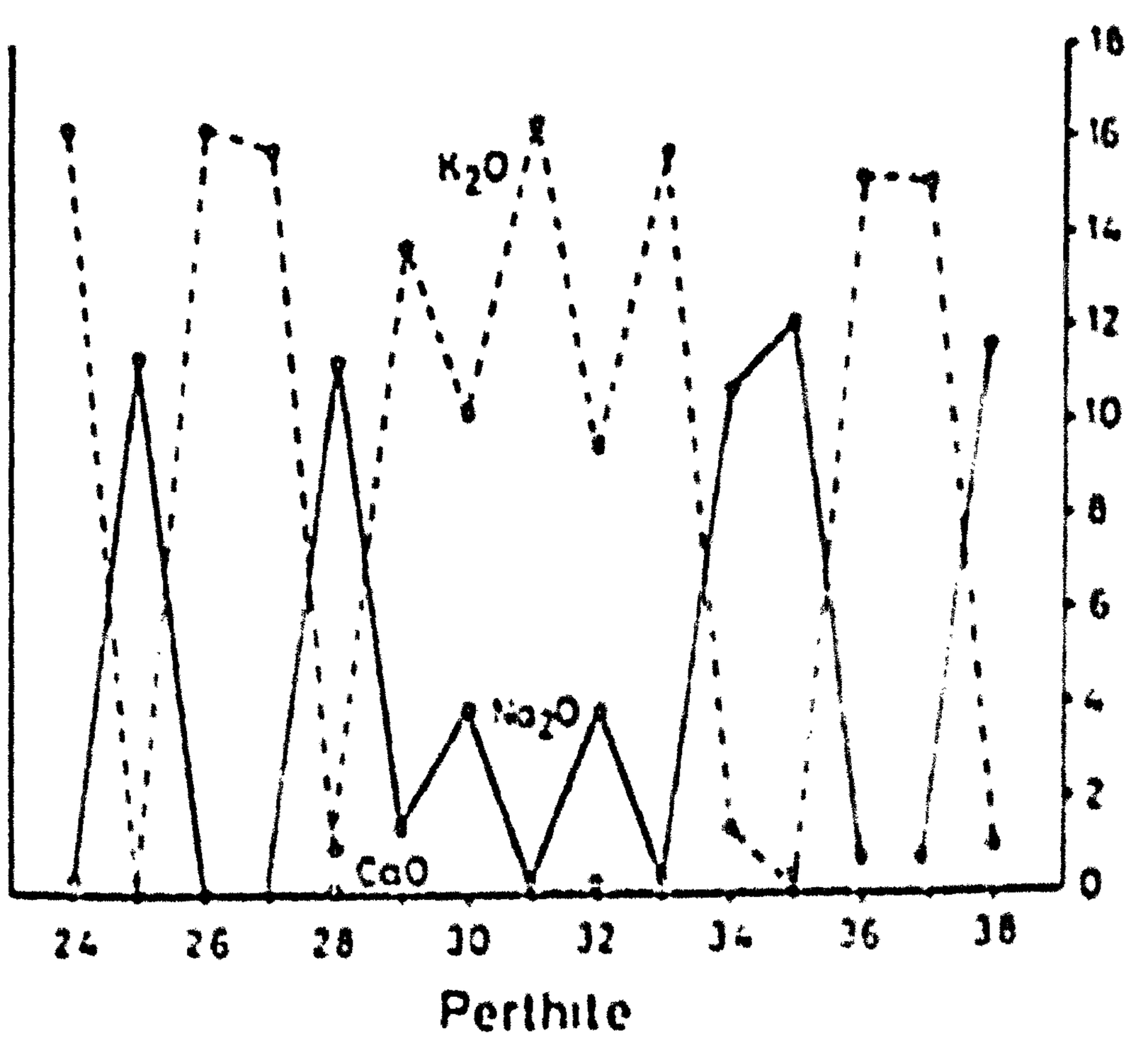

Fig. 3/6 Microprobe feldspar analyses plots for clast 101

zoning is 101 which produces the best trend in analyses (Fig. 3/6). A mildly calcic core (An07 Ab91 Or02) shows a gradual decrease in Ca and increase in Na towards the rim (Ab02 An97 Or01). All the plagioclases indicate normal zoning from calcic to sodic compositions with possible oscillatory zoning in the early formed cores. Thus in many cases plagioclase did not remain in equilibrium with the melt composition.

The potassium feldspar shows optical variation from orthoclase to microcline but the main feature is the development of perthite. This mainly takes the form of microperthite (5-100 μm) but in some cases develop s to perthite (100-1000 μm), though from now on the term perthite will be used in reference to the general morphological feature (Figs. 3/7 & 3/8). Analysis of the exsolution lamellae is presented for two granite samples, 101 and 187 (Figs, 3/4 and 3/6). The main feature of these data are the low, or zero, Ca content and the extreme composition separation (e.g. An00 Ab99 Or01 and An00 Ab03 Or97) of the lamellae. The width of the individual lamellae also varies in apparent sympathy with increasing differentiation and acidity, with the coarse perthite developed in the alkali-rich samples 186 and 187. These samples also exhibit the development of fine grained plagioclase crystals (essentially pure albite Ab100 to Ab98) between adjacent perthite grains (Figs. 3/2, 3/4 & 3/7).

The coarsening perthites and fine grained plagioclase development are both features which may be related to fluid diffusion which in turn would accord with magmatic fractionation producing the alkali-rich granites. The albitic plagioclase suggests low temperature crystallization which may be enhanced by the adjacent recrystallizing exsolution lamellae. Another explanation for the coarseness of the perthite is the lack of Ca in the lattice making exsolution easier (Parsons 1977). This again may be a function of differentiation, as is the case for hypersolvus syenites containing alkali pyroxene or amphibole in which coarse perthite exists.

Grain boundary recrystallization is also typical

of deformation but in these samples there is little evidence of tectonism. Thus an origin through increased water content as a function of fractionation is preferred. This, however, leads to one consideration in that if the water content increases exsolution may be expected to produce complete unmixing of the feldspars. Thus a careful balance between exsolution and recrystallization effects appears to exist.

Amphiboles are present in many clasts but those in the alkali-rich granites (186 & 187) show optical zoning from a dark green core to a dark blue rim (Fig. 3/2). Microprobe analyses across the amphiboles (Fig. 3/9) shows that the zoning is not particularly well reflected in the chemistry but that the margins tend to be richer in Mn and Na. Although an unequivocal classification of the amphibole type is not possible it most probably lies in the range riebeckite-arfvedsonite, typical of alkali-granites.

Granophyric intergrowths are developed in several clasts and particularly well developed in 197, 194 and 284 (Figs. 3/10 & 3/11). These indicate rapid cooling at low water pressures from near eutectic compositions and hence are typical of high level intrusions. Parsons (1972) invoked a simple pressure reduction origin but the eutectic compositions are also thought to be a pre-requisite. Other features consistent with high level intrusion are the presence of small mariolitic cavities and occasional development of myrmekitic intergrowths.

The majority of samples show no evidence of tectonic deformation but minor alteration and weathering are ubiquitous in all clasts. The main effects are sericitization and/or saussuritization of the plagioclase component producing mica (mainly in the form of sericite replacing the calcic cores), epidote and calcite. Biotite and amphibole frequently exhibit partial or complete replacement by chlorite. Minor chemical changes are associated with this but the chlorite tends to mimic the chemistry of the original ferromagnesian host. Accompanying the chlorite development is the growth of lensoid plagioclase along the biotite cleavage ranging in

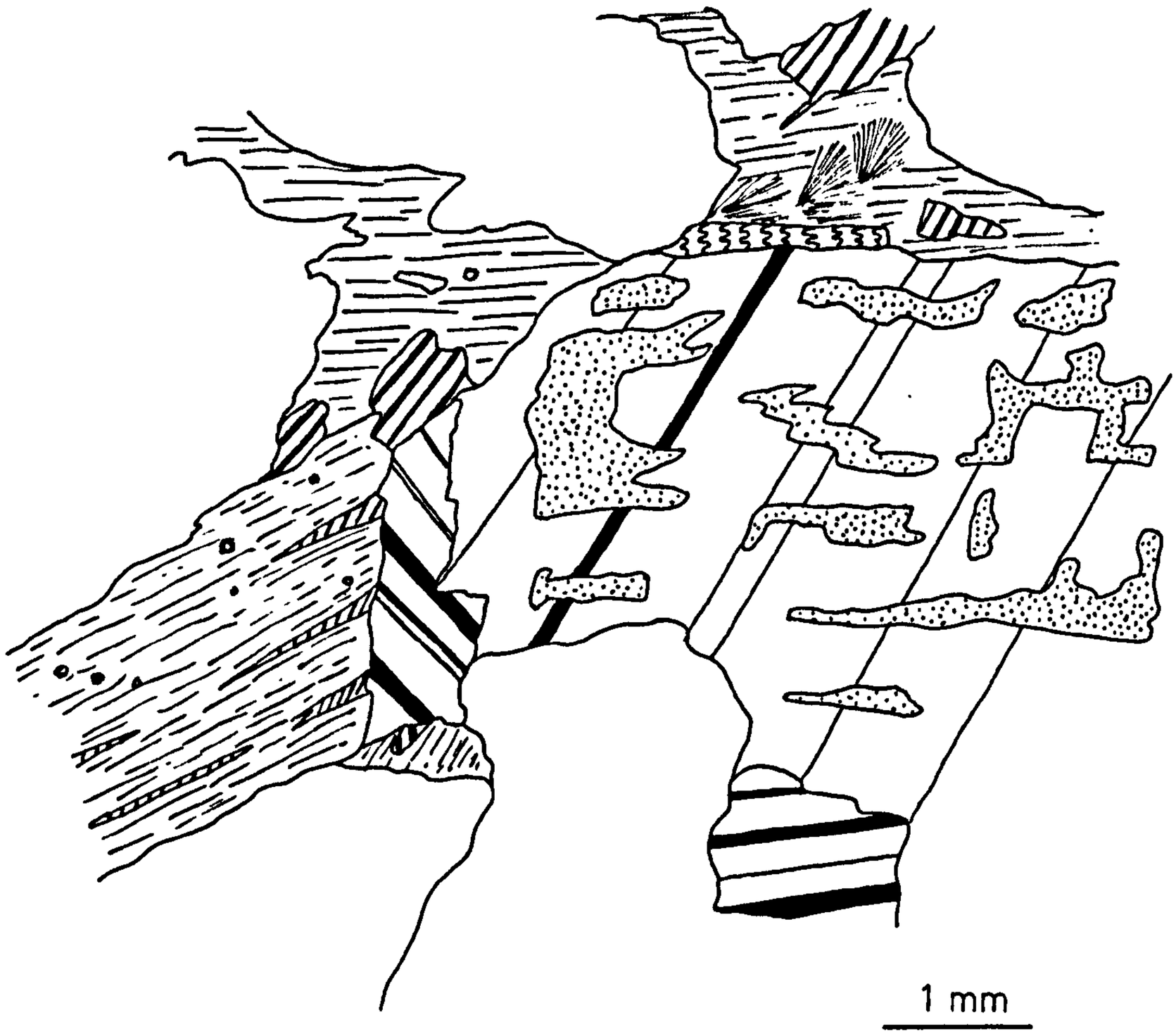

Fig. 3/7 Sketches of thin section from sample 101 showing general textural relationship, with some patch/replacement perthite and a high magnification sketch of well developed rod perthite. See Fig. 3/10 for key.

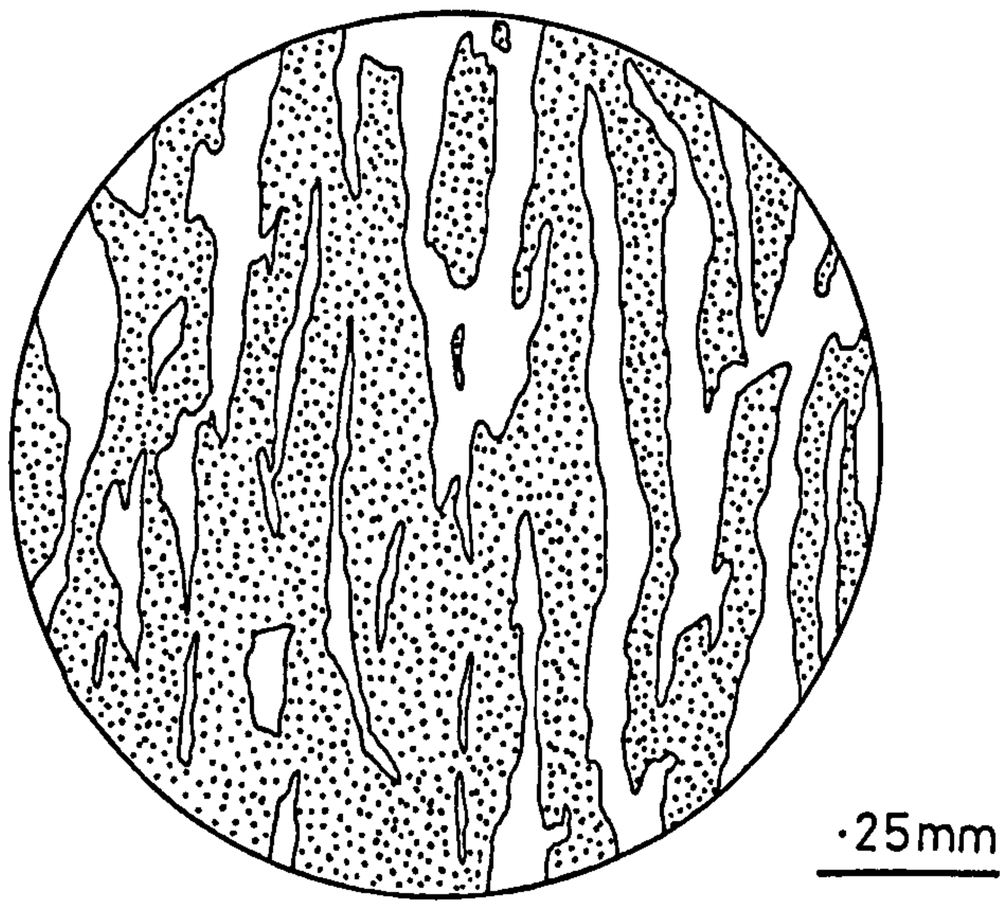

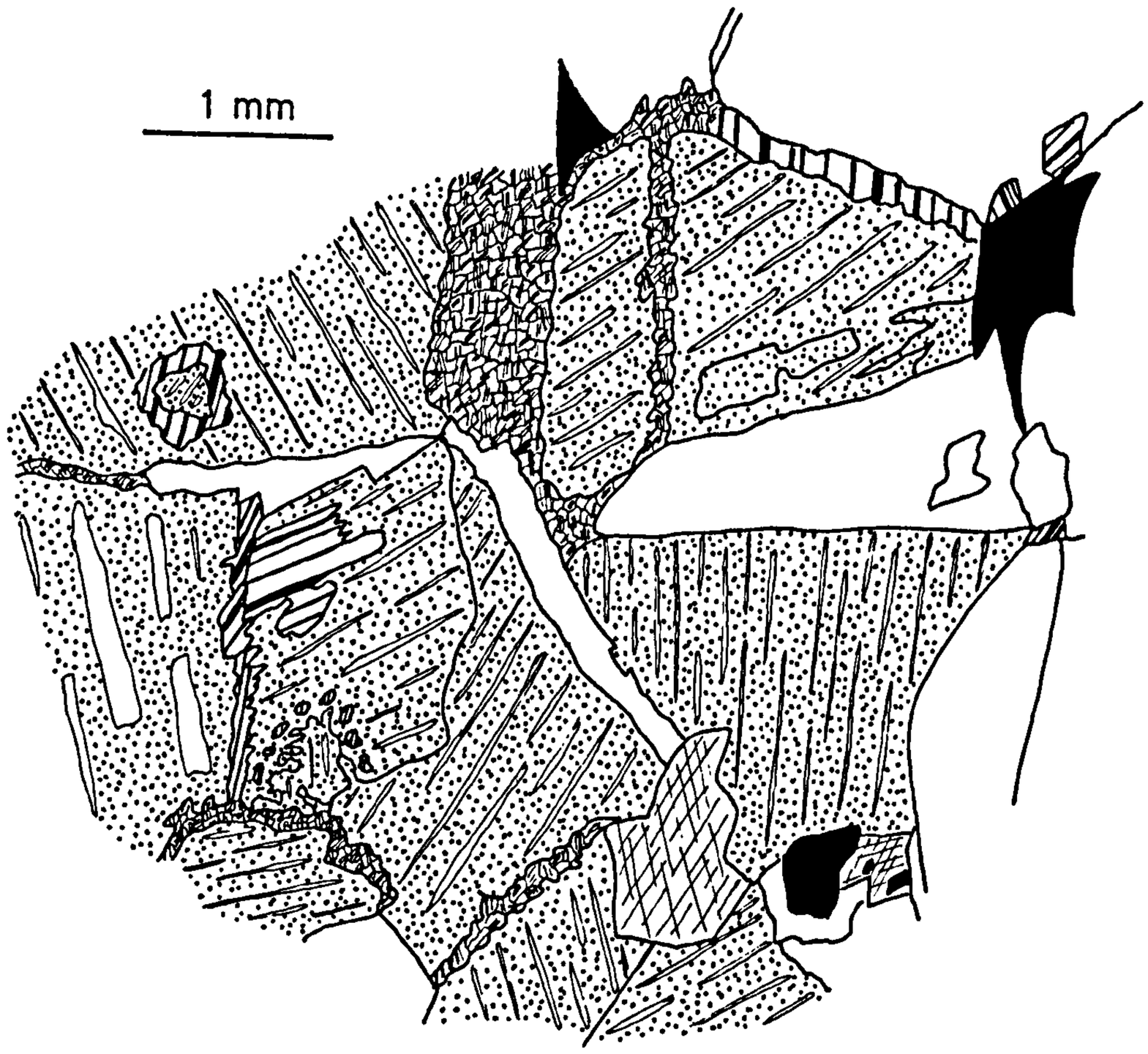

Fig. 3/8 Sketch of thin section from sample 187. This shows the well developed rod perthite and the intergrowth of small plagioclase (Albite) crystals between adjacent perthite grains. See Fig. 3/10 for key.

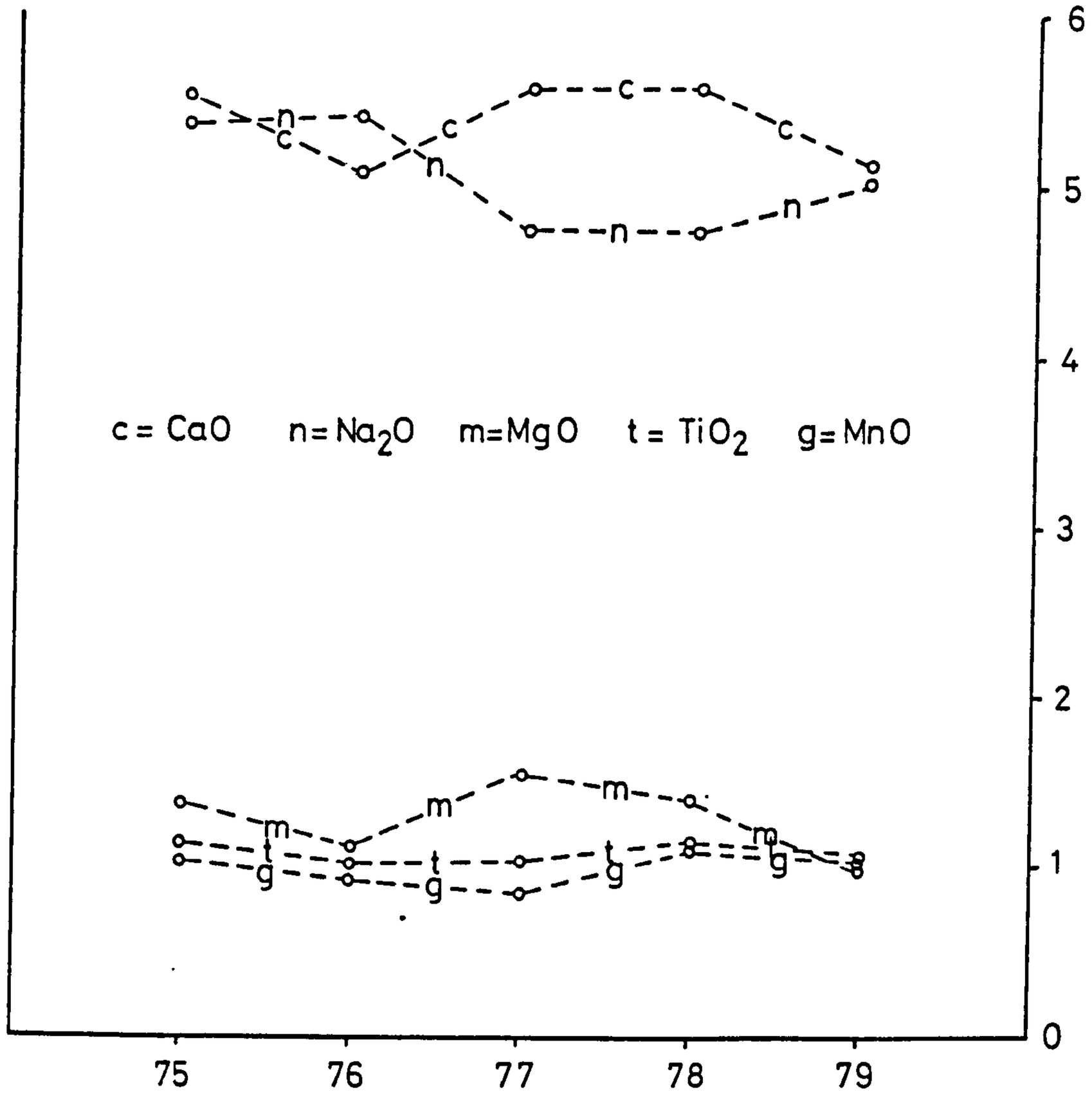

Fig. 3/9 Plot of microprobe analyses showing the compositional variation across a zoned amphibole from clast 187, an alkali-rich granite

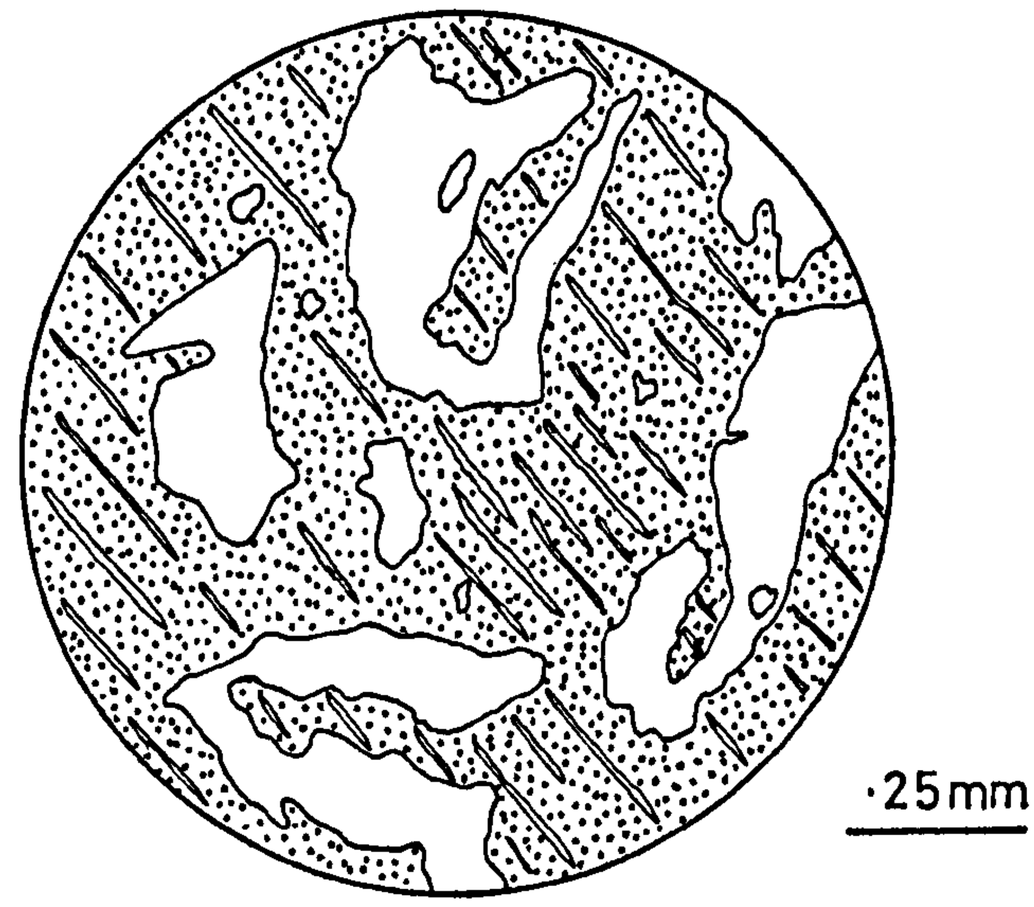

Zircons

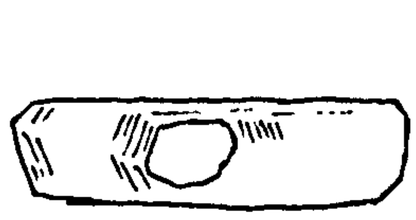

·05mm

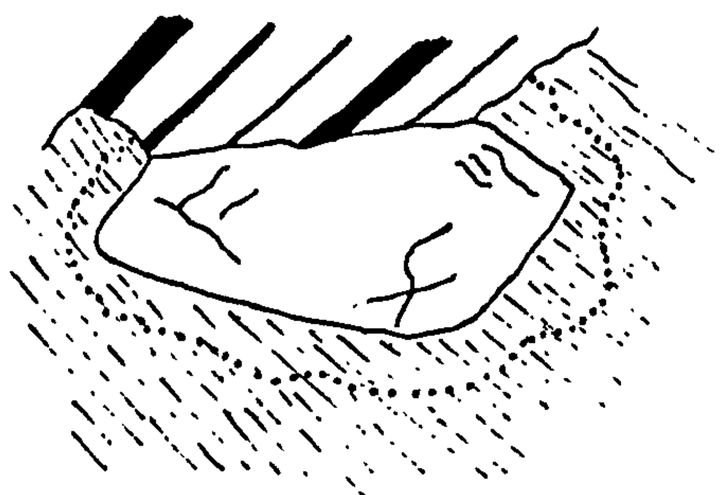

Fig. 3/10 Sketches of thin section from sample 197 showing pseudo-graphic texture and subhedral zircon crystals.

Biotite/chlorite

Hornblende

Opaques

Perthite

Plagioclase

Potassium feldspar

Muscovite

Quartz

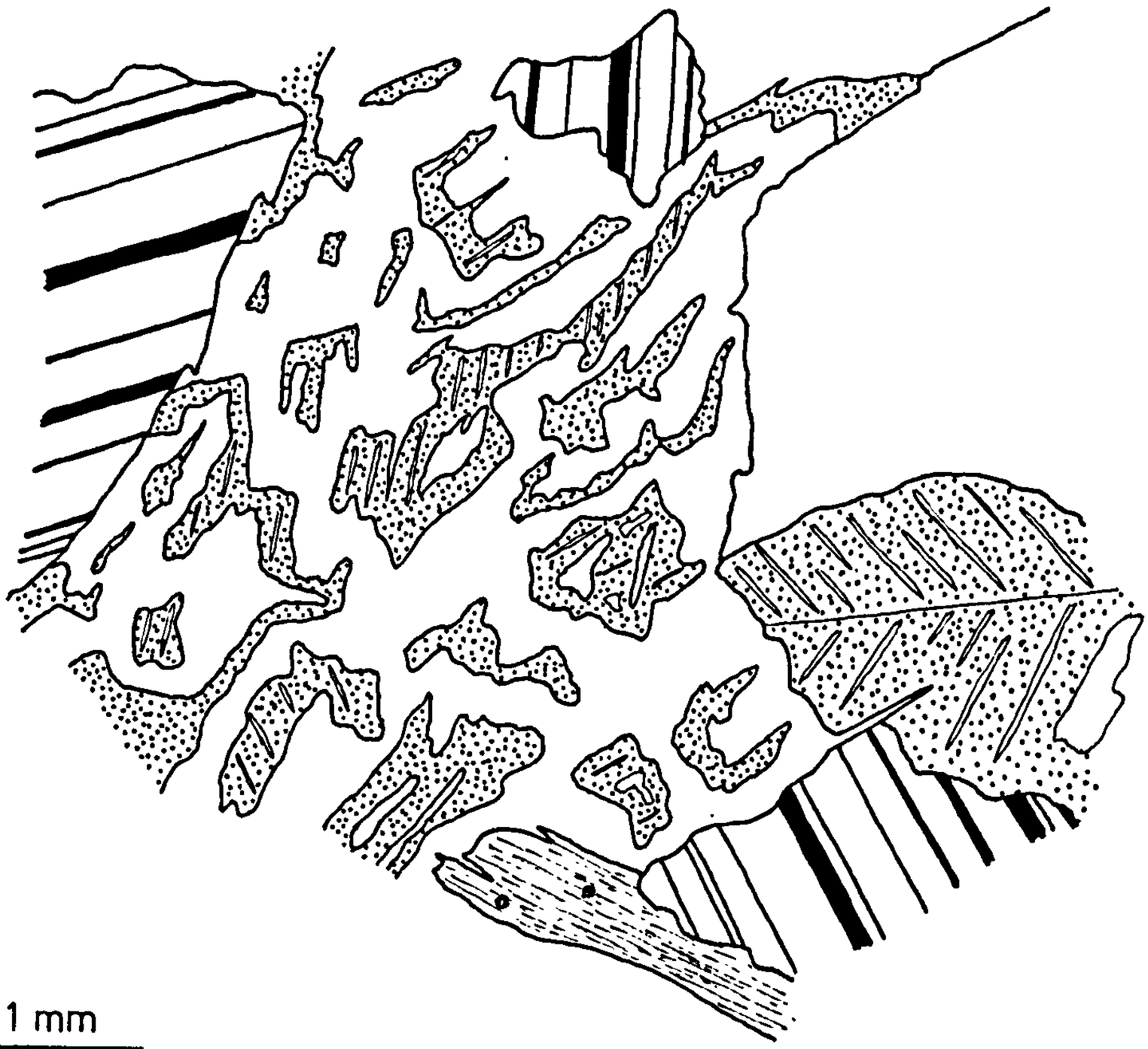

Fig. 3/11 Sketch of thin section from sample 284 exhibiting a well developed graphic texture. See Fig. 3/10 for key.

composition from Ab100 to Ab98.

Many samples also contain calcite veins and although the decalcification of plagioclase liberates calcite which may contribute to the veining, in the majority of samples the field relations indicate that the veins invaded the in situ conglomerate and hence imply a separate origin.

Some clasts show textural evidence of having been deformed and several develop a penetrative fabric. Samples from the Kirkland conglomerate (e.g. 889) show extensive deformation and calcite veining, some of which also appears to be deformed exhibiting curved twin lamellae. The other horizons have scattered examples of deformed clasts though in contrast to the Kirkland they are often foliated but with less recrystallization. The best example is clast 988, one typical of many from the Corsewall conglomerate, and containing equigranular quartz and feldspar but with elongate aligned biotite and muscovite. In general the Corsewall conglomerate contains a higher proportion of deformed clasts than the other rudaceous units.

Whilst the Kirkland conglomerate granitic clasts show definite tectonic effects it is difficult to assess the role of regional tectonism versus intrusive effects in many others. Holder (1979) noted that for the Adara pluton successive pulses of magma deform the previous pulses and the surrounding 'plastic' country rocks by 'balloon' like expansion and leave the last pulse unfoliated. Roddick & Hutchison (1974) working in the Coast Plutonic Complex, British Columbia noted that ' most of the granitic rocks exhibit some degree of foliation. In the better defined plutons foliation is best develpped near the margins and is least conspicuous or absent in the central parts'. In the Ayrshire suite the more basic samples are more frequently foliated and this may be a function of earlier intrusion in a cycle of pulses or the presence of micas and hornblendes which take up the foliation. The more acid samples rarely show foliation due to late intrusion or lack of planar minerals (?) and although some recrystallization is evident much may be due to late stage fluids (as noted earlier). The lesser content of deformed granites does, however,

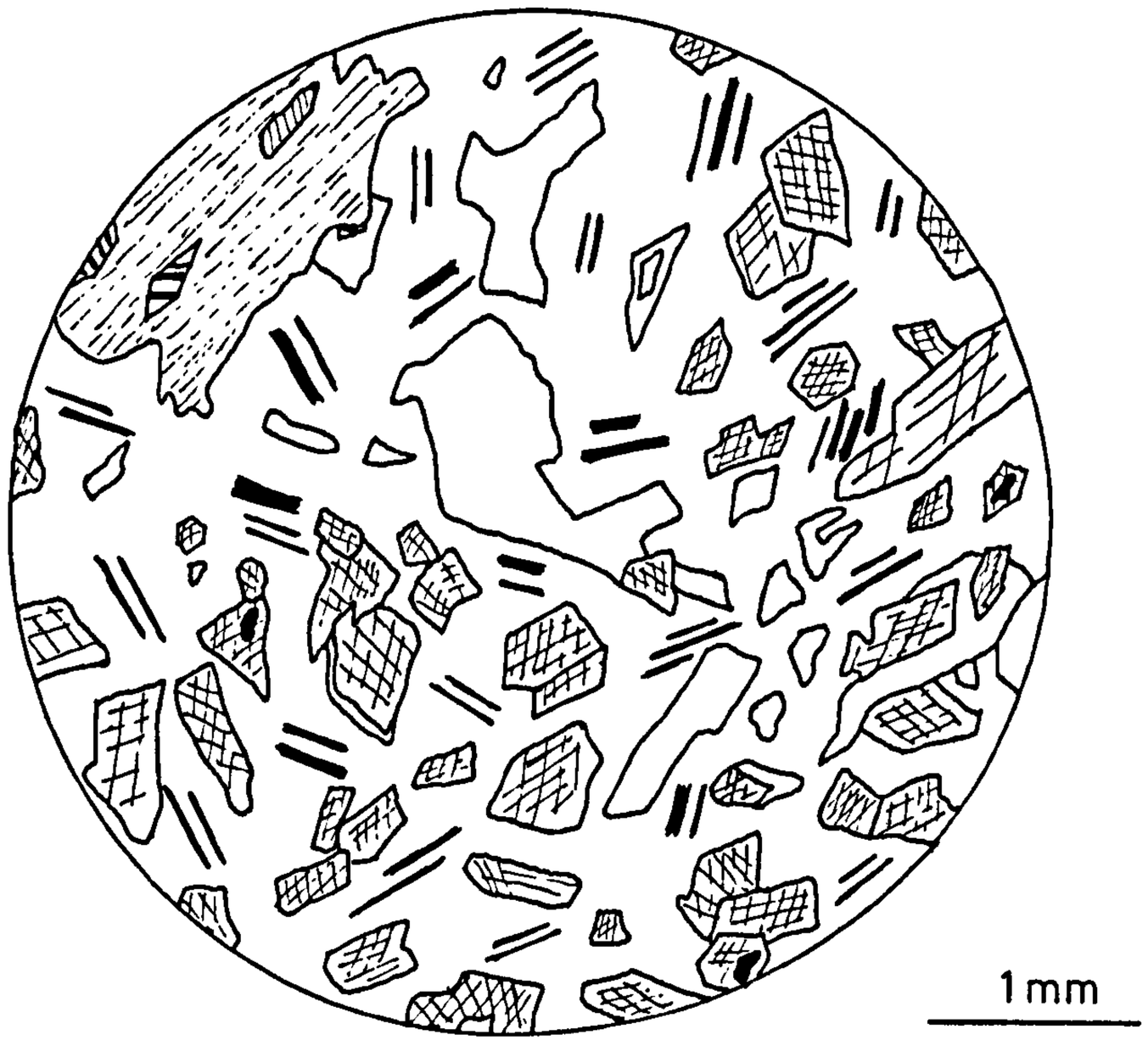

Fig. 3/12 Sketch of thin section from sample 179 (xenolith) showing subhedral hornblende in a plagioclase surroundi. See Fig. 3/10 for key.

mitigate against a regional deformation and the minor effects are probably intrusion related.

3.2.2 Xenoliths

Few samples contain visible xenoliths but two with small exotic fragments (~8 cm^3) were sectioned, clasts 994 and 179. In both cases the xenoliths are basic igneous rocks comprising subhedral hornblende in a matrix of plagioclase (Fig. 3/12). These are considered to represent early formed magmatic residua, the restite of White & Chappel (1977). In no cases were xenoliths of non igneous material found which could represent the wall rocks.

3.3 Problems of granite classification

During the course of this study the question of applying a name to the granitic clasts under investigation caused certain difficulties.

There are two diffent approaches to classifying granitic rocks, one using a modal system and the other involving varying treatments of chemical analyses. The definitive work on the classification of plutonic rocks was performed under the auspices of the International Union of Geological Sciences (IUGS), and published by Streckeisen in 1976. In this paper it is stated that the proposals are only recommendations and at best a practical compromise between various pre-existing schemes. The classification they propose is based on the modal mineral content expressed as volume percent, determined through point counting techniques and used mainly out of deference to historical tradition. In the case of the silica oversaturated plutonic rocks with a mafic content of less than 90%, a triangular plot is used with the three apices being : Q (Quartz), A (Alkali feldspar i.e. orthoclase, microcline, perthite and albite (An 00-05)) and P (Plagioclase (An 05-100)). The divisions and nomenclature within this triangle (Fig. 3/13) have been devised in an attempt to utilize natural breaks in the mineral series and terms already in use. This serves to provide petrological definitions for the rock names but uses the modal system. This tends to cause problems when comparing plutonic rocks from different areas as, in most cases today, rocks are analysed chemically and it is the chemical variation which is important in demonstrating trends and affinities. As a consequence of this the modal analysis tends to be avoided or overlooked by many authors. Streckeisen (1976) was aware of this : 'However, a system of rock chemistries may, besides the mineralogical classification of rocks, have its advantages, especially for comparison', but did not discuss the matter further.

Other authors have used the chemistry to effect a classification, but come up with a wide variety of schemes.

Chemical rock analyses are determined in weight percent oxides, and the chemically based classifications tend to be of two types; those based simply on oxide or cation ratios and those based on treatment of the normative (CIPW) mineral assemblage.

A normative classification using a ternary plot of An-Ab-Or from a Barth norm was proposed by Hietanen (1963) (Fig. 3/14). This was empirically divided using pre-existing named data, but where these names were themselves derived from is not stated. This approach was also used by O'Connor (1965), Streckeisen (1976), Glikson (1979) and Barker (1979) and their schemes are shown in Figs. 3/14 & 3/15, where again a varying number of fields are defined from clusters of previously defined data. A further refinement to the molecular norm classification was produced by Streckeisen & Le Maitre (1979). In place of the ternary diagram they used a rectangular plot of silica saturation (Q') where $Q' = 100Q/(Q + An + Ab + Or)$ against the An/Or ratio (ANOR) where ANOR is neasured as 100 An/(An + Or) (Fig.3/16). This again subdivided empirically with the authors using the nomenclature of Streckeisen (1976) and claiming good agreement with the modal system.

Viljoen & Viljoen (1969) used a simple K_2O:Na_2O ratio to define four fields and this was expanded into a ternary Ca-Na-K diagram by Condie & Hunter (1976) (Fig. 3/17). These classifications have several drawbacks in that they simply use one ratio as the discriminator and use the names tonalite - granodiorite - quartz monzonite- granite to represent the sequence of increasingly alkali-rich granites and as such it does not correspond to the nomenclature as used by Streckeisen (1976). In addition Condie & Hunter (1976) used Ca as the third apex of their ternary diagram. This is essentially useless as a discriminator in acid plutonics being coupled with Na in plagioclase and thus simply increasing towards their tonalite field. If one is to use this system an improvement may be to plot the K_2O/Na_2O ratio against a measure of the femic cations (e.g. Fe + Mg + Mn) to give some idea of the mafic mineral content. This is a view concurred with by Condie (pers. comm. 1979) and

shown in Fig. 3/18.

De la Roche et al. (1980) have gone to the other extreme in producing a chemical classification based on all the major cations (Fig. 3/19). This is a binary diagram with the two axes being $X = R_1 = 4Si - 11(Na + K) - 2(Fe + Ti)$ and $Y = R_2 = 6Ca + 2Mg + Al$ (expressed as millications) and subdivided empirically into a curvilinear grid. The complexity of producing the diagram, however, appears unwarranted in the light of the spread of named data when plotted on it.

It thus appears that the straight chemical classifications are either over simplified or over complicated and that even the best of the normative based systems lacks the consistency of application of the modal, IUGS, system. There is however, a method of calculating a mode from the chemical analysis of a specimen - although this produces a weight percent mode in contrast to the volume percent mode obtained by point counting. This involves fitting mineral analyses to the total rock analysis. The mineral phases may be determined petrographically and if microprobe analyses of the phases are available (see 3.1.3) they are ideal but if not then either end member or average compositions for phases may be used. The computer programme, XTLFRAC, devised by St ormer & Nicholls (see 3.1.5) and modified by M.R.Giles (pers. comm. 1978) uses the least squares method to equate the analyses and produces a best fit modal assemblage (Table 3D). In all cases here two end members of the plagioclase series were used to cover the variation of An content from specimen to specimen. The sum of the albite and anorthite components was then used as the plagioclase total. This means that in the recalculation the albite component goes to the plagioclase apex of the ternary diagram rather than the alkali feldspar apex in the Streckeisen (1976) classification. This, however, appears to be a minor problem as albite (An 00-05) determination in point counting is difficult and tedious and in many granitic rocks zoned plagioclase is present and also modal determination varies from section to section. In the few

samples point counted the agreement between the volume percent and weight percent mode is extremely good.

Another possibility for the Q-A-P triangle is to recalculate the co-ordinates from the normative components. This is less satisfactory as it takes no account of the mafic phases present and uses idealised compositions and relationships rather than measured mineral compositions, although it gives quite good results at the leucocratic end of the spectrum e.g. the granite field (Fig. 3/20)

On balance it seems that the best classification is that of Streckeisen (1976), particularly as it uses IUGS nomenclature. However, when chemical analyses are available and not modal data it is extremely useful to apply a calculated weight percent mode to the volume percent mode diagram of Streckeisen. In this study the nomenclature for the clasts (Table 3C) has been derived in this fashion. The weight percent mode plotted in the Q-A-P triangle is shown in Fig. 3/21. It is informative to compare this diagram with the other classifications (Figs. 3/13 to 3/20) which are plotted for comparative purposes and show the bewildering range of names it is possible to give one specimen.

NOTE : For Figs. 3/13 to 3/38

When plotted on chemical diagrams the anlyses from each conglomerate horizon are denoted in the following manner :-

Symbol	Horizon
○	Benan conglomerate
□	Kilranny conglomerate
▼	Tormitchell conglomerate
●	Craigskelly conglomerate
■	Kirkland conglomerate
×	Corsewall conglomerate

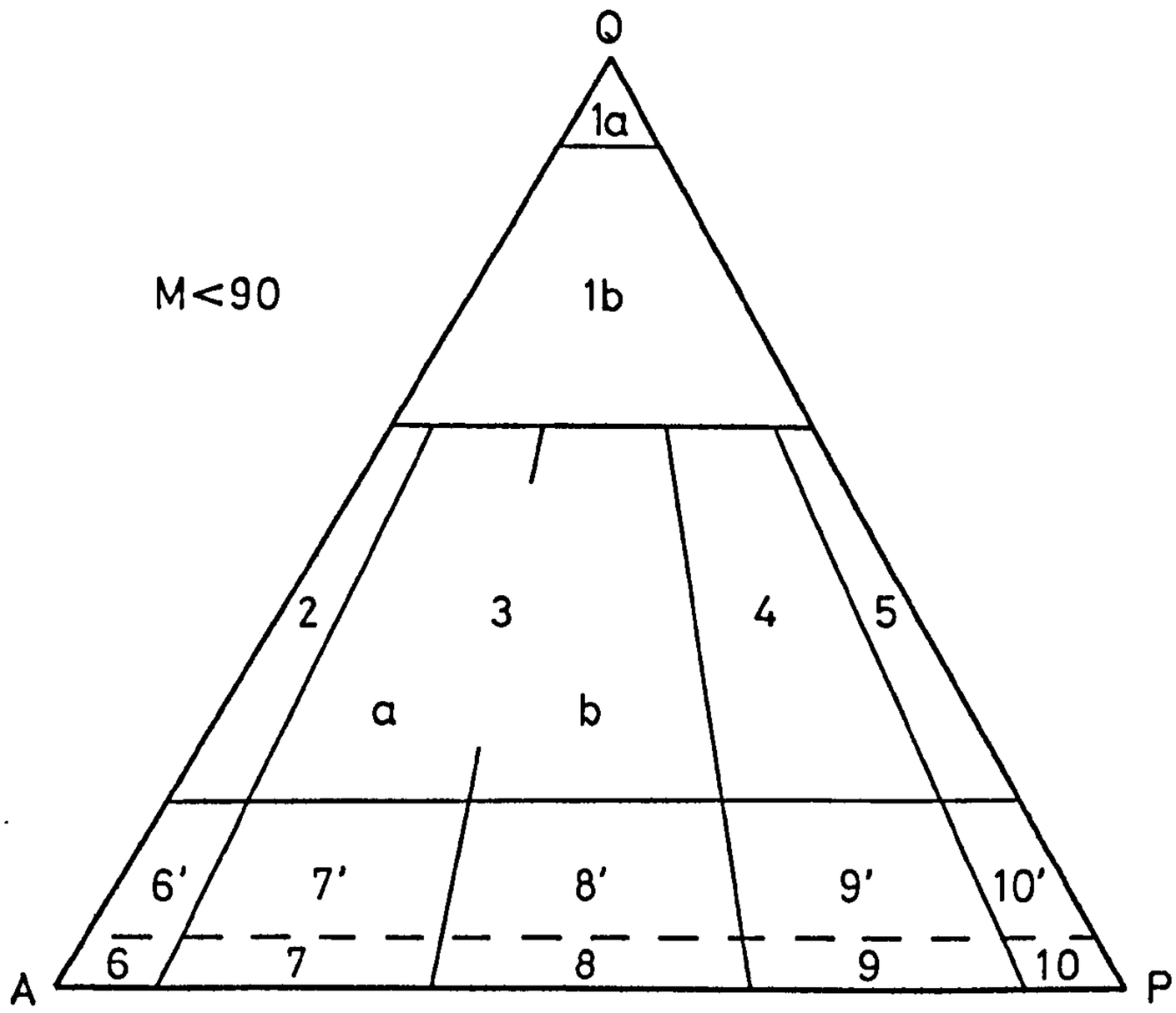

Subdivisions of the ternary field Q + A + P = 100 (volume %)

1a	Quartzolite (silexite)	
1b	Quartz-rich granitoids	
2	Alkali feldspar granite	
3a	Syenogranite)	Granite
3b	Monzogranite)	
4	Granodiorite	
5	Tonalite	
6'	Quartz alkali feldspar syenite	
7'	Quartz syenite	
8'	Quartz monzonite	
9'	Quartz monzodiorite / Quartz monzogabbro	
10'	Quartz diorite / Quartz gabbro / Quartz anorthosite	
6	Alakali feldspar syenite	
7	Syenite	
8	Monzonite	
9	Monzodiorite / Monzogabbro	
10	Diorite / Gabbro / Anorthosite	

Fig. 3/13 Nomenclature for the acid plutonic igneous rocks as proposed by the IUGS and reported in Streckeisen (1976).

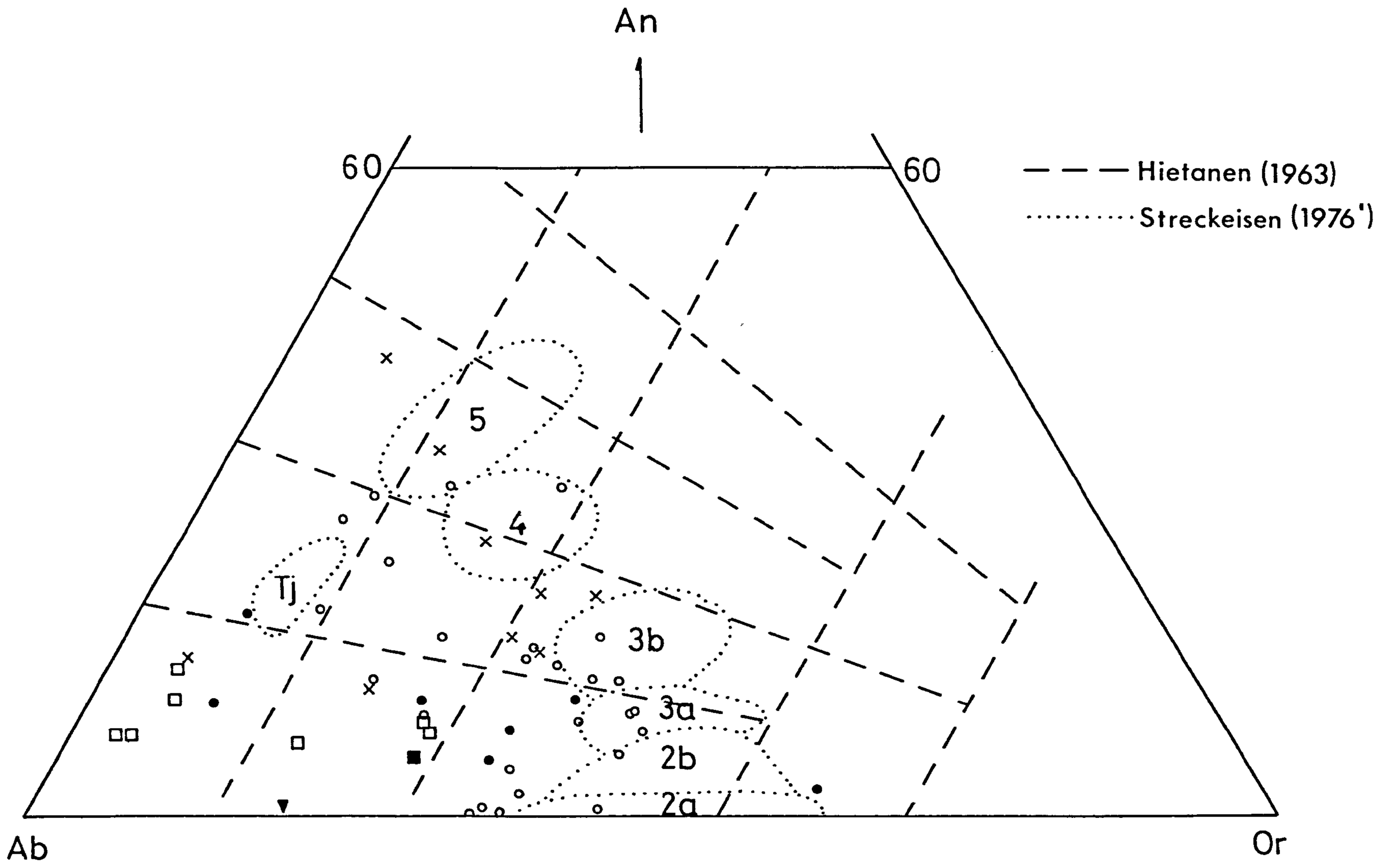

Fig. 3/14 Acid plutonic classifications using normative An-Ab-Or after Heitanen (1963) and Streckeisen (1976'). Numbered fields as for Fig. 3/13.

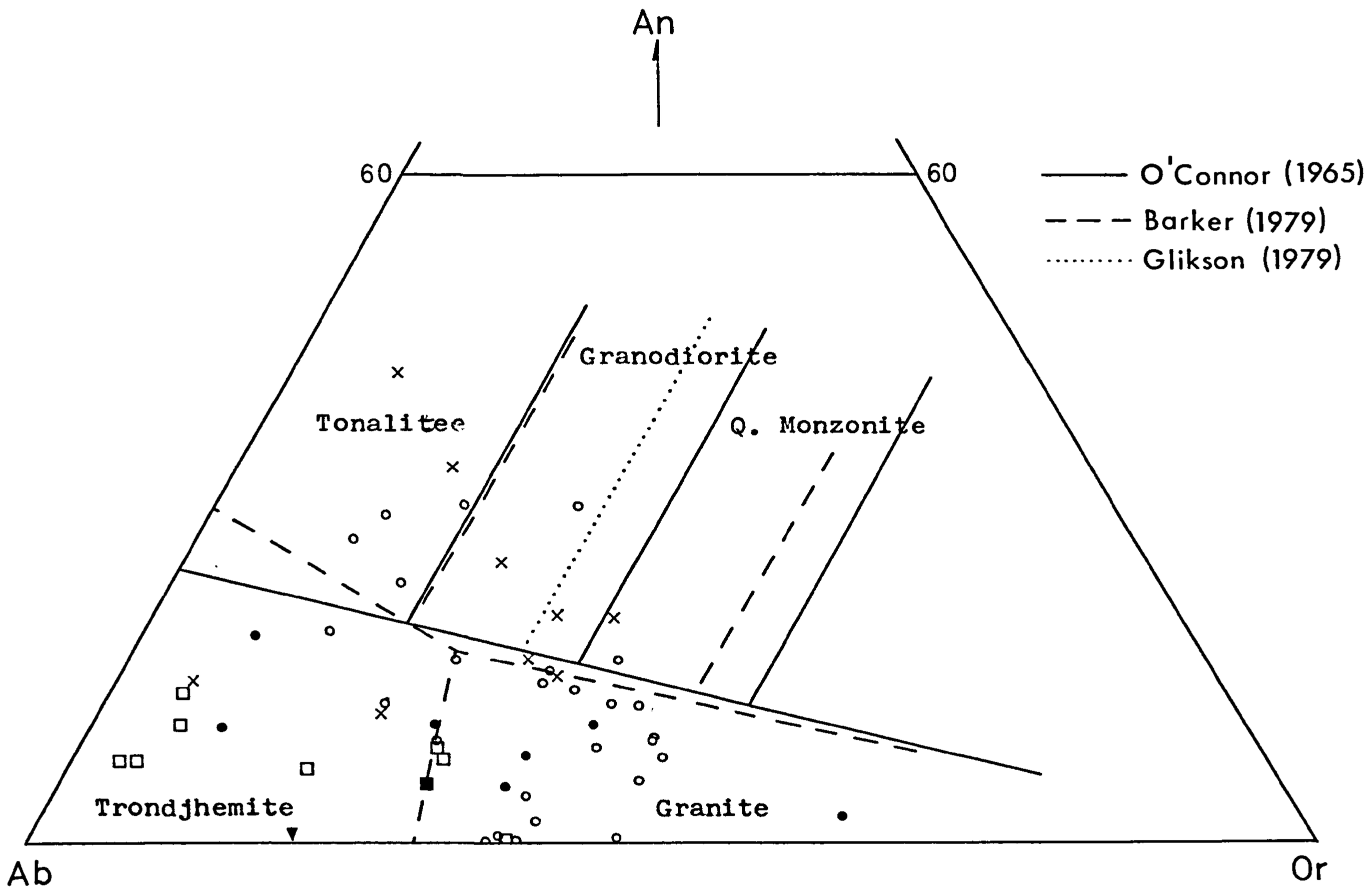

Fig. 3/15 Acid plutonic classification using normative An-Ab-Or proposed by O'Connor (1965) and modified by Barker (1979) and Glikson (1979).

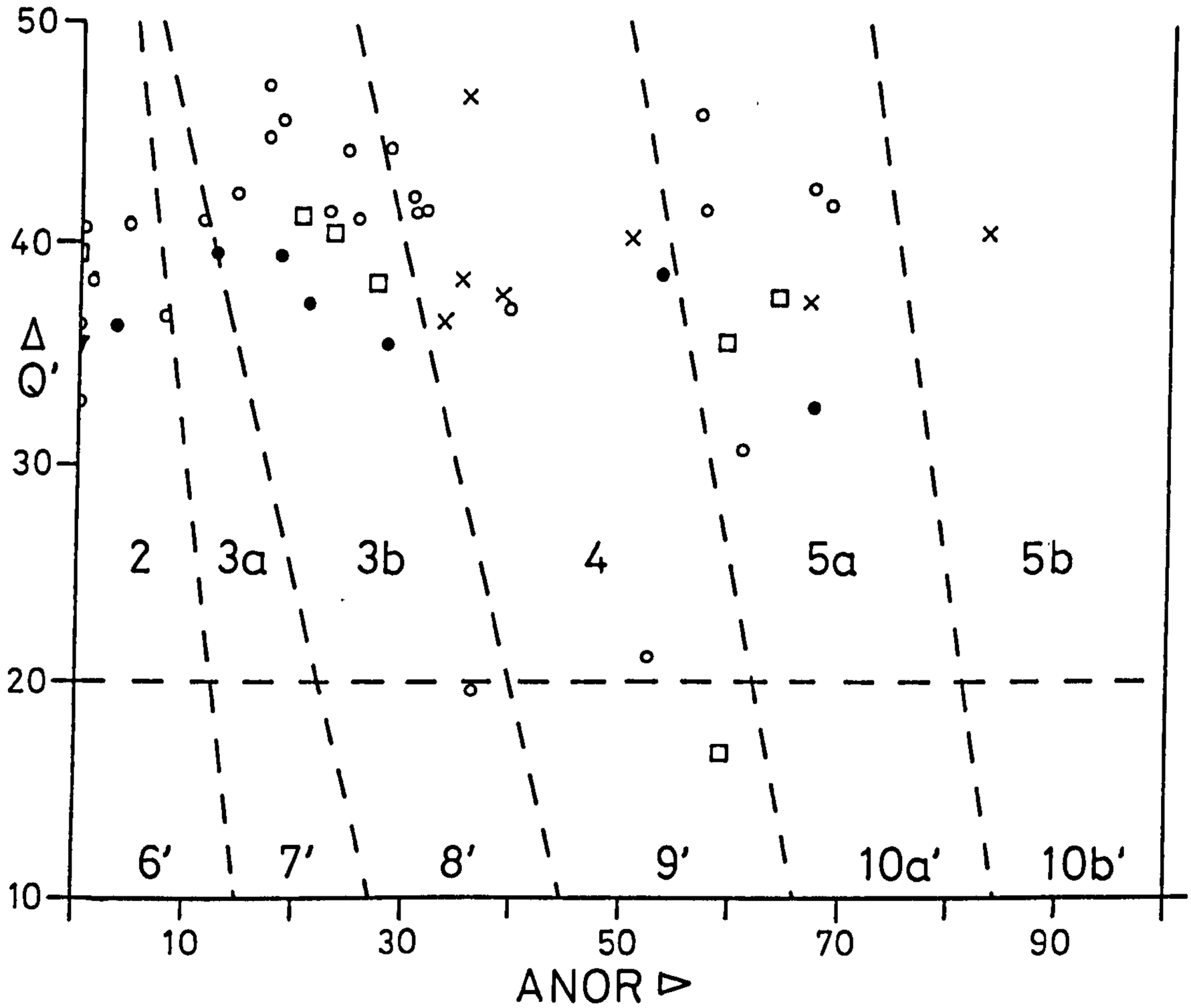

Fig. 3/163 Classification after Streckeisen & Le Maitre (1979) using normative values and subdivided empirically after Streckeisen (1976). Numbers as for Fig. 3/13.

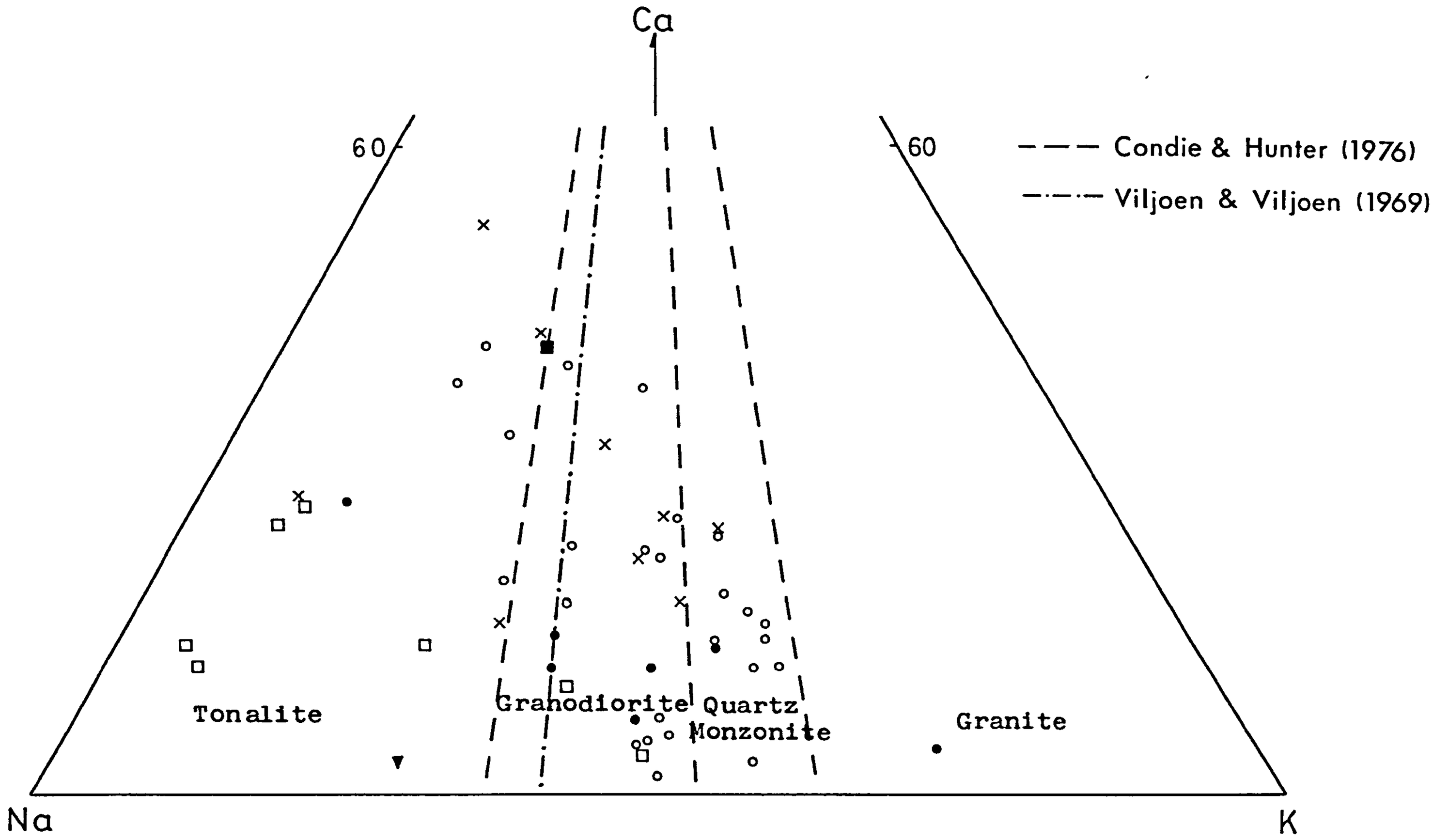

Fig. 3/17 Classifications using Ca-Na-K cation percentages after Condie & Hunter (1976) and Viljoen & Viljoen (1969), the latter modified from oxide ratios.

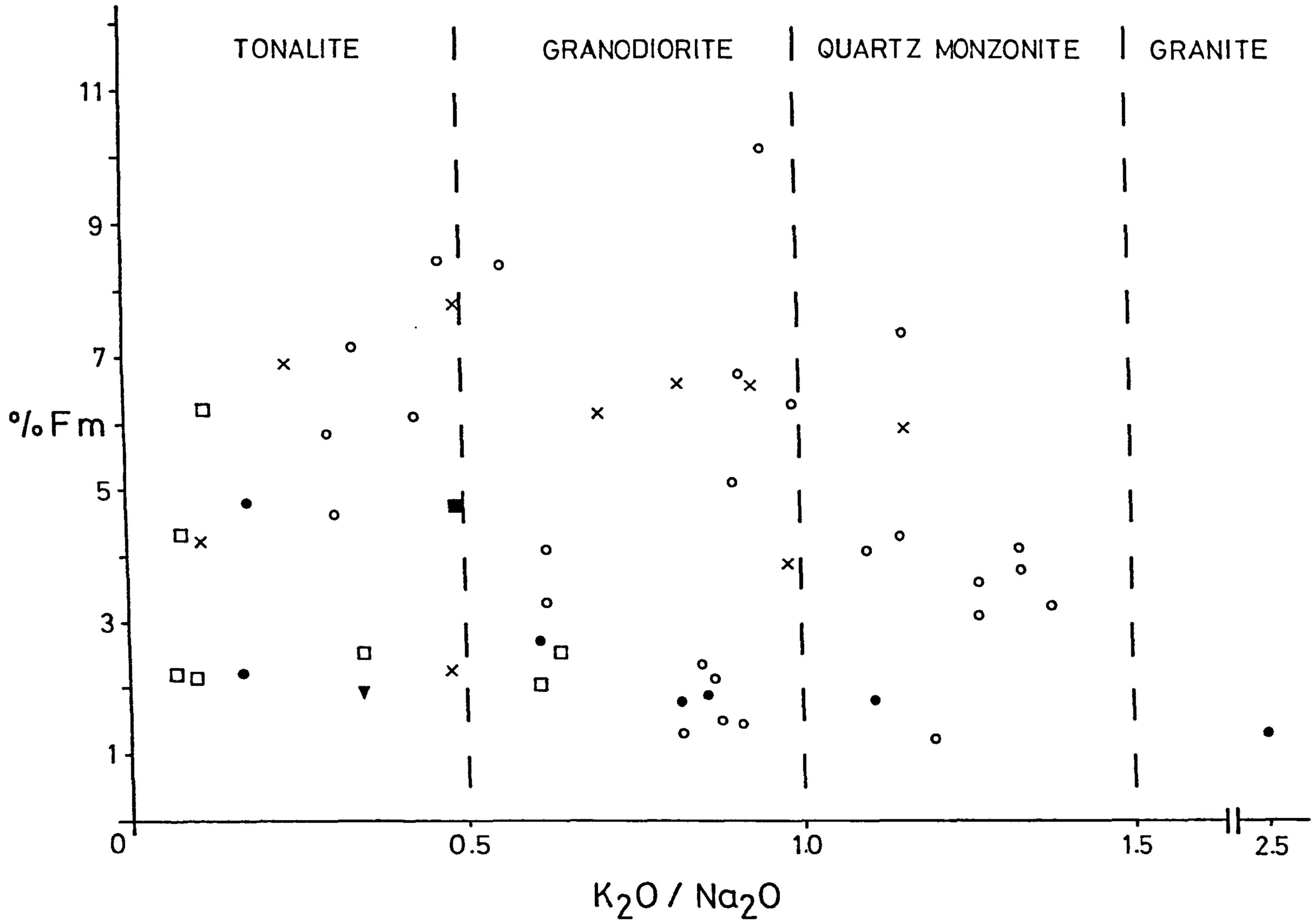

Fig. 3/18 Classification modified from Condie & Hunter (1976) to include a measure of femic cations.

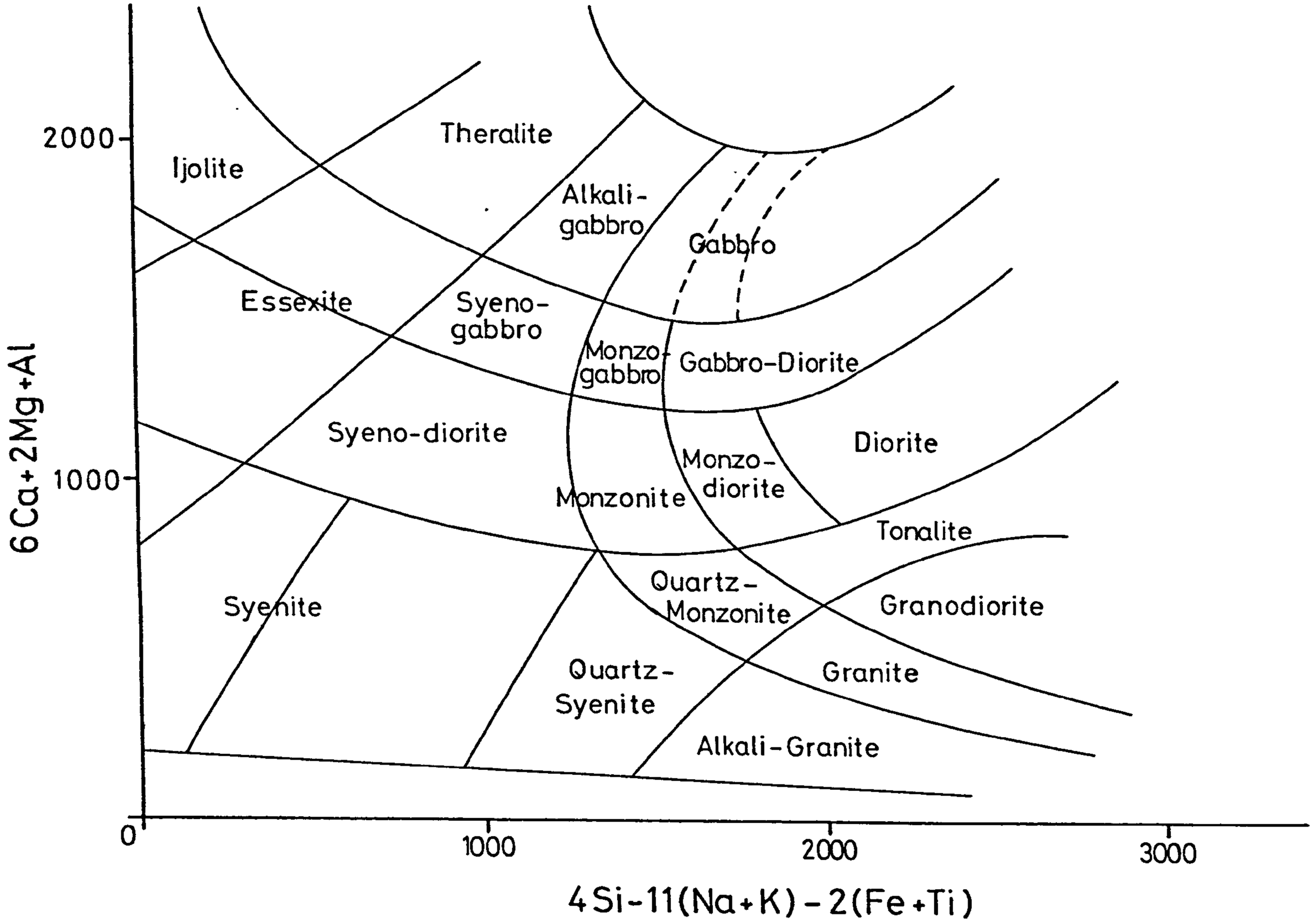

Fig. 3/19 Classification of de La Roche et al. (1980) incorporating all the major cations.

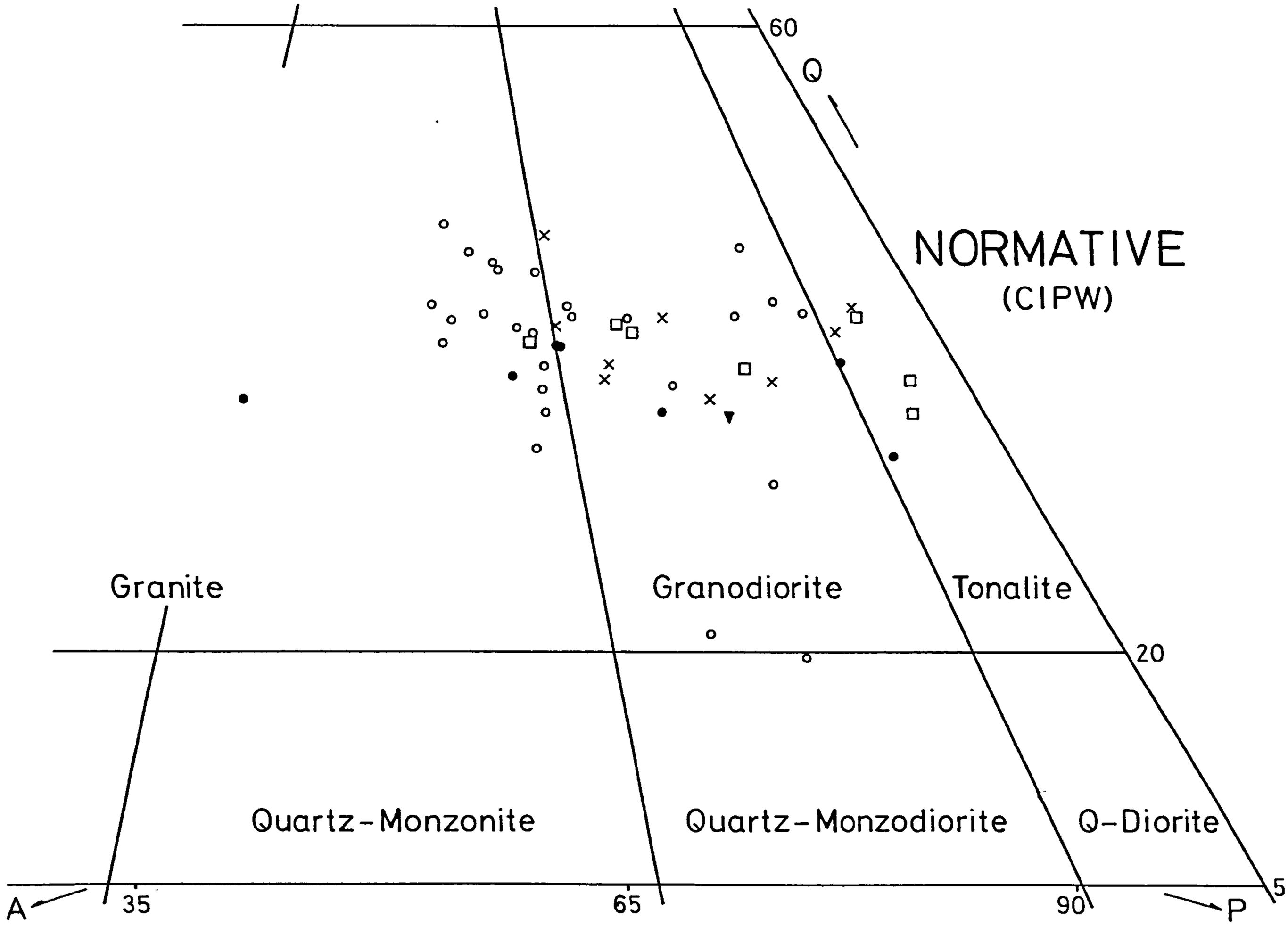

Fig. 3/20 Normative mineralogy plotted on a Streckeisen (1976) diagram.

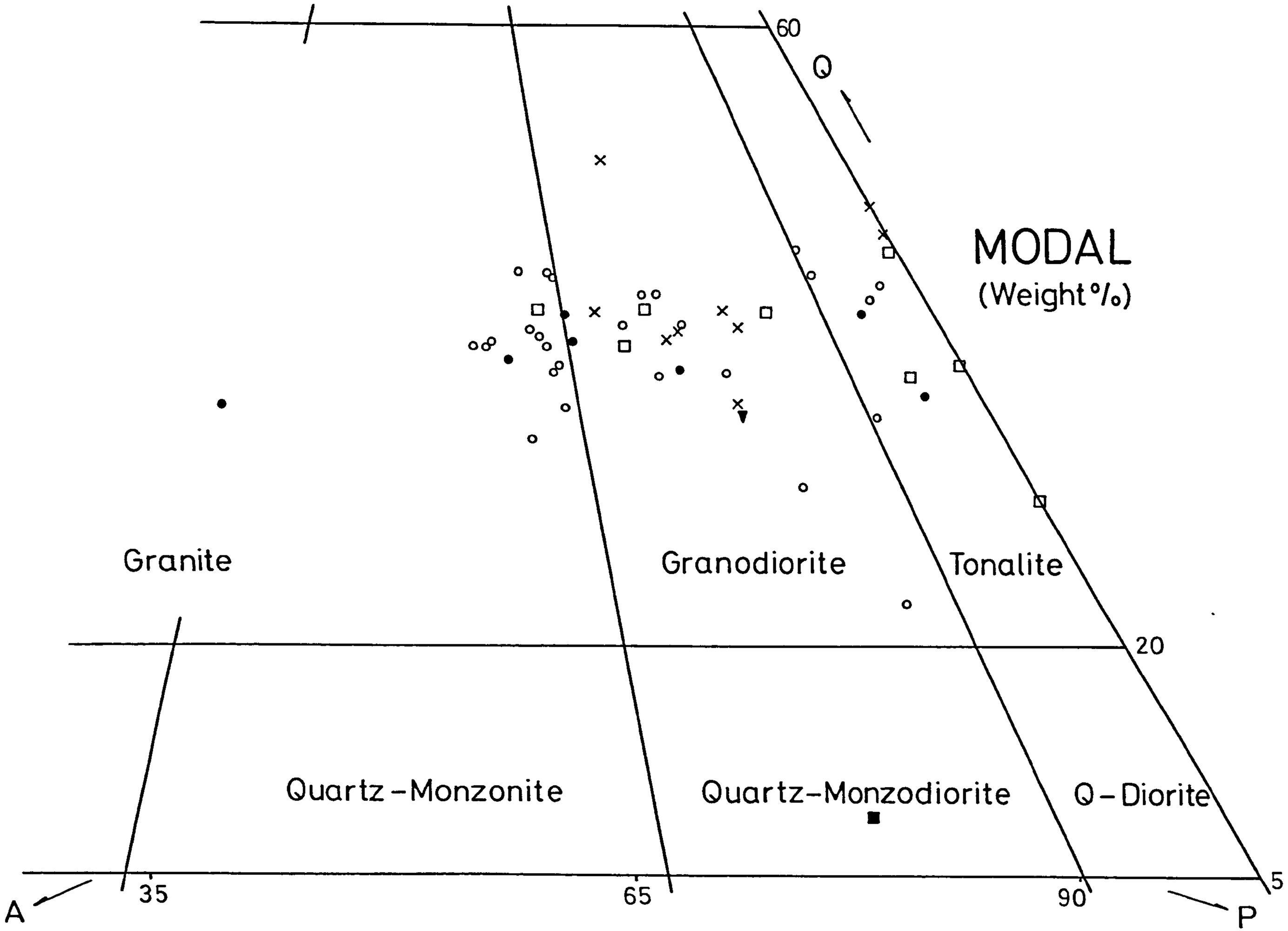

Fig. 3/21 Modal mineralogy plotted on a Streckeisen (1976) diagram.

3.4 Major element chemistry

The chemical analyses of the Ayrshire granitic suite are important in tying down their affinity and evolution. The nature of various rock associations has long been of interest and many early works still form the basis for todays magmatic series. Harker (1909) distinguished between volcanic rocks on the margins of the Pacific and Atlantic, and Peacock (1931) used the alkali-lime index (weight percent SiO_2 when $CaO = Na_2O + K_2O$) to define four arbitrary divisions; alkalic <51, alkali-calcic 51-56, calc-alkali 56-61 and calcic >61. Harker then equated Pacific with Peacock's calc-alkali and Atlantic with alkali. This classification has survived the test of time and with the advent of plate-tectonics it took on a new significance in relation to the types of plate boundaries. Calc-alkali corresponding to the suite generated in compressive regimes and alkali to the extensional suites. Within this framework little work has been done to equate the major element chemistry of plutonic rocks to the nature of the plate boundary. One notable exception is the work of Petro et al. (1979) who used Mesozoic and Cenozoic plutonics from typical anorogenic extensional and orogenic compressional plate margins to produce a series of distinguishing features. This is important in the context of this study where the chemistry forms part of a series of pieces of evidence used to determine the environment of intrusion of the host plutons.

One of the most widely used diagrams for distinguishing broad chemical trends is the ternary AFM plot modified after Wager & Deer (1939). In this instance (Fig. 3/22) all the samples plot along a typical calc-alkaline trend of increasing Al_2O_3 with increasing FeO/MgO ratio. Petro et al. (1979) demonstrated that parameters such as Differentiation Index (DI) where DI = normative Q + Or + Ab + Ne + Lc + Ks, and normative plagioclase composition show variations in frequency distribution as a function of intrusion environment. Fig. 3/23 demonstrates that the granites presented here have a unimodal

distribution for both DI and plagioclase composition indicative of a compressional origin. Peacock's alkali-lime index was also used by Petro et al. who named it the calc-alkali index. Fig. 3/24 indicates that hand drawn curves for the presented data provide a calc-alkali index of ~62, a figure well into Petro's compressional regime. These three discriminators refer to the whole plutonic suite but Petro et al. also attempted to differentiate between extensional and compressional 'granites' (referred to as specimens in the SiO_2 range 70-75 %) due to their greater abundance. Table 3E shows two of the type examples compared with the 70-78 % SiO_2 (range extended to 78 % to include more data) specimens from each conglomerate horizon. The data are less convincing but still lean toward a compressional origin.

Brown (1979) used a slightly different approach to Peacock's alkali-lime index to distinguish calc-alkaline and alkaline plutonic suites (Fig. 3/25). Again the Ayrshire suite plots on a calc-alkaline trend but the appearance of more alkaline samples is apparent. This is confirmed by reference to the alumina saturation. In the sense of Sorensen (1974) most specimens are peraluminous or subaluminous, as is typical of calc-alkaline plutons, but several exhibit a more alkaline composition and two (187 and 399) are peralkaline (This is also borne out by the petrography as these more alkaline samples are those seen to contain the riebeckite-arfvedsonite amphiboles). The relationship between alumina and the alkalis may also be represented in the form of alumina saturation (AA) where AA = (2Ca + Na + K)/Al and plotted against SiO_2 percentage. Fig. 3/26 exhibits this with the calc-alkaline trend of Strong (pers. comm. 1980) and ampphibole compositions superimposed. A similar method of representing this is to plot normative diopside (Di) versus corundum (C) against SiO_2 percentage as is done in Fig. 3/27. Both these figures exhibit a broad calc-alkali trend away from amphibole compositions and additionally the C vs. Di plot shows some division of samples from each conglomerate into independent (?) but overlapping fields, which probably reflects the variation in proportions of fractionating minerals in

conjunction with slightly different starting compositions.

Traditional major element variation diagrams are of limited use in this study. They are best suited to suites (especially volcanic) where inflection points may be used to indicate the phases, and change of phases, involved in any fractionation. The Ayrshire analyses form part of an incomplete suite of plutonic rocks as a consequence of the sampling method, and thus the interpretation of variation diagrams is non-specific. Major elements plotted against SiO_2 show the trends expected in any sequence of rocks ranging from tonalite to granite in composition e.g. with increasing SiO_2, decreasing MgO, CaO, FeO^{Total} and P_2O_5, some increase in total alkalis and an increase in the K/Na ratio. Other element-element plots may indicate the importance of fractionating phases e.g. MgO vs. P_2O_5 with respect to apatite. Fig. 3/28 shows this plotted for the granites and a slightly different slope is evident for the Craigskelly samples as compared to the rest.

Winkler & Breibart (1978) noted a procedure in which granitic rocks are plotted in the system Q-Ab-An-Or-H_2O to estimate whether the composition represents a complete melt or had a significant restite (sensu Chappel & White 1974) component. Two ternary diagrams, Q-Ab-Or and An-Ab-Or, are used with cotectic surfaces contoured for the fourth component at a specific pressure. The further away from the cotectic surface an analysis plots the greater the implied restite content. Figs. 3/29 and 3/30 show the Ayrshire granites plotted on the diagrams contoured for pH_2O = 5 Kb (taken from Winkler & Breibart 1978). In the Q-Ab-Or diagram only those analyses with Q + Ab + Or $\geq$ 80% have been plotted following the recommendations of Tuttle & Bowen (1958). Both diagrams indicate that in general the granites lie close to the cotectic in regions of medium to low temperature, as is typical of melts containing few solids. The samples that lie away from the cotectic invariably plot in the plagioclase + quartz + liquid + vapour field and indicate the importance of plagioclase as a restite, and hence fractionating,phase. In contrast to this the quartz and alkali-rich granites plot close to the cotectic

but in the alkali feldspar field, indicating the importance of potassium feldspars in their crystallization history. Another general feature is the samples plotting on the low pressure side of the cotectic which suggests that the granites were intruded at a higher level than that equivalent to 5 Kb. The alkali rich samples are, however, slightly different plotting close to the 5 Kb cotectic surface. This suggests that they equilibrated at pH_2O = 5 Kb but other evidence (see 3.2.1) indicates emplacement at higher levels.

Chappel & White (1974) and White & Chappel (1977) initiated an interesting approach to theproblem of granite genesis using the major element chemistry and mineralogy. They divided granites into two types : those derived from a sedimentary source (S types) and those from an igneous source (I types). Although in theory this sounds an attractive idea in practice it is difficult to apply with most plutons having some features from the I type pigeon-hole and other features thought to characterise the S types. Obviously one of the major problems is the composition of the theoretical source rocks, which although having some broad features must naturally show variations on both local and regional scale. Strong (in press and in prep.) produced a review of the chemistry of Newfoundland plutons in which he tried to apply the I and S classification by reference to numerous variation diagrams. He was, however, forced to conclude that the general applicability of the I & S system is of dubious merit. This is a conclusion concurred with by this study.

The major element patterns as reflected in Figs. 3/26 and 3/27 suggest that amphibole fractionation was important in the evolution of the granite suite from Ayrshire (e.g. Cawthorn & Brown 1976). The XTLFRAC computer programme (see 3.1.5) may also be used to determine the feasibility of producing one melt from another through fractionation of certain phase(s). Using the individual Ayrshire analyses the most likely minerals involved in any fractionation are plagioclase and biotite and/or hornblende.

One factor important in interpretting the chemical data is the age relationship of the clasts as they are

taken from a sedimentary sequence rather than one pluton. Talking in terms of fractionation producing an evolving magma sequence it is obviously ridiculous to model fractionation of a specimen dated at 560 Ma to one of an age of 470 Ma. However in all cases the analyses define a broad calc-alkaline trend and the XTLFRAC modelling has been performed using samples with practical age relations e.g. 475-450 Ma and 560-540 Ma.

Another feature evident from the major element studies is the presence of increasingly alkaline and marginally peralkaline samples (e.g. well seen on Fig. 3/31). The origin of these is somewhat problematical and several explanations have been proposed with reference to other areas, where they are in conjunction with calc-alkaline sequences rather than in more typical alkaline extensional environments. The fractionation biotite and plagioclase from a corundum normative calc-alkali suite could produce the necessary composition with reference to the major elements. It would, however, produce adecrease in certain trace elements in the melt e.g. Rb, Zr, Zn and Nb, whereas these are typically enriched in peralkaline granites (see Table 3C and section 3.5). Teng & Strong (1976) suggested that the origin of the St. Lawrence granite, a peralkaline Newfoundland pluton, may be through solely plagioclase fractionation from a calc-alkali magma. This is more realistic in the light of trace element enrichment. Lameyre (1980) said that alkaline compositions may be produced at the end of normal calc-alkaline evolution trends but Petro et al. (1979), using type compressional and extensional plutons stated that only extensional (and hence not calc-alkaline) suites produce peralkaline rocks. The question of the origin of these rocks is further discussed in section 3.5 where the trace element data aid investigation.

(An additional method of treating the major oxide data was also attempted. This involved using a four component projection system first reported by O'Hara (1976). This expresses analyses in terms of four end members, namely CaO, MgO, Al_2O_3 and SiO_2 (CMAS) and equating the other

oxides, through similarities in chemical behaviour, to these apices. A computer programme modified from Yarwood's Edinburgh version then computes the analyses in three dimensional space and this is reduced to two dimensions by projection from certain points onto sides of the tetrahedron. O'Hara's original version, the CMAS tetrahedron, was designed for ultrabasic rocks but by using K_2O, Al_2O_3, FeO^{Total} and SiO_2 (KAFS) as the end members a projection suited to the acid rocks results. The Ayrshire granites when plotted in this system yield a trend which may be related to the position of certain minerals in the projection e.g. biotite, hornblende and plagioclase. Detailed investigation of these plots was not, however, followed up. Although there is good potential in using this system for differentiating between acid plutonic suites from different petrotectonic environments, the amassing and comparing of pre-existing data was far beyond the scope of this project.)

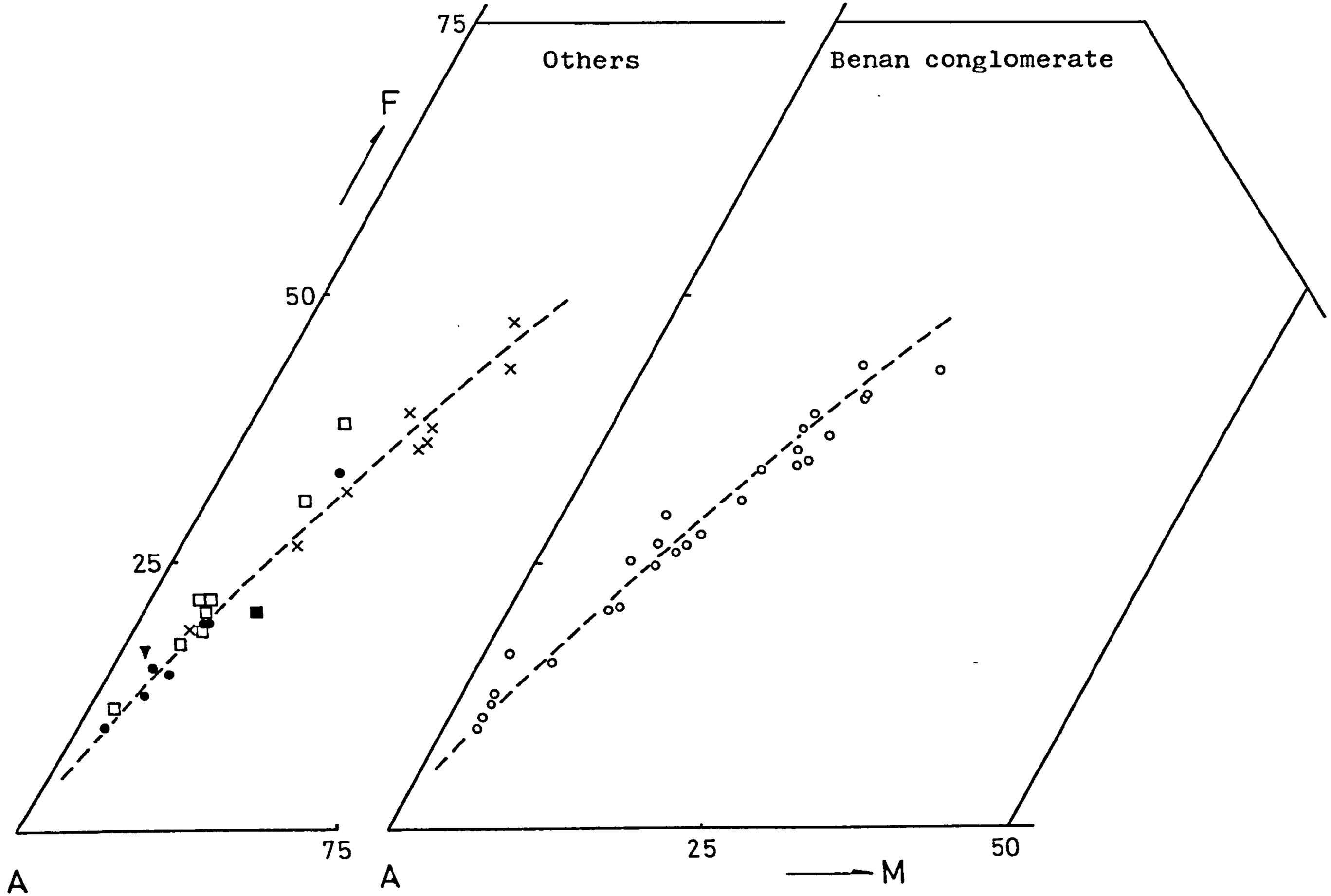

Fig. 3/22 AFM diagrams showing typical calc-alkaline trend.

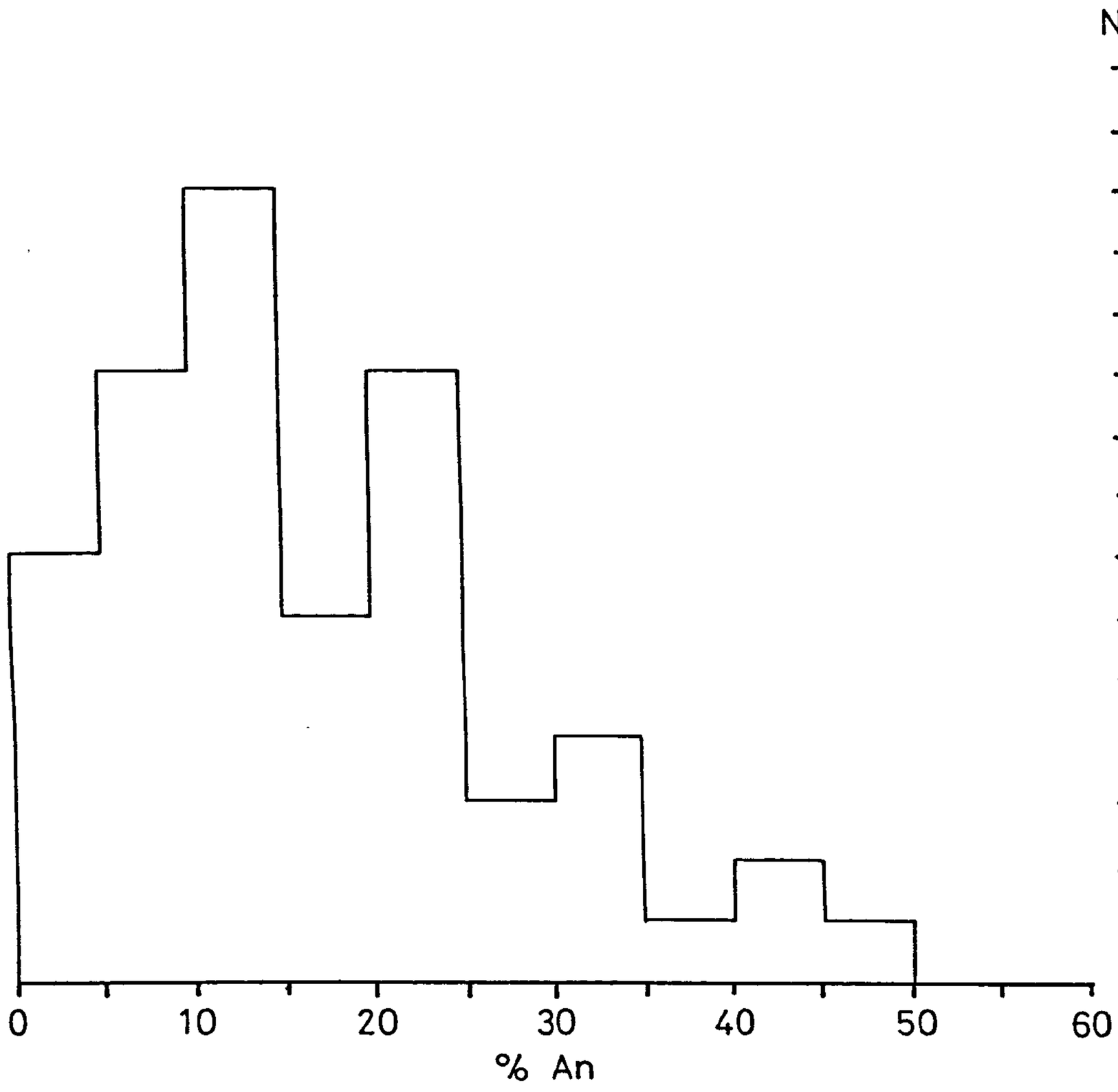

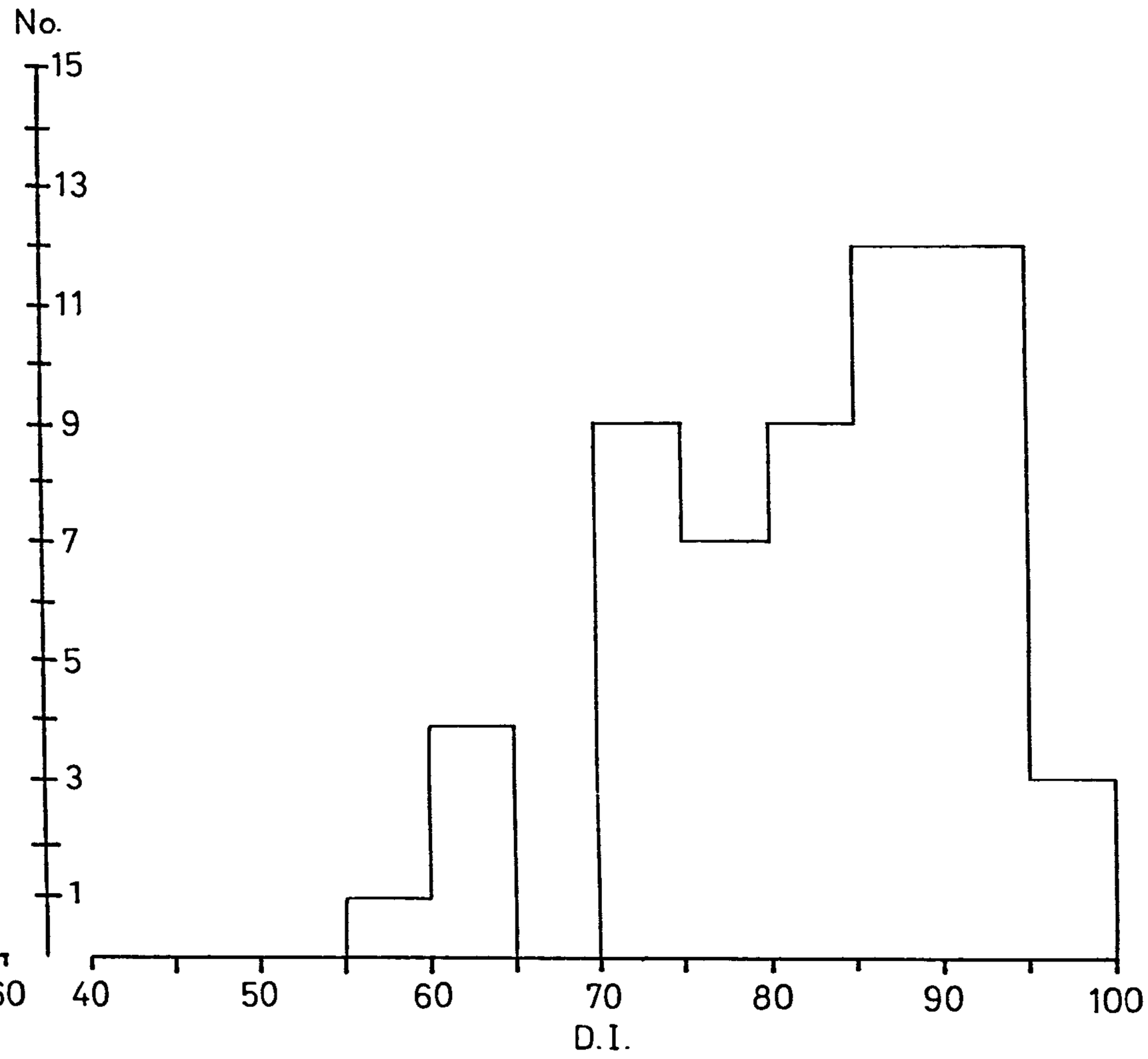

Fig. 3/23 Frequency diagrams for plagioclase composition and Differentiation Index showing unimodal distribution in both cases.

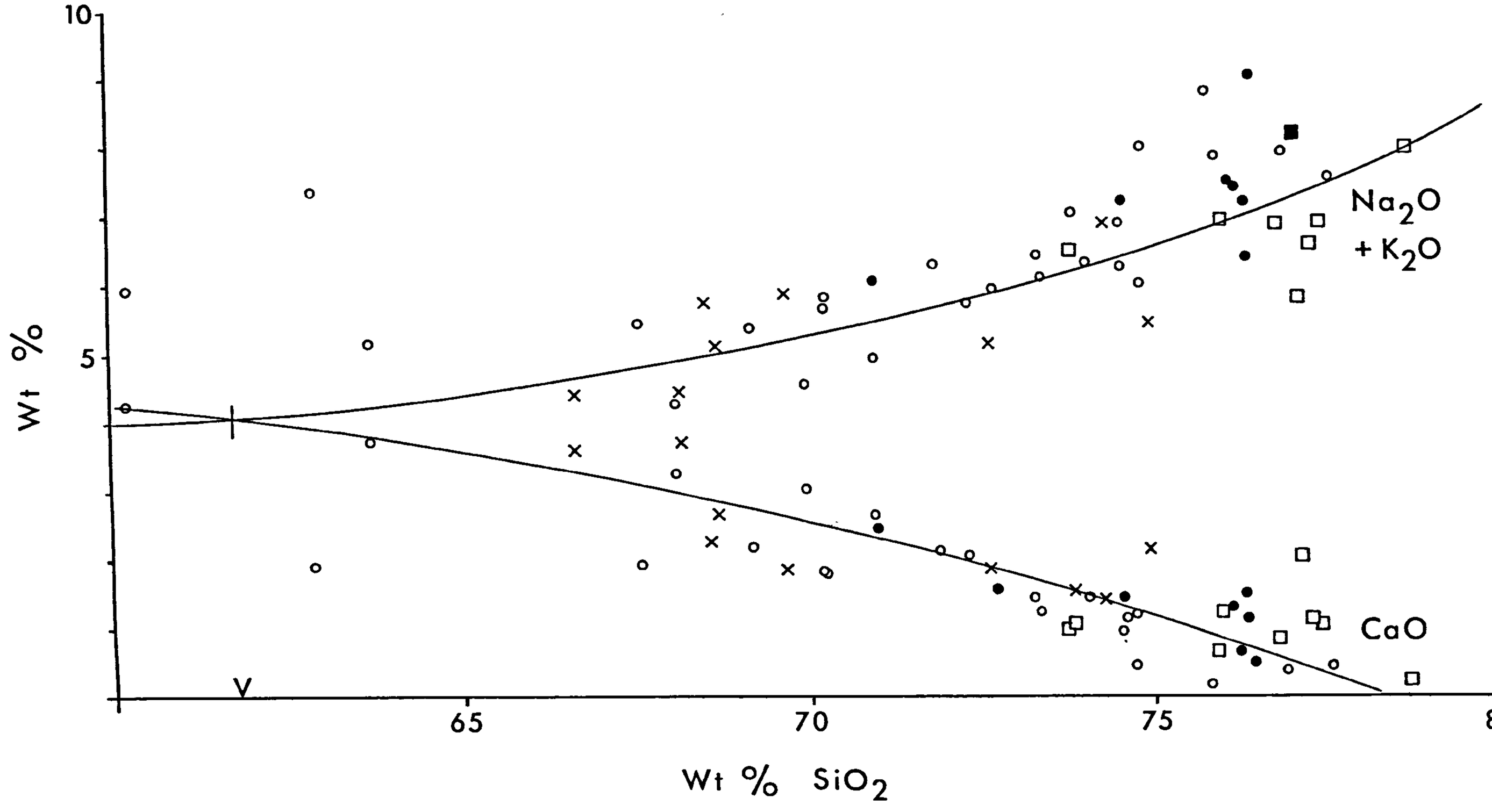

Fig. 3/24 Hand drawn curves through $Na_2O + K_2O$ and CaO values indicating a calc-alkali index of ~62.

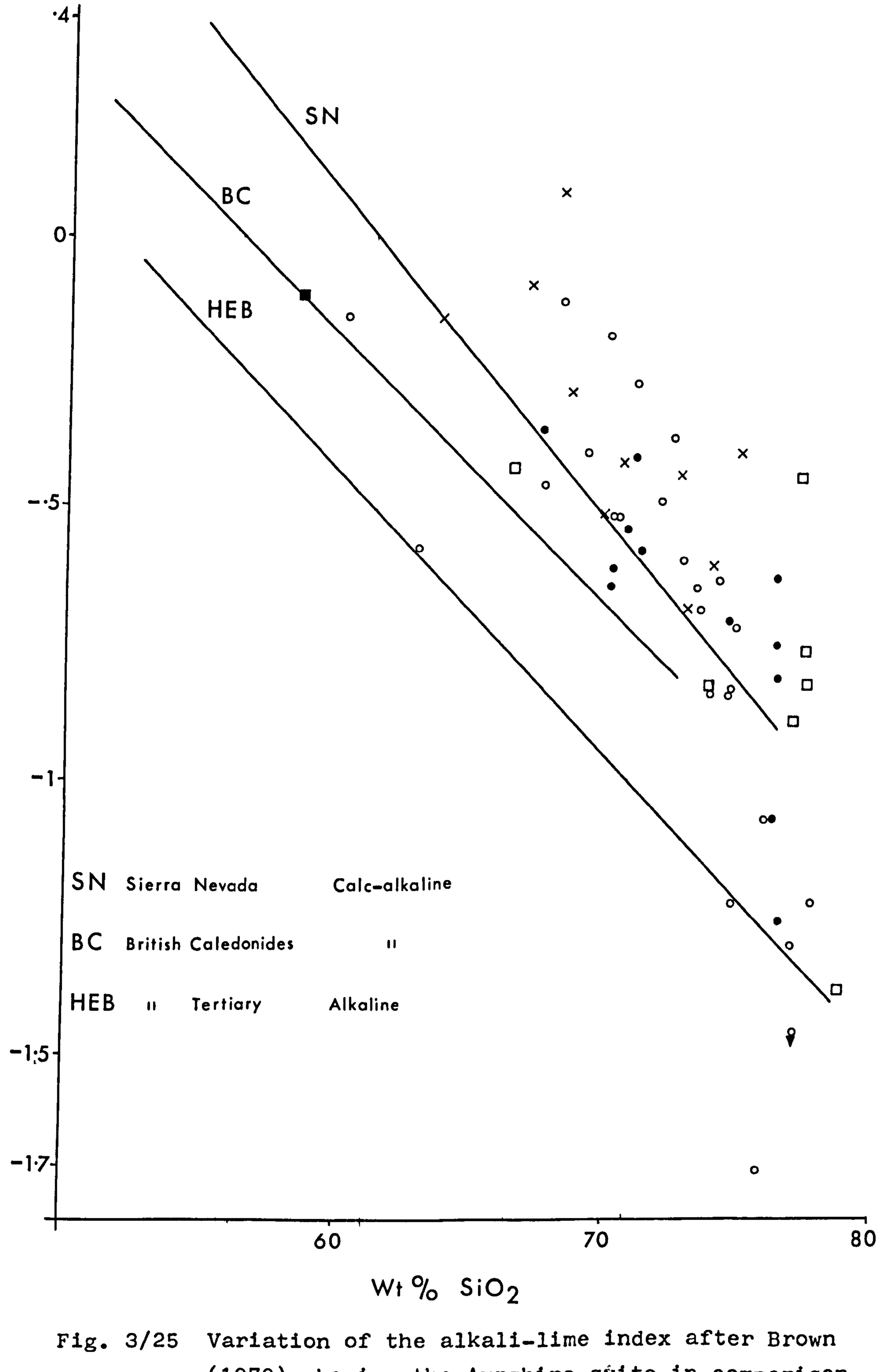

Fig. 3/25 Variation of the alkali-lime index after Brown (1979) showing the Ayrshire suite in comparison with typical calc-alkaline and alkaline suites.

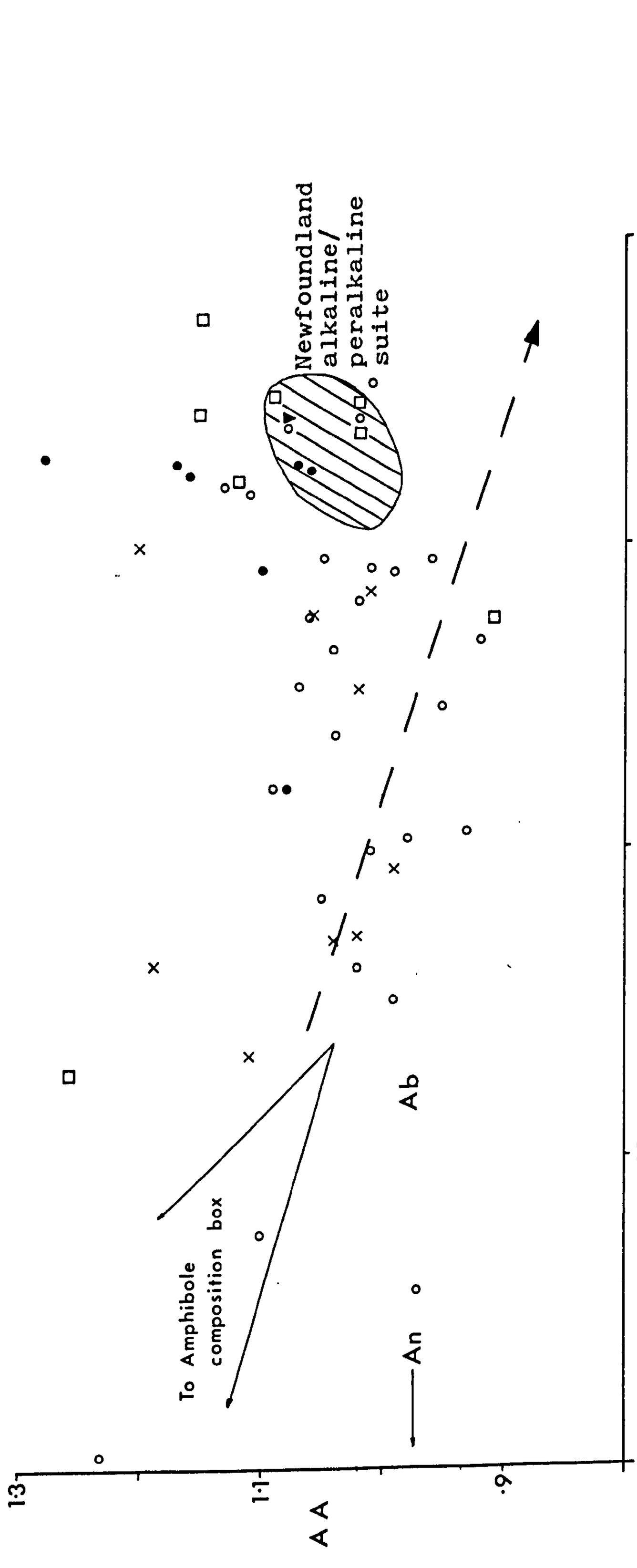

Fig. 3/26 AA vs. SiO_2 plot with the Dunnage calc-alkaline trend (- - - -) and Newfoundland alkaline/peralkaline suite after Strong (in press).

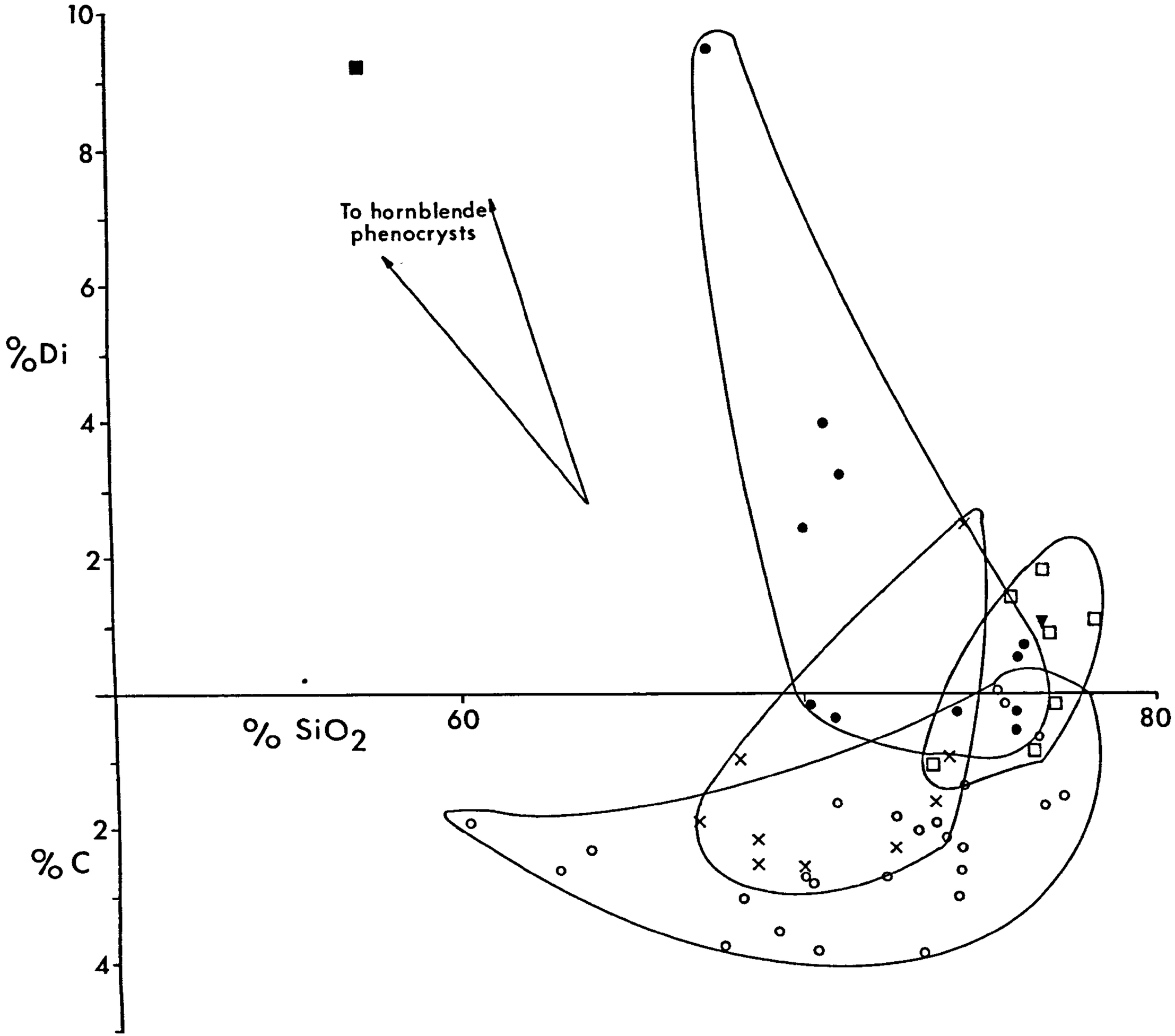

Benan conglomerate
Corsewall conglomerate
Craigskelly conglomerate
Kilranny conglomerate

Fig. 3/27 Diopside (Di) or corundum (C) content.

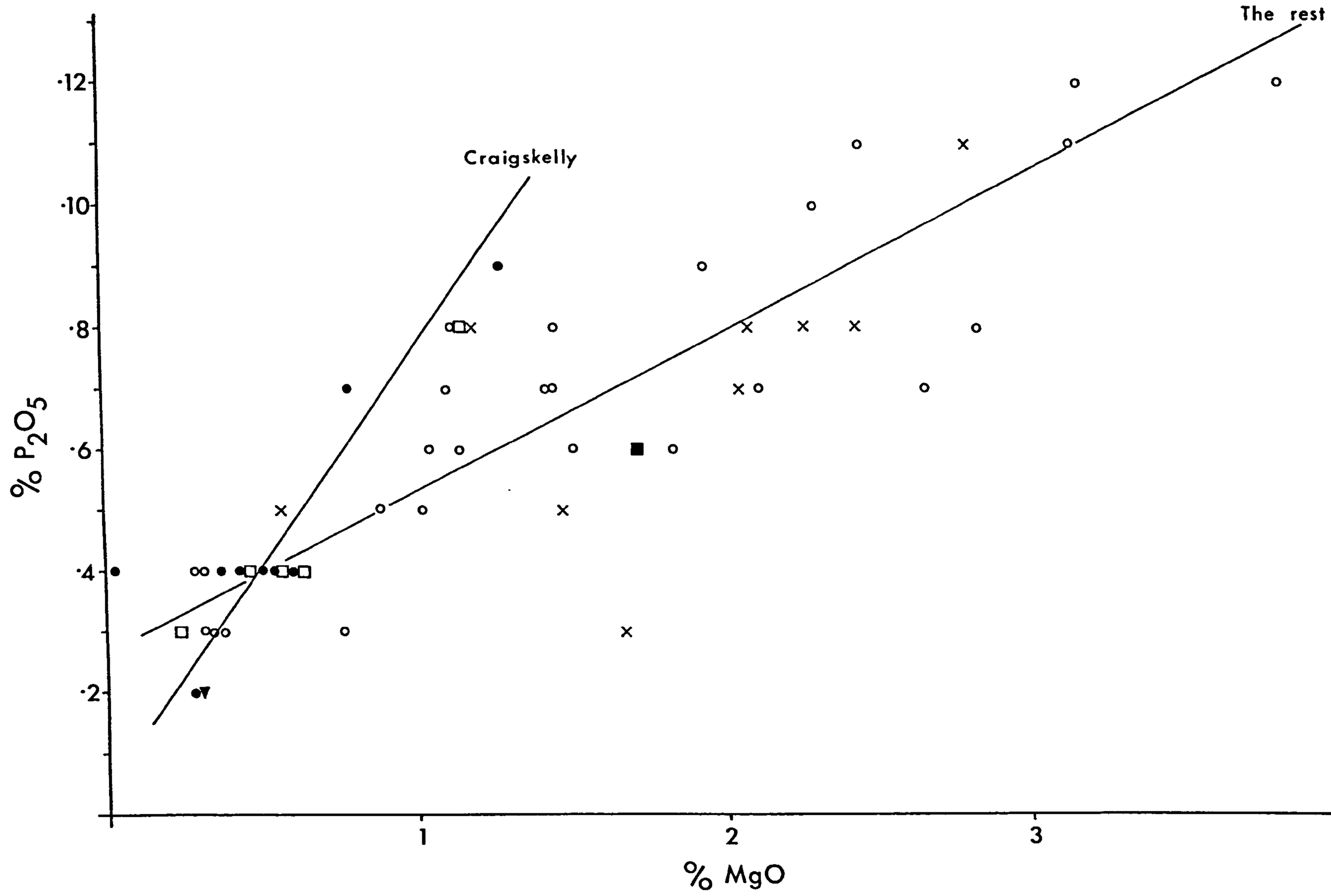

Fig. 3/28 MgO vs. P_2O_5

690 Temperature (^{o}C)

12 An content on the cotectic surface

5 An content for individual analyses

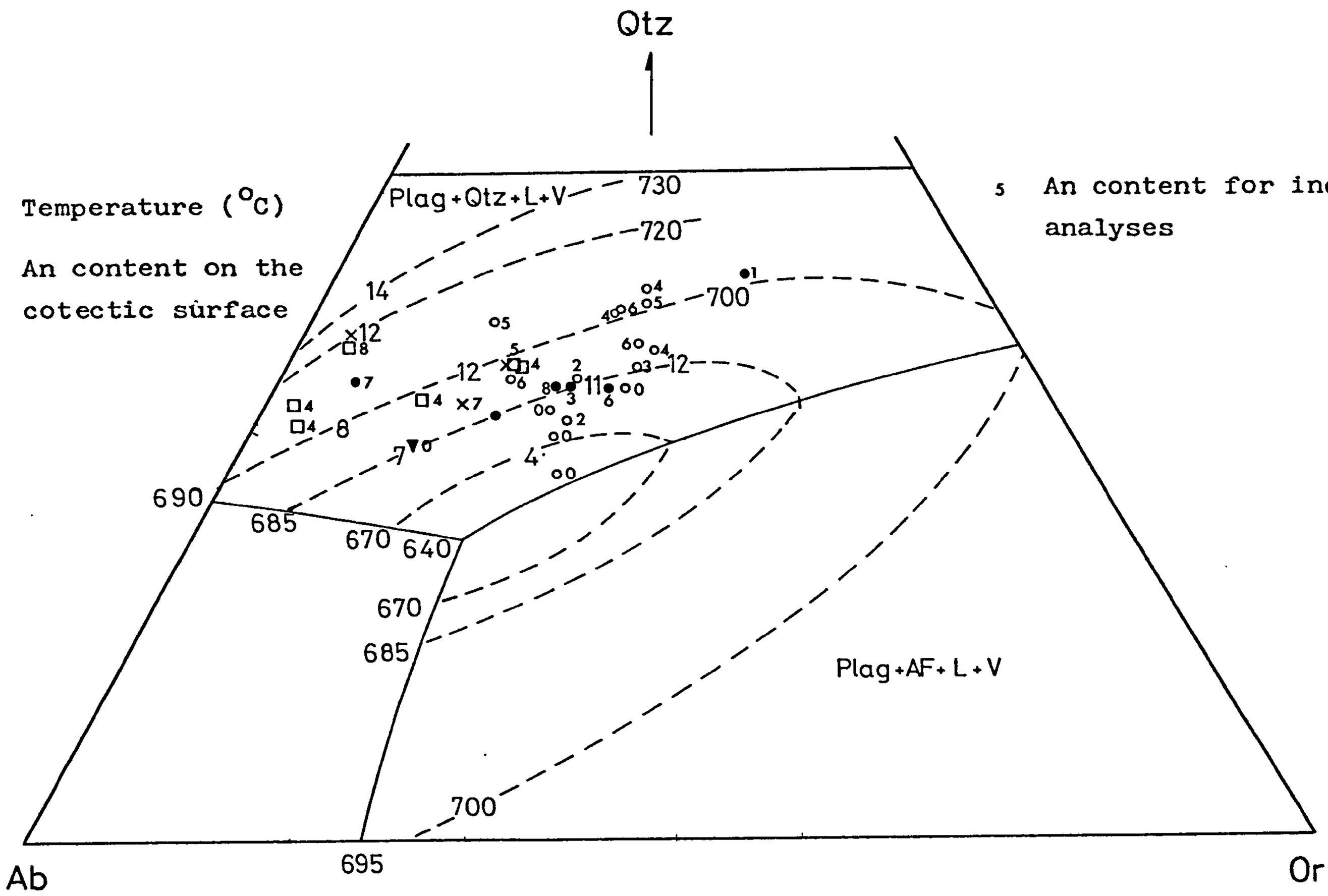

Fig. 3/29 Qtz-Ab-Or diagram showing cotectic surface at pH_2O = 5 Kb after Winkler & Breibart (1978).

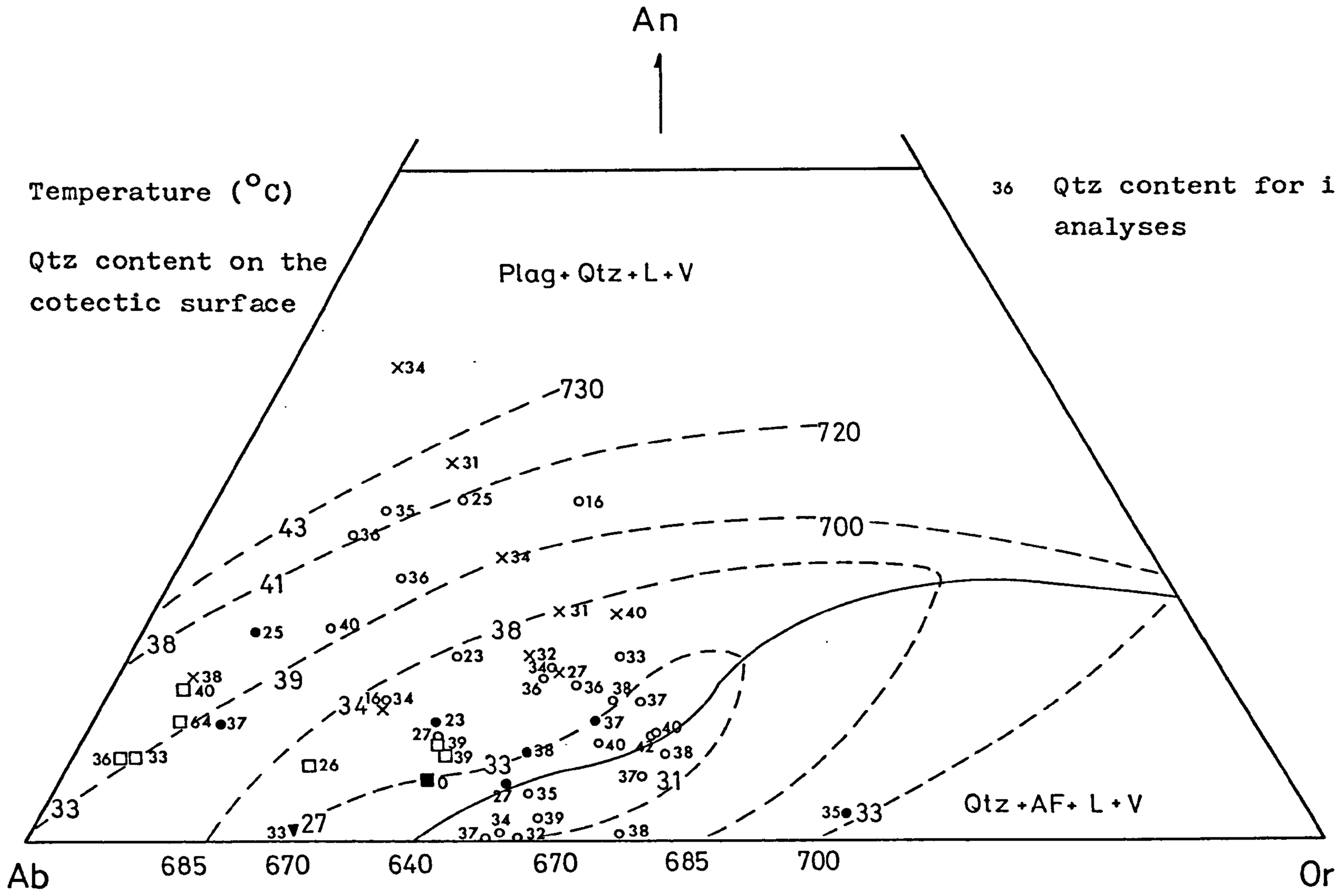

Fig. 3/30 An-Ab-Or diagram showing cotectic surface at pH_2O = 5 Kb after Winkler & Breibart (1978).

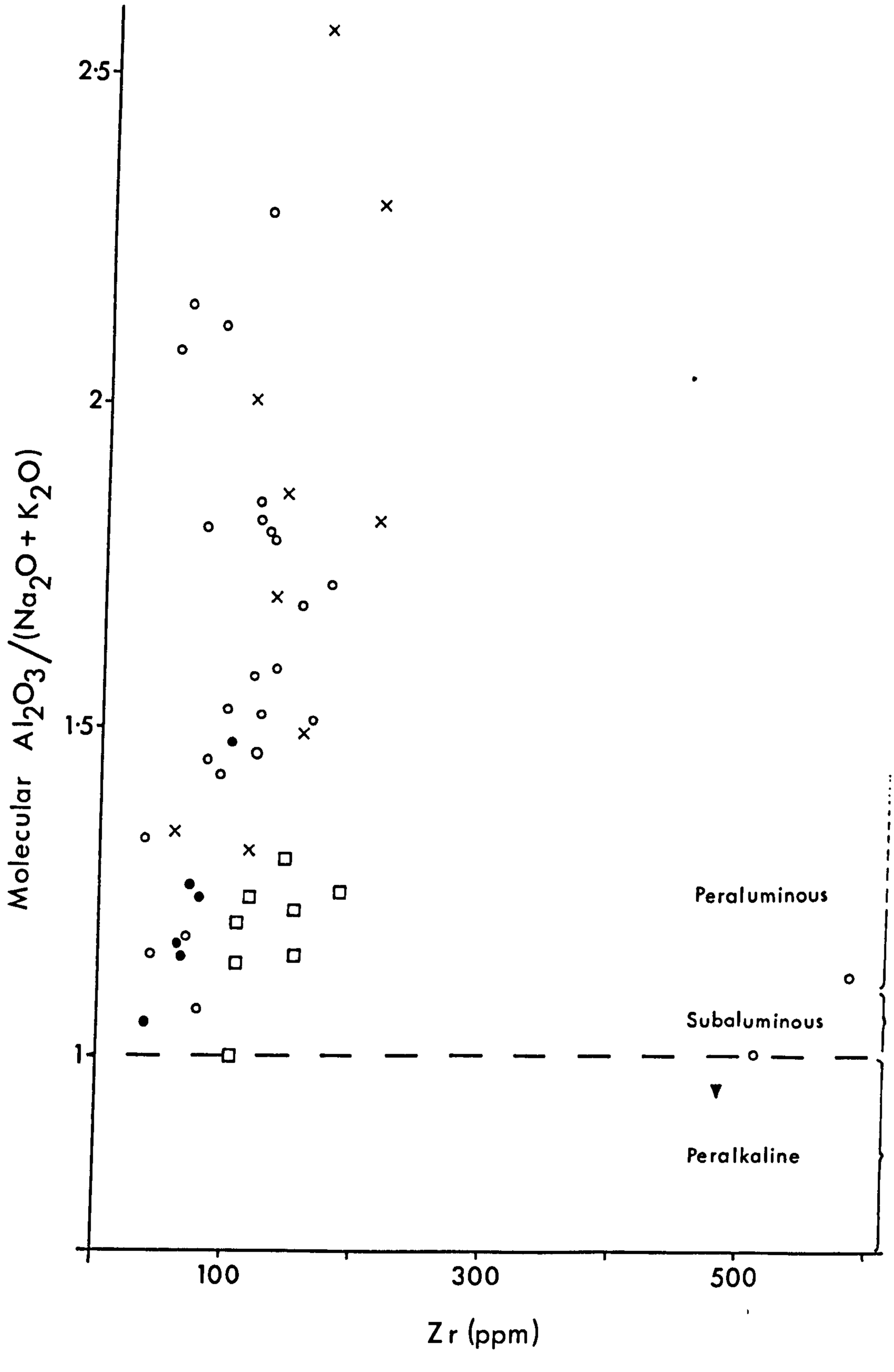

Fig. 3/31 Molecular alumina/alkalis showing the presence of peralkaline samples.

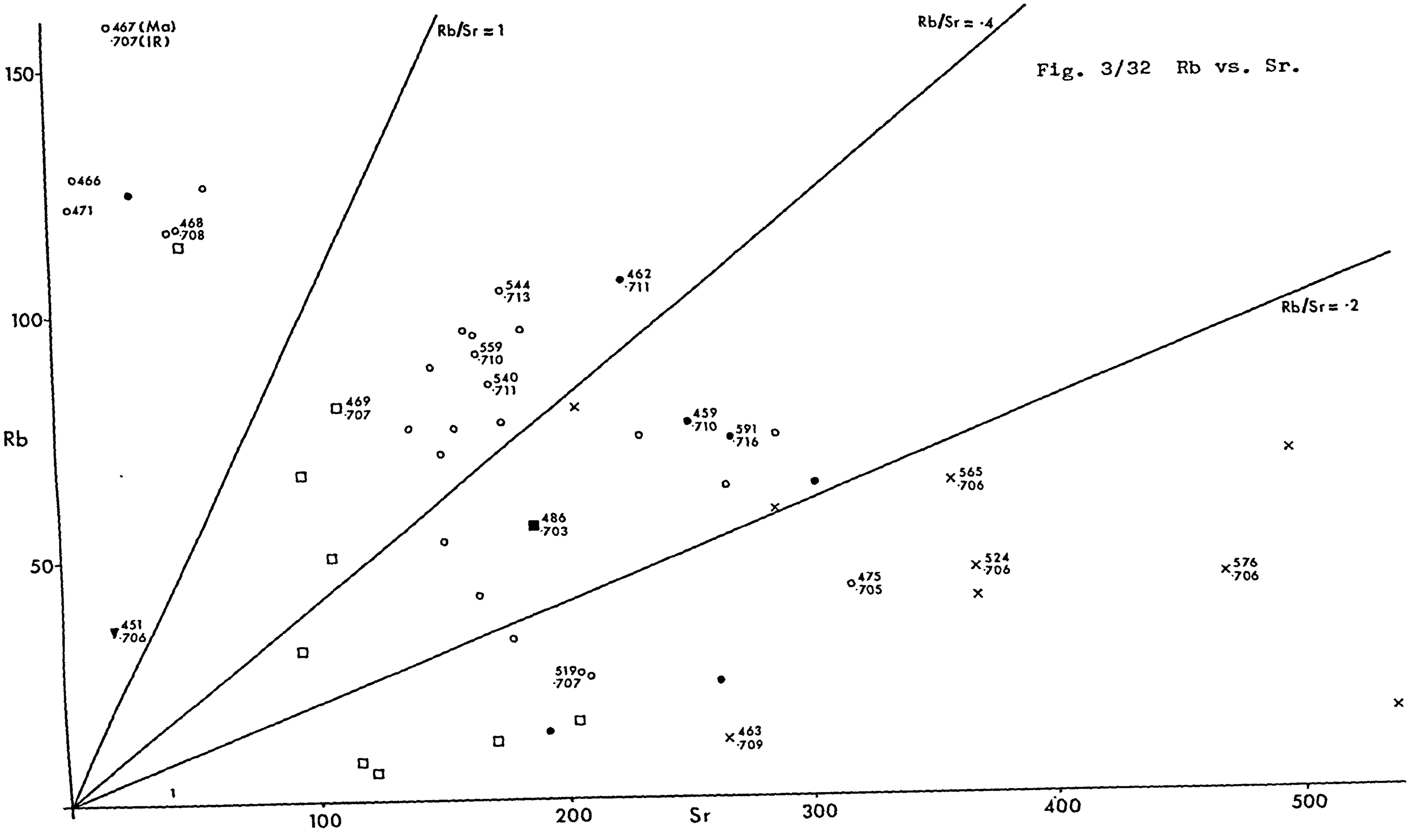

Fig. 3/32 Rb vs. Sr.

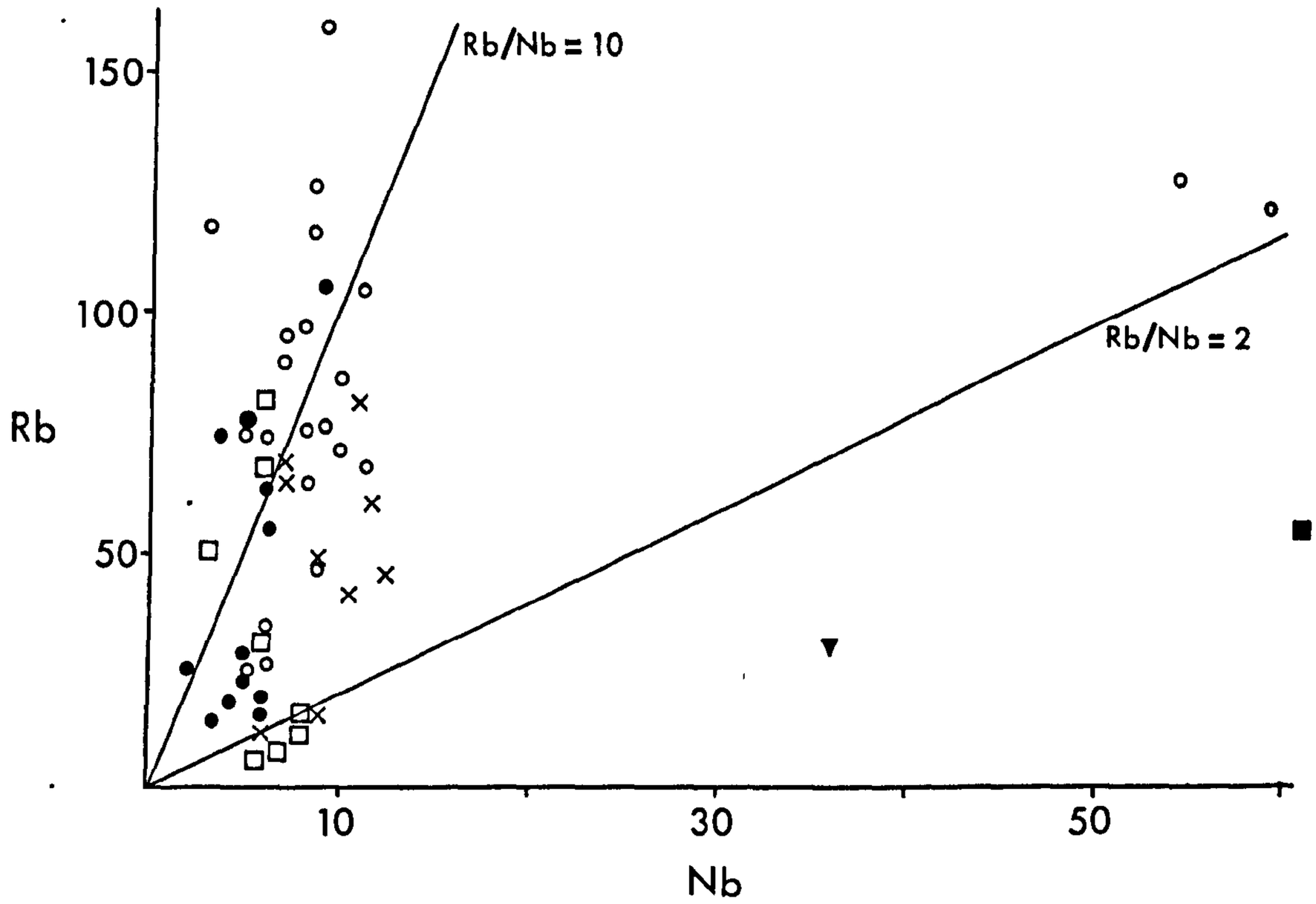

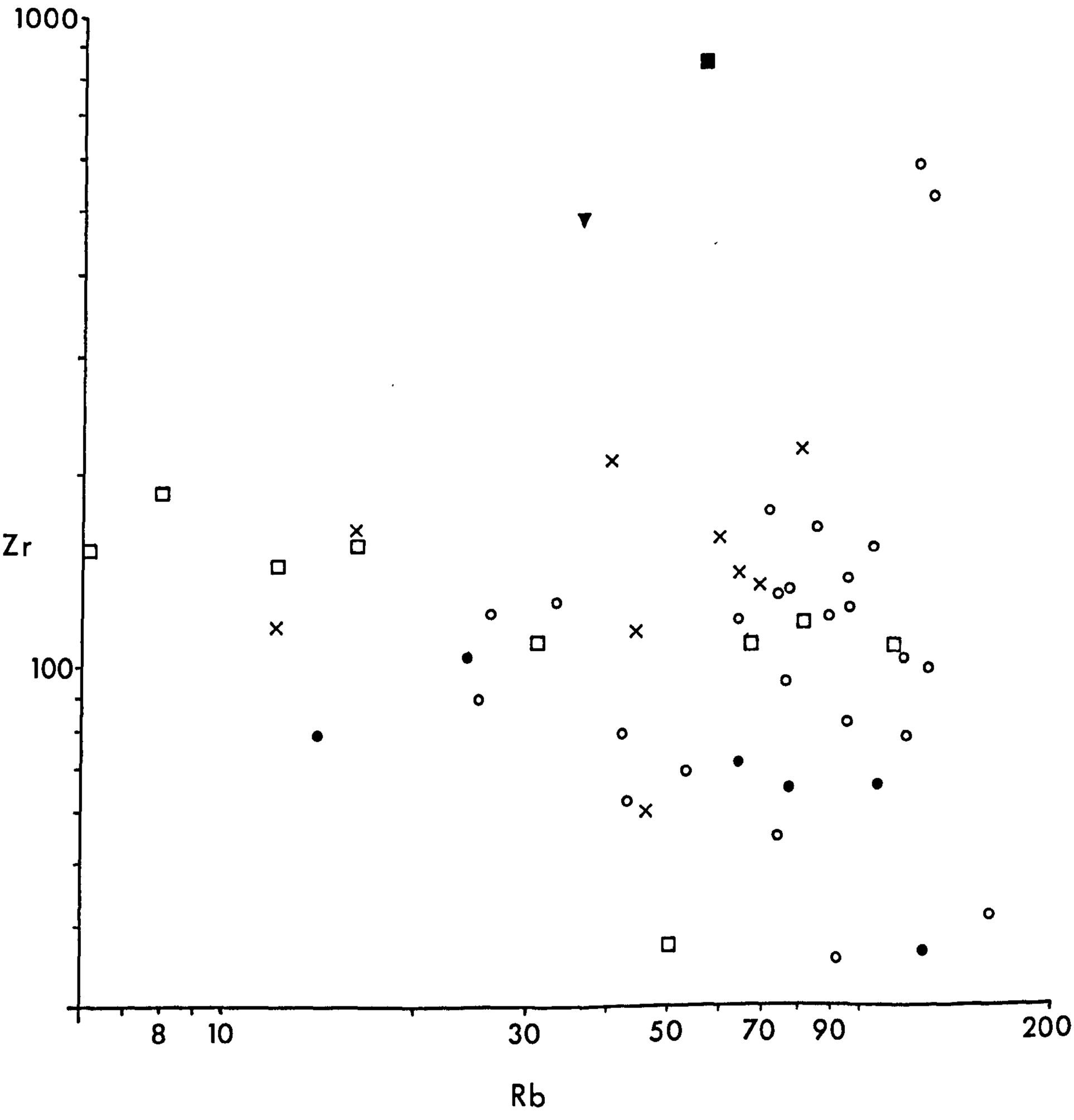

Fig. 3/33 Rb vs. Nb and Log Zr vs. Log Rb.

Parameter	Compression (Aleutians)	Extension (B.I.Tertiary)	Corsewall (4)	Craigskelly (7)	Kilranny (7)	Benan (19)	Tormitchell (1)
D.I.*	83.10	88.87	82.48	88.97	90.99	85.47	93.87
Al_2O_3	14.90	13.34	12.61	12.55	12.12	12.89	11.70
Fe_2O_3	0.73	1.23	1.17	0.74	1.06	0.93	1.08
FeO	1.13	1.97	1.75	1.04	0.86	1.50	0.67
MgO	0.52	0.31	1.18	0.61	0.57	1.12	0.30
CaO*	2.40	1.24	1.77	1.28	1.10	1.20	0.28
Na_2O	4.09	3.79	3.80	4.19	5.11	3.48	6.09
K_2O	2.62	4.78	2.17	3.11	1.76	3.22	2.16
TiO_2	0.25	0.29	0.35	0.19	0.21	0.21	0.14
Alkalis*	6.68	8.57	5.97	7.30	6.87	6.70	8.25
$CaO/(Na_2O+K_2O)$*	0.38	0.15	0.31	0.19	0.17	0.20	0.03
$Fe^TO/(Fe^TO+MgO)$*	0.79	0.91	0.71	0.74	0.77	0.71	0.85

Table 3E Compression vs. extension for granites (after Petro et al. 1979). Aleutians/Alaska and British Isles Tertiary data based on 'granites' in the SiO_2 interval 70-75%, Ayrshire samples based on 70-78% SiO_2. Parameters marked thus (*) are those most valuable for environmental distinction. Numbers in parentheses indicate the number of analyses averaged.

3.5 Trace element chemistry

The trace element variation diagrams, whether plotted against another trace element or a measure of fractionation e.g. SI, DI, Larsen Index etc., show features typical of calc-alkaline evolution. Figs. 3/32 and 3/33 present graphs of Rb vs. Sr, Rb vs. Zr and Rb/ vs. Nb, and show a progression to Rb/Sr ratios in excess of 12, increasing Rb/Zr and Rb/Nb and additionally serve to demonstrate the presence of the alkali rich granites with high Zr and Nb contents.

The ratio K/Rb, which decreases with fractionation, plotted against DI, which increases with fractionation, is a useful plot. Fig. 3/34 illustrates this for the Ayrshire suite in comparison with trends produced by some of the Andean calc-alkaline plutons. The Benan conglomerate clasts compare favourably with the Andes but the other horizons are less well defined due to a smaller range in DI (which is possibly a function of sampling).

More information may be obtained by using a ternary approach, with the elements Ba, Rb and Sr particularly useful in granitic rocks. These elements substitute widely for potassium in the major mineral phases and are not affected to a large degree by early formed constituents such as zircon, allanite etc.. El Bouseily & El Sokkary subdivided a ternary Rb-Ba-Sr diagram by empirical observation on previously defined granitoids (Fig. 3/35). They found that Ba/Rb and Ba/Sr ratios may show some variety in trends from different associations but that in a ternary sense Ba decrease was associated with an increase in Rb or Sr and hence an important governing factor in the Rb/Sr ratio. Fig. 3/35 shows the Ayrshire granite suite plotted on the ternary diagram, and a complete spread exists along the differentiation trend. El Bouseily & El Sokkary (1975) suggested that the'anomalous granites' field may correspond to granites of metasomatic origin but in this study it is thought to represent a continuum in the granite spectrum rather than a genetic difference in origin.

McCarthy & Hasty (1976) also used Ba, Rb and Sr

in an attempt to define the crystallization of granitic melts. Plotting Ba vs. Rb and Sr vs. Rb on log-log scales leads to a straight line evolution for perfect fractional crystallization and a curved path for incremental equilibrium crystallization. This, however, is not unambiguous and difficult to apply to single plutons let alone a series of granitic clasts. Also their models involve a decrease in Ba with fractionation whereas the Ayshire granites show a Ba increase with increased Rb, and hence fractionation. This relationship probably reflects the minor involvement of potassium feldspar as a fractionating phase until late in the evolution. Hence only the Ba depleted specimens are those exhibiting the more alkaline character.

Log distribution graphs can also be utilized in the manner proposed by Beckinsale (1979). The evolving composition of a melt can be modelled for fractional crystallization with respect to the phases fractionating. Assuming a trace element content in the starting melt and using distribution coefficients for elements in different phases, in conjunction with the mathematical model for Rayleigh fractionation ($C_l/C_o = F^{(D-1)}$ where C_l = melt concentration, C_o = initial composition, D = bulk distribution coefficient and F = fraction of remaining melt) trends produced by individual minerals can be plotted and annotated for percentage fractionation. Figs. 3/36, 3/37 and 3/38 show this done for Ba vs. Rb, Sr vs. Rb and Ce vs. Rb using the distribution coefficients of Hanson (1978) and Cox et al. (1979). Inspection of these figures indicates that in all cases biotite removal produces trends in opposition to those of the postulated basic to acid progression. Clino- and ortho- pyroxene show indecisive trends for Sr vs. Rb and Ba vs. Rb but are oblique to any linearity on the Ce vs.Rb plot. This and the lack of any petrographic evidence of pyroxene suggests that they took no major part in any fractionation. This leaves hornblende, plagioclase and potassium feldspar as the main possibilities. On all three plots it is feasible to reproduce the general suite trends by juggling the proportions of hornblende and plagioclase fractionating in the early evolution and then

invoking potassium feldspar as a later phase to produce the more alkaline compositions. The trace element content of the alkaline samples may, however, be due in part or whole to another cause. As noted previously (3.2.1) the alkaline specimens show evidence of late stage fluids and Mustart (1972) found that high alkali content in a fluid may directly aid trace element enrichment.

The five porphyries analysed provide a sample of the extensive range of hypabyssal acid clasts. Although this cannot be held to be representative the data are not incompatible with the plutonic suite. The very high Ba and Sr values, however, seem to preclude an origin of the porphyries as late differentiates, they must belong to a fairly primitive cycle. (See Table 3c).

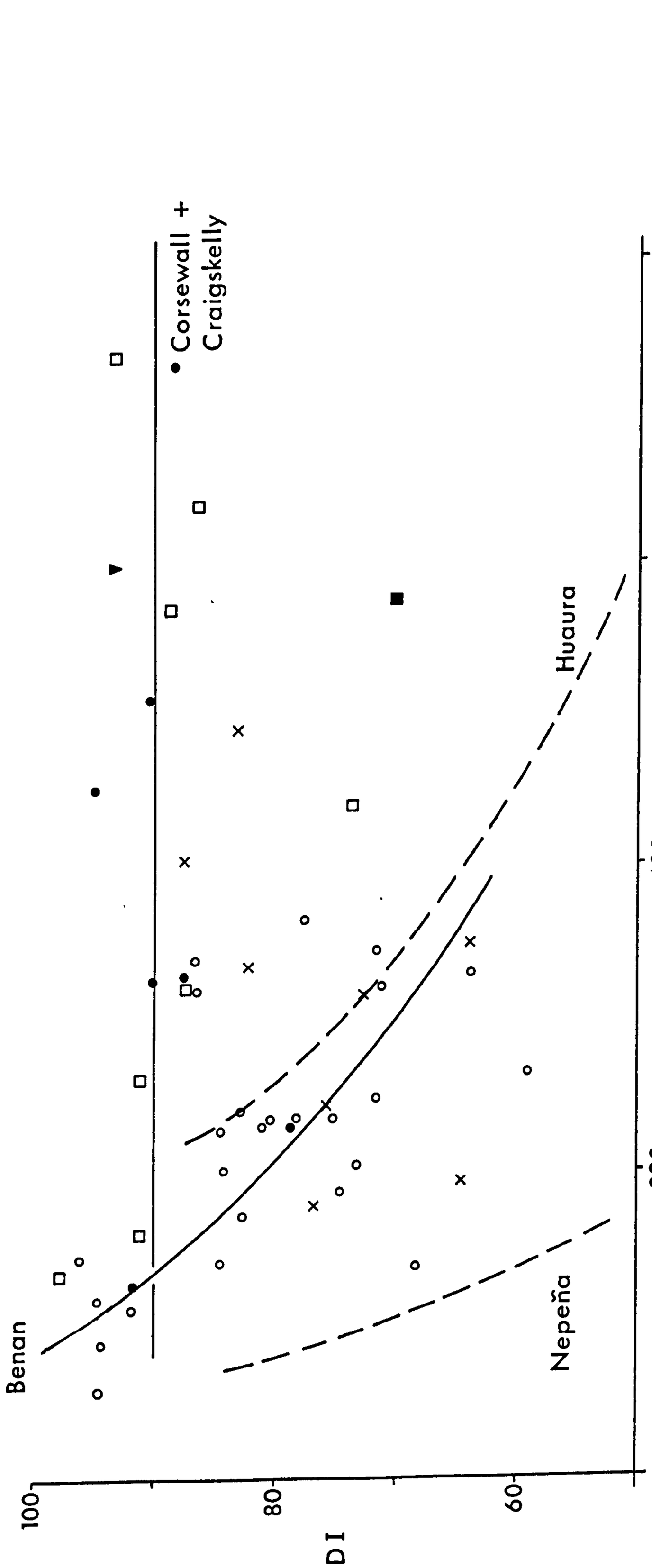

Fig. 3/34 D.I. vs K/Rb with typical calc-alkaline trends from Andean plutons superimposed after Atherton et al. (1979).

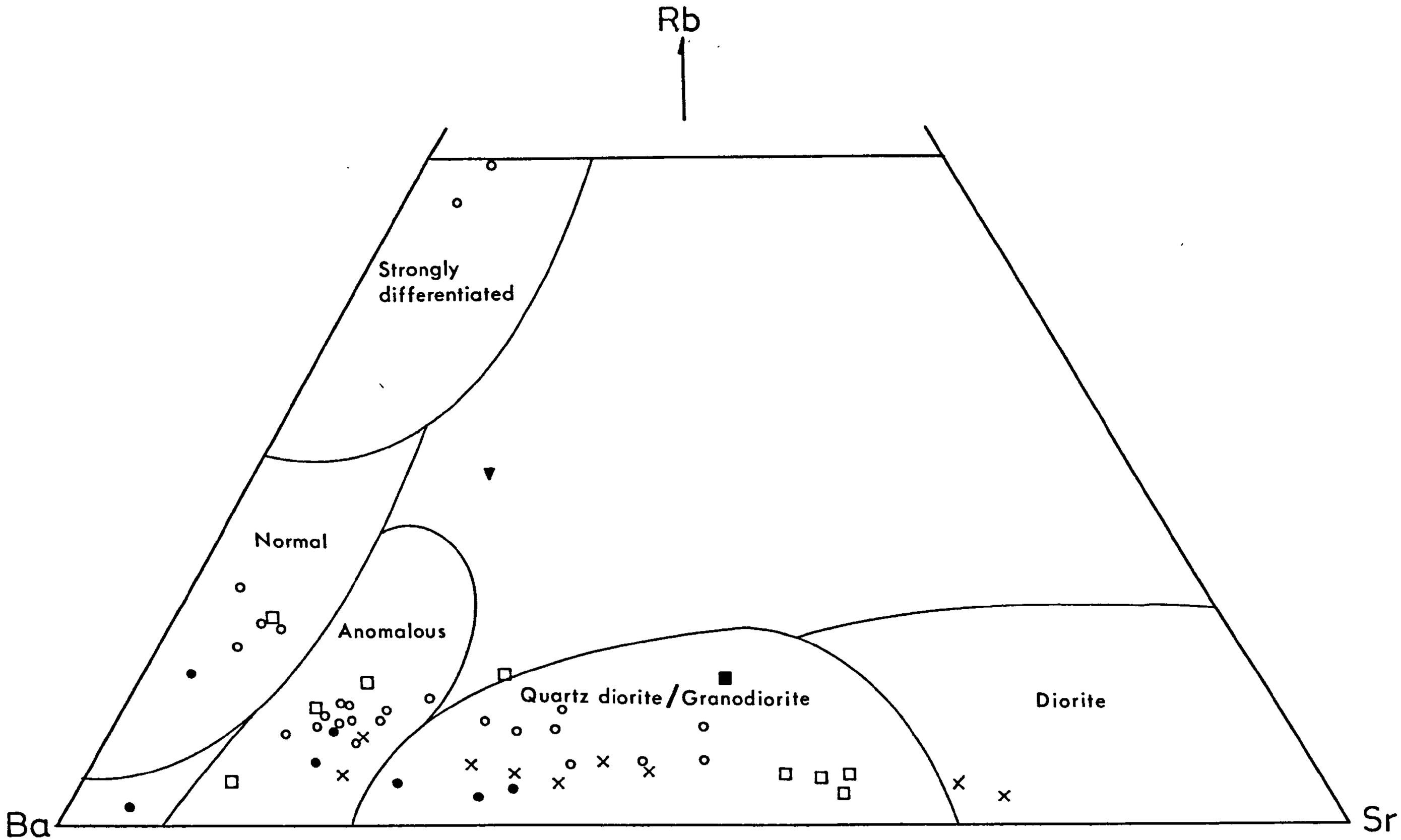

Fig. 3/35 Ba-Rb-Sr ternary diagram with granite fields after El Bouseily & El Sokkary (1975).

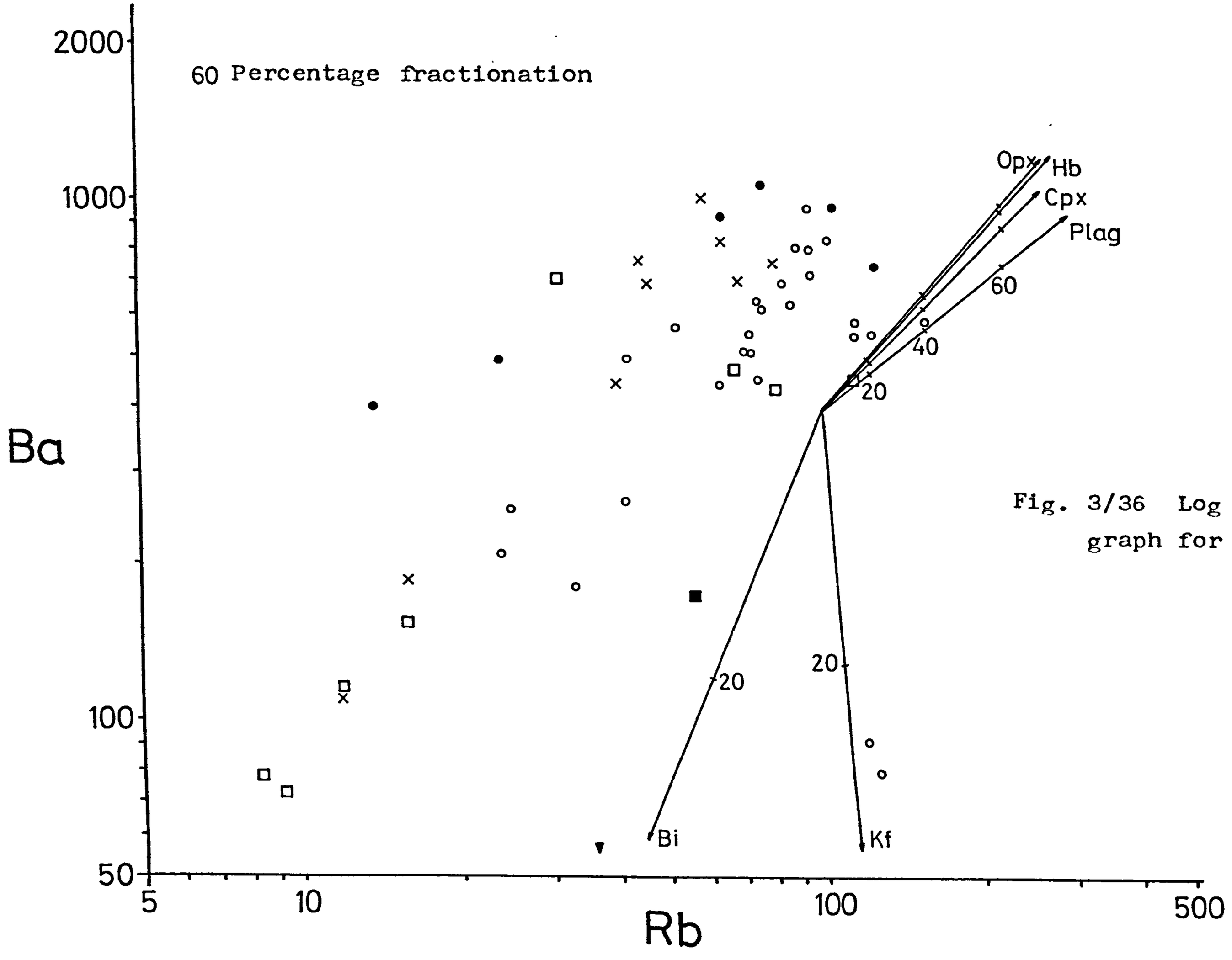

Fig. 3/36 Log distribution graph for Ba vs. Rb.

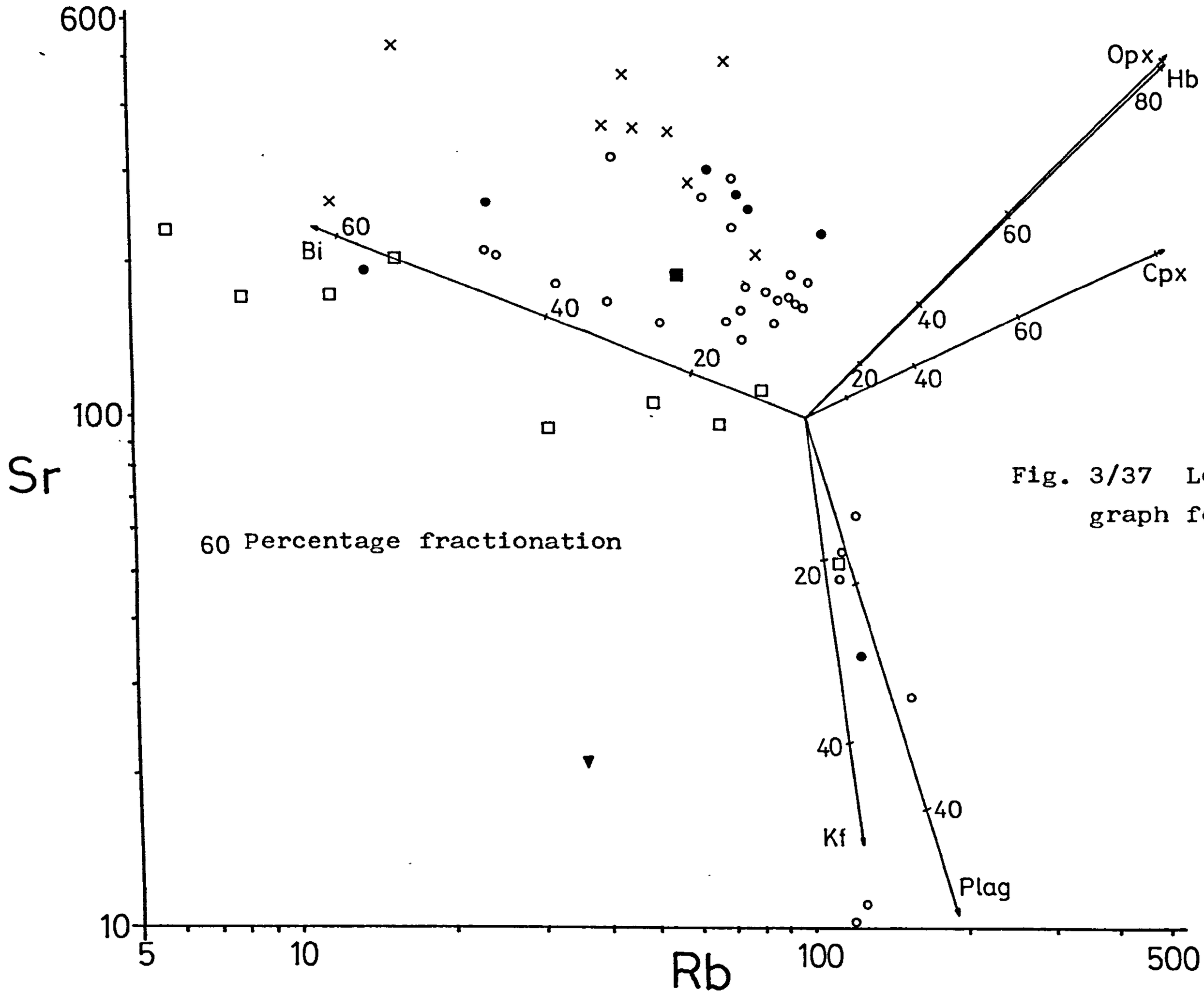

Fig. 3/37 Log distribution graph for Sr vs. Rb.

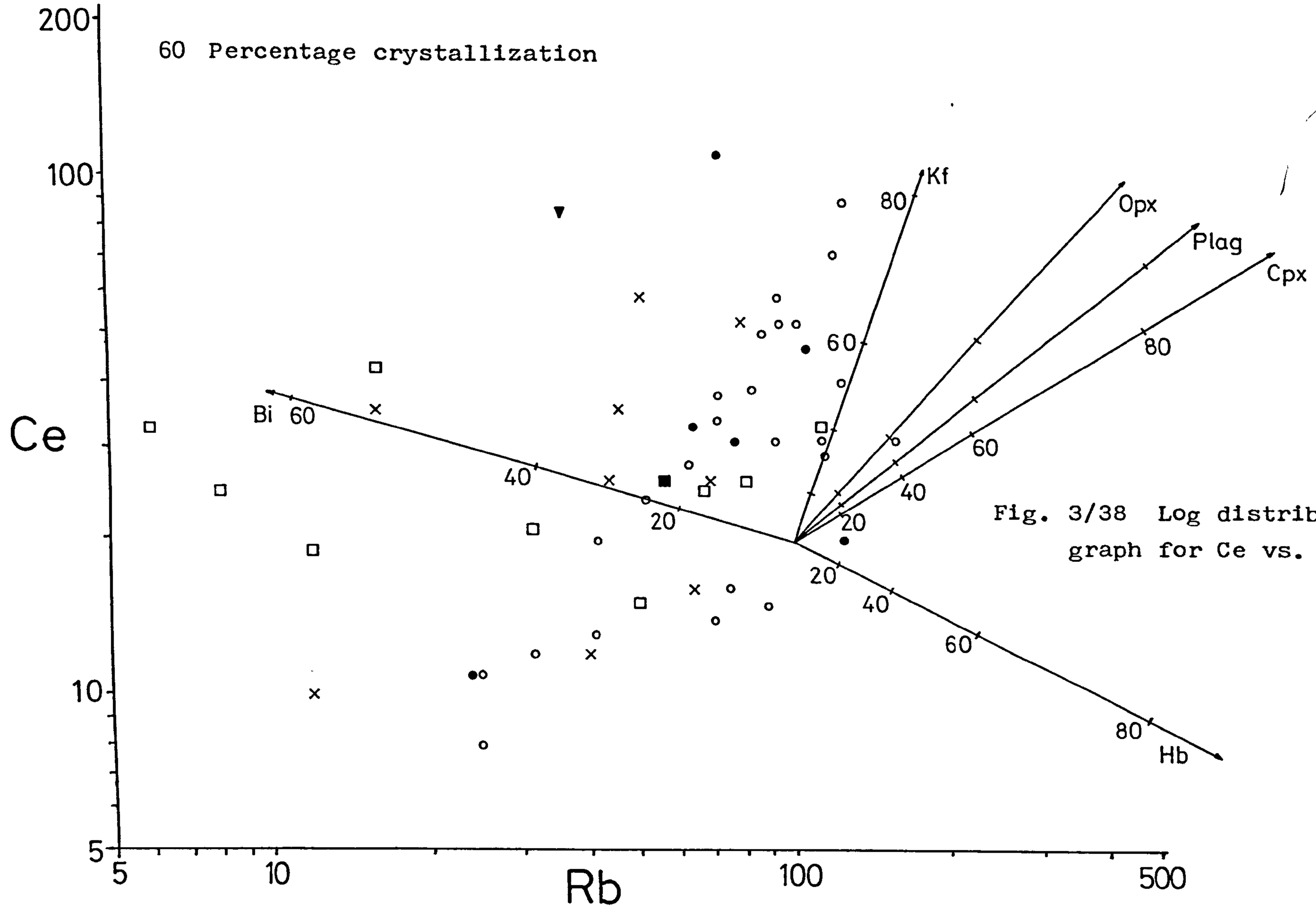

Fig. 3/38 Log distribution graph for Ce vs. Rb.

3.6 Geothermometry

Compositional analysis of the feldspars enables some geothermometry to be undertaken. There are, however, many formulated graphical and numerical thermometers, all of which appear to have had objections raised about them. In this study one of the more recent numerical variations has been employed, namely that of Powell & Powell (1977). To obtain realistic temperatures one needs a pair of co-existing plagioclase and alkali feldspars. This itself is difficult to establish in the Ayrshire clasts due to the presence of zoned plagioclases and exsolved potassium feldspar. The other factor which needs to be quantified is the pressure of crystallization. An estimate of this may be made through composition, petrography and environmental comparison and is likely to be high level (see 3.2.1) and in the range 1-3 Kb. The range in pressure, however, only produces small variations in temperature as can be seen from Powell & Powell's equation :-

$$T = \frac{-x^2_{K,Af}\,(6330 + 0.093P + 2x_{Na,Af}(1340 + 0.019P))}{R \log K_D + x^2_{K,Af}(-4.63 + 1.54\, x_{Na,Af})}$$

where $T = {}^{o}K$, P = bars, $K_D = x^{Na,Af} / x_{Na,Pl}$ and R = gas constant.

Calculations have been made using microprobe analyses from sample 101. A plagioclase core (analysis 12, see Figs. 3/2 and 3/6 for analyses) and potassium feldspar (average of analyses 24-38) yield temperatures of 593 ^{o}C at 1 Kb and 616^{o}C at 3 Kb. An average plagioclase composition (9) in conjunction with potassium feldspar (24-38) gives 570 ^{o}C at 1 Kb and 592 ^{o}C at 3 Kb. These temperatures are fairly low which may reflect high level emplacement, but the inherent uncertainties in the calculation reduce the emphasis which may be placed on these figures.

In addition to the above the geothermometer may be applied to the compositions of the perthite lamellae to estimate the temperature at which unmixing may occur. The

validity of doing this is disputed and Brown & Parsons (in preparation) argue its inapplicability due to kinetic and coherency effects during unmixing together with the difficulty of determining phase compositions. The last reason is reduced by the use of the microprobe but it does appear that the degree of unmixing within a single perthite is variable. However the following figures were obtained : analyses 17 (Pl) and 21 (Kf) yield 303 ^{o}C and 37 (Pl) and 38 (Kf) give 353 ^{o}C, both at 1Kb. Although the absolute reality of these values is questionable it does indicate that exsolution continued down to quite low temperatures.

3.7 Summary

The petrography and geothermometry suggest that the granites were mostly intruded at fairly high crustal levels. The subsolvus nature of the clasts implies a reasonable H_2O content in the melt, and the highly perthitic and more alkali rich samples of initially drier nature show evidence of some late stage fluid development.

The major and trace element chemistry define the Ayrshire suite as being of calc-alkaline affinity and produced in a compressional regime. There is a spectrum from basic to acid members though the sampling may tend to overweigh the acid end of the scale. In broad terms there is little variation between the trends from individual conglomerate horizons and all appear capable of being produced in the same manner, namely evolution through fractionation dominated by plagioclase and hornblende.

A broadly similar origin for most samples thus appears tenable. The isotopic age spread (590-450 Ma), however, obviously prevents all the samples being evolved from one intrusive event. The data thus seem to best fit a series of magmatic episodes in an environment evolving chemically on a large scale but still being in the same broad tectonic regime.

4 CALEDONIAN EVOLUTION OF SOUTHERN SCOTLAND

4.1 Previous plate-tectonic models

The development of plate-tectonic concepts in the late 1960's in conjunction with Wilson's (1966) suggestion of a proto-Atlantic ocean le d to many interpretations of the British Caledonides through plate-tectonic processes (see Fig. 4/1 and Table 4A)

The pioneer of this work was Dewey whose first model appeared in 1969 with modifications in 1970 (Bird & Dewey), 1971 and 1974. The essence of these models is that the Scottish Caledonides lay on a continental edge to the north of the proposed Iapetus Ocean. Dewey suggested a northward dipping subduction zone sited to the north of the Southern Uplands with the Midland Valley as a thickening sedimentary wedge on Dalradian terrain (Fig. 4/1). He thought of the Ballantrae Complex as being formed in a marginal basin/island arc environment but suggested that the granitic detritus in the Lower Ordovician sediments was of Highland origin. In 1970 Fitton & Hughes also produced a model involving island arc development along the margins of the Iapetus Ocean. This was for the Lake District on the south side of the ocean, however, and involved a southerly dipping subduction zone located at Moffat in the Southern Uplands.

Garson & Plant (1973) suggested progressive development with several ophiolite zones, from the Moine Thrust to the Southern Uplands Fault. One interesting addition was their suggestion of an ophiolite suite along the Highland Boundary Fault. Church & Gayer (1973) dealt mainly with the Ballantrae ophiolite but came to conclusions similar to those of Dewey with northward dipping subduction, but suggested that the additional effect of the southerly Lake District subduction would place the eventual Iapetus suture through the Solway Firth. Gunn (1973) and Jeans (1973) then provided a departure from the generally proposed model to account for the work of Powell (1971). Powell used various geophysical methods to investigate the basement to

the Southern Uplands and concluded that it was underlain by a Lewisian type basement. This threw doubt onto the Dewey type model which implied a palaeo-oceanic floor to the Southern Uplands. The essence of both Jeans' and Gunn's models is siting the Iapetus Ocean in the Midland Valley and having subduction to the north at the Highland Boundary Fault and to the south at Girvan/Ballantrae (Fig. 4/1). This, however, runs into more difficulties with the main problem at the time being the faunal province evidence of Williams (1962). More recent structural evidence along with new evidence presented herein make this interpretation broadly untenable.

Mitchell & McKerrow (1975) compared the pattern found in the Scottish Caledonides to the modern situation in the Burma orogen and as such introduced the concept of oblique rather than parallel subduction and ocean closure. Lambert & McKerrow (1976) expanded on this with oblique closure, migration of subduction zones as far north as the Highland Boundary Fault and subduction of a spreading ridge to enhance metamorphism and magma generation. Phillips et al. (1976) also favoured oblique collision giving rise to lateral motion along the Highland Boundary Fault and sketchily implied the existence of a marginal basin on the northern margin of the ocean, mainly through evidence from Ireland. Wright (1976) then treated the island arc and marginal basin development hypothesis as an integral part of the Caledonide evolution. He proposed alternating subduction directions on the north and south margins leading to small discontinuous arc-continent collisions which produced the various recognisable orogenies on the north and south continental margins. Wright (1977) continued this line and made a definite suggestion of the Highland Boundary Fault being the site of a back-arc basin.

Bamford et al. in a series of papers (1976; 1977; 1978 & 1979) used various geophysical parameters on a longitudinal profile through Britain (LISPB) to further define the basement under central and southern Scotland. This showed that the Midland Valley is floored by a fairly typical continental crust section but that the Southern

Uplands basement is somewhat anomalous. Further evidence on the base to the Midland Valley came from Upton et al. (1976) and Graham & Upton (1978) who investigated clasts in Carboniferous volcanic vents. Gneissose clasts occur in vents at both the east and west ends of the Midland Valley and have mineral assemblages typical of granulite facies and pressures and temperatures in excess of 11 Kb and 850 ^{o}C. van Breemen & Hawkesworth (1980) published Sm-Nd isotopic determinations on these clasts which indicated a Grenville model age. This data is now subject to some uncertainty due to more recent evidence on rare-earth element mobility at high pressures, but is likely to represent a minimum age for the clasts.

Moseley (1977) used the strong evidence from the LISPB profile and Powell's (1971) geophysical interpretation to imply the non-existence of large oceanic remnants under Scotland. He suggested marginal basin development and closure to give the ophiolite slivers at Ballantrae and the Highland Boundary Fault with the eventual ocean suture along the Solway Firth. McKerrow et al. (1977) investigated the stratigraphy and structure of the Southern Uplands and concluded that it matched that of accretionary prisms from modern continental margins. This provided a refinement of the subduction zone site suggesting its early position near the Southern Uplands Fault and migrating south, as accretion thickened the prism, to a final site in the Solway Firth. Mitchell (1970) again used analogies with the Burma orogen and the Himalayas to propose an arc and marginal basin situation but with early southeasterly subduction behind the arc and later northwesterly subduction. The next refinement to the Caledonide plate-tectonic model was that of Longman et al. (1979 & Appendix II) discussed more fully in 4.5. The latest contribution is that of Bluck et al. (1980) who through extremely detailed analysis of the Ballantrae Complex lend support to its origin in a marginal basin.

Continental crust

Oceanic crust

Arc basement

Volcanic arc

Sediments

Ophiolite

BC Ballantrae Complex

HBF Highland Boundary Fault

LD Lake District

MV Midland Valley

SU Southern Uplands

SUF Southern Uplands Fault

Legend for Fig. 4/1.

Dewey (1969 + 1971)

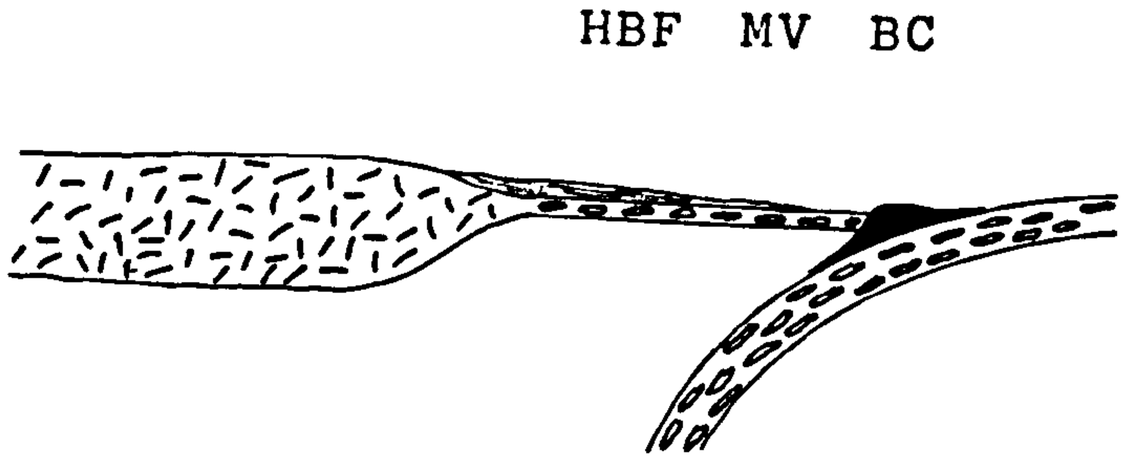

Garson + Plant (1973)

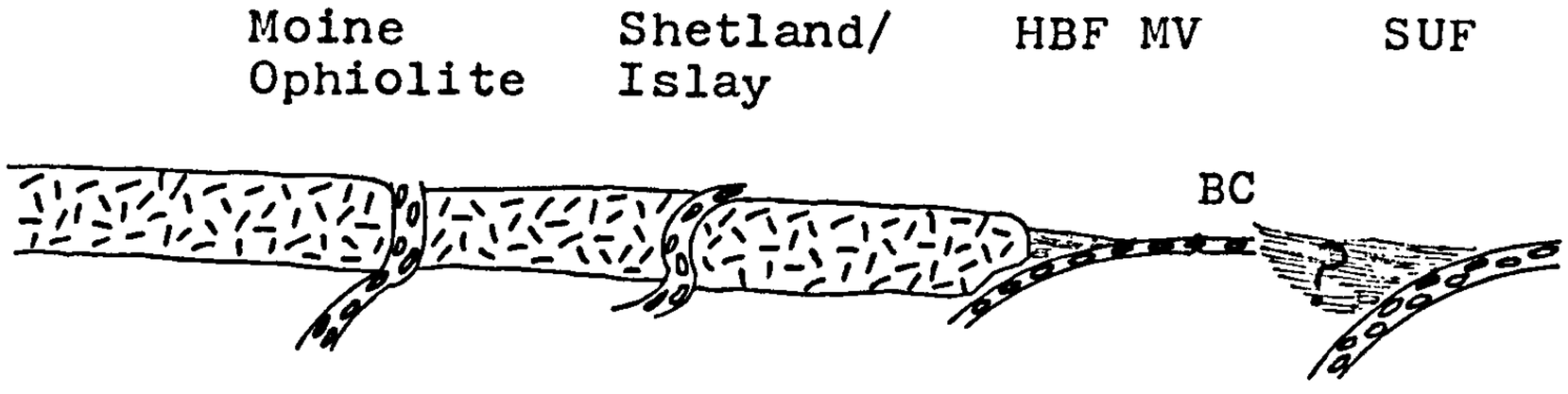

Church + Gayer (1973)

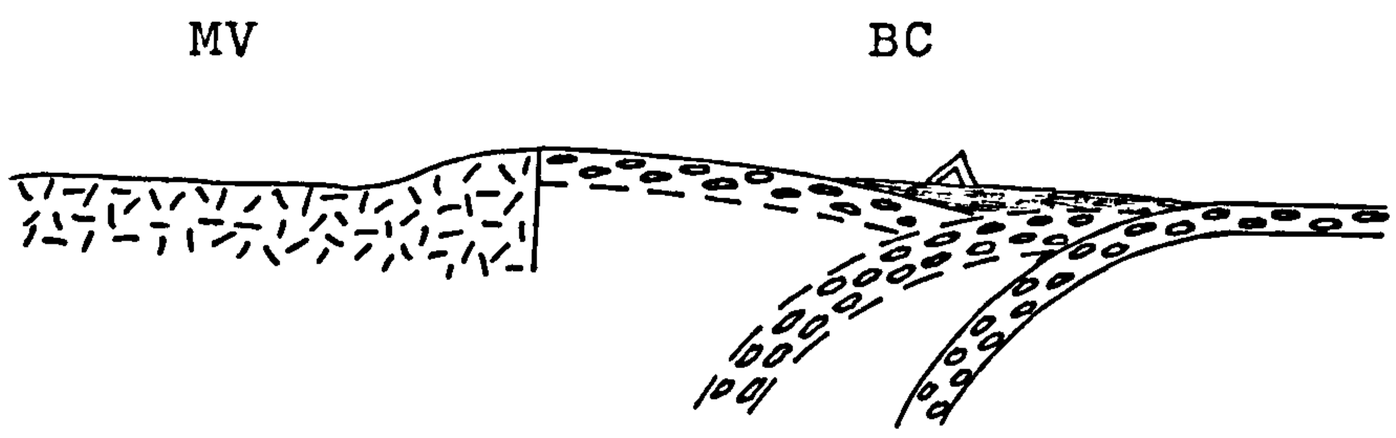

Jeans (1973) + Gunn (1973)

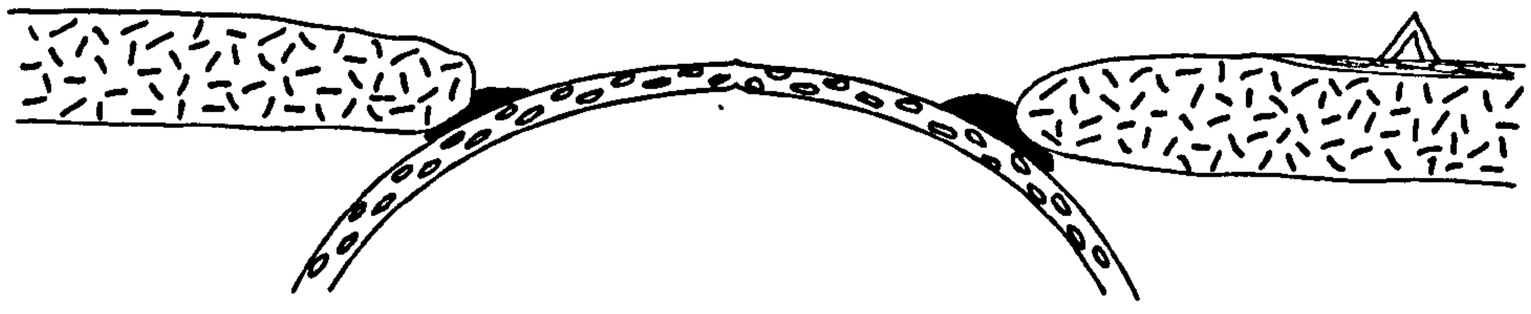

Mitchell + McKerrow (1975)

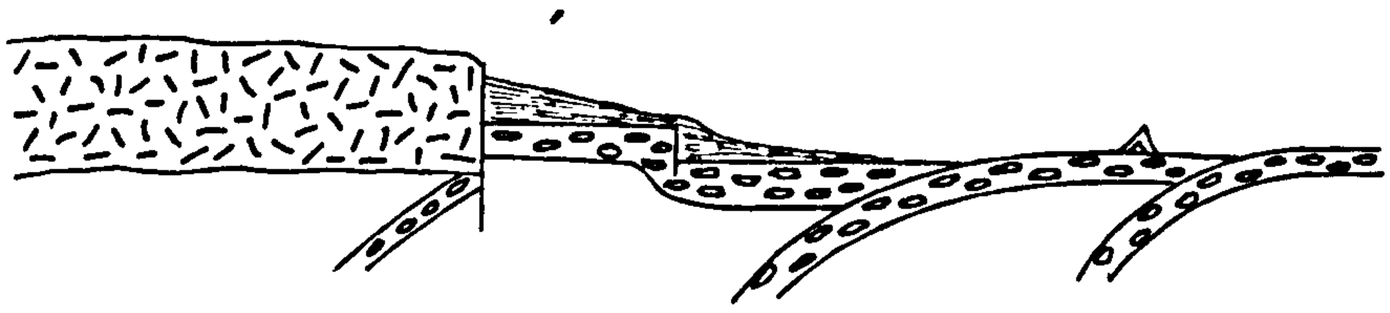

Fig. 4/1 Sketches of plate-tectonic models for the northern margin of the Iapetus Ocean.

Lambert + McKerrow (1976)

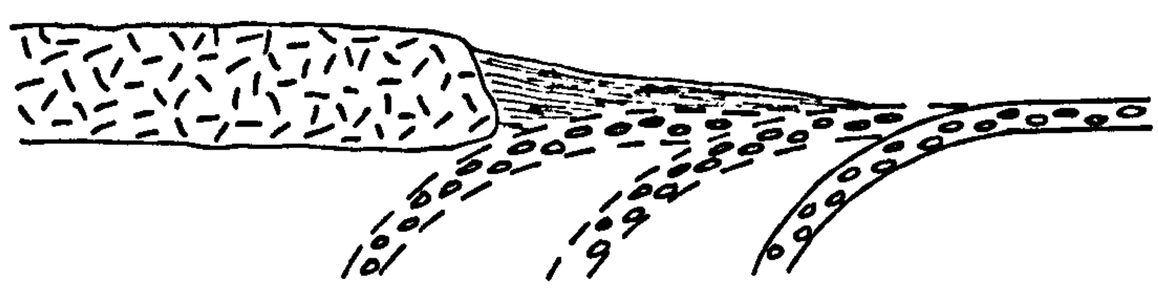

Phillips et al. (1976)

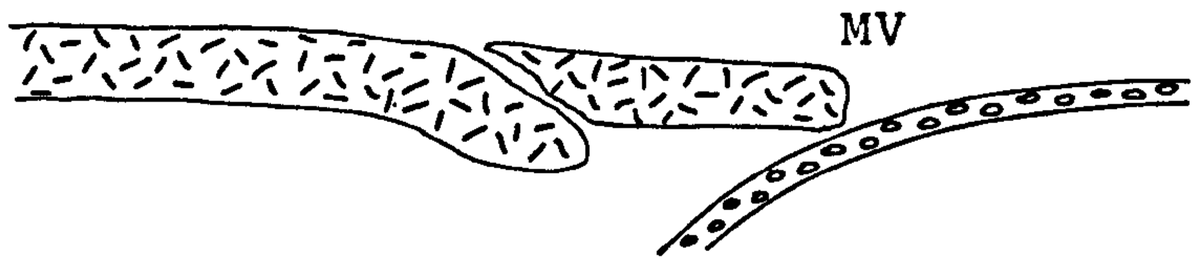

Wright (1976+1977)

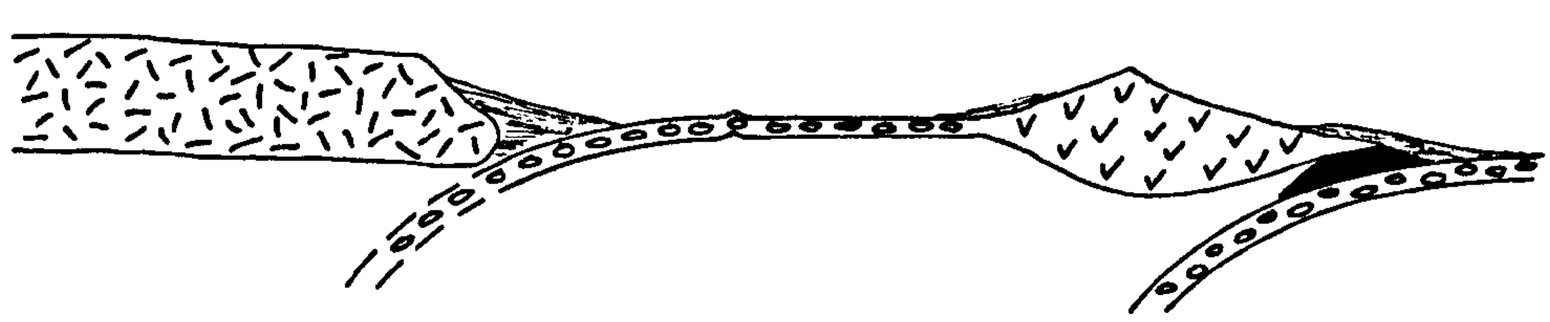

Moseley (1977)

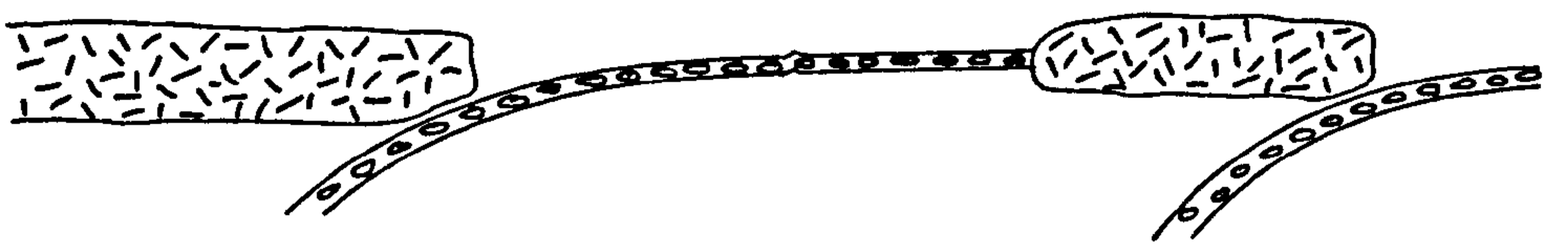

Mitchell (1977)

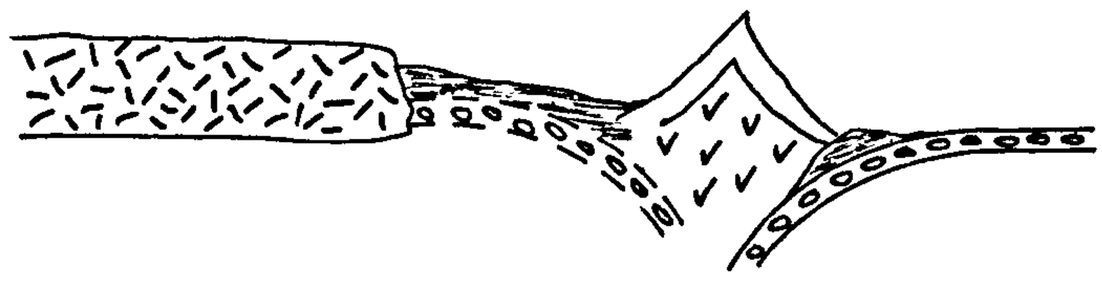

Fig. 4/1 Continued

Author	No. of Sub. zones	Position	Direction	Midland Valley basement
Dewey(1969)	1	SUF	N	Oceanic remnant
Dewey(1971)	1	SUF	N	Oceanic remnant
Garson & Plant(1973)	4	1.Moine Ophiolite 2.Shetland/Islay 3.HBF 4.SUF	N N N N	Lower Palaeozoic (?)
Church & Gayer(1973)	1	SUF	N	Continental
Gunn(1973)) Jeans(1973))	2	1.HBF 2.SUF	N S	Oceanic
Mitchell & McKerrow(1975)	3	1.HBF 2.SUF 3.Solway	N N N	Oceanic
Lambert & McKerrow(1976)	1	Migrating, SUF to HBF then jump to Solway	N	Oceanic
Phillips et al.(1976)	2	1.Moine thrust 2.Solway	S N	Continental
Wright(1976 & 1977)	3	1.N.Highlands 2.SUF 3.Solway	N N N	Thin continental or oceanic
Mosely(1977)	2	1.HBF 2.Solway	N N	Continental
McKerrow et al.(1978)	1	Solway	N	———
Mitchell(1978)	2	1.MV/HBF 2.Solway	S(?) N	Oceanic (?)

Table 4A Summary of plate-tectonic models for subduction events on the northern margin of the Iapetus Ocean. See Fig. 4/1 for equivalent diagrams.

4.2 Evidence for a fore-arc regime in the Middle + Upper Ordovician

The depositional environment discussed in section 1.5 in conjunction with the conglomerate compositions (1.6) and the broad plate-tectonic picture enable the Girvan succession to be discussed in the light of fore-arc basin development within the arc-trench gap (Fig. 4/2). Dickinson & Seely (1979) produced a synthesis of fore-arc regions and many of the features are found to be similar to those of Girvan.

The sequence at Girvan lies between the postulated position of northward dipping subduction (see 4.1) and the magmatic arc of the Midland Valley (see 4.3). This immediately places the succession geographically in a fore-arc setting, sensu Dickinson & Seely (1979). As noted in 1.6 the sequence comprises mainly clastic detritus including numerous acid and intermediate plutonic and volcanic clasts in conglomerate and greywacke facies. The environment of deposition is envisaged to be, in the framework of Williams (1962), one of a basin with a fault bounded northern margin and with a broad northward overlap onto the eroded underlying Ballantrae Complex (Fig. 1/4). At this stage it becomes important to elaborate on the nature and origin of this complex. The Ballantrae suite has long been envisaged to represent a section of oceanic crust e.g Dewey (1969) and subsequent workers, obducted onto a pre-Caledonide basement. The problem has been in deciding what type of oceanic crust it represents. Bluck (1978) and Bluck et al. (1980) provide a review of previous ideas (1978) and suggest through geochemical and field succession evidence, an origin in a marginal basin probably behind an early volcanic arc. Hence the overall sequence is fault controlled basin sediments resting on oceanic type crust trapped between the trench and arc. This is a frequently documented occurrence in fore-arc basins and referred to as a 'residual fore-arc basin' by Dickinson & Seely (1979) (Fig. 4/3).

Fore-arc basins although often subject to subsidence and varying rates of sediment input tend to 'fill up' and produce progressively shallower facies with

time. This is not simply the case in Girvan with the early platform sediments and dominant greywacke facies, though this is probably the result of syndepositional faulting undoubtedly active at the time. Another feature typical of fore-arc basins is, however, the ratio of plutonic to volcanic detritus. The peak of volcanic andesite debris occurs early in the Ordovician e.g. Kelling (1961) and then tends to give way to acid porphyries and granites. This is a frequent situation reflecting deeper erosion of a magmatic arc enhanced by rapid uplift which is itself assisted by the emplacement of the arc plutons. Even the tectonic effects of Caledonian age reported by Williams (1959), namely dominant faulting with associated folding, are somewhat typical of evolving fore-arc basins with changing subduction and accretion geometry.

A fore-arc basin setting for the Girvan succession thus appears extremely tenable as the following features all fit typical residual fore-arc basins (Fig. 4/3) :-

1. Sited between the trench and a magmatic arc.
2. Floored by oceanic crust.
3. Sedimentary infill of arc derived material.
4. Fault dominated sequence involving platform and basin sediments.

Indeed in comparing Fig. 4/3, theoretical diagrams produced by Dickinson & Seely (1979), with Fig. 4/4, a series of evolutionary diagrams modified after Longman et al. (1979) and Bluck et al. (1980), the resemblance is striking.

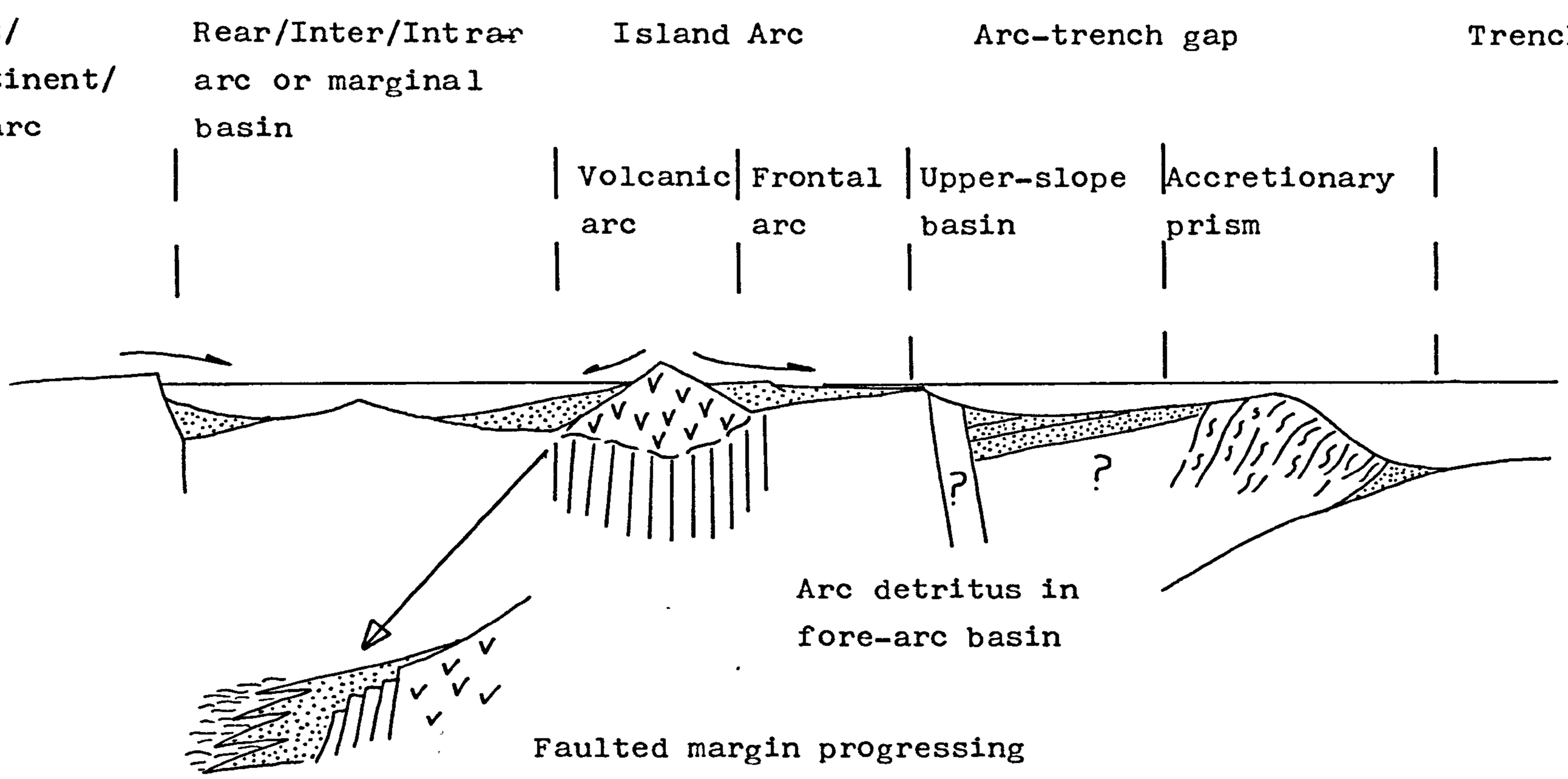

Fig. 4/2 Anatomy of a volcanic arc.

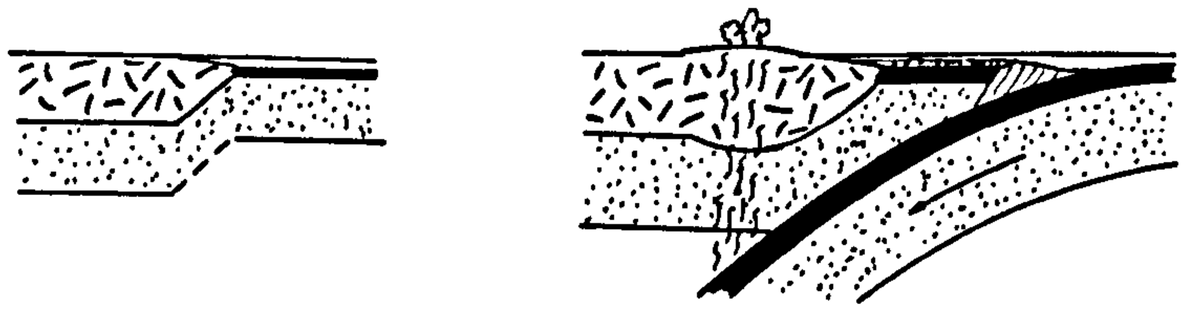

Activation of continental margin

"Detached normal subduction arc"

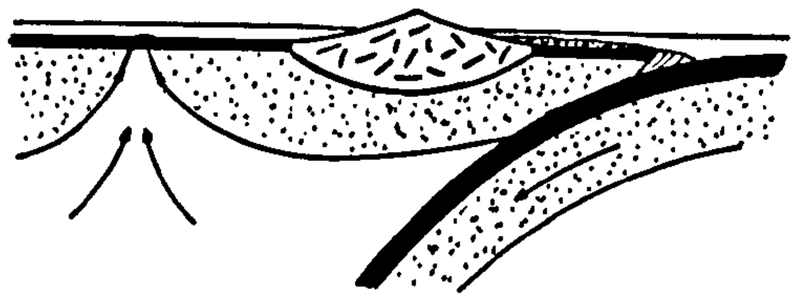

"Residual Basin" - fore-arc founded on oceanic or transitional crust

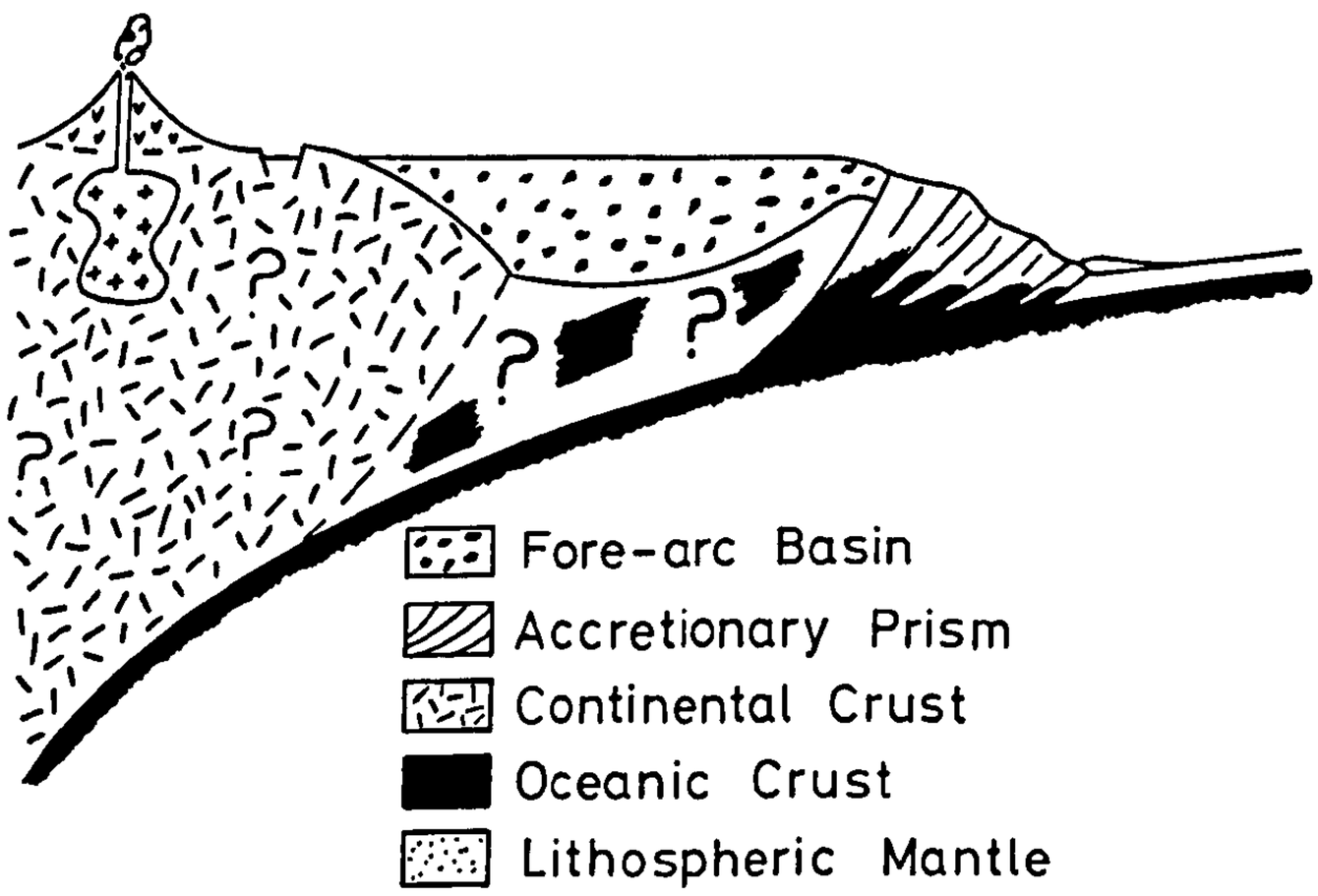

Fig. 4/3 Development of a 'residual fore-arc basin after Dickinson & Seely (1979).

PAGES
MISSING
IN
ORIGINAL

4.3 Island arc development

The presence of an island arc complex north of the site of subduction of the Iapetus crust has been suggested several times. Kelling (1961) noted the dominance of andesite fragments in Llandeilo greywackes from the Rhinns of Galloway and implied the existence of volcanic source fields. Williams (1969) in reviewing the Ordovician of Scotland suggests the existence of 'volcanic islands' and 'Ordovician igneous complexes' within the Midland Valley. Plate-tectonics transformed this into the term island arc associated with subduction. The existence of an island arc became acceptable to many authors e.g. Phillips et al. (1976), Wright (1977) and Moseley (1977) although in all cases the evidence is slender. The granitic clasts were noted by Dewey (1971) but he thought of them as being derived from the Highlands.

The presence of this island arc was speculation based on the detritus in the Girvan and Rhinns of Galloway successions. This, study, however, provides the only evidence tying the sediments to a magmatic arc. The ages obtained from the detritus also indicate that the arc is partially coeval with the sediments and as such has a great tectonic significance for the evolution of the southern Midland Valley.

The principle of using the detritus in fore-arc terrains to reconstruct the nature of any possible arc complex is well known. Dickinson (1970) discussing the Great Valley successsion in relation to the Sierran-Klamath mountains stated that 'The fundamental assumption of a volcanoplutonic provenance, upon which the detailed interpretations are based, is corroborated by the clast populations in conglomerates. Characteristically, about two-thirds of the clasts are igneous, comprising a suite ranging in texture from plutonic, mainly granite with diorite and gabbro, through hypabyssal mainly microgranite types and feldspar prophyries, to volcanic, mainly andesitic and dacitic, with lesser basaltic and rhyolitic types, including welded tuffs'. In S.W.Scotland an influx of

andesitic debris in Llandeilo greywackes from the Rhinns of Galloway occurs in conjunction with much granitic debris both in the Rhinns and in the Llanvirn-Llandovery succession at Girvan. This situation was confirmed by Kelling & Holroyd (1978) whocconcluded that for these Lower Palaeozoic conglomerates acid and basic intrusives and extrusives dominated the extra-basinal assemblage. Thus intrusive and extrusive igneous rocks appear to be a major component of the source area. As noted in 1.3 and 1.5 the source for these sediments lies in a general northerly direction (variation N.W. to N.E.). The size of some of the granitic clasts (up to 80 cm in longest dimension) indicates that the transport distance is not very large and consequently the provenance appears to be to the 'immediate' north.of the site of deposition.

The age of the granitic clasts presented in Chapter 3 shows a variation from around 580 Ma to 450 Ma. Although this represents a spread of 130 Ma there is a fairly even distribution of radiometric ages through this range, with no gap of more than 30 Ma.duration. There is a possibility of younger plutonism resetting older ones to give a spurious impression of a continuous age spectrum but this is considered unlikely in this case due to the length of the time spread and the high level intrusion with rapid cooling and uplift. The chemistry, as indicated in Chapter 2, demonstrates that there is no significant difference between clasts from Girvan, the Rhinns of Galloway or different conglomerate horizons. There is a range in composition from tonalite through to granite, typical of many major acid intrusive provinces and in particular island or continental arc environments. The clast chemistry produces a broad calc-alkaline pattern with individual clasts almost always indicating a compressional orogenic origin and showing features typical of arc granitoids. Thus the chemistry fits with the granites being of island arc affinity and the age data indicate that its development began around 580 Ma ago and continued periodically through to around 450 Ma (late Pre-Cambrian to Caradocian). Evidence of high level intrusion and the $^{87}Sr/^{86}Sr^{o}$ values of 0.706

to 0.715 are also typical of island arc environments e.g. Shibata & Ishihara (1979). The $^{87}Sr/^{86}Sr^{o}$ ratios are too high for purely mantle derivation but suggest involvement of basic lower crust or sediment. This is frequently the case in magmas generated over subduction zones, particularly during sediment subduction rather than offscraping, which itself may enhance melting and magma emplacement in an island arc environment.

Other clasts present in the conglomerate include metamorphics (dominated by metaquartzite and amphibolite) and sheared granitoids. These are not genetically associated with the island arc but are thought to indicate the nature of the basement through which the arc was intruded. The extensively deformed granitic clasts found almost exclusively in the Kirkland conglomerate yield a well defined age of 486 $\pm$ 29 Ma. The precise significance of this is uncertain. The rocks may represent basement material but the age cannot represent an orogenic event affecting the upper levels of the arc as many pre 486 Ma granites are undeformed. The age may, however, indicate the effects of repeated intrusion events partially resetting the deformed basement granitoids.

The magmatic arc being a positive feature with rapid uplift to yield boulder sized granite clasts would obstruct sediment from the north of it. The earlier views that the metamorphic material was derived from the Highlands is thus unacceptable. Moreover the size of the metamorphic clasts, although smaller than the granites, suggests a more proximal source than the Highlands. Thus the implication is now that metaquartzite, amphibolite etc. were present within and beneath the arc. Quartzite suggests ensialic deposition and as such is likely to be on continental basement. This is vindicated by the amphibolite and sheared granite and is in agreement with the interpretation of Graham & Upton (1978) based on vent derived granulite clasts. Continental basement to the arc may also support theeearly interpretations of Kennedy (1958) and George (1960) who found evidence for a southerly derivation of Upper Dalradian sediments.

Another implication from the presence of metaquartzite clasts in conjunction with undeformed granites of c. 580 Ma age is that the deformation responsible for the metaquartzite was earlier than about 580 Ma.

Thus the clast population and its age and chemistry suggest the development of a magmatic arc in the south Midland Valley, founded on continental crust, from around 580 Ma to 450 Ma.

4.4 Midland Valley as a marginal basin

The involvement of marginal basins in the evolution of the Scottish Caledonides has been postulated since Dewey (1971). Most of these early workers were, however, concerned with the origin of the Ballantrae Complex in a marginal basin rather than the possibility of the Midland Valley itself being a marginal basin. The presence of serpentinite, spilite, radiolarian chert and black shale assemblages along the Highland Boundary Fault had long been recognised, but again the advent of plate-tectonics meant that this assemblage could be interpret ed as an ophiolite suite. This fact coupled with the similar interpretation for Ballantrae Complex le d Garson & Plant (1973) to propose a model involving numerous subduction zones (Fig. 4/1) and the Midland Valley as a marginal sea.

Gunn (1973) and Jeans (1973) didn't suggest the existence of a marginal basin but had the Iapetus Ocean in the Midland Valley. Phillips et al. (1976) indicated a marginal basin to the north of the Southern Uplands but did not give any details as to why or where it is found. Wright (1976 & 1977) first postulated that the upper Dalradian Tayvallich volcanics may represent the remnants of an attempt to open a marginal basin. He then suggested that the more complete ophiolite suite at the Highland Boundary Fault chronicles the existence of a marginal basin along the line of the Highland Boundary Fault. Mosèley (1977) also used a marginal basin in the Midland Valley similar to that of Garson & Plant (1973). All these models use marginal basin development in conjunction with northward dipping subduction but Mitchell (1977) although suggesting a remnant basin in the Midland Valley area had southerly dipping subduction.

The main reason for any postulation of marginal basin development must be to account for the basic volcanic /ophiolitic suites. The Tayvallich volcanics are found within the Dalradian shallow water shelf sequence (Graham 1976) and as such cannot represent a section of oceanic crust. Their origin as early extrusion associated with

extensional rifting of attempted back-arc basin initiation does, however, seem eminently feasible. The suite along the Highland Boundary Fault has more features suggesting some oceanic type crust formation. The position adjacent to the Highland Boundary Fault means that the relation to surrounding rocks is obscured but it appears that oceanic crust originating in a marginal basin was 'subducted' along the Highland Boundary Fault during the subsequent closure of the basin.

The age of the Highland Boundary Fault ophiolite suite is probably Arenig-Llanvirn (Downie et al. 1971). This compares favourably with the data on the south Midland Valley arc (see 4.3) suggesting its existence through to the Caradoc. Overlying the ophiolite is the arenaceous Margie series involved in deformation at the site of the Highland Boundary Fault. These sediments contain varied detritus including individual feldspars and composite grains of undoubted granitic origin (Jehu & Campbell 1917). This would appear to be derived from the magmatic arc feeding the coarse sediments to Girvan on the south side and finer sediments expanding northwards over a contracting marginal basin. Although the maximum width of this marginal basin is unknown the width at the time of deposition of the Margie series must have been small enough to permit transport of the Margie sediments across it. This was probably after the maximum width during basin closure.

4.5 Plate-tectonic model for the development of southern Scotland

The aforementioned features allow a model for the Caledonian evolution of southern Scotland to be proposed (Fig. 4/4). The existence of a precursor to the Atlantic ocean, the proto-Atlantic or Iapetus Ocean, appears to be proven. The age of opening of this ocean is, however, uncertain (Anderton 1980) as is the time of initiation of subduction to the north under Scotland. The presence of granitic plutons in an island arc environment at c. 580 Ma would suggest that subduction was initiated prior to this time. Whether this is in fact the oldest granite clast present is uncertain. This fact coupled with the variable time span between subduction initiation and first volcanic arc-pluton emplacement (if, indeed an arc develop s as is not always the case) mean that no real estimate of the onset of subduction can be made from this study data.

The development of an arc took place in the south part of the area presently occupied by the Midland Valley. The volcanic and plutonic expression of this arc is evident in the sedimentary record of the semi-coeval fore-arc basin. The radiometric ages for the granitoids indicate that the arc development occurred over approximately 130 Ma from c. 580 Ma to 450 Ma. The basement to this arc is continental crust of pre-Dalradian age which may have been uplifted early in arc initiation to provide a southerly source for much of the Upper Dalradian. The magmatism appears to be more or less continuous during the arc development as indicated by the radiometric ages. In comparison with modern subduction zones e.g. Raymond & Swanson (1980) this situation appears typical of sites above subduction zones which have a small or non-existent accretionary prism and hence are subducting most of the sediment on the oceanic plate. This implication of wet sediment subduction enhancing magmatism may also point to an explanation for the lack of Cambrian sediments in the south Midland Valley and Southern Uplands.

Associated with early arc development there

also appears to have been the evolution of marginal basins. The Ballantrae Complex is thought to be of marginal basin affinity (Bluck 1978) and was obducted from the south in the middle Arenig (c. 480 Ma) (Bluck et al. 1980). The suggestion, therefore, is one of a marginal basin to the south of the Midland Valley arc and possibly to the north of another minor arc during the early Arenig (Fig. 4/4). A similar situation emerges for the area to the north of the Midland Valley arc. At some stage there occurred the opening of a back-arc or marginal basin. This opening saw the production of marginal ocean crust initiated along a line of weakness which split the continental crust founded arc from the main body of the continent to the north.

This marginal basin is today represented by the ophiolite suite along the Highland Boundary Fault. This suite is of supposed Arenig-Llanvirn age, meaning that the opening of the back-arc must have occurred in pre-Arenig times (Fig. 4/4). The width of this basin is unknown but is unlikely to have been very large. The closure appears to be through subduction related underthrusting along the line of the Highland Boundary Fault. The time is again uncertain but thought to be Caradocian and immediately after the deposition of the Margie series arenaceous 'molasse', much of which was derived from the exposed arc to the south. This closure at around 460-450 Ma (Fig. 4/4) may correspond to uplift in the Highlands and fits in with the final emplacement of the Tay nappe and associated folding (Thomas 1980).

The last radiometric age for the granitic debris is also around 450 Ma and this may be related to the closure of the marginal basin. It, however, also corresponds to the time when a major accretionary prism developed above the subduction zone to the south (McKerrow et al. 1977). This fact may serve to reduce and halt plutonism by starving the subduction zone of sediment in the manner proposed by Raymond & Swanson (1980). This accretionary prism then continued to develope moving the site of subduction further south and with the suture representing eventual Iapetus closure located in the Solway Firth.

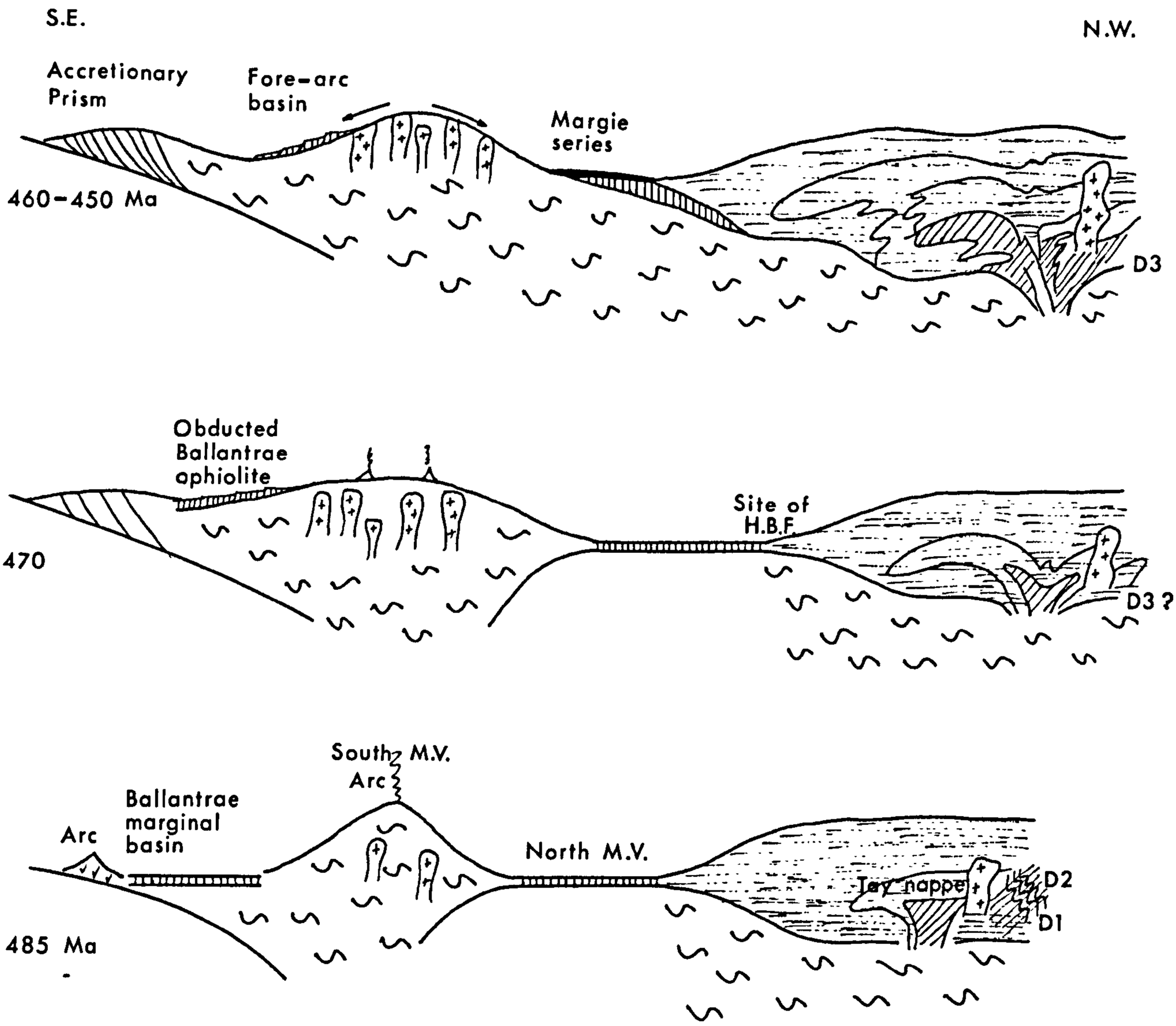

Fig. 4/4 Evolution of the Midland Valley during part of the Ordovician, incorporating data from Roberts (1974), Harris et al. (1976), Thomas (1980) and Bluck et al. (1980).

4.6 Implications of the model

4.6.1 Agreement/disagreement with previous models

The model proposed herein agrees in broad terms with several pre-existing reconstructions, notably those of Wright (1976 & 1977) but mitigates against others. The marginal basin development and closure provides a mechanism for explaining the existence of continental crust as far south as the Southern Uplands Fault as is suggested by geophysical evidence. This is in contrast to many of the early models which had oceanic crust as the basement to the Midland Valley (Dewey 1969 & 1971; Garson & Plant 1973; Church & Gayer 1973; Mitchell & McKerrow 1975; Lambert & McKerrow 1976; Mitchell 1977). The propositions of Gunn (1973) and Jeans (1973) cannot be reconciled with the present data. They ignore the faunal province evidence, no source would be available for the granitic detritus, again it implies the base to the Midland Valley being oceanic crust and the Ballantrae ophiolite is obducted from the south not the north as they proposed. Moseley (1977) accounted for the geophysical evidence by having the Midland Valley as a marginal basin. He, however, placed Girvan/Ballantrae on the south side of his Midland Valley basin which is contrary to the sedimentological evidence and recent studies on the Ballantrae Complex (Bluck et al. 1980). Of the detailed models this leaves Phillips et al. (1976) and Wright (1976 & 1977) as the most likely. The former is based mainly on data from Ireland and although the existence of an island arc of Lower Ordovician age is seen in County Mayo the pattern is only broadly translated to Scotland on a palaeogeographic reconstruction. Wright, however, referred more to Scotland than Ireland in suggesting the existence of marginal basin and island arc terrain. This study comes out in agreement with much of the broad palaeogeography of Wright but spearates the Upper Dalradian from the Highland Boundary Fault succession (see 4.6.3).

4.6.2 Dalradian sedimentation

Anderton (1980) reviewed Dalradian sedimentation with reference to the opening of the Iapetus Ocean. Most of the Dalradian sediments are predominantly derived from the northwest, but the Portaskaig tillite and Southern Highlands Group had a southeasterly source. Harris et al. (1978) used the proximal nature of the Southern Highlands Group in conjunction with the presence of metamorphic and granite detritus, including fresh angular feldspars, to propose a source adjacent and to the south. This source was referred to as the Midland Valley landmass by Anderton (1980) who thought that this uplifted area could not be large enough to feed the extensive glaciers responsible for the Portaskaig tillite which may well have ultimately been sited in northern Europe. This indicates that the Iapetus Ocean did not open until post the tillite deposition (see 4.6.3). The southerly source for the Dalradian Southern Highland Group may, however, be the early stages of development and uplift of the Midland Valley island arc. Arc plutons and metaquartzite basement providing detritus which moved northward across the Midland Valley into the Dalradian basin. This in turn implies that the marginal basin in the Midland Valley did not develop until the deposition of the Southern Highlands Group (4.6.3.)

4.6.3 Timing of events

The sequence of events postulated here can often be correlated with radiometric age determinations to provide a broad base sequence for late Pre-Cambrain to Silurian times (Table 4B). The age of opening of the Iapetus Ocean is not defined in this study. Anderton (1980), however, suggests opening after the Portaskaig tillite, the lateral equivalent of which yields a Rb-Sr age of 654 $\pm$ 23 Ma (Pringle 1973). The Tayvallich volcanics of the Dalradian Argyll Group have not been dated but they are correlated with a suite of lavas and dykes in Newfoundland. Stukas & Reynolds (1974) dated these Long Range dykes at 605 $\pm$ 10 Ma and Dewey (1969) attributed them to the opening of the

Iapetus Ocean. The work presented here appears more compatible with these Dalradian lavas representing an early attempt to develop a marginal basin along similar lines to the later, more successful, Midland Valley marginal basin. The earliest dated granite pluton in the arc complex being c. 580 Ma indicates that subduction was already occurring post an initial spreading phase. Therefore if opening did not take place until after 605 Ma very little time is available for subduction and arc development. Anderton (1980), however, uses petrographic evidence from the sedimentary succession to suggest little tectonic instability before the Tayvallichs and hence prefers it to represent the original Iapetus opening phase. The emergence of Anderton's Midland Valley landmass after the extrusion of the Tayvallich lavas is, however, probably associated with early magmatic pulses into the base of the arc to be.

Following 580 Ma the volcanic arc continued to develop in the south of the Midland Valley. The fact that many of the older granite clasts are undeformed provides several important points. The metaquartzite clasts associated with the granitoids must have been metamorphosed prior to 580 Ma, which is earlier than most of the Highland metamorphism. The continued intrusion of granitic plutons until 450 Ma, the bulk of which escaped any metamorphic effects, indicates that the island arc had a different tectonic setting to that of the Highlands. During this interval the Dalradian of the Highlands was being subjected to a series of deformation events (D_1 to D_3). The age of D_1 is uncertain but it appears that D_2 is pre 514 Ma and D_3 post 514 Ma from structural and radiometric evidence from the Ben Vuirich granite (Bradbury et al. 1976). The D_3 event has been tentatively placed at around 490 Ma (Pankhurst 1970; Pankhurst & Pidgeon 1976). The protection of the arc material from these structural events may best be achieved by having the marginal basin in existence. A balance must, however, must be made between the southerly derivation of the Southern Highland Group and the opening of the back-arc basin. Also it may be problematical to have extensional opening of a marginal basin at the same

time as the formation of the southerly emplaced Tay nappe and associated structures.

The development of another marginal basin to the south of the arc must have occurred to enable the intrusion and extrusion of the Ballantrae suite prior to its obduction at about 480 Ma (Bluck et al. 1980). The location of amphibolite and other obduction related fragments in conjunction with black shales containing graptolites of the D. nitidus zone in olistostromes and conglomerates, means that the obduction belongs to the middle Arenig.The Highland Border ophiolite assemblage has also been dated as Arenig/ Llanvirn (Downie et al. 1971) indicating the existence of both marginal basins during the Arenig.

The last arc granite at around 450 Ma corresponds to the same time as the closure of the marginal basin in the Midland Valley, after the Margie Series and in the Caradoc. This closure and the underthrusting of the ophiolite beneath the Dalradian would probably result in uplift and metamorphism of the southern Highlands. Thomas (1980) incorporated this marginal basin closure in explaining the development of Ordovician deformation in the younger Moines and the final emplacement of the Tay nappe (Fig. 4/4).

One potential problem with this pattern is the deformation of the rocks along the Highland Boundary Fault. Johnson & Harris (1967) found many aspects of the deformation history of the Highland rocks similar to that of the Highland Border Series ophiolitic rocks, recognising the D_1 and D_2(?) events. This would indicate that the Arenig is pre 514 Ma in age but this is not the case found by Bluck et al. (1980) using more reliable data. Johnson & Harris (1967) themselves appeared to be sceptical of their data as they mentioned the possibility of the similarity being due to coincidence. Henderson (in prep.) also considers the D_1 and D_2 effects to be visible in the Highland Border Series. He uses this and their downward facing nature to invoke an origin for the Highland Border Series through riding on the back of a large nappe (the Tay nappe ?). This has many problems such as the lack of metamorphism, the location of a root zone for the nappe

Ma			
400	Post-tectonic granites		
420			
440	Marginal basin closure	Peak highland uplift	
460	Highland Border Series		
		Arc Maturity (?)	
480	Ballantrae ophiolite obduction		
		491 ± 15	
500		497 ± 17	D3 ?
520	Ben Vuirich granite		------
	(514 +6)		D2 ?
	-7		
540			
560			D1 ?
580			
	First arc granite (?)	Southerly derived Dalradian	
600			
620	Tayvallich volcanism (c. 605 ± 10)		
		Initial marginal rifting	
640			
660	Port Askaig tillite (654 ± 23)		
680			
700			

Table 4B Sequence of events.

and the location of an ophiolite source. The facing direction may also be explained by later movement on the Highland Boundary Fault producing overturned beds adjacent to it. This seems a more reasonable explanation particularly as the Lower Old Red Sandstone sediments are also overturned and downward facing (I.G.S. Stirling sheet (39 W) 1974). An alternative explanation for the overall structural pattern may be found in the closure of the marginal basin which paralleled the axis of the Tay Nappe thus providing a spurious impression of structural unity.

The events up to this point combine to form the Grampian orogeny (sensu Lambert & McKerrow 1976) and as such appear to be the result of arc-continent collisions rather than a continent-continent collision. The remaining events involve the final closure of the Iapetus Ocean and associated tectonics (the Caledonian orogeny) and the emplacement of the post-tectonic suite of granites at around 400 Ma.

4.6.4 Relationship to other episodes of granitic intrusion

The Midland Valley arc pluton suite of c. 580-450 Ma forms part of a group of granites throughout Scotland between 600 and 400 Ma in age. The later post-tectonic granites forming the 400 Ma suite are found from Criffel to Ben Loyal with a spasmodic distribution and no trend in isotopic composition or chemistry. This does not, however, appear to be the case with some of the others.

Between the Solway Firth, thought to represent the site of the final Iapetus suture, and the Great Glen Fault there appears to be a pattern. The Midland Valley arc plutons range in age from c. 580 Ma to 450 Ma and have a spread in initial $^{87}Sr/^{86}Sr$ ratio of .705-.715. The Aberdeenshire granites investigated by Pankhurst (1974) produce ages of 455-445 Ma and $^{87}Sr/^{86}Sr^{o}$ values of 0.714-0.717 and intrusions in Glenkyllachy nearer the Great Glen give mineral ages c. 440 Ma and $^{87}Sr/^{86}Sr^{o}$ of 0.718 (van Breemen & Piasecki in press). In addition to this, much granitic detritus is found in the Devonian Dunnottar group

in the Stonehaven district. These granites have a northerly source (B.J.Bluck pers. comm. 1980) and give ages and $^{87}Sr/^{86}Sr^{o}$ values of 460-450 Ma and 0.710-0.720 respectively (van Breemen & Bluck in press). This provides a series of granitic intrusions becoming more corundum rich and muscovite bearing e.g. Busrewil et al. (1975), decreasing in age and increasing in $^{87}Sr/^{86}Sr^{o}$ moving north (Fig. 4/5). This situation can be explained by increasing the crustal contribution in the granites further north which in turn may fit generation at increasing depths and greater crustal assimilation on passing through older continental (Lewisian?) basement. This is shown in Fig. 4/5 where the Midland Valley arc plutons are derived at shallow depths involving some oceanic sediments but probably dominated by upper mantle melts above the subduction zone and incorporating only small amounts of crustal material in the melt. The Aberdeenshire suite ,in contrast, may represent melting above the slab now subducted at depth and crustal assimilation or melts from the base of the crust induced by heating from the consumed slab. This situation is similar to that found in western America (Kistler & Peterman 1973; Armstrong et al. 1977) where subduction produces increased $^{87}Sr/^{86}Sr^{o}$ and decreased age away from the trench.

A feature described by Pidgeon & Aftalion (1978) is the absence of any inherited zircons in granitoids to the south of the Highland Boundary Fault, whereas to the north they found a significant amount of relict 1600 Ma zircons. The one sample in this study with zircon analysis (101) shows no inherited component and as such fits the previous pattern. Pankhurst & Pidgeon (1976) favoured the non-inheriting granites being derived from Palaeozoic crust, but the arc plutons here appear to be predominantly mantle and oceanic sediment derived,alternatively accounting for the lack of inherited zircons.

580-440 Ma
0.705-0.715

460-450 Ma
0.710-0.720

455-445 Ma
0.714-0.717

440-430 Ma
0.718

South

North

Devonian
Dunnottar
Group
clasts

Glenkyllachy

N.E.Aberdeen

GGF

Magmatic arc

Ballantraee
basin

Midland Valley

HBF

?

?

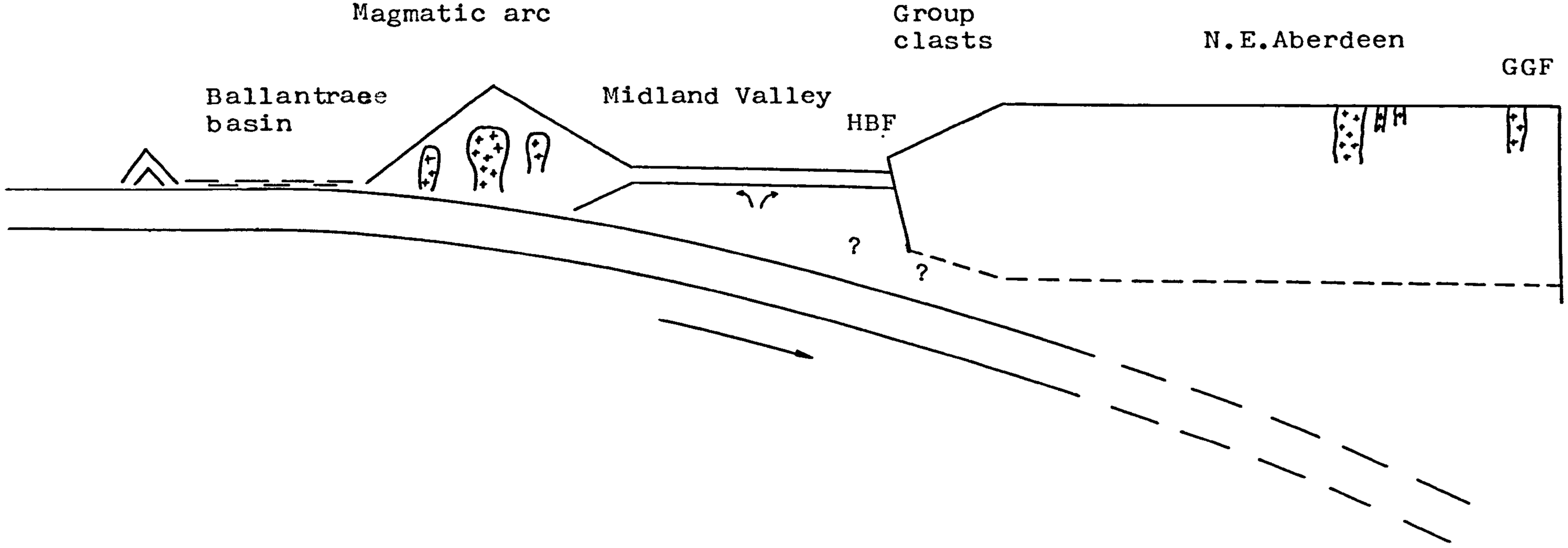

Fig. 4/5 Diagram showing postulated northward subduction and the age and $^{87}Sr/^{86}Sr^{o}$ values for granitoids moving progressively northwards.

4.7 Correlation to the east and west

The Caledonides of Scotland form only a part of an orogenic belt extending from N.E. America to Scandinavia and East Greenland. The pattern of development proposed for Scotland involves the growth of island arcs and marginal basins on the southern margin of a continent to the north of the Iapetus Ocean. The closure of basins on this fragmented continental margin then caused individual orogenic events. Does this pattern fit in with other workers models for other parts of the Caledonide belt ?

In Newfoundland extensional volcanics are found which may represent the initial or final splitting of the Iapetus Ocean, and are correlated with the Tayvallich volcanics. The Holyrood plutonic series dated at around 570 Ma (McCartney et al. 1966) is thought to represent the the construction of an island arc complex (Hughes & Bruckner 1971). These are just two examples of a wealth of evidence pointing to the development of island arc and marginal basin terrain in Newfoundland. In Scandinavia,Gale & Roberts (1974) describe several instances of volcanic assemblages considered to indicate island arc and back-arc environments. Closer to the west Phillips et al. (1976) found evidence of island arc propagation in County Mayo.

It would thus appear that the model proposed here is compatible on a broad scale with other models involving the development of island arcs and marginal basins on the northern edge of the Iapetus Ocean , and the closure and destruction of which produced many of the distinctive orogenic events recognised.

5 ORDOVICIAN TIME SCALE

5.1 Present research applications

The present study has provided additional data points which help to define the "absolute" Ordovician time scale. The stratigraphic ages of the conglomerate horizons are well defined (see 1.5) and the radiometric ages of some clasts are close to published dates for their respective stratigraphic levels. Thus if an assessment of the time span between pluton emplacement and deposition of granitic detritus can be obtained, a maximum age estimate for the stratigraphic horizon ensues.

5.2 Published time scales

There is a paucity of reliable, stratigraphically controlled radiometric ages for the Lower Palaeozoic, although the situation is beginning to improve. Harland (1964) noted few ages for the Ordovician system and Fitch et al. (1976) used a number of poorly defined figures to delimit the top, middle and base of the Ordovician (Table 5A, where all ages are calculated or recalculated to $\lambda^{87}Rb = 1.42 \times 10^{-11} y^{-1}$). The latter authors were forced, however, to conclude (quite rightly!) that "a satisfactory Ordovician time scale is not available at present".

The first attempt at producing a detailed time scale for the Ordovician was that of Churkin et al. (1977). They used published ages for worldwide Ordovician horizons in conjunction with sedimentation rates (obtained by extrapolation from Deep Sea Drilling Project results) for a sequence of graptolitic shales within the Cordilleran foldbelt of western U.S.A.. This scale (Table 5A) suffered from a slight internal inconsistency and it transpires that in compiling the data the authors overlooked 27.4 metres of the Caradoc succession (Carter pers. comm. 1980). The consequence of this is that the ages for the Caradoc and Lower Ordovician are now increased by about 7 Ma (Table 5A) and internal consistency is achieved.

Two more recent publications (Rundle 1979; Gale

et al. 1979) show fair agreement with the Churkin et al. scale for the Lower Ordovician (Table 5A) but use a recent age determination on the Stockdale (Yarlside) rhyolite (Cautleyan stage) from the English Lake District to redefine the Upper Ordovician. Although the age for the Stockdale rhyolite appears to be well defined figures from rhyolites frequently give good looking results that are known to be too young through other evidence. It may thus be rash to place too much emphasis on this value. Bluck et al. (1980) have used radiometric age determinations together with graptolite zonation from the Ballantrae Complex to constrain the Middle Arenig at around 480 Ma (Table 5A), providing an additional data point for the Lower Ordovician.

All the time scales referred to thus far are based mainly on Rb-Sr and K-Ar radiometric ages, although the Gale et al. version includes some fission track data, and show some agreement towards the top or bottom of the Ordovician system. In contrast to this Ross et al. (1978) expanding on Ross et al. (1976 & 1977), proposed a scale based solely on fission track ages obtained from volcanic horizons interstratified with thettype Ordovician series (Table 5A). Their figures show some agreement with the previous studies for the Ordovician-Silurian boundary but are signifi.cantly older for the rest of the Ordovician succession.

Correlating between one time scale and another is problematical. Churkin et al. and Ross et al. use graptolite zones as an integral part of their successsion, Rundle refers to stages and graptolite zones and Gale et al. use only series and stage names. The graptolite zones in Britain and North America have some species/assemblages in common and a correlation between them is possible. However, graptolite zones are diachronous and the base of a named zone in N. America may not represent the same time plane as the base of the same zone in the British Isles. The N. American series and stage names are different from those in Britain and do not correspond to the same stratigraphic levels. Taking the above features into account in compiling Table 5A I have used, where possible, graptolite zones as the mainstay of the correlation with British stage names as an additional guideline.

5.3 Implications of present data

5.3.1 Pluton emplacement to erosion timespan

The environment into which the plutons were intruded is envisaged to be an active magmatic arc (see Chapter 4 & Longman et al. 1979). To estimate the time before plutonic detritus may be expected to be present in the sedimentary cycle a comparison with other ancient and modern magmatic arcs is made.

In the N. American Cordillera Mesozoic plutons are thought to have been emplaced at a depth of 3-5 Km. in a magmatic arc undergoing rapid uplift of a pulsatory nature. One documented case is the Hotailuh batholith (H.Gabrielse pers. comm. 1979). This pluton is intrusive into a Karnian succession which is overlain conformably by Norian sediments. (The Karnian and Norian are together the standard European equivalents of the locally named Keuper series (Upper Triassic)). A conglomerate horizon placed at the Karnian-Norian boundary by ammonite correlation, contains clasts petrographically and radiometrically equivalent to the Hotailuh granite. The Hotailuh batholith itself gives K-Ar ages around 225 Ma and the Karnian-Norian boundary is placed at about 210-215 Ma. Unfortunately although this case appears well defined there are problems with calibrating the late Triassic/early Jurassic radiometric time scale with the biostratigraphy, leading to some uncertainty on the Karnian-Norian boundary age.

In Japan, itself a magmatic arc, presently observed rates of uplift are up to a staggering 76.2 m/ 1000 years (Blatt, Middleton & Murray 1972) and plutons yielding radiometric ages of 10 Ma are currently exposed and providing detritus for the sedimentary cycle (Shibata & Ishihara 1979).

These figures, although not abundantly available, indicate that a 10 Ma interval between intrusion and erosion is the best available estimate for plutonic intrusions in active orogenic areas of magmatic arc type.

5.3.2 Maximum age estimates for stratigraphic horizons

Bearing in mind the constraints referred to above figures for the maximum radiometric age of the conglomerate horizons can now be obtained by subtracting 10 Ma from the youngest age determined on the granitic clasts from each conglomerate. Clearly in many cases the granitic clasts will be substantially older than the stratigraphic level in which they occur, and in this instance the figures are of little practical value. However, in the case of two conglomerates sampled in this study the resulting figures provide useful ages for the Benan and Tormitchell horizons.

A suite of samples from the Benan conglomerate give Rb-Sr ages of 467-475 Ma (see Chapter 2). One sample (101) provided zircon analyses which gave a U-Pb age and mean (Of 5) Pb-Pb age of 475^{+17}_{-9} and 475 $\pm$ 3 Ma respectively compared with 467 $\pm$ 3 Ma by the Rb-Sr method. These figures show a limited spread of ages around 470 Ma which is taken to represent a significant magmatic event and the latest intrusive episode sampled by the detritus of the Benan conglomerate. The one clast dated from the Tormitchell conglomerate yields an age of 451 $\pm$ 8 Ma from a well constrained isochron.

The stratigraphic ages of these units (see 1.5 & Table 5A) have been determined as lower Llandeilo (Nemagraptus gracilis) for the Benan conglomerate and lower Caradoc (Climacograptus wilsoni) for the Tormitchell conglomerate.

Combining the radiometric age, emplacement to unroofing timespan and stratigraphic age leads to the following figures :-

1. Maximum age for the lower Llandeilo (N. gracilis) of 460-465 Ma.

2. Maximum age for the lower Caradoc (C. wilsoni) of 440-450 Ma.

5.3.3 Comparison with previous time scales

Table 5A shows that these figures are in good agreement with those time scales based on Rb-Sr and K-Ar

radiometric ages. They are very close to the revised figures of Churkin et al. and on the right side of the Rundle and Gale et al. values. In contrast to this they are at variance with the fission track age scale of Ross et al., their figures for the lower Caradoc and lower Llandeilo being older than the maximum age estimates presented here and in Longman et al. (in press). (Appendix III).

	Series	Stage	British Graptolite Zone	Fitch et al. 1976	Churkin, Carter & Johnson 1977	Carter (unpub)	Ross et al. 1978	Rundle 1979	Gale et al. 1979	Bluck et al. 1980	This Study
SIL	LLVY	Rhuddanian	M. cyphus C. vesiculosus Of. acuminatus G. persculptus	430±10	433 Volcanic breccia, Alaska. Hb. K/Ar ±3 435	435	437 Low Birkhill Shales Fission-track, Bentonite (FTB) ±11		418		
ORDOVICIAN	ASHGILL	Hirnantian									
		Rawtheyan	D. anceps					421 Stockdale (Yarlside) Rhyolite Whole rock (WR) Rb/Sr ±3	421 Stockdale rhyolite WR Rb/Sr ±3		
		Cautleyan									
		Pusgillian	D. complanatus P. linearis		438	438					
	CARADOC	Onnian				438.5					
		Actonian	D. clingani				468 Acton Scott Beds zircon ±12				
		Marshbrookian			444 Bentonite, Tennessee Zircon U/Pb						
		Longvillian						429 Eskdale granite, WR Rb/Sr ±4			
		Soudleyan	D. multidens: C. wilsoni		445						Max. 440-450
		Harnagian	D. multidens: C. peltifer								
		Costonian		459±10	448	455			434		
	LLANDEILO	Upper	N. gracilis					Threlkeld microgranite WR Rb/Sr 459±25			
		Middle						458 Great Cockup Diorite Hb K/Ar 458±9			Max. 460-465
		Lower	G. teretiusculus		456	464					
	LLANVIRN	Upper	D. murchisoni		458	466	477 Bach-y-Graig, FTB ±11		453		
		Lower	D. bifidus		463	471					
	ARENIG	Upper	D. hirundo				487 Stapeley Volcanic Gp	468 Carrock gabbro / Eycott lavas, Bi K/Ar ±10	464		
		Lower	D. gibberulus D. nitidus D. deflexus T. approximatus	493±10	Bay of Islands, Newf Hb Ar/Ar 469±5 470 Ballantrae Complex Bi. K/Ar 484?		493 Llyfnant Flags, FTB±11		482	478 Ball Oph Hb K/Ar ±8	

Table 5A. Ordovician time scales (Ages in Ma)

APPENDIX I

Thin section descriptions

The nomenclature for the clasts is that derived from the weight percent mode (see 3.3). The grain size limitations are rather old fashioned but for plutonic rocks give more idea of grain size variation, namely coarse 3 cm-5 mm, medium 5mm-1mm and fine 1mm.

101 Medium-fine grained granite containing quartz, plagioclase, potassium feldspar, chlorite, muscovite, zircon, spene and opaques (Fig. 3/7). Potassium feldspar is present ascrod microperthite and as larger patches in more extensively unmixed (or possibly replaced) crystals. Albitic plagioclase is sericitized in the core and occasionally in the rim. Chlorite contains pleochroic haloes after biotite.

198 Medium grained granite with quartz, plagioclase, potassium feldspar, biotite (more or less chloritized), hornblende, epidote, sphene and opaques. Potassium feldspar is present as minor discrete crystals and the oligoclase is extensively altered to sericite and epidote. Some opaques form cores to biotite and hornblende, the former of which shows some kinking, and both are more or less replaced by chlorite. Strained quartz contains elongate subgrains.

197 Medium-fine grained granite containing quartz, plagioclase, potassium feldspar, biotite and opaques. Potassium feldspar as string microperthite and replacing oligoclase. Plagioclase shows some zoning with cracked cores and epidote infill. Perthite and quartz are grown together in a granophyric/graphic texture (Fig. 3/10). Biotite again being replaced by chlorite and contains pleochroic haloes around well developed zircons (Fig. 3/10). Some minor recrystallization.

196 Medium-coarse grained tonalite comprising quartz, plagioclase, potassium feldspar, hornblende, biotite and o paques. Dominated by 6 mm hornblendes with inclusions of

plagioclase and opaques. Zoned plagiolclases are highly sericitized and biotites variably chloritized. Quartz shows undulose extinction.

194 As for 197 though better developed graphic texture.

192 Medium-coarse tonalite containing quartz, plagioclase, potassium feldspar (?), biotite, hornblende and opaques. 4mm biotites are often kinked and chloritized. Some degenerating hornblende and highly sericitized plagioclase.

188 Medium grained granite with quartz, plagioclase, potassium feldspar, biotite, apatite and opaques. Some plagioclases zoned with coarse sericite (.04 mm) developed in core. Biotite with chlorite replacement. Potassium feldspar often encloses plagioclase.

187 Medium grained granite comprising quartz, plagioclase, potassium feldspar, amphibole, biotite, zircon and opaques. Potassium feldspar is present as rod and patch perthites exhibiting Carlsbad twinning. Early plagioclases are heavily corroded and some are enclosed by perthites. Large amphiboles are zoned from a dark green core to a dark blue rim and have a riebekite/arfvedsonite composition (3.2.1). Small hornblendes of a different generation are associated with biotite and opaques. Adjacent perthite grains exhibit the development of small albite crystals between them (see 3.2.1 and Fig. 3/8).

186 Granite similar to 187 though with no clean hornblende and more extensive chloritization of mafics and infiltration along perthite strands. (Contains small plagioclase and chlorite xenolith).

179 Xenolith containing quartz, plagioclase, hornblende, chlorite, opaques and clinopyroxene (?). Large chlorites after biotite (some kinked) enclose partially resorbed hornblende. Numerous small, often twinned,subhedral hornblendes (16^{o} extinction) with anhedral highly sericitized oligoclase. Quartz is either interstitial or'semi-ophitic' (Fig. 3/12).

176 Medium grained granite with quartz, plagioclase, potassium feldspar, biotite, sphene and opaques. Plagioclase is extensively zoned (Fig. 3/3) with the calcic cores highly sericitized. Potassium feldspars are often large with some minor exsolution picked out by alteration products, and may enclose early plagioclases. Biotite variably replaced by chlorite and contains many opaques (ilmenite/magnetite). Some potassium feldspars show pseudo-albite twinning.

299 Medium grained tonalite containing quartz, plagioclase, potassium feldspar, chlorite, epidote and opaques. Plagioclase sericitized and mafics largely replaced by chlorite. Some granophyric texture.

286 Medium grained granodiorite comprising quartz, plagioclase, potassium feldspar, biotite, epidote and opaques. Zoned plagioclase with 'coarse' sericite developed in the cores. Perthites intergrown with quartz to give granophyric/graphic texture. Biotite partially replaced by chlorite. Some myrmekite.

284 Medium grained granodiorite similar to 286 though with better developed graphic texture (Fig. 3/11).

399 Medium grained granodiorite comprising quartz, plagioclase, potassium feldspar, amphibole and opaques. Extensive perthites with plagioclase development between adjacent crystals (c.f. 187 & 186). Anhedral amphiboles showing alkali colouration.

591 Medium-fine grained deformed tonalite with quartz, plagioclase, potassium feldspar, amphibole, biotite and opaques. Amphibole and biotite are both chloritized and the

plagioclase sericitized. Some calcite veining.

587 Medium-fine grained granodiorite containing quartz, plagioclase, potassium feldspar, biotite, muscovite, zircon and opaques. Plagioclase is sericitized and the muscovite associated with chloritization of biotite.

580 Medium grained granite with quartz, plagioclase, potassium feldspar, biotite, muscovite and opaques. The plagioclase is sericitized and the biotite chloritized. Muscovite associated with alteration. Recrystallization at grain boundaries though no fabric development.

579 Medium grained granodiorite comprising quartz, plagioclase, potassium feldspar, biotite, epidote and opaques. Plagioclase, frequently zoned, is sericitized and the biotite chloritized. Potassium feldspar is present as discrete grains and patch/rod perthite. Extensive quartz and calcite veining.

889 Medium grained rock of quartz-monzonite composition containing plagioclase, potassium feldspar, biotite, quartz calcite, epidote and opaques. The potassium feldspar is unaltered as is the plagioclase. Some remnant perthite and biotite show chloritization. Extensive deformation and calcite veining which itself appears deformed, e.g. kinked twin lamellae.

996 Medium-fine grained foliated granodiorite with quartz, plagioclase, potassium feldspar, biotite and opaques. Some large microcline (2 mm) and zoned plagioclase exhibiting much sericitization. Biotite is partially replaced by chlorite.

993 Medium grained granodiorite comprising quartz,

plagioclase, potassium feldspar, biotite and opaques. The plagioclase is occasionally zoned and heavily sericitised. Biotite almost completely replaced by chlorite and epidote. Unduloze quartz and some epidote veining.

988 Medium-fine grained foliated granodiorite containing quartz, plagioclase, potassium feldspar, biotite, muscovite, zircon and opaques. Plagioclase is often sericitized and the potassium feldspar is present as both large and interstitial crystals. Biotite contains zircons and shows some chlorite replacement. Muscovite appears as large plates and also intimately associated with chlorite in the biotite breakdown. Veined by calcite.

985 Medium grained tonalite with quartz, plagioclase, biotite and opaques. Much alteration and quartz/epidote veining.

982 Medium grained granodiorite comprising quartz, plagioclase, potassium feldspar, biotite, hornblende and opaques. Zoned plagioclase is sericitized and enclosed by quartz. Potassium feldspar may enclose quartz and replace plagioclase. Biotite replaced by chlorite and epidote. Subhedral hornblendes contain feldspar inclusions.

APPENDIX II

Copy of :-

Longman, C.D., Bluck,B.J. & van Breemen,O. Ordovician conglomerates and the evolution of the Midland Valley. Nature 280, 578-581 (1979).

(Reprinted from Nature Vol. 280, No. 5723, pp. 578-581, August 16 1979)

Ordovician conglomerates and the evolution of the Midland Valley

ORDOVICIAN and Silurian marine clastic sequences containing boulder bearing conglomerates overlie the Ballantrae ophiolite complex in South-west Ayrshire, Scotland. These conglomerates are thought to have been emplaced by submarine slides[1] or less viscous marine currents[2]. The Ordovician conglomerates accumulated at the toes of contemporary submarine faults downthrowing to the south[3] and in both their stratigraphy and palaeocurrents there is substantial evidence for a northerly source. The conglomerates contain clasts of the underlying ophiolite, metamorphic rocks, acid and intermediate volcanic and hypabyssal rocks and clasts of undeformed pink granite some of which are >80 cm in largest dimension. Dewey[4] and many subsequent workers[5] envisage these sediments as having accumulated on the southern margin of a continent under which oceanic plate was being consumed in a northerly dipping subduction zone. The time span of this subduction is subject to much speculation[6] but is generally thought to have ceased by Devonian time. We report here our investigations of the clasts in the southern Ayrshire conglomerates to elucidate (1) the nature and extent of plutonic activity in the area to the north of the subduction zone, and (2) the nature of the crust into which the plutons were emplaced.

Rb–Sr isotope dilution analyses of these clasts follow the analytical methods described by Blaxland *et al.*[7]. Rb–Sr ages have been calculated, or recalculated, using $\lambda^{87}Rb = 1.42 \times 10^{-11}\ yr^{-1}$. Analytical uncertainties at the 1σ level for $^{87}Rb/^{86}Sr$ and $^{87}Sr/^{86}Sr$ isotope ratios are ±0.7% and ±0.03% respectively. Seven analyses of the NBS 607 potassium feldspar standard yield average $^{87}Rb/^{86}Sr$ and $^{87}Sr/^{86}Sr$ values of 24.21 ± 11 (1σ) and 1.2006 ± 6 (1σ) respectively. The average $^{87}Sr/^{86}Sr$ value for NBS 987 standard $SrCO_3$ is 0.71020 ± 5 (1σ). Rb–Sr isochron ages were calculated using the least squares method of York[8]. All isochrons are concordant (MSWD < 2.5) or near concordant suggesting the observed scatter to be analytical rather than geological.

Table 1 Analytical data

Sample	Phase	Rb (p.p.m.)	Sr (p.p.m.)	$^{87}Rb/^{86}Sr$	$^{87}Sr/^{86}Sr$
17600	Whole rock	94.9	177.8	1.5640	0.72212
17607	Plagioclase	57.8	374.8	0.4465	0.71274
17613	Alkali feldspar	264.0	130.0	5.9044	0.75801
17616		287.7	106.9	7.8362	0.77133
17617		296.1	100.1	8.6205	0.77687
17618		312.3	92.5	9.8451	0.78417
10100	Whole rock	163.8	27.1	17.6832	0.82536
10107	Perthite	35.2	86.0	1.1833	0.71460
10113		450.6	21.5	63.1951	1.13128
10115		591.6	17.7	103.374	1.39660
10116	Muscovite	1049.1	4.8	1084.75	8.17221
10104*	Perthite	284.3	35.0	23.8428	0.86476
10108*		389.5	25.6	45.3412	1.00714
10111*		445.5	21.0	64.1603	1.13346
10113*		521.6	18.1	88.2863	1.29343
10114*		607.6	16.9	111.411	1.43777
18600	Whole rock	112.0	10.5	33.8337	0.92777
18605	Perthite	173.3	14.0	36.7596	0.94866
18612		244.5	13.6	53.9222	1.06083
18613		258.9	13.7	56.7424	1.08367
18700	Whole rock	127.1	11.1	33.9507	0.92320
18705	Perthite	142.4	13.7	30.6406	0.90431
18709		227.1	13.7	49.2947	1.02998
18711		226.9	13.4	50.5927	1.03354
18713		235.9	13.4	52.6500	1.05118
18714		258.0	13.4	57.8238	1.08135
19700	Whole rock	117.2	48.1	7.0899	0.75569
19704	Alkali feldspar	133.2	65.4	5.9144	0.74731
19706		256.6	45.8	16.4009	0.81789
19708		280.2	45.4	18.0603	0.82799
19709		306.0	43.5	20.6541	0.85765
19710		364.9	41.7	25.7471	0.87975
19400	Whole rock	117.4	61.2	5.5704	0.74441

All mineral separates are of a size fraction 210–175 μm except those marked * which are 500–210 μm.

Rb–Sr analytical data are shown in Table 1. Mineral isochrons determined for five different granite clasts (minimum of 30 cm in longest dimension) and one composite whole rock isochron are plotted in Fig. 1.

The age values obtained suggest a two-fold division defining one event at ~560 Myr and another at ~470 Myr. Sample 176, an undeformed non-perthitic biotite–chlorite bearing subsolvus granodiorite[9] yields an age of 559 ± 20 Myr. The other four clasts, 101, 196, 187 and 197 yield ages of 469 ± 5, 471 ± 13, 466 ± 14 and 468 ± 5 Myr respectively. These samples are less mafic, commonly microperthite-bearing subsolvus granites. The four whole rock points from the samples defining the ~470 Myr event were plotted along with another whole rock point from a chemically and petrographically similar clast (Fig. 1). These define a tentative isochron of 459 ± 10 Myr.

The initial $^{87}Sr/^{86}Sr$ ratios of three younger samples agree within experimental error (those for 186 and 187 were excluded as being ill defined and anomalously low) ranging from 0.7067 ± 8 to 0.7087 ± 15 and giving a mean of 0.7078 ± 10. The initial $^{87}Sr/^{86}Sr$ ratio for sample 176 is 0.7095 ± 11.

The age and stratigraphic position of the granite clasts places constraints on the Ordovician time scale. The dated clasts come from the Benan conglomerates of Llandeilo age. Petrographically similar clasts are, however, found in conglomerates ranging through to Llandovey in age[10]. Presently observed rates of uplift and erosion[11] suggest that surface exposure of the granites is possible in <10 Myr. This gives a maximum age for the base of

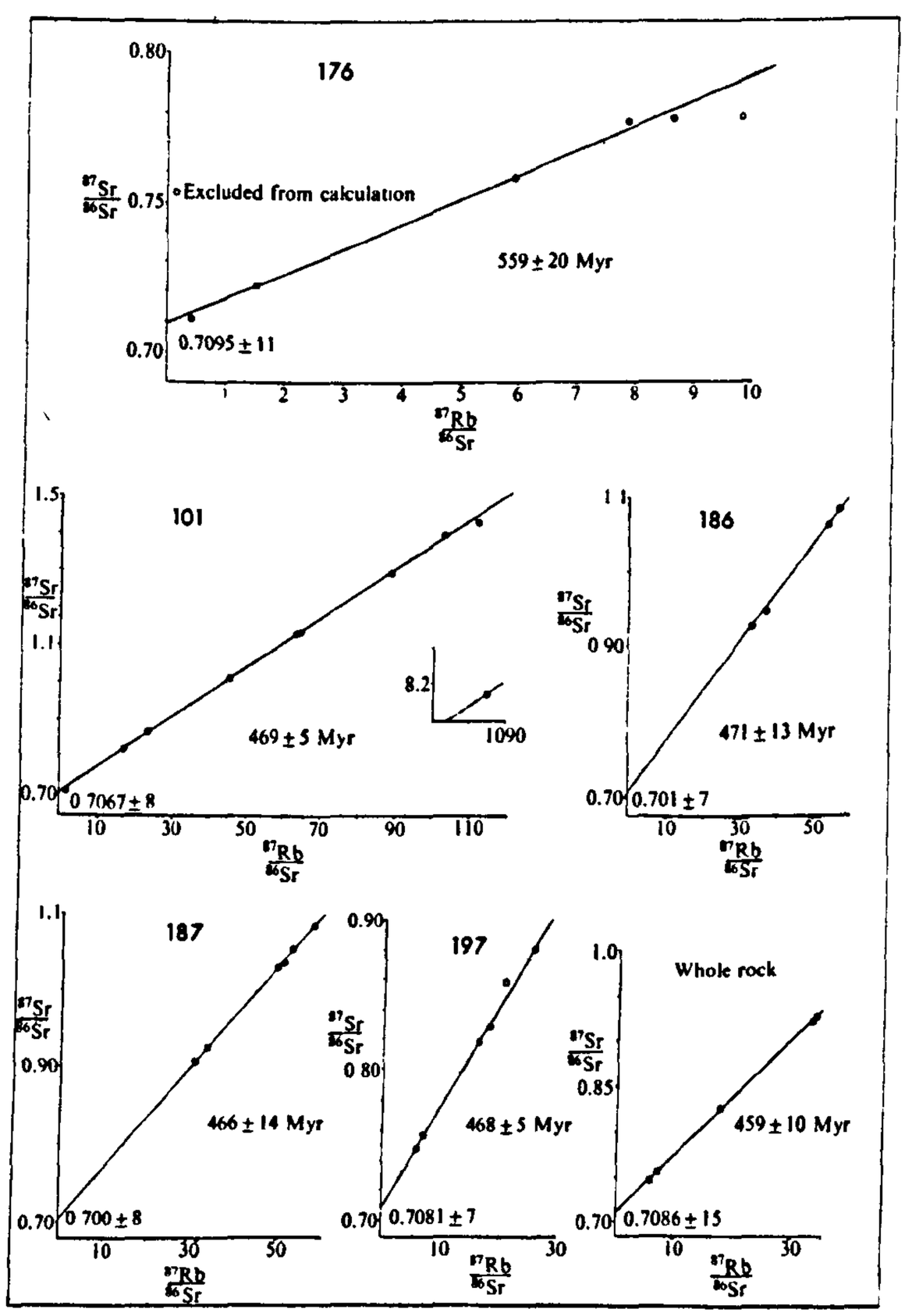

Fig. 1 Mineral isochrons of five different granite clasts and one composite whole rock isochron.

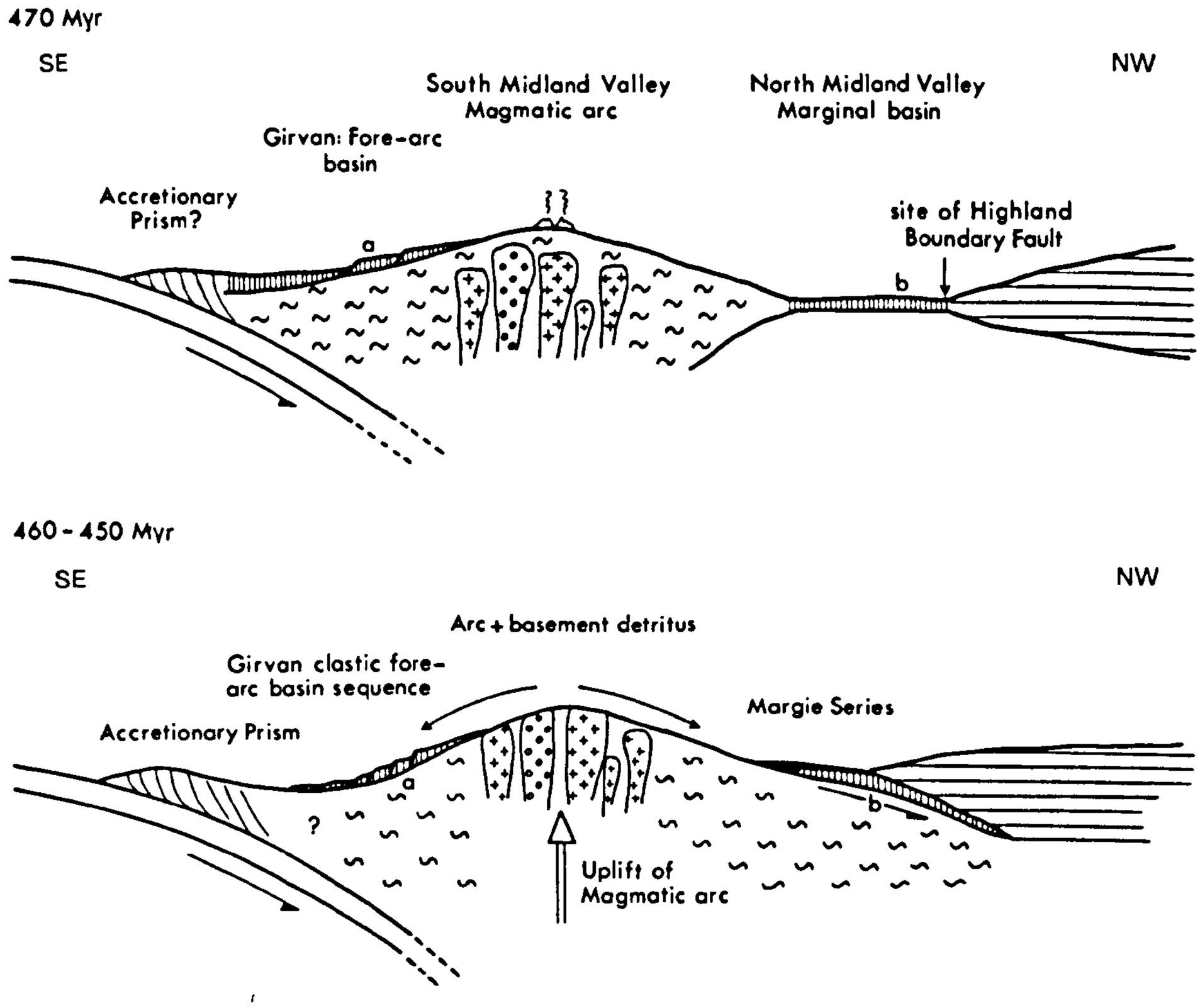

Fig. 2 Reconstruction of the Midland Valley during the Ordovician.

the Llandeilo of about 460 Myr. This figure is in reasonable agreement with some published Ordovician time scales[12,13] based largely on K–Ar and Rb–Sr ages, but is irreconcilable with older ages based on fission track data[14].

Consideration of dispersal of the conglomerates and the size of the granite clasts indicate a provenance to the immediate north, in the south-west margin of the Midland Valley. The granite clasts have a similar petrography and age to the exposed pre and late tectonic granites in the Highlands. Ages of ~450 Myr are reported for many of the smaller granites of North-east Scotland[15] whereas the Carn Chuinneg–Inchbae granite is dated at 560 ± 10 Myr[16,17]. The known pre and late tectonic plutonic activity which preceded the ubiquitous ~400 Myr granites, relating to the final closure of the Iapetus Ocean, is therefore extended south of the Highlands.

The initial $^{87}Sr/^{86}Sr$ ratio of the Carn Chuinneg granite (0.710 ± 2)[16] is similar to that of sample 176—unless the 559 ± 20 Myr age for this rock is a cooling age and the high $^{87}Sr/^{86}Sr$ ratio reflects Sr isotopic equilibration on a mineral scale. In contrast, the initial $^{87}Sr/^{86}Sr$ ratios of around 0.708 for the ~470 Myr suite are significantly lower than the values of 0.714–0.717 for the ~450 Myr suite of Aberdeenshire granites[15]. Taken together, the 470–450 Myr Midland Valley–Aberdeenshire granites show a northerly increase in initial $^{87}Sr/^{86}Sr$ ratios. This pattern together with the high normative corundum and presence of muscovites in the northern granites[18] can be explained by increasing crustal involvement in the northern source. Although this evidence does not prove northward subduction the data are consistent with $^{87}Sr/^{86}Sr$ isotope ratio patterns of Mesozoic and Cenozoic subduction related granites in the western US[19,20] and such a model accords with many views on plate configuration in this region at that time[21].

The discovery of granite boulders of this age, together with consideration of the type and distribution of clasts in other Midland Valley conglomerates helps to refine existing models. Boulders and large cobbles of granite, quartz-porphyry, rhyolite and andesite present in Ordovician and Silurian conglomerates, suggest major intrusive and extrusive activity in the source area. The plutonic activity is now dated, and Kelling[22] in recording an influx of andesite fragments in Llandeilo greywackes has suggested volcanic fields in this region at the same general time as the intrusion of the younger granites of this study. This evidence is consistent with the development of an island arc in the southern margin of the Midland Valley reaching maturity in Lower Ordovician time. The existence of an island arc associated with the northward subduction has been previously postulated[4,23,24] but hitherto no evidence for its existence has been available.

Cobbles and boulders of metaquartzite, amphibolite and sheared granite occur in the northerly derived Ordovician conglomerates discussed here and the southerly derived Silurian conglomerates of the southern Midland Valley[25]. Metaquartzite thus formed part of the provenance in the Midland Valley at this

time. However, as the 560 Myr granite is unfoliated it seems likely that the event which created the metamorphic assemblage pre-dated the early igneous episode. Furthermore, the presence of metaquartzite suggests ensialic deposition. Thus the evidence points to the existence of Precambrian basement under the Midland Valley, in accord with the original interpretation placed on granulite clasts of intermediate composition found in Carboniferous vents[26]. Mineral chemistry of these clasts indicate pressures and temperatures of metamorphism exceeding 11 kbar and 850 °C (ref. 27) and recent Sm–Nd isotopic work indicates a maximum Grenville age[28]. This evidence for late Precambrian continental basement under the Midland Valley agrees well with the LISPB north–south seismic profile across Scotland[29] and possibly supports both Kennedy[30] and George[31] who found evidence of a southerly source for the Upper Dalradian sediments.

The temporal and spatial setting of the probable post-Grenville quartzite deposition and its metamorphism in the late Precambrian, possibly very early Cambrian time, is critical to the evaluation of the early history of the Midland Valley block. It would, nevertheless, seem likely (also with evidence for Grenville basement under the Dalradian[32,33]) that the Midland Valley began its separate development after the rifting associated with the extrusion of the Tayvallich volcanics[34] which initiated the southward derived sediments of the Upper Dalradian.

The Tayvallich volcanism has been correlated with similar basic volcanism in Newfoundland (dated at 605 ± 10 Myr[35]) which has been attributed to the opening of Iapetus[36]. Our evidence, however, suggests that this rifting event was related to the formation of the first marginal basin along the southern margin of the North American Continent[23].

The serpentinite, spilite, radiolarian chert and black shale assemblages along the Highland Boundary Fault (HBF) are probably of Arenig–Llanvirn age[37]. The new data make it likely that these rocks were deposited behind the magmatic arc, in a marginal basin. The later closure of this basin, by subduction related under thrusting, then resulted in the preservation of a thin ophiolitic sliver along the HBF (see Fig. 2). This closure is likely to have occurred in Caradocian time, immediately after the deposition of the arenaceous 'molasse' of the Margie series, also preserved along the HBF. The closure resulted in the Highland Border rocks having a structural grain similar to those of the adjacent Dalradian, thus giving a spurious impression of structural unity in them both.

The evidence from the Tayvallich volcanics, the HBF suite and also the Ballantrae Complex[38] indicate that the southern margin of the North American continent comprised a series of marginal basins and associated microcontinents. It therefore seems improbable that the Grampian Orogeny resulted from a large-scale continent–continent collision. Consequently we conclude that the landmass which supplied the sediments of the Upper Dalradian was emplaced beneath the latter (see Fig. 2) resulting in the symmetrical folding and mushrooming of the Grampian orogeny and the dramatic uplift along the HBF[39].

We thank J. H. Hutchinson for help with the mass spectrometry. C.D.L. acknowledges the support of a NERC grant. The Isotope Geology Unit of the Scottish Research Reactor Centre is supported by a NERC Research grant.

C. D. LONGMAN
B. J. BLUCK

Department of Geology,
The University,
Glasgow, UK

O. VAN BREEMEN

Reactor Centre,
East Kilbride, UK

Received 8 May; accepted 10 July 1979.

1. Kuenen, P. H. *Konikl Ned. Akad. Wet. Verh., Afh. Natuurk* **20**, 1–47 (1953).
2. Hubert, J. F. in *North Atlantic—Geology and Continental Drift* (ed. Kay, M.) 267–282 (American Association of Petroleum Geologists, Tulsa, 1969).
3. Williams, A. *Mem. geol. Soc. Lond.* **3**, 265P (1962).
4. Dewey, J. F. *Scott. J. Geol.* **7**, 219–240 (1971).
5. Phillips, W. E. A., Stillman, C. J. & Murphy, T. *J. geol. Soc. Lond.* **132**, 579–609 (1976).
6. Lambert, R. St. J. & McKerrow, W. S. *Scott. J. Geol.* **12**, 271–292 (1976).
7. Blaxland, A. B., van Breemen, O., Emeleus, C. H. & Anderson, J. G. *Bull. geol. Soc. Am.* **89**, 231–244 (1978).
8. York, D. *Earth planet. Sci. Lett.* **5**, 320–324 (1969).
9. Streckeisen, A. *Earth. Sci. Rev.* **12**, 1–33 (1976).
10. Ingham, J. K. *Geol. J. Spec. Issue* No. **10**, 115–138 (1978).
11. Blatt, H., Middleton, G. & Murray, R. *Origin of Sedimentary Rocks* (Prentice-Hall, Englewood Cliffs, 1972).
12. Churkin, M. Jr, Carter, C. & Johnson, B. R. *Geology* **5**, 452–456 (1977).
13. Rundle, C. C. *J. geol. Soc. Lond.* **136**, 29–38 (1978).
14. Ross, R. J. Jr *et al. U.S. Geol. Surv. Open File Rep.* 78–701, 363–365 (1978).
15. Pankhurst, R. J. *Bull. geol. Soc. Am.* **85**, 345–350 (1974).
16. Long, L. E. *J. geophys. Res.* **69**, 1589–1597 (1964).
17. Pidgeon, R. T. & Johnson, M. R. W. *Earth planet. Sci. Lett.* **24**, 105–112 (1974).
18. Busrewil, M. T., Pankhurst, R. J. & Wadsworth, W. J. *Miner. Mag.* **40**, 363–376 (1975).
19. Kistler, R. W. & Peterman, Z. E. *Bull. geol. Soc. Am.* **84**, 3489–3512 (1973).
20. Armstrong, R. L., Thorbeneck, W. H., & Hales, P. O. *Bull. geol. Soc. Am.* **88**, 397–411 (1977).
21. Moseley, F. *Bull. geol. Soc. Am.* **88**, 764–768 (1977).
22. Kelling, G. *J. geol. Soc. Lond.* **117**, 37–75 (1961).
23. Wright, A. E. *Estudios geol.* **33**, 303–313 (1977).
24. Mitchell, A. H. G. *J. Geol. Chicago* **86**, 643–646 (1977).
25. McGiven, A. thesis, Univ. Glasgow (1967).
26. Upton, B. G. J., Aspen, P., Graham, A. M. & Chapman, N. *Nature* **260**, 517–518 (1976).
27. Graham, A. M. & Upton, B. G. J. *J. geol. Soc. Lond.* **135**, 219–228 (1978).
28. van Breemen, O. & Hawkesworth, C. J. (in the press).
29. Bamford, D., Nunn, K., Prodehl, C. & Jacobs, B. *J. geol. Soc. Lond.* **133**, 481–488 (1977).
30. Kennedy, W. Q. *Trans. geol. Soc. Glasg.* **23**, 107–133 (1958).
31. George, T. N. *Trans. geol. Soc. Glasg.* **24**, 32–107 (1960).
32. Pankhurst, R. J. & Pidgeon, R. T. *Earth planet Sci. Lett.* **31**, 55–68 (1976).
33. van Breemen, O., Halliday, A. N., Johnson, M. R. W. & Bowes, D. R. *geol. J. Spec. Issue* No. 10, 81–106 (1978).
34. Graham, C. *J. geol. Soc. Lond.* **132**, 61–84 (1976).
35. Stukas, V. & Reynolds, P. H. *Earth planet. Sci. Lett.* **22**, 256–266 (1974).
36. Dewey, J. F. *Nature* **222**, 124–129 (1969).

APPENDIX III

Copy of :-

Longman,C.D., Bluck,B.J., van Breemen,O. & Aftalion,M. Ordovician conglomerates : Constraints on the time scale, in 'Numerical dating of the stratigraphic column', Ed. Odin, G.S. (Wiley & Sons) (in press).

Ordovician conglomerates : Constraints on the time scale

C.D.Longman, B.J.Bluck, O. van Breemen & M.Aftalion.

Ordovician conglomerates within a clastic sequence overlying the Ballantrae ophiolite in S.W.Scotland contain numerous granitic clasts. The succession represents sediment accumulation on the southern margin of a continent to the north of the Iapetus Ocean (Dewey 1971). Stratigraphy, palaeocurrent analysis and clast size (some >80 cm in longest dimension) indicates that the conglomerates had a source to the immediate north. The granite clasts were thus dated by the Rb-Sr and U-Pb techniques, and analysed to elucidate the nature of the northern margin of the closing Iapetus Ocean (Longman et al. 1979). The age data obtained, however, also have implications concerning the Ordovician time scale due to the proximity of the stratigraphic and radiometric ages.

The two horizons constrained by this study, the Benan and Tormitchell conglomerates, are exposed in the Girvan region, Ayrshire (Scotland). Williams (1962) investigated the stratigraphy and brachiopod fauna of the area and advocated a Caradocian age for both horizons. More recent work, however, on the conodont, graptolite and trilobite fauna (Ingham 1978; Tripp 1980) has placed a lower Llandeilo (Nemagraptus gracilis) age on the Benan conglomerate and a lower Caradoc (Climacograptus wilsoni) age on the Tormitchell conglomerate.

The sample data presented here (Tables 1 & 2) are from aseries of analyses on clasts collected (by C.D.L.) to encompass the range pf granitic clasts present, which in all cases were >30 cm in longest dimension. Conglomerates being the host rock for the granite clasts means that the samples have been subjected to atmospheric weathering. This weathering, evident as chloritization of biotite and sericitization of the plagioclase, appears to be limited and to have occurred during a short erosion/sedimentation phase as the presently exposed conglomerates are not unduly

weathered.

Rb-Sr isotope dilution analysis follows the procedure of Blaxland et al. (1978). Mineral separates were obtained by utilizing heavy liquid and magnetic techniques on sieved size fractions (generally 210-175 um). Zircon separation and analysis follows the procedure of Pidgeon & Aftalion (1978). The earlier Rb-Sr analyses were performed on an AEI MS12 mass spectrometer but some later Rb-Sr and the U-Pb analyses were done on a semi-automated Micromass MM30 machine. Analytical uncertainties at the 1σ level for $^{87}Rb/^{86}Sr$ and $^{87}Sr/^{86}Sr$ are $\pm$ 0.7% and $\pm$ 0.03% respectively. Seven analyses of NBS 607 (Potassium feldspar) give averages of 24.11 $\pm$ 11 (1σ) for $^{87}Rb/^{86}Sr$ and 1.2006 $\pm$ 6 (1σ) for $^{87}Sr/^{86}Sr$ and the mean value for NBS 987 ($SrCO_3$) is 071020 $\pm$ 5 (1σ). Corrections for common lead in the zircon analyses were made using $^{206}Pb/^{204}Pb = 17.3$, $^{207}Pb/^{204}Pb = 15.5$ and $^{208}Pb/^{204}Pb = 37.1$.

Analytical data are presented in Tables 1 & 2. Rb-Sr isochron results, using one whole rock point and a variable number of mineral separates, and following the least squares method of York (1969) are shown in Table 3 along with U-Pb concordia ages and a mean Pb-Pb age. Values used for the decay constants are as follows : $^{87}Rb = 1.42 \times 10^{-11} y^{-1}$, $^{238}U = 1.55125 \times 10^{-10} y^{-1}$ and $^{235}U = 9.84850 \times 10^{-10} y^{-1}$ (Steiger & Jäger 1977).

The Rb-Sr ages for the clasts are based mainly on whole rock and potassium feldspar data points, the latter of which show little or no effects of weathering, and thus should be representative of the age of emplacement. The one sample on which zircon analyses have been undertaken gives and upper intercept U-Pb age and a Pb-Pb age of 475^{+17}_{-9} and 475 $\pm$ 3 Ma respectively compared with 460 $\pm$ 3 by the Rb-Sr method. Although there is some overlap this may suggest possible minor pulling down of the Rb-Sr ages for individual clasts. However, the limited spread of ages around 470 Ma for the Benan conglomerate samples appears to represent a real magmatic event.

The radiometric ages for the clasts can be used to delimit the age of their stratigraphic horizons by

estimating the emplacement to unroofing timespan. The environment into which the granites were intruded is envisaged to be an active magmatic arc (Longman et al. 1979). Presently observed rates of uplift and erosion (Blatt, Middleton & Murray 1972) and comparison with arc related Mesozoic plutons in the North American Cordillera (H.Gabrielse pers. comm. 1979) indicate unroofing in less than 10 Ma. This then places maximum age figures of c. 460-465 Ma on the lower Llandeilo (N. gracilis) and c. 440-450 Ma on the lower Caradoc (C. wilsoni).

These figures are in good agreement with the Ordovician time scales based on Rb-Sr and K-Ar age determinations (Churkin et al. 1977; Rundle 1979; Gale et al. 1979 (the latter also contains fission track ages)) but is at variance with that based mainly on fission track data (Ross et al. 1978).

Our thanks go to J.H.Hutchinson for help with the mass spectrometry and J.Jocelyn for the zircon separation. C.D.L. acknowledges receipt of a NERC grant and the Isotope Geology Unit of the Scottish Universities Research and Reactor Centre is supported by a NERC research grant.

C.D.Longman & B.J.Bluck
Department of Geology
Glasgow University
Glasgow G12 8QQ
Scotland

O. van Breemen & M.Aftalion
S.U.R.R.C.
National Engineering Laboratory
East Kilbride G75 OQU
Scotland

Sample	Rb (ppm)	Sr (ppm)	$^{87}Rb/^{86}Sr$	$^{87}Sr/^{86}Sr$
101	163.8	27.1	17.6832	0.82536
10107	35.2	86.0	1.1833	0.71460
10113	450.6	21.5	63.1951	1.13128
10115	591.6	17.7	103.374	1.39660
10116*	1049.1	4.8	1084.75	8.17221
10104*	284.3	35.0	23.8428	0.86476
10108*	389.5	25.6	45.3412	1.00714
10111*	445.5	21.0	64.1603	1.13346
10113*	521.6	18.1	88.2863	1.29343
10114	607.6	16.9	111.411	1.43777
186	112.0	10.5	33.8337	0.92777
18605	173.3	14.0	36.7596	0.94866
18612	244.5	13.6	53.9222	1.06083
18613	258.9	13.7	56.7424	1.08367
187	127.1	11.1	33.9507	0.92320
18705	142.4	13.7	30.6406	0.90431
18709	227.1	13.7	49.2947	1.02998
18711	226.9	13.4	50.5927	1.03354
18713	235.9	13.4	52.6500	1.05118
18714	258.0	13.4	57.8238	1.08135
196	40.7	322.1	00.3655	0.70749
19607	45.9	285.8	0.4634	0.70832
19608	85.4	291.4	0.8476	0.71078
19609	135.2	232.4	1.6843	0.71649
197	117.2	48.1	7.0899	0.75569
19704	133.2	65.4	5.9144	0.74731
19706	256.6	45.8	16.4009	0.81789
19708	280.2	45.4	18.0603	0.82799
19709	306.0	43.5	20.6541	0.85765
19710	364.9	41.7	25.7471	0.87975
399	32.1	22.2	4.2060	0.73299
39905	40.8	16.5	7.2044	0.75291
39907	54.8	17.5	8.9957	0.76343
39909	75.8	18.0	12.2792	0.78506
39911	118.8	18.0	18.2032	0.82275

All mineral separates are of a size fraction 210-175 μm except those marked thus (*) which are 500-210 μm.

Table 1 Rb-Sr Analytical Data

Sample	Size (μm)	Pb(ppm)	U(ppm)	$^{206}Pb/^{204}Pb$	^{206}Pb	^{207}Pb (Atomic %)	^{208}Pb	$^{207}Pb/^{206}Pb$	$^{207}Pb/^{235}U$	$^{206}Pb/^{238}U$
101688	-85+65 NM	104.6	1379	1095	81.9040	4.63519	13.4608	0.056593	0.56308	0.072156
101689	-85+65 M1°	202.3	2694	1319	81.4381	4.59876	13.9632	0.056469	0.55320	0.071046
101690	-65+53 M1°	195.3	2591	1503	81.2092	4.59973	14.1910	0.056641	0.55532	0.071103
101707	-85+65 M3°	249.1	3424	699	80.7374	4.57366	14.6890	0.056649	0.53170	0.068085
101708	-65+53 M3°	228.7	3139	838	80.5922	4.55403	14.8538	0.056507	0.53149	0.068212

Table 2 U-Pb Analytical Data

Horizon	Sample	Method	Age (Ma ± 2σ)	No. of points	MSWD
Benan Conglomerate	101	Rb-Sr	467 ± 3	9	1.12
		Rb-Sr	469 ± 5	10 (incl. musc.)	3.66
		U-Pb Concordia	U.I. 475 $^{+17}_{-9}$ L.I. -1 $^{+121}_{-123}$	5	1.49
		Pb-Pb	475 ± 3	Mean of 5	----
	186	Rb-Sr	471 ± 13	4	0.72
	187	Rb-Sr	466 ± 13	5	1.46
	196	Rb-Sr	475 ± 12	4	0.17
	197	Rb-Sr	468 ± 5	5	0.57
Tormitchell Conglomerate	399	Rb-Sr	451 ± 8	5	1.02

Table 3 Age Data

REFERENCES

Anderton, R. (1980) Did Iapetus start to open during the Cambrian ?. Nature 286, 706-708.

Armstrong, R.L., Taubeneck, W.H. & Hales, P.O. (1977) Rb-Sr and K-Ar geochronometry of Mesozoic granitic rocks and their Sr isotopic composition, Oregon, Washington and Idaho. Bull. geol. Soc. Am. 88, 397-411.

Bamford, D. & others (1976) A lithospheric seismic profile in Britain - I preliminary results. Geophys. J. R. astron. Soc. 44, 145-160.

Bamford, D., Nunn, K., Prodehl, C. & Jacobs, B. (1977) LISPB - III Upper crustal structure of northern Britain. J. geol. Soc. Lond. 133, 481-488.

Bamford, D., Nunn, K., Prodehl, C. & Jacobs, B. (1978) LISPB - IV Crustal structure of northern Britain. Geophys. J. R. astron. Soc. 54, 43-60.

Bamford, D., Jentsch, M. & Prodehl, C. (1979) P_n anisotropy studies in northern Britain and western United States. Geophys. J. R. astron. Soc. 57, 397-429.

Barker, F. (1979) Tröndhjemite : definition, environment and hypotheses of origin. in Trodhjemites, dacites and related rocks, Ed. Barker, F. (Elsevier).

Barth, T.F.W. (1955) Presentation of rock analyses. J. geol. 63, 340-363.

Beckinsale, R.D. (1979) Granite magmatism in the tin-belt of S.E. Asia. in Origin of Granite Batholiths : Geochemical evidence (Shiva publishing limited).

Bergström, S.M. (1971) Conodont biostratigraphy of the Middle and Upper Ordovician of Europe and eastern North America. Mem. geol. Soc. Am. 127, 83-157.

Bird, J.M. & Dewey, J.F. (1970) Lithosphere plate-continental margin tectonics and the evolution of the Appalachian orogen. Bull. geol. Soc. Am. 81, 1031-1060.

Blatt, H., Middleton, G. & Murray, R. (1972) Origin of sedimentary rocks (Prentice-Hall).

Bluck, B.J. (1978) Geology of a continental margin 1 : the Ballantrae Complex. in Geol. J. Spec. Issue No. 10, 151-162.

Bluck,B.J., Halliday, A.N., Aftalion, M. & MacIntyre, R.M. (1980) Age and origin of the Ballantrae ophiolite and its significance to the Caledonian orogeny and Ordovician time scale. Geology 8, 492-495.

Bradbury, H.J., Smith, R.A. & Harris, A.L. (1976) 'Older' granites as time-markers in Dalradian evolution. J. geol. Soc. Lond. 132, 677-684.

Brooks, C., Wendt, I. & Harre, W. (1968) A two-error regression treatment and its applications to Rb-Sr and initial $^{87}Sr/^{86}Sr$ ratios of younger Variscan granitic rocks from the Schwarzwald Massif, Southwest Germany. J. geophys. Res. 73, 6071-6084.

Brooks, C., Hart, S.R. & Wendt, I. (1972) Realistic use of two-error regression treatments as applied to Rubidium-Strontium data. Rev. Geophys. 10, 551-577.

Brown, G.C. (1979) The changing pattern of batholith emplacement during Earth history. in Origin of Granite Batholiths : Geochemical evidence (Shiva publishing ltd.).

Busrewil, M.T., Pankhurst, R.J. & Wadsworth, W.J. (1975) The origin of the Kennethmont granite-diorite series, Insch, Aberdeenshire. Mineralog. Mag. London 40, 363-376.

Cawthorn, R.G. & Brown, P.A. (1976) A model for the formation and crystallization of corundum normative calc-alkaline magmas through amphibole fractionation. J. Geol. Chicago 84, 467-476.

Chappell, B.W. & White, A.J.R. (1974) Two contrasting granite types. Pacific Geology 8, 173-174.

Church, W.R. & Gayer, R.A. (1973) The Ballantrae ophiolite. Geol. Mag. 110, 497-510.

Churkin, M.Jnr., Carter, C. & Johnson, B.R. (1977) Subdivision of Ordovician and Silurian time scale using accumulation rates of graptolitic shale. Geology 5, 452-456.

Cocks, L.R.M. & Toghill, P. (1973) The biostratigraphy of the Silurian rocks of the Girvan district, Scotland. J. geol. Soc. Lond. 129, 209-243.

Condie, K.C. & Hunter, D.R. (1976) Trace element geochemistry of Archean granitic rocks from the Barberton region, South Africa. Earth Planet. Sci. Lett. 29, 389-400.

Cox, K.G., Bell, J.D. & Pankhurst, R.J. (1979) The interpretation of igneous rocks (George, Allen & Unwin).

Cross, W., Iddings, J.P., Pirsson, L.V. & Washington, H.S. (1906) Quantitative classification of igneous rocks (University of Chicago Press).

de la Roche, H., Letterier, J., Grandeclaude, P. & Marchel, M. (1980) A classification of volcanic and plutonic rocks using R_1-R_2 diagram and major-element analyses - its relationship with current nomenclature. Chem. Geol. 29, 183-210.

Dewey, J.F. (1969) Evolution of the Caledonian/Appalachian Orogen. Nature 222, 124-129.

Dewey, J.F. (1971) A model for the Lower Palaeozoic evolution of the southern margin of the early Caledonides of Scotland and Ireland. Scott. J. Geol. 7, 219-240.

Dewey, J.F. (1974) The geology of the southern termination of the Caledonides. in Ocean basins and margins, 2, The North Atlantic (Eds. Nairn, A.E.M. & Stehli, F.) (Plenum Press).

Dewey, J.F., Rickards, R.B. & Skevington, D. (1970) New light on the age of Dalradian deformation and metamorphism in western Ireland. Nor. geol. Tiddskr. 50, 19-44.

Dickinson, W.R. (1970) Relation of andesites, granites and derivative sandstones to arc-trench tectonics. Rev. Geophys. Space Phys. 8, 813-860.

Dickinson, W.R. & Seely, D.R. (1979) Structure and stratigraphy of fore-arc regions. Bull. Am. Assoc. Petrol. Geol. 63, 2-31.

Downie, C., Lister, T.R., Harris, A.L. & Fettes, D.J. (1971) A palynological investigation of the Dalradian rocks of Scotland. Inst. Geol. Sci. Rept. 71/9.

El Bouseily, A.M. & El Sokkary, A.A. (1975) The relation between Rb, Ba and Sr in granitic rocks. Chem. Geol. 16, 207-219.

Fitch, F.J., Forster, S.C. & Miller, J.A. (1976) The dating of the Ordovician. in The Ordovician System (The University of Wales Press), 15-27.

Fitton, J.G. & Hughes, D.J. (1970) Volcanism and plate tectonics in the British Ordovician. Earth planet. Sci. Lett. 8, 223-227.

Gabrielse, H. & Reesor, J.E. (1974) The nature and setting of granitic plutons in the central and eastern parts of the Canadian Cordillera. Pacific Geology 8, 109-138.

Gale, G.H. & Roberts, D. (1974) Trace element geochemistry of Norwegian Lower Palaeozoic basic volcanics and its tectonic implications. Earth planet. Sci. Lett. 22,380-390.

Gale, N.H., Beckinsale, R.D. & Wadge, A.J. (1979) A Rb-Sr whole rock isochron for the Stockdale Rhyolite of the English Lake District and a revised mid-Palaeozoic time-scale. J. geol. Soc. Lond. 136, 235-242.

Garson, M.S. & Plant, J. (1973) Alpine type ultramafic rocks and episodic mountain building in the Scottish Highlands. Nature (phys. Sci.) 242, 34-38.

George, T.N. (1960) The stratigraphical evolution of the Midland Valley. Trans. geol. Soc. Glasgow 24, 32-107.

Glikson, A.Y. (1979) Early Precambrian tonalite-trondhjemite sialic nuclei. Earth Sci. Rev. 15, 1-73.

Graham, C. (1976) Petrochemistry and tectonic significance of Dalradian metabasaltic rocks of S.W. Scottish Highlands. J. geol. Soc. Lond. 132, 61-84.

Graham, A.M. & Upton, B.G.J. (1978) Gneisses in diatremes, Scottish Midland Valley : petrology and tectonic implications. J. geol. Soc. Lond. 135, 219-228.

Gunn, P.J. (1973) Location of the Proto-Atlantic suture in the British Isles. Nature 242, 111-112.

Hanson, G.N. (1978) The application of trace elements to the petrogenetis of igneous rocks of granitic composition. Earth planet. Sci. Lett. 38, 26-43.

Harker, A. (1909) The natural history of igneous rocks. (MacMillan).

Harland, W.B. (1964) The Phanerozoic time-scale. Spec. Publ. geol. Soc. London 5.

Harland, W.B. & Gayer, R.A. (1972) The Arctic Caledonides and earlier oceans. Geol. Mag. 109, 289-314.

Harris, A.L., Bradbury, H.J. & McGonigal, M.H. (1976) The evolution and transport of the Tay nappe. Scott. J. Geol. 12, 103-113.

Harris, A.L., Baldwin, C.T., Bradbury, H.J., Johnson, H.D. & Smith, R.A. (1978) in Geol. J. Spec. Issue No. 10, 115-138. Ensialic basin deposition : the Dalradian Supergroup.

Henderson, S.M.K. (1935) Ordovician submarine disturbances in the Girvan district. Trans. R. Soc. Edinburgh 63, 487-509.

Hietanen, A. (1963) Metamorphic and igneous rocks along the northwest border zone of the Idaho batholith. Prof. Pap. U. S. geol. Surv. 344-D.

Holder, M.T. (1979) An emplacement mechanism for post-tectonic granites and its implications for their geochemical features. in Origin of granite batholiths : Geochemical evidence (Shiva Publishing Limited).

Hubert, J.F. (1969) Late Ordovician sedimentation in Caledonian geosyncline, southwestern Scotland. in North Atlantic - Geology and Continental Drift (Ed. Kay, M.), 267-283.

Hughes, C.J. & Bruckner, W.D. (1971) Late Precambrian rocks of Eastern Avalon peninsula, Newfoundland - A volcanic island complex. Can. J. Earth Sci. 8, 899-915.

Ingham, J.K. (1978) Geology of a continental margin 2 : middle and late Ordovician transgression, Girvan. in Geol. J. Spec. Issue No. 10, 163-176.

Ingham, J.K. & Wright, A.D. (1970) A revised classification of the Ashgill series. Lethaia 3, 233-242.

Jeans, P.F.J. (1973) Plate-tectonic reconstruction of the southern Caledonides of Great Britain. Nature (phys. Sci.) 245, 120-122.

Jehu, T.J. & Campbell, R. (1917) The Highland Border rocks of the Aberfoyle district. Trans. R. Soc. Edinburgh 52, 175-212.

Johnson, M.R.W. & Harris, A.L. (1967) Dalradian -? Arenig relations in parts of the Highland Border, Scotland, and their significance in the chronology of the Caledonian orogeny. Scott. J. Geol. 3, 1-16.

Kelling, G. (1961) The stratigraphy and structure of the Ordovician rocks of the Rhinns of Galloway. J. geol. Soc. Lond. 117, 37-75.

Kelling, G. & Holroyd, J. (1978) Clast size, shape and composition in some ancient and modern fan gravels. in Sedimentation in submarine canyons, fans and trenches (Eds. Stanley, D.J. & Kelling, G.) (Howden).

Kelsey, C.H. (1965) Calculation of the CIPW norm. Mineralog. Mag. London 34, 276-282.

Kennedy, W.Q. (1958) The tectonic evolution of the Midland Valley of Scotland. Trans. geol. Soc. Glasgow 23, 107-133.

Kistler, R.W. & Peterman, Z.E. (1973) Variations in Sr, Rb, K, Na and initial $^{87}Sr/^{86}Sr$ in Mesozoic granitic rocks and intruded wall rocks in central California. Bull. geol. Soc. Am. 84, 3489-3512.

Krogh, T.E. (1973) A low-contamination method for hydro-thermal decomposition of zircon and extraction of U and Pb for isotopic determinations. Geochim. cosmochim. Acta 37, 485-494.

Kuenen, Ph.H. (1953) Graded bedding with observations on Lower Palaeozoic rocks of Britain. K. Ned. Akad. Wet. Afd. Nat. Verh. 20, 1-47.

Kuenen, Ph.H. (1956) The difference between sliding and turbidity flows. Deep Sea Res. 3, 134-139.

Lambert, R.St.J. & McKerrow, W.S. (1976) The Grampian Orogeny. Scott. J. Geol. 12, 271-292.

Lameyre, J. (1980) Les magmas granitiques : leurs comprtements, leurs associations et leurs sources. Mém. h. sér. Soc. géol. de France No. 10.

Lamont, A. & Lindström, M. (1957) Arenigian and Llandeilian cherts identified in the Southern Uplands of Scotland by conodonts etc.. Trans. Edinb. geol. Soc. 17, 60-70.

Lapworth, C. (1882) The Girvan succession. J. geol. Soc. Lond. 38, 537-666.

Leake, B.E. & others (1969) The chemical analysis of rock powders by automatic X-ray fluorescence. Chem. Geol. 5, 7-86.

Longman, C.D., Bluck, B.J. & van Breemen, O. (1979) Ordovician conglomerates and the evolution of the Midland Valley. Nature 280, 578-581.

Longman, C.D., Bluck, B.J., van Breemen, O. & Aftalion, M. (in press) Ordovician conglomerates : Constraints on the time scale. in Numerical dating of the stratigraphic column (Ed. Odin, G.S.) (Wiley)

MacIntyre, G.A., Brooks, C., Compston, W. & Turek, A. (1966) A statistical assessment of Rb-Sr isochrons. J. geophys. Res. 71, 5459-5468.

McCarthy, T.S. & Hasty, R.A. (1976) Trace element distribution patterns and their relationship to the crystallization of granitic melts. Geochem. cosmochem. Acta 40, 1351-1358.

McCartney, W.D., Poole, W.H., Wanless, R.K., Williams, H. & Loveridge, W.D. (1966) Rb-Sr age and geological setting of the Holyrood granite, southeastern Newfoundland. Can. J. Earth.Sci. 3, 947-957.

McKerrow, W.S., Legget, J.K. & Eales, M.H. (1977) Imbricate thrust model of the Southern Uplands of Scotland. Nature 267, 237-239.

Mitchell, A.H.G. (1977) The Grampian Orogeny in Scotland : Arc-continent collision and polarity reversal. J. Geol. Chicago 86, 643-646.

Mitchell, A.H.G. & McKerrow, W.S. (1975) Analogous evolution of the Burma orogen and the Scottish Caledonides. Bull. geol. Soc. Am. 86, 305-315.

Moseley, F. (1977) Caledonian plate tectonics and the place of the English Lake District. Bull. geol. Soc. Am. 88, 764-768.

Mustart, D.A. (1972) Phase relations in the peralkaline portion of the system Na_2O - Al_2O_3 - SiO_2 - H_2O. Unpubl. PhD thesis, Stanford University.

Nicolaysen, L.O. (1961) Graphic interpretation of discordant age measurements on metamorphic rocks. Ann. New York Acad. Sci. 91, 198-206.

Niggli, P. (1954) Rocks and mineral deposits (Freeman).

O'Connor, J.T. (1965) A classification of quartz-rich igneous rocks based on feldspar ratios. Prof. Pap. U. S. geol. Surv. 525-B.

O'Hara, M.J. (1976) The CaO - MgO - Al_2O_3 - SiO_2 projection. in Progress in experimental petrology, Third Report, 109.

Pankhurst, R.J. (1970) The geochronology of the basic complexes (N.E. Scotland). Scott. J. Geol. 6, 83-107.

Pankhurst, R.J. (1974) Rb-Sr whole-rock chronology of Caledonian events in northeast Scotland. Bull. geol. Soc. Am. 85, 345-350.

Pankhurst, R.J. & Piggeon, R.T. (1976) Inherited isotope systems and the source region pre-history of early Caledonian granites in the Dalradian series of Scotland. Earth planet. Sci. Lett. 31, 55-68.

Peach, B.N. & Horne, J. (1899) The Silurian rocks of Britain, Volume 1, Scotland. Mem. Geol. Surv.

Peacock, M.A. (1931) Classification of igneous rock series. J. Geol. Chicago 39, 54-67.

Petro, W.L., Vogel, T.A. & Wilband, J.T. (1979) Major element chemistry of the plutonic rock suites from compressional and extensional plate boundaries. Chem. Geol. 26, 217-235.

Pettijohn, F.J. (1943) Archaean sedimentation. Bull. geol. Soc. Am. 54, 925-972.

Phillips, W.E.A., Stillman, C.J. & Murphy, T. (1976) A Caledonian plate-tectonic model. J. geol. Soc. Lond. 132, 579-609.

Pidgeon, R.T. & Aftalion, M. (1978) Cogenetic and inherited zircon U-Pb systems in granites : Palaeozoic granites of Scotland and England. in Geol. J. Spec. Issue No. 10, 183-220.

Powell, D.W. (1971) A model for the Lower Palaeozoic evolution of the southern margin of the early Caledonides of Scotland and Ireland. Scott. J. Geol. 7, 369-372.

Powell, M. & Powell, R. (1977) Plagioclase-alkali feldspar geothermometry revisited. Contrib. Mineral. Petrol. 41, 253-256.

Pringle, I.R. (1973) Rb-Sr age determinations on shales associated with the Varanger Ice Age. Geol. Mag. 109, 465-472.

Raymond, L.A. & Swanson, S.E. (1980) Accretion and episodic plutonism. Nature 285, 317-319.

Roberts, J.L. (1974) The structure of the Dalradian rocks in the S.W. Highlands of Scotland. J. geol. Soc. Lond. 130, 93-124.

Roddick, J.A. & Hutchison, W.W. (1974) Setting of the coast plutonic complex, British Columbia. Pacific Geology 8, 91-108.

Ross, R.J.Jnr., Naeser, C.W. & Izett, G.A. (1976) Apatite fission-track dating of a sample from the type Caradoc (Middle Ordovician) Series in England. Geology 4, 505-506.

Ross, R.J.Jnr., Naeser, C.W. & Izett, G.A. (1977) Fission track dating of Lower Palaezoic bentonites in British stratotypes. U. S. Geol. Surv. Open-File Report 77-348.

Ross, R.J.Jnr. & others (1978) Fission track dating of Lower Palaeozoic volcanic ashes in British stratotypes. U.S. Geol. Surv. Open-File Report 78-701, 363-365.

Rundle, C.C. (1979) Ordovician intrusions in the English Lake District. J. geol. Soc. Lond. 136, 29-38.

Shibata, K. & Ishihara, S. (1979) Initial $^{87}Sr/^{86}Sr$ ratios of plutonic rocks from Japan. Contrib. Mineral. Petrol. 70, 381-390.

Sorensen, H. (1974) The alkaline rocks (Wiley).

Statham, P.J. (1976) A comparitive study of techniques for quantitative analysis of the X-ray spectra obtained with a Si(Li) detector. X-ray Spectrometry 5, 16-28.

Steiger, R.H. & Jäger, E. (1977) Subcommision on geochronology : Convention on the use of decay constants in geo- and cosmo- chronology. Earth planet. Sci. Lett. 36, 359-362.

Stormer, J.C.Jnr. & Nicholls, J. (1978) XTLFRAC : a program for the interactive testing of magmatic differentiation models. Computers and Geosci. 4, 143-159.

Streckeisen, A. (1976) To each plutonic rock its proper name. Earth Sci. Rev. 12, 1-33.

Streckeisen, A. (1976') Classification of the common igneous rocks by means of their chemical composition. Neues Jahrb. Mineral. Monatsch., 1-15.

Streckeisen, A. & Le Maitre, R.W. (1979) A chemical approximation to the modal QAPF classification of the igneous rocks. Neues Jahrb. Mineral. Abhandlungen 136, 169-206.

Stukas, V. & Reynolds, P.H. (1974) $^{40}Ar/^{39}Ar$ dating of the Long Range dykes, Newfoundland. Earth planet. Sci. Lett. 22, 256-266.

Suess, E. (1906) Face of the Earth II (Oxford University Press).

Teng, H.C. & Strong, D.F. (1976) Geology and geochemistry of the St. Lawrence granite and associated fluorspar deposits, southeast Newfoundland. Can. J. Earth Sci. 13, 1374-1385.

Thomas, P.R. (1980) The stratigraphy and structure of the Moine rocks north of the Schiehallion complex, Scotland. J. geol. Soc. Lond. 137, 469-486.

Titterington, D.M. & Halliday, A.N. (1979) On the fitting of parallel isochrons and the method maximum likelihood. Chem. Geol. 26, 183-195.

Toghill. P. (1970) Highest Ordovician (Hartfell Shales) graptolite faunas from the Moffat area, south Scotland. Bull. Br. Mus. nat. Hist. (Ser. Geol.) 19, 1-26.

Topping, J. (1965) Errors of observation and their treatment. (Chapman & Hall Limited).

Tripp, R.P. (1980) Trilobites from the Ordovician Balclatchie and Lower Ardwell groups of the Girvan district, Scotland. Phil. Trans. R. Soc. Ed. (E. Sci.) 71, 123-145.

Tuttle, O.F. & Bowen, N.L. (1958) Origin of granite in the light of experimental studies in the system $NaAlSi_3O_8$ - $KAlSi_3O_8$ - SiO_2 - H_2O. Mem. geol. Soc. Am. 74.

Upton. B.G.J., Aspen, P., Graham, A.M. & Chapman, N. (1976) Pre-Palaeozoic basement of the Scottish Midland Valley. Nature 260, 517-518.

van Breemen, O. & Hawkesworth, C.J. (1980) Sm-Nd isotopic study of garnets and their metamorphic host rocks. Trans. R. Soc. Edinburgh (E. Sci.) 71, 97-102.

van Breemen, O. & Upton, B.G.J. (1972) Age of some Gardar intrusive complexes, south Greenland. Bull. geol. Soc. Am. 83, 3381-3390.

Viljoen, M.J. & Viljoen, R.P. (1969) Geol. Soc. S. Africa Spec. Publ. 2.

Wager, L.R. & Deer, W.A. (1939) Geological investigation in E. Greenland : Part III, The petrology of the Skaergaard intrusion, Kangerdlugssuaq, East Greenland. Medd. Gronland. 105, No. 4.

Walton, E.K. (1956) Two Ordovician conglomerates in south Ayrshire. Trans. geol. Soc. Glasgow 22, 133-156.

Walton, E.K. (1963) Sedimentation and structure in the Southern Uplands. in The British Caledonides (Oliver & Boyd).

Wetherill, G.W. (1956) Discordant uranium-lead ages. Trans. Am. geophys. Union 37, 302-326.

White, A.J.R. & Chappell, B.W. (1977) Ultrametamorphism and granitoid genesis. Tectonophysics 43, 7-22.

Williams, A. (1959) A structural history of the Girvan District, S.W. Scotland. Trans. R. Soc. Edinburgh 63, 629-667.

Williams, A. (1962) The Barr and Lower Ardmillan series (Caradoc) of the Girvan district, south-west Ayrshire. Mem. geol. Soc. London 3.

Williams, A. (1969) Ordovician of the British Isles. in North Atlantic geology and continental drift (Ed. Kay, M.) (AAPG).

Williams, A. & others (1972) A correlation of the Ordovician rocks in the British Isles. Geol. Soc. Lond. Spec. Rep. No. 3.

Wilson. J.T. (1966) Did the Atlantic close and then reopen ? Nature 211, 676.

Winkler, H.G.F. & Breibart, R. (1978) New aspects of granitic magmas.Neues. Jahrb. Mineral. Monatsh. 10, 463-480.

Wright, A.E. (1976) Alternating subduction direction and the evolution of the Atlantic Caledonides. Nature 264, 156-160.

Wright, A.E. (1977) The evolution of the British Isles in the late Pre-Cambrian. Estudios geol. 33, 303-313.

York, D. (1966) Least squares fitting of a straight line. Can. J. Phys. 44, 1079-1086.

York, D. (1969) Least squares fitting of a straight line with correlated errors. Earth planet. Sci. Lett. 5, 320-324.